EPRI

Evaluation of the Proposed High-Level Radioactive Waste Repository at Yucca Mountain Using Total System Performance Assessment

Phase 6

Technical Report

Main Library - No
EPRI

Evaluation of the Proposed High-Level Radioactive Waste Repository at Yucca Mountain Using Total System Performance Assessment

Phase 6

1003031

Final Report, February 2002

EPRI Project Manager
J. Kessler

EPRI • 3412 Hillview Avenue, Palo Alto, California 94304 • PO Box 10412, Palo Alto, California 94303 • USA
800.313.3774 • 650.855.2121 • askepri@epri.com • www.epri.com

DISCLAIMER OF WARRANTIES AND LIMITATION OF LIABILITIES

THIS DOCUMENT WAS PREPARED BY THE ORGANIZATION(S) NAMED BELOW AS AN ACCOUNT OF WORK SPONSORED OR COSPONSORED BY THE ELECTRIC POWER RESEARCH INSTITUTE, INC. (EPRI). NEITHER EPRI, ANY MEMBER OF EPRI, ANY COSPONSOR, THE ORGANIZATION(S) BELOW, NOR ANY PERSON ACTING ON BEHALF OF ANY OF THEM:

(A) MAKES ANY WARRANTY OR REPRESENTATION WHATSOEVER, EXPRESS OR IMPLIED, (I) WITH RESPECT TO THE USE OF ANY INFORMATION, APPARATUS, METHOD, PROCESS, OR SIMILAR ITEM DISCLOSED IN THIS DOCUMENT, INCLUDING MERCHANTABILITY AND FITNESS FOR A PARTICULAR PURPOSE, OR (II) THAT SUCH USE DOES NOT INFRINGE ON OR INTERFERE WITH PRIVATELY OWNED RIGHTS, INCLUDING ANY PARTY'S INTELLECTUAL PROPERTY, OR (III) THAT THIS DOCUMENT IS SUITABLE TO ANY PARTICULAR USER'S CIRCUMSTANCE; OR

(B) ASSUMES RESPONSIBILITY FOR ANY DAMAGES OR OTHER LIABILITY WHATSOEVER (INCLUDING ANY CONSEQUENTIAL DAMAGES, EVEN IF EPRI OR ANY EPRI REPRESENTATIVE HAS BEEN ADVISED OF THE POSSIBILITY OF SUCH DAMAGES) RESULTING FROM YOUR SELECTION OR USE OF THIS DOCUMENT OR ANY INFORMATION, APPARATUS, METHOD, PROCESS, OR SIMILAR ITEM DISCLOSED IN THIS DOCUMENT.

ORGANIZATION(S) THAT PREPARED THIS DOCUMENT

Risk Engineering, Inc.
EPRI, Inc.

ORDERING INFORMATION

Requests for copies of this report should be directed to EPRI Orders and Conferences, 1355 Willow Way, Suite 278, Concord, CA 94520, (800) 313-3774, press 2 or internally x5379, (925) 609-9169, (925) 609-1310 (fax).

Electric Power Research Institute and EPRI are registered service marks of the Electric Power Research Institute, Inc. EPRI. ELECTRIFY THE WORLD is a service mark of the Electric Power Research Institute, Inc.

Copyright © 2002 Electric Power Research Institute, Inc. All rights reserved.

CITATIONS

This report was prepared by

Risk Engineering, Inc.
4155 Darley Avenue, Suite A
Boulder, Colorado 80303

Principal Investigators
J. Vlasity
R. McGuire

Authors
J. Kessler, EPRI, Inc.
J. Vlasity, Risk Engineering, Inc.
R. McGuire, Risk Engineering, Inc.
A. Long, University of Arizona
S. Childs, Kennedy Jenks, Inc.
B. Ross, Disposal Safety, Inc.
F. Schwartz, Ohio State University
D. Shoesmith, University of Western Ontario
J. Massari, Constellation Nuclear Services, Inc.
W. Zhou, Monitor Scientific, LLC.
R. Arthur, Monitor Scientific, LLC.
M. Apted, Monitor Scientific, LLC.
E. Sudicky, Groundwater Simulations Group

This report describes research sponsored by EPRI.

The report is a corporate document that should be cited in the literature in the following manner:

Evaluation of the Proposed High-Level Radioactive Waste Repository at Yucca Mountain Using Total System Performance Assessment: Phase 6, EPRI, Palo Alto, CA: 2002. 1003031.

REPORT SUMMARY

A successful license application for the candidate spent-fuel and high-level waste repository at Yucca Mountain depends on a robust demonstration of long-term safety. This report presents EPRI's evaluation of, and makes a case for, the suitability of the Yucca Mountain repository using a Total System Performance Assessment (TSPA). The report discusses factors that make the Yucca Mountain repository system suitable for continued development and initiation of the licensing process. Information in this Phase 6 TSPA report provides insight in defining important barriers to radionuclide release and the anticipated travel time to the accessible environment, once a release is assumed. Health impacts from such releases are estimated to remain small at all times in the future.

Background

Regulations limiting the negative impacts of the potential high-level waste repository as well as the current site recommendation process require a quantitative assessment of total performance. The iterative TSPA process can most wisely be used to refine models and improve databases in order to reduce conservatisms and/or uncertainties. When applied in this manner, the TSPA can guide the allocation of future resources toward repository system components with the greatest impact on overall performance and away from components not affecting performance. Both the EPA and the NRC have issued new risk-based evaluation criteria mandating that applicants show the importance of each system and subsystem used to demonstrate compliance to the EPA's accessible environment standard dose regulations. This Phase 6 TSPA continues to play a crucial role in development of the associated safety case for Yucca Mountain.

Objective

To provide an independent technical review of whether the Yucca Mountain site appears suitable for continued development and licensing.

Approach

EPRI used its Integrated Multiple Assumptions and Release Code (IMARC) model to probabilistically evaluate the performance of the proposed Yucca Mountain site. The code, now in its sixth phase, has been updated to include new data as appropriate. The code divides the repository system into several sections—1) climate and net infiltration, 2) near-field thermal and hydrologic effects, 3) drip shield, container, and cladding degradation, 4) release from the near-field, 5) far-field flow and transport, and 6) biosphere. Abstractions of the behavior of each section (lookup tables or computer submodels) are combined in the probabilistic IMARC "shell" computer model to calculate probability-weighted mean doses to a "reasonably maximally exposed individual" (RMEI). Many studies on a single scenario are conducted to evaluate the sensitivity of various parts of the repository system on overall performance. Analyses were also conducted to understand the relative importance of 12 different barriers within the Yucca

Mountain system. A "barrier" is a set of repository features and processes that retain radionuclides within the repository, limit the rate of radionuclide release from the repository, limit radionuclide transport to the biosphere, or dilute the concentrations of radionuclides in the groundwater.

Results

There is high confidence that the proposed Yucca Mountain system, including the present engineering design, will provide a large degree of safety. A brief safety case is made in the first chapter of this report. When compared to the regulatory criteria, the IMARC analyses indicate the criteria are met by over six orders of magnitude of margin. Furthermore, the peak dose—which occurs well beyond 10,000 years—is still about 1000 times lower than natural background radiation levels.

The barrier analyses indicate that many independent barriers contribute to overall safety, as measured by the ability of individual barriers to lower the estimated dose rates to an RMEI. Several natural and engineered barriers each contribute greatly to overall dose reduction, though no single barrier contributes a major share to the overall dose reduction. Furthermore, several backup barriers—such as used fuel cladding and the drip shield in the engineered part of the system along with the alluvium in the saturated zone—will also contribute to overall dose reduction in the unlikely event that other barriers do not function as anticipated.

EPRI Perspective

This report was prepared at the time the Yucca Mountain repository was recommended by the Secretary of Energy and the President to Congress for continuation into the next stage of repository development—application to the NRC for a license to construct the repository. Congress must now decide whether to authorize the DOE to proceed with licensing. A high level of confidence needs to be established to justify continuing to this next step. This level of confidence must be based on what is now known combined with the risks of proceeding given uncertainties about very long-term behavior of the repository system. EPRI feels that the level of confidence is high, and the DOE is properly managing these uncertainties, as discussed in this report. EPRI therefore recommends that the DOE proceed with preparation of the license application.

Keywords

Yucca Mountain
High-level radioactive waste
Spent-fuel disposal
Total System Performance Assessment

CONTENTS

LIST OF FIGURES

LIST OF TABLES

1

SITE RECOMMENDATION CONSIDERATIONS AND SUMMARY OF MAIN RESULTS

At the time of this writing, the U.S. Congress has just been presented with a recommendation by the Secretary of Energy and the President to proceed with the development of the Yucca Mountain system as the repository for much of the nation's high-level radioactive waste (HLW). The HLW proposed to be disposed of at Yucca Mountain includes: commercial used nuclear fuel, used nuclear fuel from the Department of Navy, and a variety of high-activity wastes generated by the Department of Energy (DOE). Analysis presented in this report supports this recommendation to Congress.

1.1 Summary of Arguments Why Development at Yucca Mountain Should Proceed

The following considerations presented in this report support a decision to allow the Yucca Mountain Project to proceed into the licensing phase:

- *The existing knowledge base about the Yucca Mountain area is extensive.* Over the past 20 years, DOE has collected a large amount of information about the natural system in the Yucca Mountain vicinity. This includes information on rock properties, groundwater flow, and past climate states. The Yucca Mountain area is one of the most studied geologic formations on the planet.
- *The combination of DOE data and analyses show a high level of confidence that the proposed repository will protect public health and safety.* DOE has incorporated the extensive data collected into detailed models to estimate that the dose to the RMEI will be well below the regulatory limits. Furthermore, doses due to the repository at Yucca Mountain are likely to be significantly less than that caused by natural background radiation at *all* times in the future.
- *Yucca Mountain is an arid site in an enclosed geologic basin.* The site is arid, which strongly supports the capability of the repository to retain the vast majority of the radionuclides until they have decayed away to negligible levels. The aridity also prevents the release of the majority of the longer-lived radionuclides by limiting the amount of groundwater that contacts the waste, as well as slowing the transport of that small fraction of those radionuclides that may escape from the repository. Finally, the aridity means that the number of people that can be supported by the available groundwater is limited. This effectively caps the number of people that could theoretically receive doses as high as the RMEI's.[1]

---

[1] The RMEI, by definition, is somebody who uses a relatively large amount of local groundwater.

The fact that Yucca Mountain is in an enclosed geologic basin means that groundwater can only carry the small fraction of radionuclides, which may escape the repository, over a relatively small distance. The groundwater passing beneath Yucca Mountain is not connected to any major rivers or lakes. This significantly limits the number of people who could ever come into contact with the radionuclides that may have escaped from the repository.

- *The natural features of Yucca Mountain contribute mightily to the overall safety of the Yucca Mountain repository system.* Analysis in this report shows that the "natural" features *alone* act to reduce the dose rate to the RMEI to below levels we all receive from natural radiation sources. This is powerful evidence that DOE is not "engineering their way around a bad site". Multiple barriers to the release or transport of wastes from the repository to the biosphere are present.
- *The engineered barriers (e.g., waste containers and drip shields) will last many thousands of years.* DOE has chosen to make the "drip shields" and containers out of metals that are among the most corrosion-resistant currently available. DOE is conducting tests on the long-term durability of these materials. Data from these tests to date, along with other available data have been used to estimate that these materials will be expected to last, on average, many thousands of years before even the smallest opening through the drip shield or container wall appears. EPRI estimates that approximately three out of four waste containers will still be intact after one million years. By that time, the vast majority of the radionuclides inside the containers will have decayed away.
- .*Any radionuclides escaping the repository will take thousands of years to reach the accessible environment.* The features of the groundwater and rock through which the groundwater passes are such that any radionuclides escaping the repository will travel very slowly. EPRI estimates it will take several thousand years for radionuclides to move 18 kilometers downstream. The nearest member of the public to Yucca Mountain is about 20 kilometers downstream.
- *The established regulations are very protective of public health.* There are several main aspects to the regulations that provide a high degree of protection. Those aspects governing long-term disposal (i.e., after the repository is loaded and closed) are:
  - DOE is required to assume individuals living in the Yucca Mountain vicinity in the far future are "reasonably maximally exposed individuals" (RMEIs). These hypothetical individuals are those who are living directly over the potential waste plume carried in the groundwater for his or her entire lifetime, and are engaged in activities that would cause them to receive the highest dose from any wastes that might seep out of the Yucca Mountain repository. For example, the RMEI meets all of his/her drinking water needs from the contaminated groundwater plume; he/she is assumed to grow much of his/her food crops using contaminated groundwater; and he/she is assumed to spend much time outdoors on land that is irrigated by contaminated groundwater. Thus, DOE must calculate the dose to the RMEI rather than to a more "average" individual who would likely receive a lower dose.
  - The dose rate limit to the RMEI is only a small fraction (less than 10%) of the dose that is received by the general population each year from natural sources. Thus, the incremental

dose allowed to be received by the RMEI is limited to only a small increase over natural background levels.

  - The regulations require DOE to demonstrate that the repository's natural features will provide significant protection. This is accomplished by requiring DOE so show there are a combination of natural and engineered barriers to mitigate the release or transport of wastes from the repository to the biosphere.

- *While uncertainties about the long-term behavior of the Yucca Mountain repository system remain, DOE has instituted a program that effectively manages those uncertainties. This provides high confidence that it is safe to proceed to the next step of repository development.* Indeed, more could be known about the very long-term behavior of the Yucca Mountain system to improve confidence in our understanding and our projections of long-term dose. DOE has done the following to provide the necessary confidence to proceed with repository development:

  - *Margin*: DOE's dose estimates to the RMEI are well below the regulatory limits. EPRI analyses in this report provide even lower estimates. This allows for the possibility that the resulting higher dose estimates would still be in compliance with the regulations, even if future information suggests that the repository system would not perform as well as currently projected.

  - *Multiple barriers:* EPRI shows in this report that DOE has many engineered and natural features that are effective "barriers" within the Yucca Mountain system that contribute to overall safety. Thus, if the long-term behavior of one or more of those barriers turns out to be less favorable than currently projected, EPRI analyses suggest it is likely that overall repository performance from the remaining features would still protect public health and safety.

  - *Conservatism:* In many instances in the DOE analyses for which there is uncertainty about future behavior, DOE introduces conservatisms in their analysis such that RMEI dose rates are likely to be overestimated. In this case, additional data collected in the future may allow for current dose estimates to be lowered.

  - *Long-term committed R&D ("performance confirmation") program:* The regulations require, and DOE has committed to a research program to collect, a variety of "confirmatory" data all the way through the repository construction, loading, and operation stages (assuming DOE is licensed to do so). These data will provide increased confidence that the appropriate decision-making with regard to either proceeding, or not, will be implemented.

  - *Natural analogues:* Obviously, it is not possible to observe directly the behavior of the Yucca Mountain repository system over ten thousand years or more. However, there are many "analogues" to the conditions that would exist at Yucca Mountain in the world, which have existed for thousands to millions of years. These analogues provide an understanding of the long-term evolution of systems similar to Yucca Mountain, and confidence that long-term projections of Yucca Mountain evolution are qualitatively reasonable. DOE has already embarked on collecting natural analogue information, and will continue to do so if further site development is approved.

  - *Reversibility:* DOE is required to develop, and is developing, a repository design such that if future information suggests that Yucca Mountain is not a safe site to dispose of

HLW, then DOE has the ability to reverse course. Thus, DOE has designed a repository from which waste can be retrieved relatively easily all the way up to the time of repository closure. Even after repository closure, waste retrieval remains possible.

For all the above reasons, there is sufficient confidence to proceed into the licensing stage of Yucca Mountain repository development. Some of the EPRI analyses supporting the above points are summarized in the remaining part of this chapter. The bulk of the analyses are presented in the following chapters.

1.2 Summary of the Main EPRI Performance Assessment Results

Performance assessments use calculations of radionuclide release and transport via groundwater to evaluate a repository's performance. The calculations presented in this section focus on estimating dose to the reasonably maximally exposed individual (RMEI) located 18 km downstream from the repository boundary (i.e., 18 km from within the footprint of the proposed repository). This distance was chosen because it is the position established in the final regulations for Yucca Mountain at which the public nearest the repository is assumed to live.

Furthermore, it is assumed that the radiation exposure of the RMEI comes via a plume of contaminants being carried downstream in the groundwater that is the source of the water used at the surface. People living downstream of Yucca Mountain are assumed to use the contaminated groundwater for drinking, and to irrigate crops or raise livestock subsequently eaten by these same people. It is also assumed that these same people spend part of their time outdoors on the land they irrigated with contaminated groundwater. Thus, they are assumed to receive additional radiation exposure from either direct "shine" from contaminants in the irrigated soil or from inhaling contaminated dust coming from the irrigated soil. Most of the results and sensitivity studies are presented as doses to the RMEI for all exposure pathways (e.g., via drinking water, consumption of food grown on contaminated land, direct exposure, and inhalation of dust from contaminated land). Some of the results and sensitivity analyses are for only the drinking water pathway, because there are additional regulatory limits on RMEI dose rates via drinking water only.

The dose rates shown are the "probability-weighted mean dose" to the RMEI. Many characteristics of the Yucca Mountain system are not uniform (i.e., heterogeneous). This results in "variability" of the estimated dose rates due to these inhomogeneities. Also, much of the very long-term behavior of the system is uncertain. This results in "uncertainty" in the estimated results. The computer model used in the analyses presented here captures both the "variability" and "uncertainty" by assigning a probability that the repository system exists in a specific state. Since this state evolves with time, this is called a "scenario". Each assumed repository scenario is assigned a probability such that the sum of probabilities for all the repository scenarios assumed is equal to one. In the probabilistic computer model used for this study, the dose rate to the RMEI versus time after repository closure is calculated for each individual repository scenario considered. The "probability-weighted mean dose" is calculated by multiplying each individual scenario dose by its probability and then adding all of these results together. What this means is that the dose rates for some individual scenarios will be higher than the probability-weighted mean, while others will be lower. However, since the mean is strongly affected by those scenarios with the highest doses, it is felt to be a reasonably conservative indicator of overall repository performance.

The analyses provide in the following section are for the "normal release" scenarios of repository evolution only. They do not consider scenarios involving igneous activity or human intrusion. Neither do we consider colloid-aided transport, as discussed briefly in Chapter 6.

1.2.1 Estimated Dose Rates to the RMEI Are Low at All Times in the Future

Figure 1-1 provides a plot of probability-weighted mean dose rate versus time after repository closure from the ten major radionuclides contributing to dose from all exposure pathways. Natural background levels are in the 100 to 300 millirem per year range.[2] The estimated mean dose rate is a flat line across the bottom that is indistinguishable from zero at this scale.

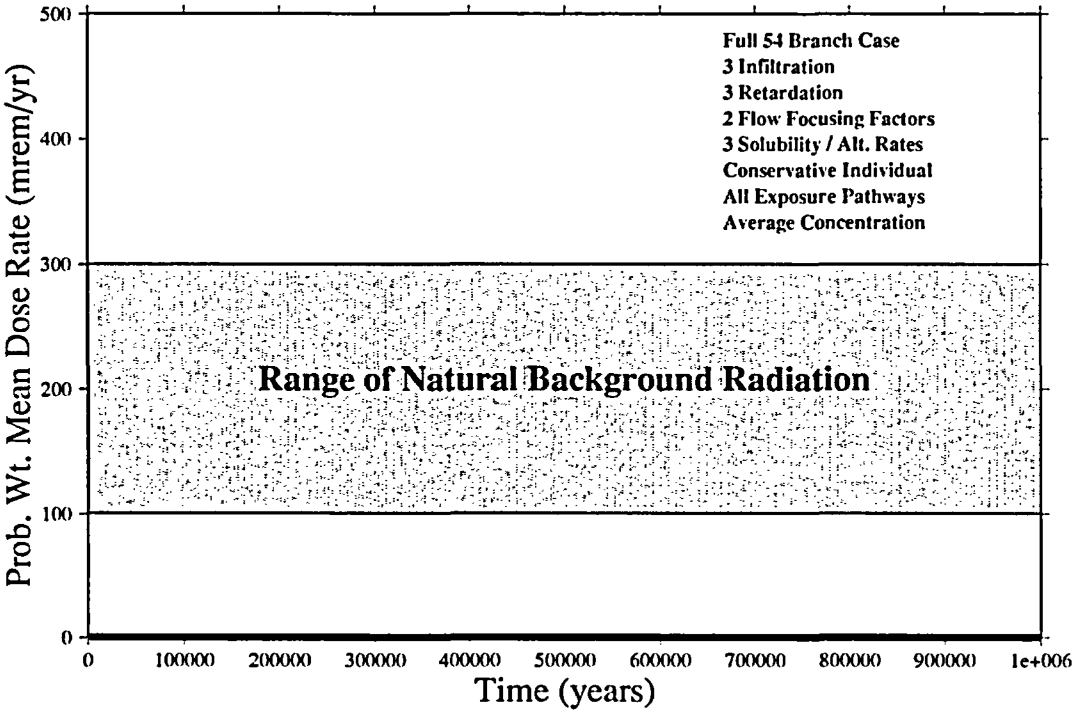

Figure 1-1
Probability-Weighted Mean Annual Dose Versus Time 18 km Downstream, All Exposure Pathways

Figure 1-2 is the same plot with the vertical scale expanded by a factor of ten (i.e., instead of the scale being zero to 500 mrem/yr, it is now from zero to 50 mrem/yr). For this figure, the natural background range is off the top of the scale. Instead, the regulatory limit of 15 mrem/yr is shown, although it only applies for the first 10,000 years. Again, the estimated dose rate even at this scale is indistinguishable from zero.

---

[2] A dose level from natural sources of 300 millirem per year is a more typical value for persons living in the Yucca Mountain vicinity.

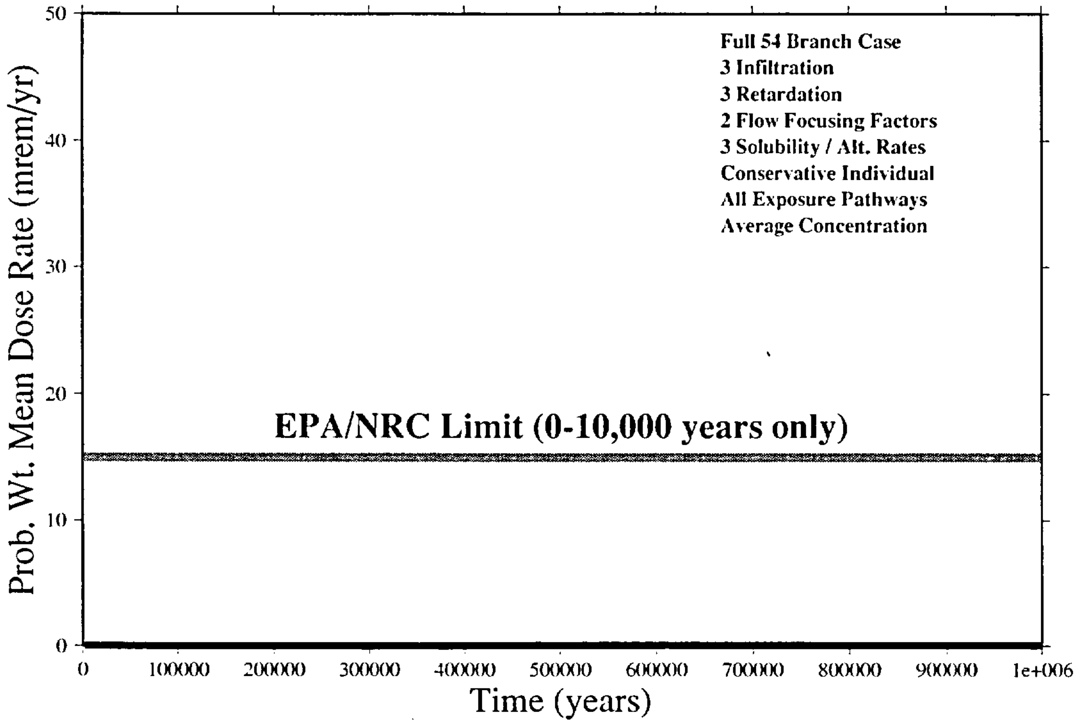

Figure 1-2
Probability-Weighted Mean Annual Dose Versus Time 18 km Downstream, All Exposure Pathways

The next expansion of ten in the vertical scale (now from zero to just 5 mrem/yr) is shown in Figure 1-3. For this figure, the estimated dose rate versus time curve finally appears to rise a very small distance off of the zero line.

The next expansion of ten in the vertical scale (now from zero to just 0.5 mrem/yr) is shown in Figure 1-4. The dose rate curve is now clearer, but still has not risen very far toward the top of the figure.

The final expansion is a factor of five in the vertical scale (from zero to only 0.1 mrem/yr), and is shown in Figure 1-5. For this curve, it can be seen that the dose rate rises above zero at about 200,000 years. For perspective, 200,000 years are about 20 times longer than the earliest recorded human history.

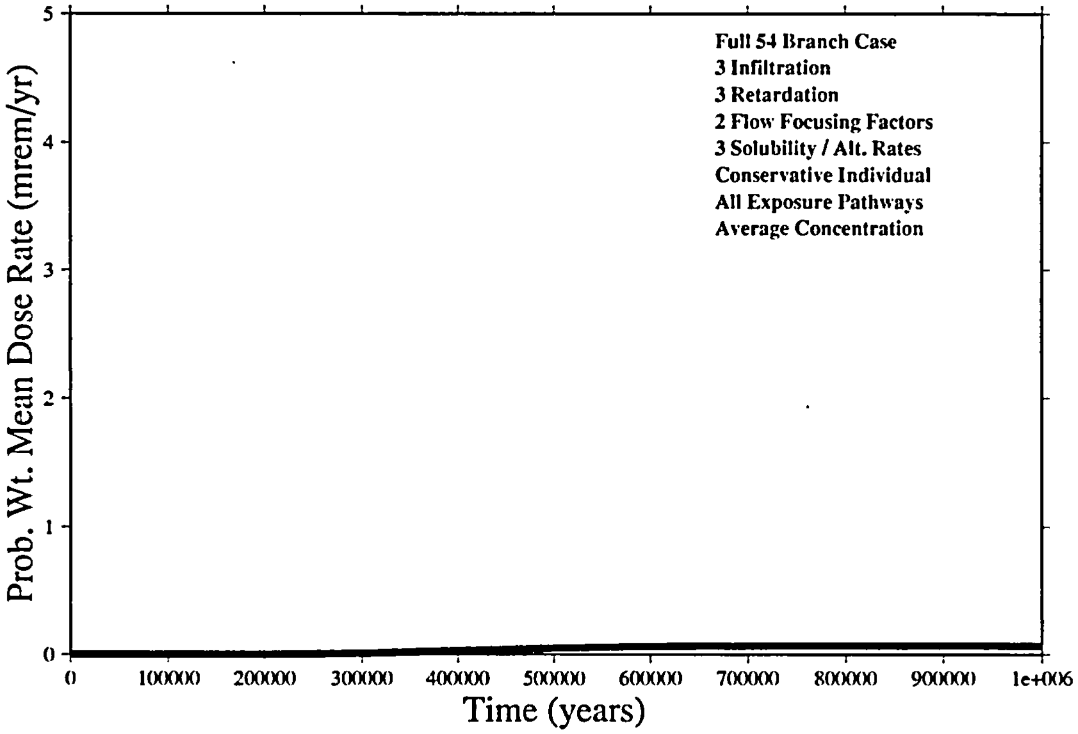

Figure 1-3
Probability-Weighted Mean Annual Dose Versus Time 18 km Downstream, All Exposure Pathways

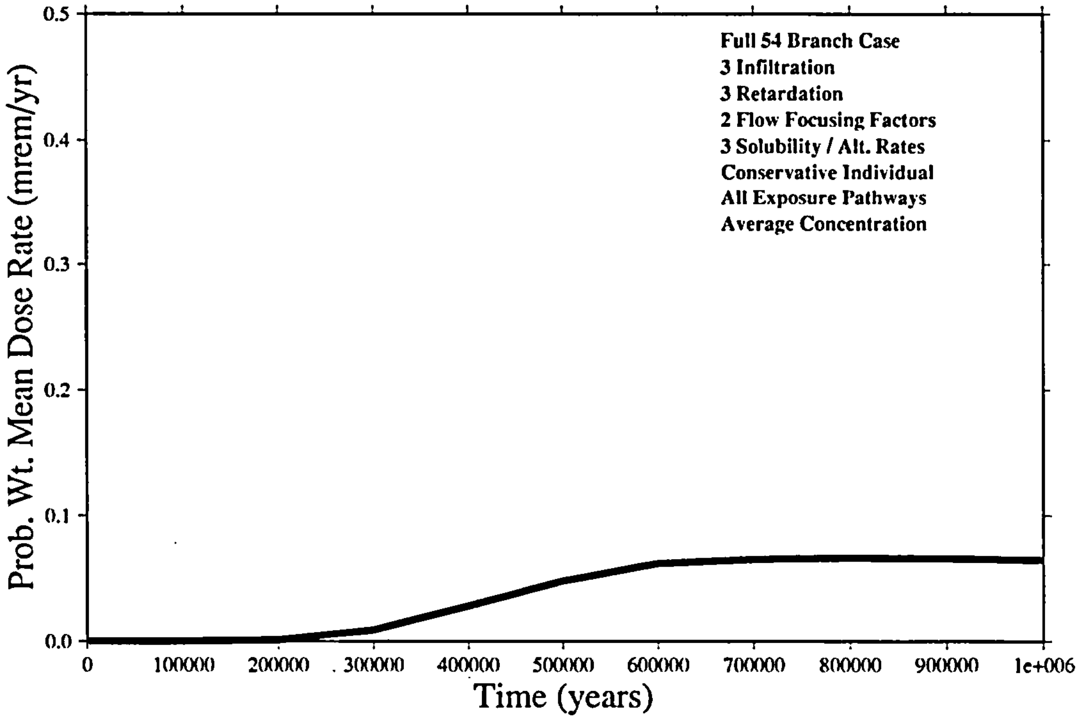

Figure 1-4
Probability-Weighted Mean Annual Dose Versus Time 18 km Downstream, All Exposure Pathways

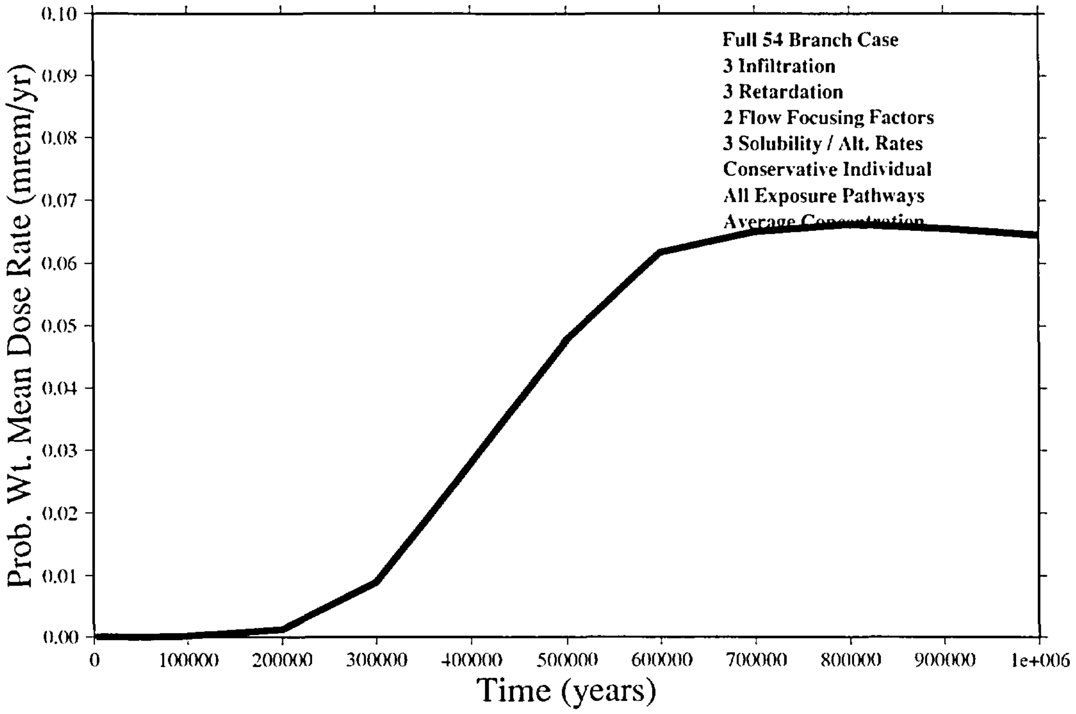

Figure 1-5
Probability-Weighted Mean Annual Dose Versus Time 18 km Downstream, All Exposure Pathways

Furthermore, as illustrated graphically in Figure 1-6,for the "normal" release scenario envisioned for the Yucca Mountain repository system, the probability-weighted mean dose to the RMEI adds less than one part in one thousand more to the dose the RMEI would receive annually from natural radiation sources. In other words, one would multiply the natural background dose by just 1.001 to obtain the RMEI dose that includes both natural radiation and that due to the "normal" release scenario from Yucca Mountain.

Figure 1-7 is the same probability-weighted mean annual dose curve shown in the previous figures, except the axes are now in logarithmic scale. The figure also shows the dose contributed by the ten radionuclides that contribute the most to dose from all exposure pathways considered in the biosphere model – the "base case".[3] As in the previous figures, this figure shows the annual dose from all exposure pathways. Dose rates prior to 10,000 years are significantly lower than 10^{-6} mrem/year – more than ten million times lower than the 15 mrem/yr limit in 10 CFR Part 63 [NRC, 2001]. Since the Part 63 annual dose limit applies to the first 10,000 years, this result suggests there is a "margin" of at least a factor of ten million in the estimated performance of the Yucca Mountain system. This provides confidence that even if some parts of the Yucca Mountain system are found to perform not as well as currently projected, there is still a high level of confidence that compliance with the regulation would still be achieved.

---

[3] The U-236 curve does not appear on this figure because it lies directly under the U-238 curve. It so happens that the product of the ratio of the number of moles of each radionuclide times the ratio of the dose conversion factors for these two radionuclides [Ci/mole] is very nearly one.

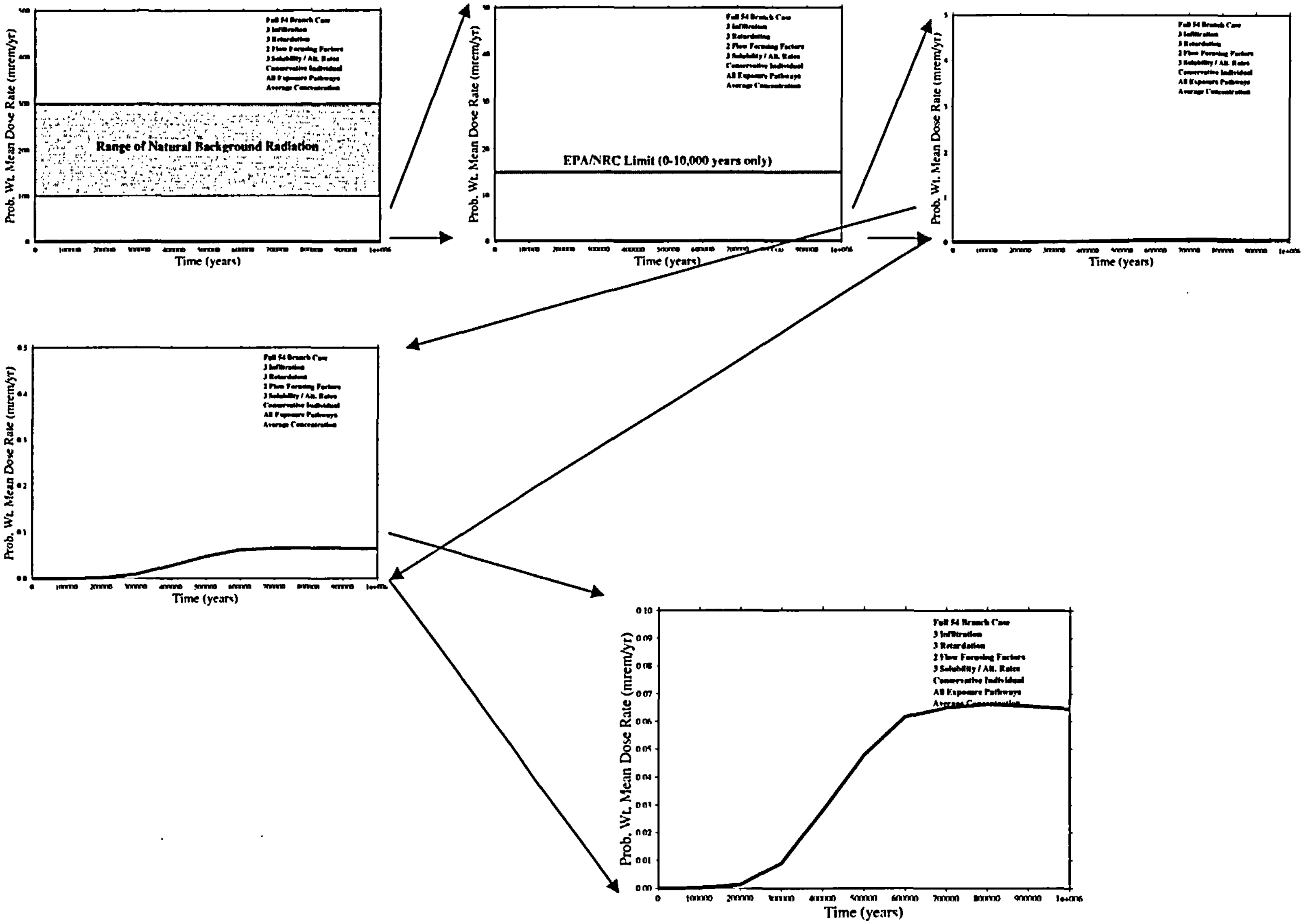

Figure 1-6
Expansion of Vertical Axes From Figure 1-1 through 1-5. Arrows indicate expansion of axes from the previous figure

Peak annual doses from all pathways occur at about 600,000 years and are on the order of 0.1 mrem. Even though the regulatory limit does not apply at these very long times, the peak dose rate is still about 100 times lower than the 15 mrem/year limit. This provides even more confidence that the Yucca Mountain system can adequately protect human health over the longest envisioned time horizons. The general character of the dose curves shown in Figure 1-7 is as follows: the ^{237}Np decay chain (^{237}Np, ^{233}U, and ^{229}Th) dominates RMEI doses at all times considered, because ^{237}Np is available in adequate inventories, dose conversion factors for the chain are relatively high, and it is not significantly retarded in geologic strata during transport. It was necessary to have the vertical axis on this plot start at an extremely small annual dose to show the earliest breakthrough at 18 km before 100,000 years. This very long delay is mainly caused by the very long combined lifetime of the engineered barriers considered in this model: the drip shield, container, and cladding. Delay is also caused by the relatively long travel times through the unsaturated (UZ) and saturated (SZ) zones.

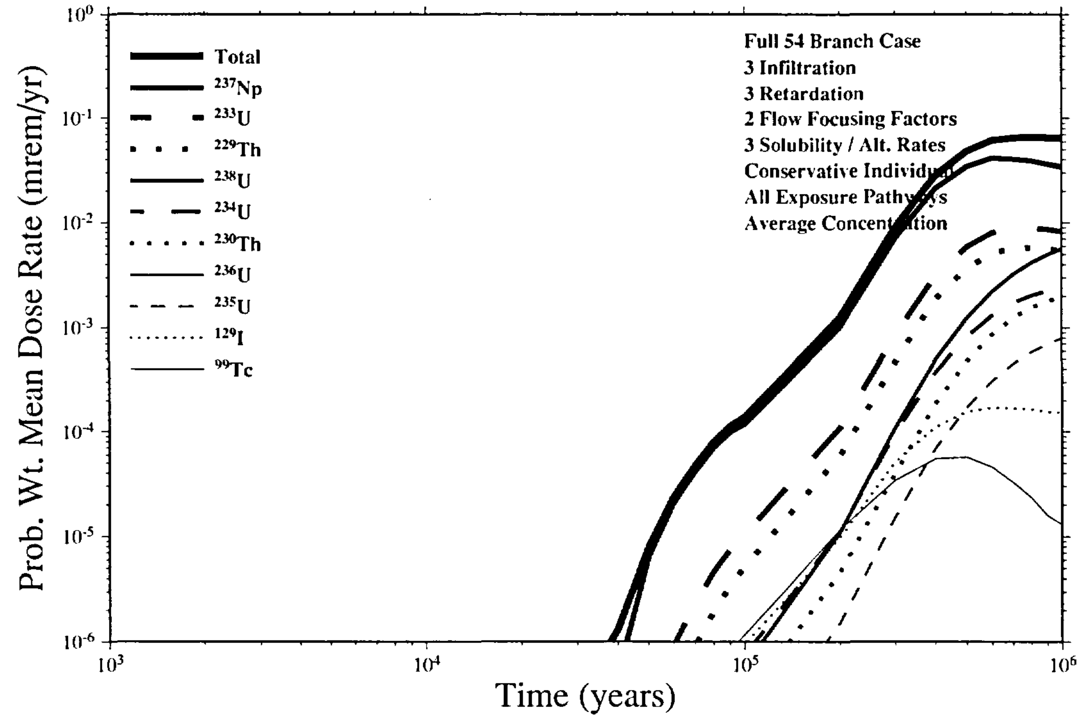

Figure 1-7
Probability-Weighted Mean Annual Dose Versus Time 18 km Downstream, All Exposure Pathways

1.2.2 There are Multiple Barriers that Contribute to Overall Safety

A "barrier" is assumed to be any single or readily distinguishable suite of features, events, and processes (FEPs) that act to:

- prevent or substantially delay[4] movement of the radionuclides to the biosphere; and/or
- substantially reduce their concentration[5] by action of either radioactive decay *or dilution*

A series of analyses presented in this report explored the individual contribution to safety of 12 different "barriers", some of which were mostly "natural", some of which were mostly "engineered", and some of which were combinations of the two. Examples of "natural" barriers include the rock formation above the repository, which affects the amount of groundwater that can drip into the tunnels containing the waste, and the rock formation downstream of the repository, which slows the transport of radionuclides that may be released from the repository. Examples of "engineered" barriers are the drip shields, the containers ("waste packages"), and the metal cladding immediately surrounding the used nuclear fuel itself.

The analyses suggested the following:

- There are multiple "engineered" and "natural" barriers that contribute significantly to overall safety. Specifically, while the waste package is an important "barrier", it is by no means the only significant barrier;
- The "natural" barriers, as a group, generally contribute more to overall peak dose reduction than do the "engineered" barriers. In fact, "natural" barriers *alone* can provide a sufficient degree of safety. This is discussed in more detail in the next section;
- Many barriers that may otherwise appear unimportant can contribute significantly to overall dose reduction if several other barrier functions are assumed to fail. Thus, they can be considered important "backup" barriers. A specific example is that of metal cladding immediately surrounding the used fuel waste form. If both the drip shield and container are assumed to fail immediately after the repository is closed, the cladding will contribute substantially to overall dose reduction.

The fact that multiple barriers exist, several of which being "backup" barriers, provides further confidence that even if some barriers fail to perform as anticipated, overall goals would still likely be achieved. As long as most of the barriers perform approximately as projected, given today's understanding, it is safe to proceed with the development of Yucca Mountain, even if it turns out that several barriers do not perform as well as presently projected.

---

[4] A 'substantial' delay may be on the order of 10^4 years or longer since both EPA and NRC have proposed the time period of regulatory compliance be 10,000 years.

[5] A 'substantial' concentration reduction is arbitrarily assumed to be a factor of ten or larger.

1.2.3 "Natural" Barriers Alone Could Provide A Sufficient Degree of Safety

Some of the analyses presented in this report very pessimistically assumed that the function of each of the three major "engineered" barriers was completely "neutralized". In this analysis, it was assumed that:

- The drip shields did not prevent groundwater from dripping directly onto the top of the emplaced waste packages;
- The containers did not prevent groundwater from dripping directly onto the used nuclear fuel assemblies containing the waste form; and
- The cladding in the assemblies surrounding the waste form did not prevent groundwater from dripping directly onto the waste form.

Thus, it was assumed that any groundwater entering the tunnels could drip directly onto the waste itself.

The analysis was performed on only a single scenario in which it was assumed that the conditions of the rock were such that dripping into the tunnels could occur, the "maximum likelihood 'wet' branch".[6] Figure 1-8 shows the annual dose to the RMEI for this single scenario for two cases. The solid line shows the case for which the functions of the drip shield and container have been "neutralized". The dashed line is the case for which the function of the cladding was neutralized as well. The "double hump" in the curve for the case where all three engineered barriers is neutralized is caused by the more rapid movement through the natural system of some of the radionuclides (specifically ^{99}Tc and ^{129}I) compared to others (generally, the major actinides).

While dose rates are higher and earlier for these cases in which the major engineered barriers are "neutralized", it can be seen that the peak annual RMEI dose is still less than about 100 (10^2) mrem. This is less than the annual dose received from natural radiation sources. *This suggests that the natural barriers* ***alone*** *can provide an adequate degree of protection to future members of the public in the extremely unlikely event that all three of the major engineered barriers completely fail immediately after the repository is closed.*

---

[6] Actually, there is a high probability that the natural conditions of the rock will be such that dripping of groundwater into the tunnels would not happen. Thus, using the assumption that it does is even more pessimistic.

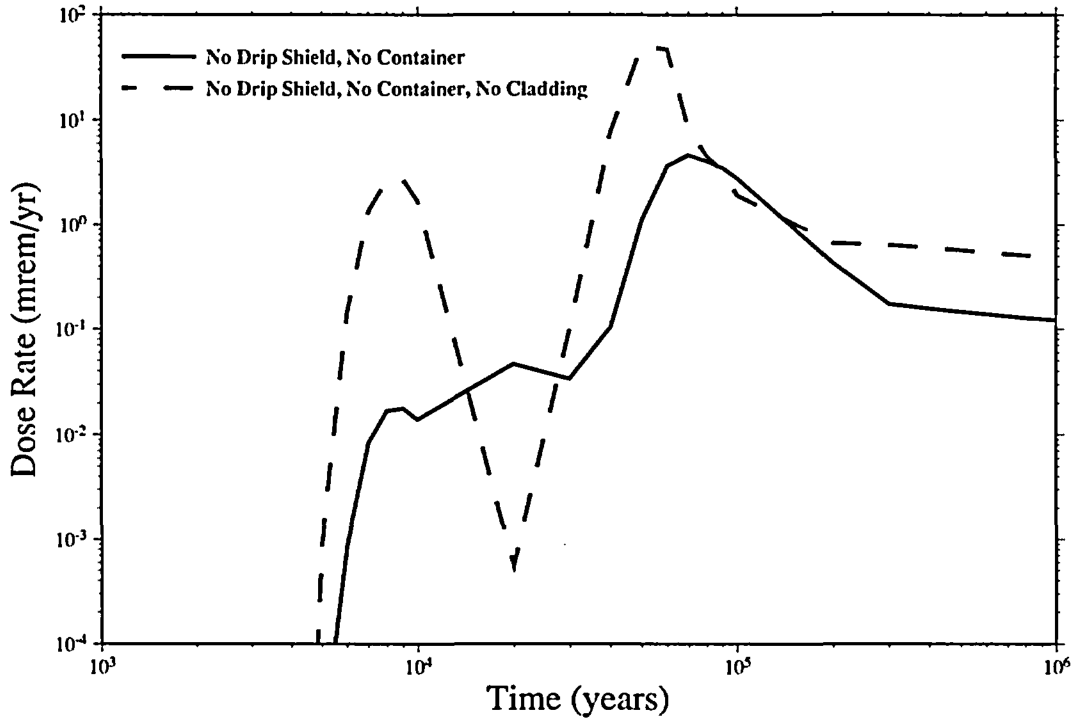

Figure 1-8
Annual Dose from the Maximum Likelihood "Wet" Branch Assuming the Drip Shield, the Waste Container, and Cladding Barriers are All Neutralized

For the reasons outlined above, there is a high degree of confidence that it is appropriate to proceed to the next stage of Yucca Mountain repository development.

The following chapters describe in more detail the basis for the conclusions presented in this chapter, and present analyses that provide significant additional insight.

2

INTRODUCTION TO IMARC PHASE 6

Significant resources and effort have been expended by EPRI over the past few years in modeling and understanding issues related to high-level radioactive waste disposal. Previous reports (EPRI, 1990; 1992; 1996; 1998; 2000) have documented the general model used in the EPRI work and specific inputs to that model for examination of the potential repository at Yucca Mountain, Nevada. Modeling of the potential Yucca Mountain site is an on-going process, and new data are being collected with which to evaluate and modify models of physical processes.

There are several purposes of the current report. The main purpose of this report is to describe the subsystem and total system performance models and present results and analysis of the results. The evaluation is based on the DOE's current design, which was first presented in DOE's Site Recommendation Characteristics Report (SRCR), although a few modifications to the design have been made since then. This design is called a 'line-loading' of the waste packages in the emplacement drifts. As is seen in Figure 2-1, this allows the emplacement drifts to be spread apart. The separation distance provides a shedding zone where mobilized moisture can drain. Figure 2-2, provides a look inside of the emplacement drifts. The design has a waste package spacing of 0.10 meters, a waste package with an outer shell of Alloy 22, a waste package pallet also made of Alloy 22, a drip shield to preclude dripping water on the waste package, an invert design that allows moisture to pass through, and a drift support system that is not continuous.

The first part of this report describes the new EPRI model, labeled 'IMARC (Integrated Multiple Assumptions And Release Code) Phase 6'. The report also identifies the key technical components of the candidate spent fuel and HLW disposal facility at Yucca Mountain using IMARC Phase 6, and provides an assessment of the overall technical suitability of the candidate High Level Waste (HLW) disposal facility at Yucca Mountain.

A series of analyses for the 'normal release' scenario are conducted using IMARC Phase 5. The cases focus on a dose rate end point calculated over times scales that exceed the time of peak release into the accessible environment (biosphere), on the order of several hundred thousand years. Expert judgement is used to evaluate and select data from published sources. Recognizing both current uncertainties and, in some cases, paucity of data, emphasis is placed on selection of "best estimate" values, with higher and lower values representing conservative bounding values. In certain areas, alternative conceptual models are compared as to their impact on overall repository performance.

Many people have contributed to development and application of the EPRI model, and to its documentation in this report. Austin Long of the University of Arizona provided an analysis of the future climates and wrote the first part of Chapter 3. Stuart Childs of Kennedy Jenks, Inc. provided the input to IMARC-6 related to net infiltration. Our net infiltration model is unchanged from that presented by Stuart in Chapter 3 of IMARC-5 [EPRI, 2000], so is simply summarized at the end of Chapter 3. The IMARC-6 model for thermohydrologic effects and percolation rates into the repository drifts is presented in Chapter 4, and was prepared by Benjamin Ross of Disposal Safety, Inc. Ben models repository conditions with respect to repository temperature, the fraction of the repository assumed wet, and flow rates through the "wet" portions as a function of time. The containment barrier system model was developed and documented in Chapter 5 by David Shoesmith of University of Western Ontario and John Massari. A summary of the somewhat revised model of the source term, along with updated information on elemental solubilities and corrosion product sorption coefficients was documented (Chapter 6) by Michael Apted, Wei Zhou, Matt Kozak, and Randy Arthur of Monitor Scientific LLC. Chapter 7 includes a brief review of the flow and transport models developed by Ed Sudicky of Groundwater Simulations Group, as well as some relevant sensitivity studies on important saturated zone properties. Frank Schwartz, from Ohio State University, also provided updated estimates of hydrologic parameters in Chapter 7. The biosphere dose model used to estimate doses has been significantly revised in IMARC-6. The biosphere model was developed by Graham Smith and others from QuantiSci, Ltd. This model was summarized in Chapter 8.

Chapter 9 describes the overall structure of the IMARC Phase 6 model and how the subsystem models are integrated. This chapter also provides a general discussion of the assumptions and expert judgment that went into the development of the models. Chapter 9 was written by John Vlasity of Risk Engineering, Inc. The IMARC Phase 6 calculations were performed at Risk Engineering by John Vlasity. They are reported by John Kessler and John Vlasity in Chapter 10.

Finally, Appendix A includes a discussion of possible approaches to defense-in-depth. This appendix was prepared by Michael Apted of Monitor Scientific.

All of these contributors have helped develop the current version of the EPRI model over the past few years, and any measure of success that this model has in providing insights and guidance regarding repository issues is due to their hard work, imagination and cooperation.

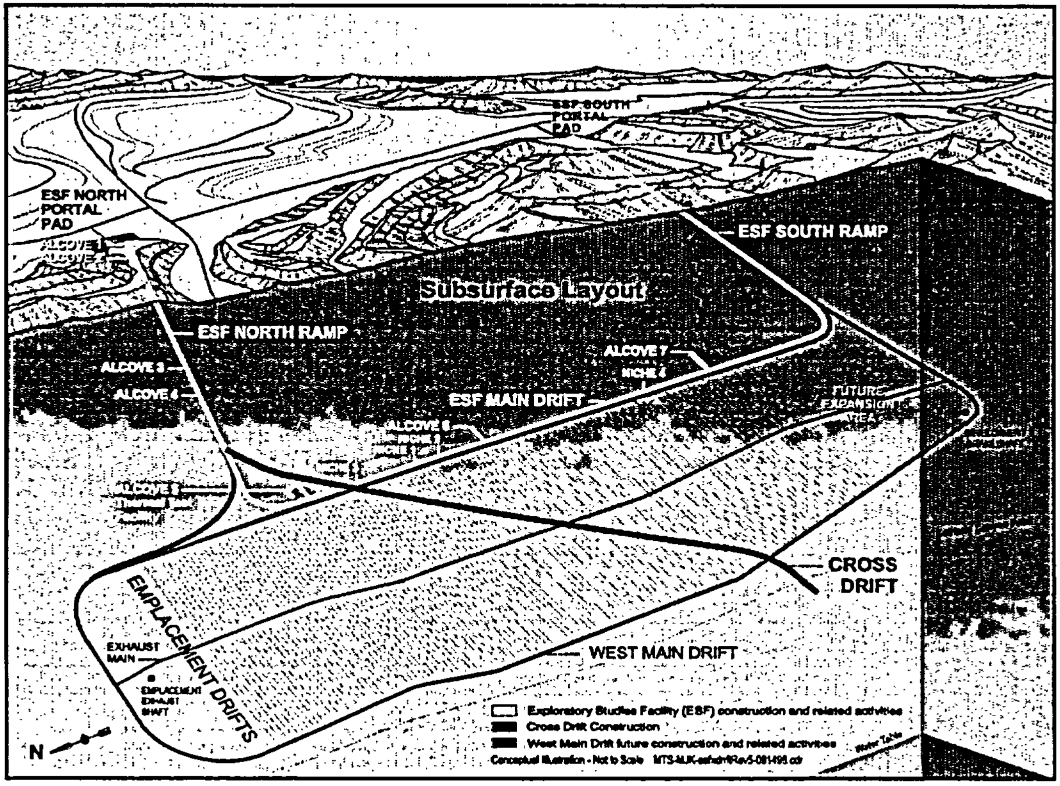

Figure 2-1
Proposed Repository Layout and Test Facilities

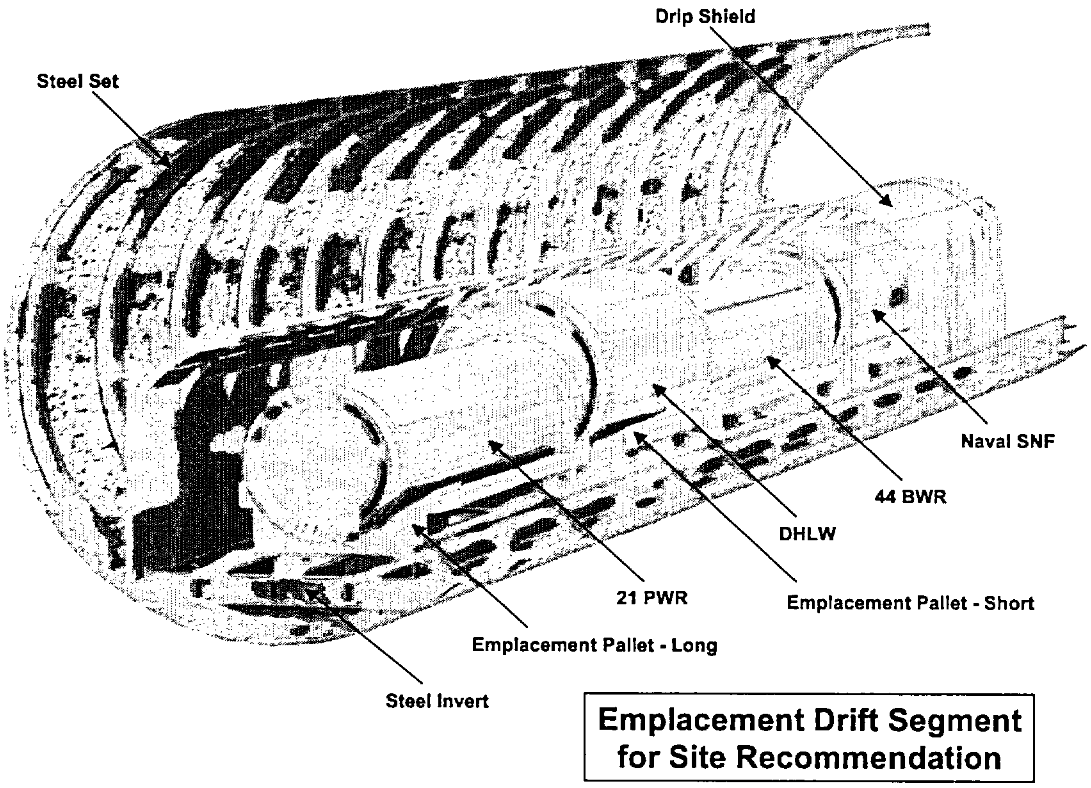

Figure 2-2
Site Recommendation Characteristics Report, Drift Configuration

2.1 References

CRWS M&O (2000). Drift Scale Thermal Analysis. CAL-WIS-TH-000002 Rev. 00.

EPRI (1990). *Demonstration of a risk-based approach to high-level waste repository evaluation*, EPRI NP-7057, Electric Power Research Institute, Palo Alto, October.

EPRI (1992). *Demonstration of a Risk-Based Approach to High-Level Waste Repository Evaluation: Phase 2*, EPRI TR-100384, Electric Power Research Institute, Palo Alto, May.

EPRI (1996). *Yucca Mountain Total System Performance Assessment, Phase 3*, EPRI TR-107191, Electric Power Research Institute, Palo Alto, December.

EPRI (1998). *Alternative Approaches to Assessing the Performance and Suitability of Yucca Mountain for Spent Fuel Disposal*, EPRI TR-108732, Electric Power Research Institute, Palo Alto CA, November.

EPRI (2000). *Evaluation of the Candidate High-Level Radioactive Waste Repository at Yucca Mountain Using Total System Performance Assessment: Phase 5*, Report number 1000802, EPRI, Palo Alto, CA, December.

3

FUTURE CLIMATE AND NET INFILTRATION

3.1 Future Climate – Summary of Model

The basic climate types adopted in the previous IMARC analyses [EPRI, 2000] have been maintained. We reject the "monsoon" climate proposed by the M&O, but maintain that a "greenhouse" climate, as described in EPRI [1998] will begin almost immediately. Given the above analysis, it may be that the greenhouse climate will continue for hundreds to perhaps 1,000 years. Since the IMARC code has initial time steps of 1,000 years we therefore assume that the "greenhouse" climate begins at the time of repository closure and continues for 1,000 years. From 1,000 to 2,000 years it is assumed there is a return to a climate state similar to that experienced by Yucca Mountain today, termed the "interglacial" state in EPRI [1996; 1998].

The climate scenario we choose still preserves the basic notions that:

- Greenhouse effects are, indeed, likely to occur for some time into the near future;
- Interglacial (present day) climates are the exception rather than the norm; and
- Glacial climates will predominate in the future, as they have over the past million years or so.

Consequently, we continue to use the following climate scenario without exception [EPRI, 2000]:

- 0 to 1000 years postclosure: "greenhouse" climate as defined in EPRI [1996; 1998];
- 1000 to 2000 years postclosure: "interglacial" (present day) climate also as defined in previous IMARC analyses;
- beyond 2000 years postclosure: "full glacial maximum" as defined in EPRI [1996; 1998].

We have chosen this simplified climate because we found no huge changes in results from carrying along three different future climate scenarios. We also selected the "full glacial maximum" as the long-term climate because this conservatively supplies the highest net infiltration rates resulting in the highest estimated future dose rates.

3.2 Brief Review of the DOE Climate Model

3.2.1 Summary of the DOE Model

The DOE Total System Performance Assessment (TSPA) model documentation is comprehensive in scope and vast in size. It considers all aspects of the potential hazards to the human environment related to emplacement of high-level radioactive waste (spent fuel rods) in Yucca Mountain.

The DOE TSPA considers two time ranges: present to 10,000 years, and 10,000 to 100,000 years. In the case of past climates, the ranking hypothesis is that changes in major climate modes were driven by rhythmic changes in solar insolation onto the Earth. The TSPA assumes that these solar-terrestrial forcing factors will continue into the indefinite future. Past global climate variations are recorded in stable oxygen isotope variations marine sediment fauna carbonate and in groundwater-deposited vein-fill carbonate at a site close to Yucca Mountain, Devil's Hole, Nevada. Climate variations are also recorded in microfaunal species variations in lake and bog deposits. All of the deposits are well-dated radiometrically, thus providing a firm time base.

The timing and generally the magnitudes of past climates inferred from the stable isotope variations near Yucca Mountain and in marine and lake deposits are generally consistent in timing and in magnitude with inferred past climates in other parts of the Earth, thus are evidently global in nature. The dominant hypothesis explaining the similarity of proxy climate inferrences is that global climate changes are driven by regular, systematic variations in the angle and intensity of insolation on the Earth caused by the different periods of the Earth's orbital parameters (eccentricity or Earth's elliptical orbit about the Sun), obliquity of the orbit, and precession of the Earth's rotational axis. This concept of the forcing factor in past climate changes is well entrenched in the literature.

The DOE TSPA assumes that inasmuch as this Earth-orbital hypothesis well explains the past climate changes, it will continue to dominate future climate changes. Correspondingly, the future pattern of changes in temperature and precipitation will match those of the past.

The next step in establishing the future temperature and precipitation at Yucca Mountain taken in the DOE TSPA is to identify present-day analogs to past and proposed future climate modes. The primary link from the past to the future is by means of micropaleontology. Fossils, particularly the various ostracode species and species assemblages, are climate sensitive. Thus, if an assembly of fossil species living today is restricted to certain climate constraints, those climate constraints can be assumed to apply to the past. It is therefore possible to designate the past climate constraints on fossil microfossils found in dated cores drilled in lakes and bogs. Fossil pollen in sediments can likewise indicate climate-sensitive trees and other plants grown nearby in the past. Based on the climate conditions required by the dominant species at particular times in the past near Yucca Mountain, the DOE TSPA divides the major past and future climate modes into 5 categories: Interglacial (present-day), Monsoon and Intermediate for the next 10,000 years; Interglacial, Intermediate/Monsoon, Glacial and Intermediate for the following 10,000 to 1 million years. This sequence repeats with a 400,000-year periodicity.

The TSPA future climate reports do not attempt to quantify the probability of a near-future climate change, such as global warming resulting from industrial carbon dioxide emissions: "Unanticipated, unknown, and unmeasurable future events and human-induced (anthropogenic) can be considered, but cannot be predicted." [TDR-MGR-MD-00000 REV 00, 2001]

TDR-CRW-GS-000001 details the proposed future climate sequence for Yucca Mountain for the next 10,000 years:

Modern-like climate would last for the next 400-600 years

The monsoon climate extends for the following 900-1400 years

The glacial transition interval for the following 8700 years

Table 3.3.1-1 [TDR-MGR-MD-00000 REV 00, June 2001] shows mean, upper bound and lower bound annual precipitation for the three future climate stages during the next 10,000 years.

Table 3.3.1-2 [TDR-MGR-MD-00000 REV 00, 2001, June 2001] shows mean, upper bound and lower bound temperatures for the three climate stages.

The values show little or no differences within each climate mode.

Table 3.3.1-3 [TDR-MGR-MD-000007 REV 00, 2001, June 2001] shows the timing of climate stages from 10ka to 1 million years in the future. This includes climate changes induced by an additional Earth orbital cycle with a periodicity of 400,000 years. Climate states added for the extended time frame are "Intermediate Monsoon", "Glacial", and "Intermediate Monsoon".

3.2.2 Reviewer's Comments on the Current DOE Climate Model

The future climates proposed in the TSPA and highlighted here are fully documented and clearly the result of a collaboration involving knowledgeable scientists. Attempts to infer future climates are always fraught with uncertainties, and simplifications are often necessary. This review suggests a few areas of improvement that may make some differences in the modeled net infiltration.

With the exception of the near future, the next 500 to 1000 years, the DOE TSPA climate model is acceptably broad. The model has wide upper and lower bounds for annual precipitation, ranging over a factor of 2 in the Monsoon and Glacial phases.

This review suggests a few areas of improvement that may make some difference in the near-future modeled infiltration.

Differentiate Seasonality of Precipitation.

Less comprehensive is that the DOE TSPA model presents only average annual precipitation, it may be missing the fact the nature of evapotranspiration in the Yucca Mountain vicinity may differ significantly between winter and summer. In the Southwest US winter precipitation events tend to extend over longer time periods than in summer. Also in winter, evapotranspiration is likely to be less in winter, allowing for possibly higher net infiltration.

Probability of Anthropogenic Climate Modification

This is another aspect of the TSPA climate model that has not been included. Although the degree to which anthropogenic pollutants will affect future climates is stated as "unpredictable" (TDR-MGR-MD-0000-REV00), the non-zero probability that it will affect future climates should not be ignored. An assembly of climatologists (Intergovernmental Panel on Climate Change, http://www.ipcc.ch/) released their 3rd report in 2001. The 3rd report includes documentation of recent data indicating anthropogenic climate change, which if it continues as models predict, will impact global climate, most notably warming, for several hundred to a thousand years (see, for example, *Consequences*, Vol. 4, no. 1, 1998).

Greenhouse-Driven Increase in El Nino frequency and Intensity.

A high-resolution sea-surface temperature model (Timmermann *et al. Nature*, 22 April 1999) predicts a 3-4 K sea-surface temperature rise by AD 2100 for a "business as usual" carbon dioxide emissions scenario. Such a rise would increase sea-surface evaporation and induce more frequent and more intense El Niño rainstorm events. The likely consequence for Yucca Mountain is greater net infiltration.

3.2.3 Summary

The DOE TSPA infiltration module for Yucca Mountain would be more comprehensive by considering the following:

- The seasons of the year have different temperatures and precipitation modes. Thus treating them separately could alter the net infiltration.
- The probability of near-future anthropogenically induced climate change is not zero, and can be treated probabilistically. More frequent and more intense summertime storms may persist for several hundred years after closure.
- The Yucca Mountain area is particularly prone to El Niño-type weather patterns and storms, which may increase during the next several hundred years.

3.3 EPRI Net Infiltration Calculations

EPRI's net infiltration modeling has not changed since Phase 4 [EPRI, 1998]. We use a "high", "moderate" and "low" values of net infiltration that are averages across the entire repository. These are summarized in Chapter 9.

3.4 References

EPRI (1996). *Yucca Mountain Total System Performance Assessment, Phase 3*, EPRI TR-107191, Electric Power Research Institute, Palo Alto, December.

EPRI (1998). *Alternative Approaches to Assessing the Performance and Suitability of Yucca Mountain for Spent Fuel Disposal*, EPRI TR-108732, Electric Power Research Institute, Palo Alto CA, November.

EPRI (2000). *Evaluation of the Candidate High-Level Radioactive Waste Repository at Yucca Mountain Using Total System Performance Assessment: Phase 5*, Report number 1000802, EPRI, Palo Alto, CA, December.

4

THERMOHYDROLOGY AND SEEPAGE

4.1 Introduction

Because the Yucca Mountain repository will be located in the vadose zone, water will be present in both liquid and vapor phases and migration can occur in either phase. This migration will be strongly affected by the presence of the repository. Two principal features of the repository that will change water flow are the heat output of the waste and the presence of excavated drifts.

Heat produced by decay of spent fuel will perturb subsurface conditions at the Yucca Mountain repository. Water will condense or evaporate as temperatures change and as fluids flow across temperature gradients, and the combined effects of evaporation, condensation, and convection create a system in which fluid flow and heat transfer influence each other reciprocally. The study of coupled flow and heat transfer phenomena in the subsurface is referred to as thermohydrology.

Openings in unsaturated rock also perturb moisture movement. In the vadose zone, capillary forces tend to pull water into smaller openings. This "capillary barrier" effect will tend to exclude water from the drifts, and thus will reduce the contact between spent fuel and water. Only to the extent that the capillary barrier is overcome will water seep into the drifts.

This chapter explores the thermohydrologic and seepage behavior of the Yucca Mountain repository and the computer models that the DOE is using to simulate thermohydrologic processes. These processes are complex in Yucca Mountain, where the rock contains both fractures and small pores, and fluids behave differently in the two kinds of openings. These phenomena had been studied very little before the Yucca Mountain project began, and DOE has made a significant commitment to research on the relevant science as a basis for repository design and performance assessment.

In the last year, DOE has continued to make progress in understanding thermohydrologic and seepage processes at Yucca Mountain and in developing computer models to simulate repository behavior. Areas where new information has significantly altered previous conclusions, or where the DOE has addressed new phenomena, include:

- **Focused flow** - Downward water flow is distributed non-uniformly in the rock, creating localized concentrations of water, potentially overcoming capillary barrier effects that otherwise can exclude water from the drifts. DOE has refined its modeling of this phenomenon.
- **Episodic flow** - Water can flow discontinuously in fractures; the DOE has developed a new model of this process.

- **Ventilation efficiency** - A new model of heat transfer during ventilation suggests that, for a given rate of air flow, more heat may be removed from the repository than previously believed.

The design of the repository has also evolved in the last year. The principal changes that affect thermohydrology are:

- **Increased ventilation rate** - The throughput of ventilation air has increased.
- **Low temperature operating mode** - Until recently, all repository designs led to drift temperatures that rise above boiling for some period of time. An alternative design concept has been introduced in which temperatures are held below boiling.

In this chapter, we critically review new thermohydrologic and seepage analyses by the Yucca Mountain project. From these results, we abstract values and probabilities for thermohydrologic and seepage parameters entering the IMARC model.

The first section of the chapter addresses new scientific analyses. The second section discusses design changes and alternate design concepts. The final section presents a newly emerging design concept that rests on the evolving scientific understanding of heat transfer during ventilation.

4.2 New DOE Scientific Analyses

Capillary barrier effects tend to exclude water from open cavities in the unsaturated zone, making it possible for waste packages to remain dry despite the presence of water in the rock above them. Because most waste package degradation mechanisms require the presence of water, repository performance depends on the fraction of the total number of waste packages that get wet, referred to as the seepage fraction.

The seepage fraction depends, of course, on the amount of water percolating through the rock. Using detailed statistical models of water flow in unsaturated fractured rock, the DOE has developed curves relating the seepage fraction to the instantaneous local percolation rate. The seepage fraction is read off the curve as a function of the instantaneous local percolation rate.

The instantaneous local percolation rate may differ from the average percolation rate due to variability in space (referred to as flow focusing) or time (referred to as episodic flow), or due to excavation-induced concentration of flow near drifts. The instantaneous local percolation rate is calculated by multiplying the average percolation rate by enhancement factors reflecting these three processes.

The DOE has developed revised or new scientific models of each element of this calculation. Our evaluation of the new DOE work and resulting changes to the IMARC model are discussed in this section.

4.2.1 Curves of Seepage Fraction versus Percolation Rate

The DOE has recalibrated its model of seepage into drifts to reflect new experimental data. The results of the recalibration are curves of seepage fraction and seep flow rate as functions of local percolation rate. The new curves, derived from Table 4.3.1-1 of the SSPA, are shown in Figures 4-1 and 4-2. For any value of percolation rate, there are triangular probability distributions of seepage fraction and seep flow rate. Each of these two probability distributions is defined by three values, the minimum, peak (corresponding to the apex of the probability distribution), and maximum values.

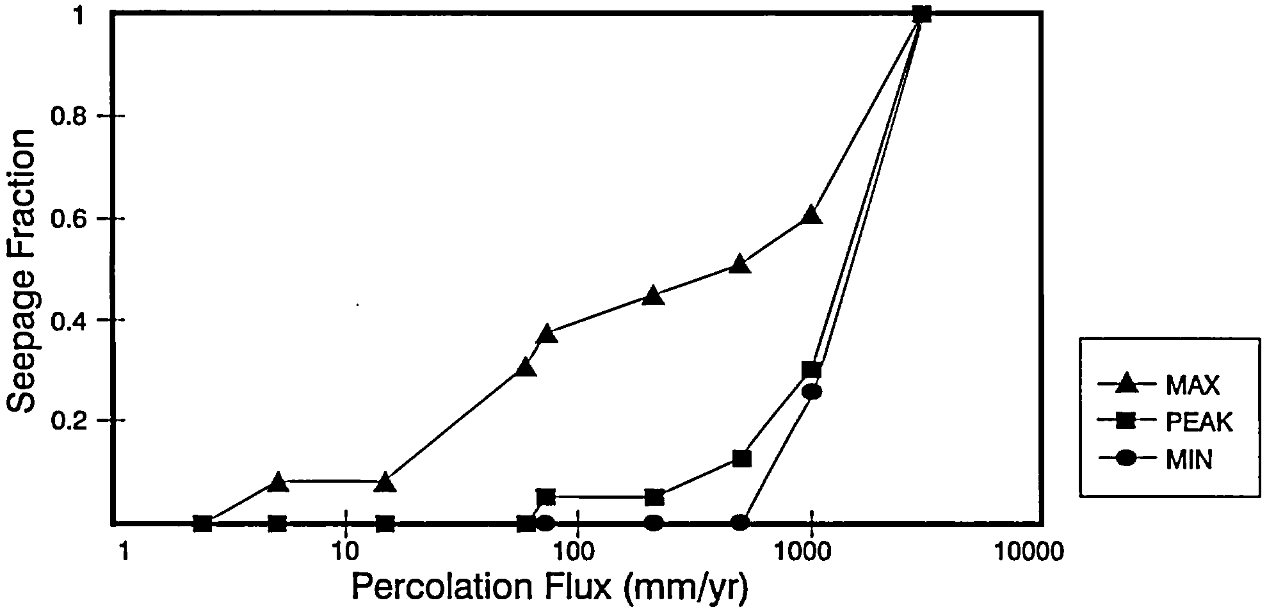

Figure 4-1
Seepage Fraction as a Function of Percolation Flux.

The main change from the previous values (shown in Figures 4-4 and 4-5 of the IMARC-5 report) is a shift to the right of the curve showing peak-probability seepage fraction as a function of percolation rate. The main reason for this shift is incorporation of data from the lower non-lithophysal unit, a horizon where a large portion of the repository will be built. The minimum and maximum curves are little changed.

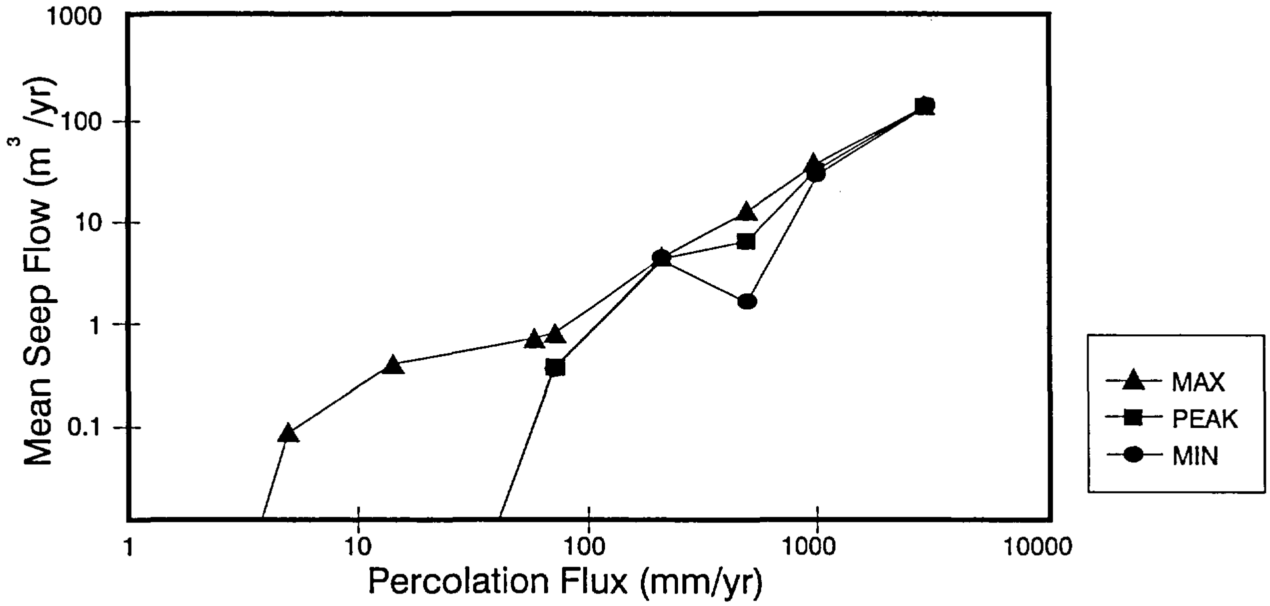

Figure 4-2
Mean Seep Flow Rate as a Function of Percolation Flux.

4.2.2 Flow Focusing

In the "active fracture" model of water flow through unsaturated fractures, water flows only in portions of the fracture network. This model has implications for seepage into drifts. The amount of water impinging on the top of a drift will tend to be greater than the average percolation flux in the area of active fractures and less elsewhere. This may cause the local percolation rate, which determines the seepage fraction, to differ from the average percolation flux.

This phenomenon is captured in the models by a "flow focusing factor", F, which is the ratio between the local flux in the wet areas and the average flux. For simplicity, the flow focusing factor is defined so that all flow passes through the wet areas — for example, if the flow focusing factor is 4, the flux is 4 times average in one quarter of the area, and zero elsewhere.

The DOE has developed a new probability distribution for the flow focusing factor. This was done by conducting finely gridded simulations of flow in two dimensions with heterogeneous fracture permeability [SSPA, p. 3-10]. The results indicated that F was usually less than 3 and always less than 6. Based on these simulations, the Yucca Mountin projected adopted a new distribution of the flow focusing factor: a declining exponential function with a minimum value of 1 and a mean value of 2. Mathematically, this distribution is

$$p(F) = e^{1-F} \qquad \text{for } F > 1 \tag{4-1}$$

This distribution was considered to be a conservative bound on the simulation results.

The IMARC model requires a set of discrete values for each uncertain parameter rather than a continuous curve of probability density. The discrete values were selected by noting that the seepage fraction becomes greater than zero only for local percolation rates greater than 60 mm/yr. For the baseline infiltration rate of 19.6 mm/yr under glacial climate conditions, this implies that seepage will occur only if the flow focusing factor is greater than 3. We therefore divided the probability distribution into one bin for F less than 3 and a second bin for F greater than 3. The probability that the factor will be greater than 3 is

$$\int_{3}^{INFINITY} e^{1-F}dF = \frac{1}{e^{2}} = 0.135 \qquad \text{4-2}$$

The average value of F for this part of the distribution is

$$\frac{1}{F^{2}} \int_{3}^{INFINITY} F e^{1-F}dF = 4 \qquad \text{4-3}$$

The remainder of the distribution was assigned a flow focusing factor of 1, representing no significant flow focusing, and had a probability of 0.865.

4.2.3 Episodic Flow

Experimental studies of unsaturated-zone flow show that water movement often varies in time, with intervals of intermittent flow interspersed among periods with little water movement. If such episodic flow occurs, the local percolation rate during the periods of flow will be greater than the average over time. The ratio of the percolation rate during the flow period to the average percolation rate is called the "intermittency factor". To an even greater degree than flow focusing, intermittent flow if it were to occur, would tends to cause an increase in seepage.

In an effort to quantify this phenomenon, the Yucca Mountain Project has analyzed one mechanism of such intermittent flow. This is the accumulation of water above an asperity due to capillary barrier effects. If a narrow pore zone created by the asperity opens into a wider cavity as shown in Figure 4-3(a), water will not flow into the larger cavity until a sufficient head of water collects above the asperity to overcome the capillary pressure at the outlet. When water accumulates to a certain height, referred to as the "capillary rise", it will break through into the larger cavity below and quickly drain. Unpublished two-dimensional analyses of this situation by C.H. Ho are summarized in Section 3.2.2.4 of the SSPA. Based on Ho's calculations, a log-uniform distribution of intermittency factors between 1 and 10^{4} is recommended in the SSPA.

Real fracture asperities will, of course, have a variety of geometries. One alternative is shown in Figure 4-3(b). Flow through a constriction of this form has been analyzed by Dullien [1992, Eq. (2.3.1)]. Dullien shows that the amount of capillary rise depends on the angle of the opening, 2φ, and the contact angle of water and rock, θ. If $\varphi+\theta$ is less than 90°, there will be no capillary rise at all. The situation analyzed by Ho is $\varphi+\theta=180°$. If $\varphi+\theta$ is between 90° and 180°, the capillary rise will be less than in the Ho case by a factor of $\cos(\varphi+\theta)$.

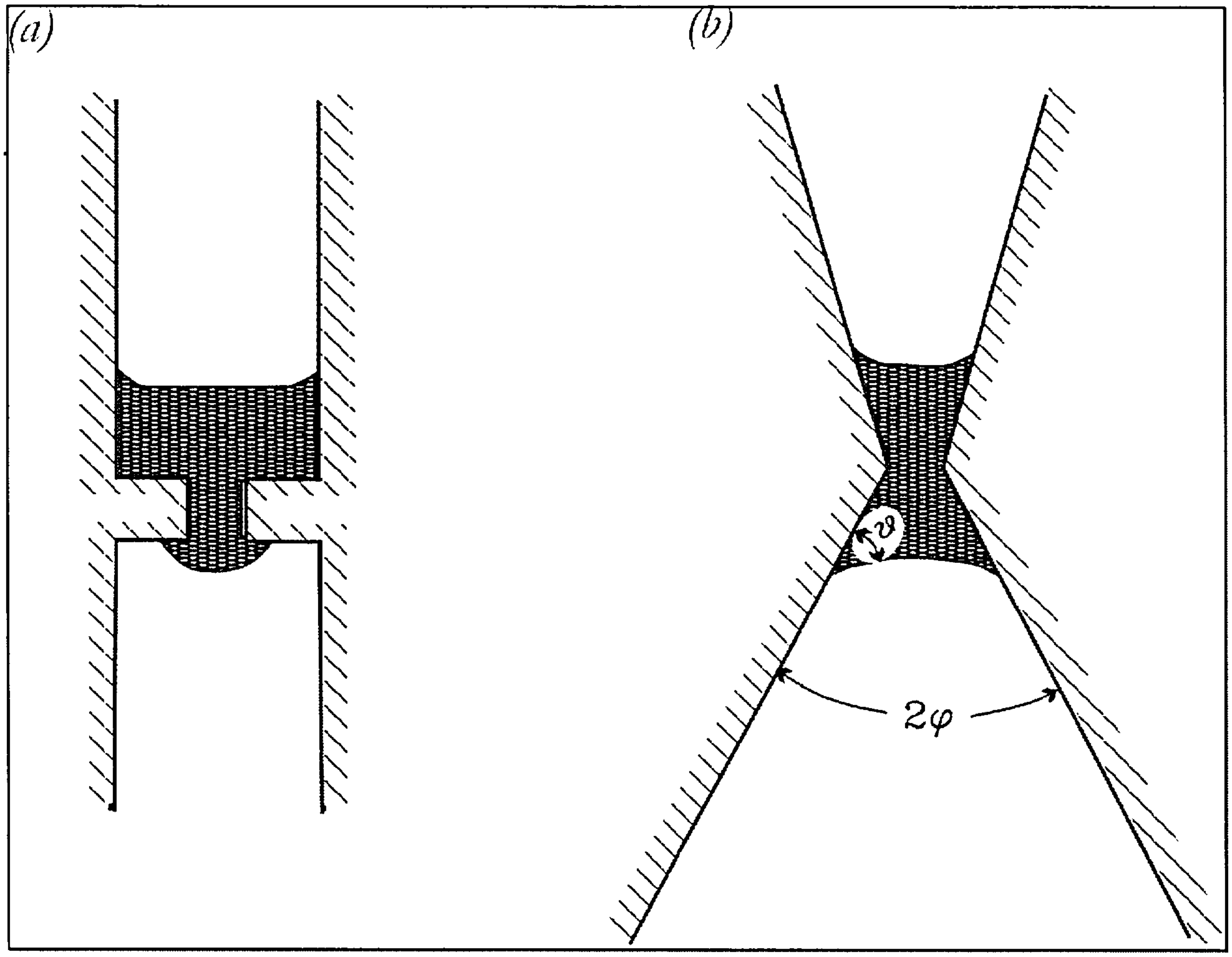

Figure 4-3
Alternative Conceptual Models of Fracture Asperities

Because fracture apertures are very small compared to the other two dimensions of the fracture, f will ordinarily be small. Furthermore, in a two-dimensional fracture, constrictions ordinarily will have some horizontal extent. The quantity f will generally vary across the constriction. It will be easiest for the water to move downward at the point where f is smallest (that is, the point where the fracture is narrowest beneath the pinch). Once water begins to drain, it will drain from the entire reservoir, and therefore the smallest value of f will determine the magnitude of the capillary rise.

If, as is believed to be the case at Yucca Mountain, the rock is water-wetting, ? will be less than 90°. With f small, f+? will then be less than 90°, and there will be no capillary rise. Based on this reasoning, the intermittent flow factor discussed in the SSPA has not been included in the IMARC model.

4.2.4 Drift Degradation and Rock Bolts

The DOE has conducted further studies of seepage enhancement as a result of drift degradation and rock bolts. These studies, discussed briefly in Section 3.2.2.5 of the SSPA, "show that there is probably no significant increase of seepage because of drift degradation or the presence of rock bolts."

This result is consistent with the current conceptual understanding of unsaturated zone water flow. Water flowing in fractures either is guided by capillary forces, or runs down the fracture in a localized "active fracture" zone. In the former case, capillary forces attract water to the narrowest part of the fracture; in the latter case, fracture aperture has little influence on water movement. In neither case would creation of larger openings as a result of drift degradation or drilling of rock bolt holes lead to a significant increase in water flow.

The DOE seepage abstraction model has nevertheless retained a 50% increase in seep flow rates to account for drift degradation, on the basis that it will make little difference to performance assessment results. This conservatism has not been included in the IMARC model.

4.2.5 In-Drift Condensation

On entry to the ECRB (east-west test drift), regions have been observed with water droplets hanging from various surfaces. These water droplets are believed to have been formed by evaporation of water from the rock matrix and subsequent condensation within the drift, but all conclusions about this water are preliminary because very few measurements of this water have as yet been reported and the mechanisms driving condensation have not yet been elucidated.

Given these uncertainties, it is too early to tell whether such condensation might occur in the repository. Therefore, in-drift condensation has not been included in the baseline IMARC model as a source of seepage onto waste packages. However, to begin assessing the possible implications of this observation, a sensitivity analysis has been done to see the consequences if 25% of waste packages are wetted by condensate.

4.3 Design Changes

The most significant development in repository design, as far as thermohydrology is concerned, is the introduction of an alternative approach to repository thermal design. This approach is the "low temperature operating mode" or cool repository.

To date, performance assessments for the Yucca Mountain repository have been based on designs in which the temperature of the drifts rises above boiling for hundreds or thousands of years. The SSPA introduces a new design concept, referred to as the low temperature operating mode. In this concept, the maximum temperature of the waste packages is near or below 85°C. The SSPA describes five different design approaches to reduce temperature, involving various combinations of decreased areal mass loading, extended ventilation, and surface aging of the waste.

Even the hot repository has a zone in the pillars where temperatures stay below boiling at all times. Experimental studies indicate strongly that water mobilized by high temperatures will drain through such a zone rather than accumulate above a boiling zone [IMARC-5 Report, Section 4.1.3.1]. These experiments have been incorporated into the DOE and IMARC seepage models, leading to the conclusion that the seepage rate differs between hot and cool repository concepts only during the period beginning after closure and ending when the hot repository cools below boiling. When the temperature of the hot repository is above boiling, seepage is zero from the hot repository. When the temperature is below boiling, seepage is independent of temperature.

The potential of coupled thermal-hydrological-chemical interactions to plug fractures and thereby affect seepage has been the subject of much discussion. Fracture plugging is of much less concern in unsaturated rock than it would be below the water table, because water drainage is localized in a small fraction of the total fracture area. If minerals precipitate in the area where the water drains and block the drainage path, the water can simply move around the plug. Furthermore, plugging is less likely if the temperature stays below boiling because water evaporation will be slower and may not go to dryness.

Thus, in current performance assessments, the temperature influences repository performance primarily through its effect on corrosion rates rather than by mobilizing water.

4.4 High Efficiency Ventilation

Ventilation can affect repository performance even beyond the period of ventilation. The heat load applied to the rock will be reduced by the amount of heat removed in ventilation air. Temperature will therefore be sensitive to the duration and thermal efficiency of ventilation. This section describes current uncertainties in heat removal by ventilation and explores the implications of these uncertainties for repository design and licensing strategies.

4.4.1 Models of Ventilation Heat Removal

In principle, the duration and thermal efficiency of ventilation are controllable parameters. The duration and the air flow rate can, within limits, be varied by repository operators. However, the relationship between air flow rate and ventilation efficiency is not well understood. This relationship is difficult to simulate because it involves several kinds of non-linear heat transfer (conductive, convective, and radiative) in the tunnels; sharply contrasting air flow regimes (turbulent pipe flow in the tunnel and porous-medium seepage in the rock); and dual-porosity flow of vadose-zone moisture, all in a complex three-dimensional geometry. These complications cannot be accomodated in a repository thermal model; it is necessary to run a separate ventilation model to determine the ventilation efficiency and adjust the thermal load downward accordingly in the repository-scale model.

In the Total System Performance Assessment, the Yucca Mountain project did thermal analyses for two ventilation cases. In these analyses, ventilation efficiency was assumed to be 70% for a ventilation duration of 50 years and 80% for a duration of 300 years.

These values are based on calculations with the ANSYS code. This model treats convective heat removal by dry air flowing in the tunnels, with conductive heat transfer in the rock, and does not consider latent heat. Assumptions and parameter values in the ANSYS code were selected to be conservative — that is, to err on the side of underestimating the amount of heat removed.

More recently, a second, more elaborate, ventilation model has been developed. This model, called MULTIFLUX, includes latent heat in the tunnel and moisture movement in the rock. Gas and moisture movement in the rock is simulated with the NUFT code — also used for such calculations in LLNL's multiscale thermohydrologic model — which is coupled to a lumped parameter ventilation simulator. The two models also make different assumptions about such parameters as thermal conductivity and convective heat transfer coefficients for turbulent gas flow. A newer version of MULTIFLUX, which improves some of the physics and corrects errors found in the first version, is currently being tested. MULTIFLUX has much less built-in conservatism than ANSYS.

A series of ventilation cases have been simulated with both ANSYS and MULTIFLUX. Ventilation efficiencies predicted by ANSYS are considerably smaller than those predicted by MULTIFLUX. Table 4-1 compares the results of the two models. For comparison, the assumptions made in repository thermal analysis are shown in the last column.

Preliminary results of two quarter-scale ventilation tests suggest that ANSYS underestimates heat removal. ANSYS predicted 74% heat removal in both tests, but measured efficiencies were 83% and 86%. Simulations of these tests by MULTIFLUX are not reported.

The new ventilation modeling has brought to light an inconsistency in thermal analysis of current repository designs. Host rock thermal conductivity is uncertain. For a given heat input, lower thermal conductivity implies higher drift temperatures. The repository design is constrained by the need to keep temperatures within required limits even if rock thermal conductivity is low. But lower thermal conductivity also implies higher heat removal for a given rate of long-term ventilation, because heat transferred to the rock in early years will remain close to the drift where it can be removed by ventilation air in later years. In the current design basis, temperatures are calculated using a low thermal conductivity in the rock, yet the ventilation heat removal in the calculation is based on a high rock thermal conductivity. This yields an overconservatism; the calculated temperatures are higher than they would be if a high or a low thermal conductivity were applied consistently through the computation.

In summary, evidence suggests that ventilation efficiencies may be greater than predicted by ANSYS. Whether ventilation efficiencies will be as large as predicted by the first round of MULTIFLUX simulations is unclear as yet. The physical processes involved in ventilation heat removal are so complex that a sizable effort will be required to understand the differences between the two models and determine what the right answer is. Until this work is complete, the feasibility of achieving very high ventilation heat removal will be uncertain.

Table 4-1
Comparison of Modeled Ventilation Efficiencies (%)[a]

Duration (yr)	Air Flow Rate (m^3/s)	ANSYS	MULTIFLUX	Assumed in Thermal Model
50	10	68	91	70
50	15	74	94	
100	10	73	93	
100	15	78	95	
200	10	77	96	
200	15	82	97	
300				80

[a] Source: SSPA, Section 5.3.2.4.1

4.4.2 Relationship Between Efficiency and Duration of Ventilation

What would be the impact of very high ventilation efficiency on repository design, operation, and performance? The greatest effect would be on the low-temperature operating mode, because this design strategy relies on ventilation to remove enough heat to keep temperatures below boiling. In current concepts, extremely long periods of ventilation are required to attain this objective. How much time would it require to remove the same amount of heat with a greater ventilation efficiency?

The ANSYS results summarized in Table 4-1 indicate that with a ventilation rate of 15 m^3/s per drift, ventilation efficiencies in the range of 94% to 95% are achievable with ventilation periods of 50 to 100 years. The difference between the 70% to 80% ventilation efficiencies assumed in TSPA thermal modeling and 94% is much greater than appears at first glance. Ventilation with 70% heat removal efficiency leaves 30% of the heat in the rock, while 94% efficiency leaves only 6% — one-fifth as much.

The time dependence of the heat source further magnifies the significance of more efficient ventilation. During the first three hundred years after the end of repository operations, the dominant source of heat in spent fuel will be decay of cesium-137. The thermal output will decline exponentially with the 30-year half-life of this isotope. This exponential decline implies that most of the heat is produced in the first decades after closure.

In these circumstances, higher efficiencies greatly shorten the duration of ventilation needed to remove a given amount of heat. The Yucca Mountain Project has analyzed a low-temperature operating mode in which the repository is ventilated for 300 yr with 80% efficiency. Calculated maximum drift temperatures for this case are 90°C for the baseline rock thermal conductivity, or 95°C if the thermal conductivity is reduced to reflect the insulating effect of lithophysae (air-filled voids in the welded tuff). Thus, with the ventilation efficiencies predicted by ANSYS, centuries of ventilation are required to hold the maximum repository temperature below boiling.

As calculated in Appendix B, if the ventilation efficiency were 94%, consistent with the MULTIFLUX calculations, only 83 years of ventilation would be required to remove the same amount of heat. Thus improved efficiency greatly reduces the duration of ventilation required to remove a given amount of heat.

4.4.3 Implications for Design and Licensing

If the MULTIFLUX results are correct, the temperature constraint on high-temperature operation (70% heat removal is needed to keep pillar temperatures below boiling and allow condensate drainage) could be satisfied with a lesser flow of ventilation air, and a low-temperature operating mode could be achieved with a much shorter period of ventilation than believed heretofore. There would then be much less need for repository designs to "push the envelope" in order to meet operating and performance constraints. The door would open to concepts that provide more flexibility and a greater degree of defense in depth.

One example of a more flexible operating mode suggested by the MULTIFLUX results is a mode with the following characteristics:

- Line loading, with waste density as now envisaged for the high temperature operating mode, and a total emplacement area of 1150 acres.
- Planned duration of forced ventilation, at a rate of 15 m^3/s, approximately 80 to 100 years. (Modeling studies are needed to better determine the needed duration.) No credit taken for natural ventilation after forced ventilation ceases.
- Maximum drift wall temperatures below boiling.

As ventilation proceeds, new options would open for repository operators. If long-term monitoring of thermohydrology and waste package performance reveals that the design is based on overly conservative temperature constraints, significant cost savings could be obtained by turning off the ventilation early. On the other hand, if performance confirmation testing fails to support design basis assumptions, compensatory actions could be taken at the end of the planned ventilation period. For example, if ventilation does not remove heat as efficiently as predicted, or if long-term testing of waste package materials reveals the need for a lower operating temperature, either forced or ventilation could continue to yield lower temperatures.

Efficient heat removal would also facilitate retrievability of waste packages during the operational period.

Adoption of a flexible repository design based on highly efficient ventilation would have vast implications for repository licensing:

- The repository would be licensed in a low-temperature operating mode without the need to address the insitutional, geotechnical, and regulatory issues involved in ensuring that ventilation systems operate for more than a century.
- The repository could operate in low-temperature mode without going beyond the planned 1150-acre footprint.
- Defense in depth would be available to compensate for uncertainty in thermohydrologic processes. Extended ventilation beyond the planned period could compensate for unexpected problems.

Further modeling of ventilation is needed to determine the feasibility of a repository licensing strategy that relies on high-efficiency heat removal. But even before the uncertainties about ventilation are resolved, the implications of efficient heat removal need to be understood, at least in general terms, so that the program can prepare itself to take advantage of opportunities that may open up. This will allow the project to avoid premature commitments to strategies that could turn out to be suboptimal when ventilation efficiency is better understood.

4.5 Reference

F.A.L. Dullien, *Porous Media: Fluid Transport and Pore Structure*, 2d ed., Academic Press, San Diego, 1992.

5

ENGINEERED BARRIERS SYSTEM DEGRADATION

As the primary engineered barriers within the overall repository design, the design and fabrication of the drip shield/waste package combination can be adapted in attempts to reduce both the uncertainties inherent in natural geologic barriers and the uncontrollable features of barriers such as the wasteform. This adapability has led to the perception that the accumulation of uncertainties in performance in all pre- and post-waste package barriers can be dealt with by improving the design and durability of the waste package. As a consequence, the waste package tends to be viewed as the principal focal point for insuring the overall repository performance.

It is not surprising, therefore, that of the many performance issues of importance to the Yucca Mountain repository, the drip shield/waste package performance has received intense scrutiny and review. This last year two major panels were convened to review their performance, the Nuclear Waste Technical Review Board (NWTRB) International Panel, and the Waste Package Materials Performance Peer Review Panel convened for the U.S. Department of Energy by the Management and Operations organization, Bechtel SAIC. In very general terms both of these review panels concluded that, while the prospects for long term radionuclide containment with the present DS/WP design looked positive, a significant number of technical issues remained to be resolved. It should be noted that the Bechtel SAIC panel has only reported its preliminary findings and continues to review the issues.

In this section we describe the changes we have made to the model published in IMARC 5 (EPRI, 2000) to accommodate the primary issues raised by these reviews and by other deliberations on DS/WP performance which have occurred since that model was published. In particular, we have revisited the issues of localized corrosion, the temperature-dependence of both localized and general passive corrosion, and the possible consequences of a significant groundwater fluoride concentration. The persistence of these issues reflects the continuing uncertainties in specifying, with any degree of quantitative confidence, the nature of the environments to which the DS/WP will be exposed. Consequently, as a prelude to describing our model and the rationale behind the selection of specific parameter values, we briefly review the present state of understanding of anticipated exposure environments.

The primary purpose of our model, as in IMARC 5 (EPRI, 2000), is to determine the total period of protection of the waste form from the time the waste is emplaced in the repository to the time when it is exposed to groundwater and release of radionuclides can commence. Failure of the engineered barrier is defined as the time when the DS and WP have failed, and the decay heat of the waste form is sufficiently reduced so as to allow water entry into the failed package. Since, failure is predicted to be by a general passive corrosion process, the breach in the waste package allowing a water pathway is likely to be of significant size. The distribution of predicted failure times is then taken as input to the source term model within IMARC. A fuel cladding failure distribution is included but, since it is unchanged from IMARC 5, it is not redescribed here. The cladding failure distribution is treated as a separate input to the COMPAS source term model used in IMARC, and is used to define the fraction of the waste form that is subject to alteration and transport at a given time following breach of the waste package.

The modeling approach adopted here, and in our previous model in IMARC 5, captures a wide range of the uncertainties in both the specification of the repository environment and the corrosion performance of the engineered barrier system materials. Our aim in adopting this approach is to demonstrate that the engineered barrier system, as presently designed, is sufficiently robust to provide the required containment despite the many residual uncertainties.

5.1 Exposure Environment and the Establishment of Aqueous Conditions

The question of the nature and concentration of aqueous environments that could arise on the drip shield and waste package surfaces has, and continues, to receive considerable study. This is as it should be, since environmental definition remains a key uncertainty in determining the corrosion performance of the engineered barriers. The repository features that control this exposure environment include, the volume and concentration of seepage waters, the hygroscopic nature and chloride content of salts introduced during ventilation, the solubilities of gaseous species such as O_2 and CO_2 and how they will be influenced by salinity and temperature, the nature and attainable concentration of minor groundwater constituents such as Pb and As.

Aqueous conditions could be established by the formation on metal surfaces of thin films of water formed by vapour condensation. The composition of these environments will be determined by the nature of the soluble species present in the repository atmosphere or present as deposits on the DS/WP surfaces. For relatively clean surfaces these environments would be expected to be relatively dilute and only passive general corrosion would be anticipated.

However, it is anticipated that particulate matter entrained in air flowing through the drifts during an early period of ventilation could lead to the deposition of inorganic (and organic) material on the engineered barrier surfaces. Once ventilation is ceased and the relative humidity within the drifts increases, the hygroscopic nature of these deposits, assisted by capillary condensation processes in the pores of the particulates, could lead to the establishment of aqueous conditions at lower relative humidities (and, hence, higher temperatures) than would be anticipated for condensed water vapour on relatively clean metallic surfaces. This process introduces the possibility of establishing more aggressive (corrosive) conditions on the waste packages. This process would occur prior to the emplacement of the drip shield.

The National Atmospheric Deposition Program/National Trends Network has been monitoring the deposition of ionic species throughout the United States (NADP/NTN 2001). One such monitoring station is located in Red Rock Canyon in Nevada. Consequently, the nature of the particulates deposited would be expected to be close to those anticipated within Yucca Mountain. The data from Red Rock Canyon show that the deposition rates for nitrate and sulphate are well in excess of those for chloride. Consequently, once ventilation ceased and wetting of these particulates occurred, the potential for a more concentrated environment would exist. The combination of a relatively high sulphate content, the availability of CO_2 and a significant amount of silicate (universally present in dust) would be expected to prevent the concentration of Ca^{2+} and Mg^{2+} in the aqueous solutions that form (Gdowski, 2001). The nitrate-containing solution anticipated would not be capable of supporting localized corrosion of the waste package and only passive general corrosion would be expected. The Ti-7 drip shield is expected to be resistant to localized corrosion irrespective of the composition of the exposure environment.

Consequently, only in the presence of seepage drips does the development of very aggressive chemistries appear possible, and recent studies appear to have placed reasonable bounds on the exposure environments feasible via this route. From a combination of evaporative studies on representative groundwaters from the Yucca Mountain area and a consideration of the concentrated brines that occur in many arid regions in the south western USA, two limiting compositions have been defined (Gdowski et al 2001). These are near neutral and high pH brines.

In high pH brines, cations such as Mg^{2+} and Ca^{2+} are removed by precipitation as insoluble carbonates and silicates, and mixed chloride/nitrate solutions with a pH possibly in excess of 12 are possible. The composition of near neutral brines will vary depending on the relative concentrations of Ca^{2+}, SO_4^{2-} and CO_3^{2-}. For high Ca^{2+}/Mg^{2+} contents all the SO_4^{2-} and CO_3^{2-} can be precipitated and the final environment would be a near neutral Mg^{2+}/Ca^{2+} chloride-dominated brine. Experimental and numerical studies at LLNL (Gdowski et al 2001, Rosenberg et al. 2000) have shown that evaporation of groundwaters such as the standard J-13 well water are likely to lead to mixed anion (Cl^-/NO_3^-) alkaline brines, whereas the evaporation of unsaturated zone pore waters has the potential to produce near-neutral Mg^{2+}/Ca^{2+} chloride-dominated brines. These studies have identified the nature of the precipitates likely to form as well as the concentration profiles along the evaporative pathway. From the perspective of drip shield (DS) and waste package (WP) corrosion there are two key features of these two bounding environments;

(i) the deliquescence point of the salt mixture, which will determine the relative humidity at which these salts can first form aqueous conditions; and

(ii) the relative concentrations of aggressive (Cl^-) and benign (NO_3^-) anions, which will determine the corrosivity of the environment.

From a corrosion perspective the alkaline mixed anion brines can be considered considerably less aggressive that the near-neutral brines. For mixed anion brines, the most hygroscopic solid would be $NaNO_3$ and measurements of deliquescence points (Gdowski et al. 2001) indicate that aqueous conditions would be possible for a relative humidity (RH) of ~ 50%. Based on laboratory tests (CRWMS M&O 2000a, 2000b), this threshold RH is related to temperature and translates to the establishment of aqueous conditions around ~ 120 °C. Since the deliquescence point of salt mixtures can be lower than those of the individual component salts, the establishment of aqueous conditions could be feasible at slightly higher temperatures depending on the exact solution composition (Gdowski, 2001). As will be seen below, this should have only a minor influence on the predicted corrosion behaviour.

The relationship between RH and temperature allows us to specify a threshold temperature for the establishment of an aqueous environment under conditions where seepage water contacts the drip shield and waste package. This relationship between RH and temperature was discussed in more detail in IMARC 5, and a temperature of 120 °C was taken to be the maximum temperature at which aqueous conditions could be established. Based on repository cooling curves this temperature can then be used to determine the earliest time at which significant corrosion can occur on either the drip shield or waste package on exposure to seepage water.

A similar consideration of deliquescence points indicates that the near neutral Ca^{2+}/Mg^{2+} brines could allow the establishment of aqueous conditions at an RH as low as ~20% which would correspond to a threshold temperature of around 160 °C. Since these brines are also chloride-dominated, their potential corrosiveness would be high. The establishment of such potentially aggressive solutions is thought unlikely, since pore water is not easily extracted from the rock and a concentration factor of ≥ 5000 would be required; i.e. a large quantity of dilute pore water would have to contact the hot surfaces to achieve such saturation. The passage of such large volumes of seepage water through the repository drifts seems unlikely at such high temperatures, and as temperatures decrease salts precipitated during the evaporative process would redissolve to yield a mixed anion solution less aggressive to the drip shield and waste packages (CRWMS M&O 2001).

Based on these analyses, we choose to define 160 °C as the maximum temperature and 120 °C as the probable temperature at which aqueous conditions will be first established in the presence of seepage drips. Also, we retain the assumption we adopted in IMARC 5 (EPRI, 2000) that such groundwater concentration processes will not occur in the absence of seepage drips onto the DS/WP surfaces. The adoption of this assumption means that, providing the drip shield functions as designed, the waste package would not experience contact with seepage drips and hence would not be exposed to such aggressive brines.

Based on these discussions it is assumed in our calculations below that aqueous conditions are possible on both the WP and the DS once the relative humidity is ≥ 50% ; i.e. the surface temperatures are ≤ 120 °C. In the case of the DS, which could be subjected to evaporate processes leading to near neutral Mg^{2+}/Ca^{2+} chloride-dominated brines, it is assumed there is a probability that aqueous conditions could be established at a temperature as high as 160 °C. Since, presently, the probability of formation of such as aggressive environment is not known, we have taken the 120 °C temperature threshold (T_{AQ}) for our base case and adopt a threshold temperature of 160 °C in sensitivity studies.

In this scenario, the probability that the waste package will be exposed to seepage drips then becomes the probability that the drip shield is improperly placed over the waste package, and that improper emplacement guarantees that the waste package will be subjected to seepage drips (and, hence, the evaporative evolution of a corrosive environment). In IMARC 5 (EPRI, 2000), we estimated this probability to be 10^{-4} per waste package (CRWMS M&O 2000c). Consideration of the effects of rock fall increased this probability to 1.5×10^{-3}. These probabilities are retained in the present analysis, and the reader is referred to IMARC 5 (EPRI, 2000) for further details.

5.2 Drip Shield Corrosion

In IMARC 5 (EPRI, 2000), we assumed two possible failure mechanisms for the drip shield; general passive corrosion and hydrogen-induced cracking (HIC) as a consequence of hydrogen absorbed during the passive corrosion process. These two processes are interlinked, since the rate of hydrogen absorption is taken to be directly proportional to the rate of passive corrosion, with a proportionality constant given by a term for the hydrogen absorption efficiency (f_H). This leads to two potential failure modes; (a) wall penetration by passive corrosion, (b) hydrogen-induced cracking once a critical hydrogen concentration of 1000 ± 200 $\mu g.g^{-1}$ is achieved. A more extensive discussion of these procedures and the source of parameter values is given in IMARC 5 (EPRI, 2000).

By reviewing the literature on titanium corrosion in various brines, we demonstrated that the database of passive corrosion rates from weight loss measurements on specimens exposed in the Long Term Corrosion Test Facility (TCFTF) at LLNL was consistent with published rates measured using a wide range of techniques. The rates from the LTCTF (CRWMS M&O 2000d) have been fitted to a Weibull cumulative distribution

$$f(t) = 1 - \exp\left[-\left\{\frac{t-\theta}{\alpha}\right\}\right] \qquad \textbf{5-1}$$

96500

× 365 × 24 × 3600

with α = 34.946, β = 0.0802 and θ = 6, Figure 5-1.

In model calculations in IMARC 5, we then chose to use the full database (3.5 nm/year (0 percentile) to 350 nm/year (100 percentile) for drip shields exposed to seepage drips and a reduced set of lower rates (10 ± 2.5 nm/year) for those shields not exposed to seepage drips. ? However, in this version of our model we abandon this separation and use only the full database for drip shield corrosion under all cases. This acknowledges the uncertainty inherent in the environments that could develop due to the deposition of salts during the period of ventilation employed immediately after waste package emplacement. While the aqueous environments expected due to the absorption of water by these potentially hygroscopic salts are not anticipated to be as aggressive as those produced by evaporative concentration of seepage waters (see section 5.1) it is likely that they will be quite concentrated. It seems judicious, therefore, to widen the corrosion database to encompass the full range.

A significant issue, which has arisen as a consequence of various Panel reviews of engineered barrier corrosion processes conducted over the past year or so, is that of the temperature dependence for corrosion processes. The rates measured for Ti-7 in the LTCTF at LLNL showed no temperature dependence over the measurement range of 60 °C to 90 °C. However, since under extreme environmental conditions an aqueous environment could form at a temperature of 160 °C, our decision not to include a temperature dependence for passive corrosion needs revisiting.

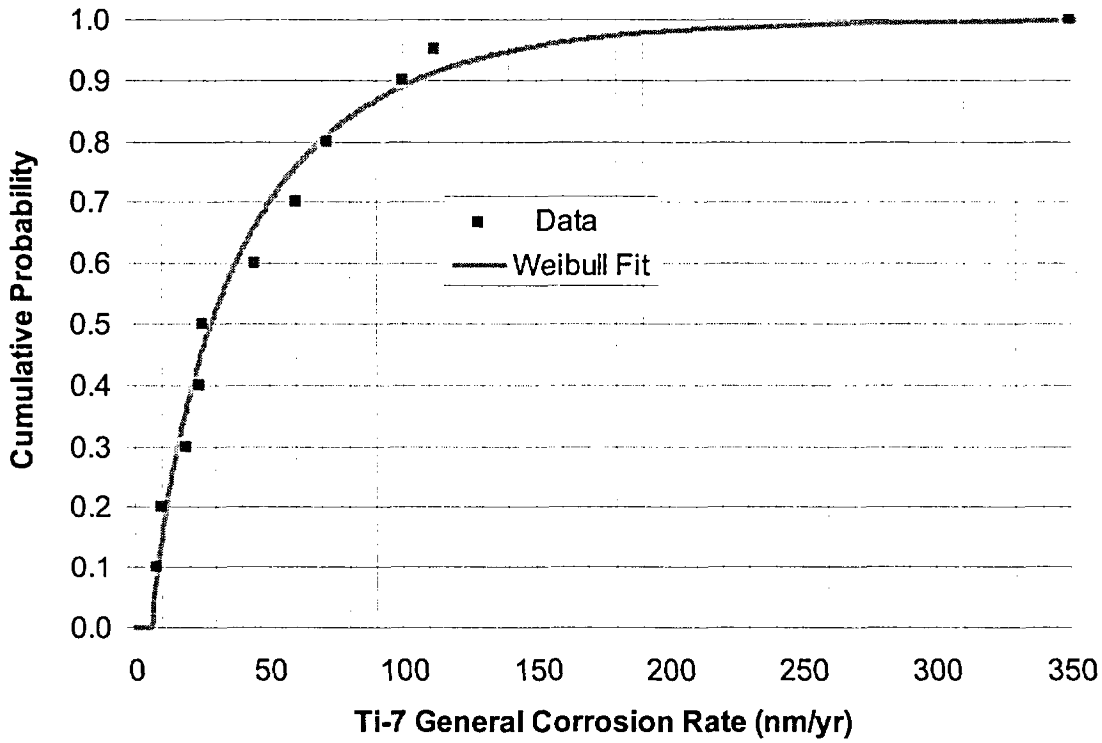

Figure 5-1
Weibull Fit of Titanium General Corrosion Rates

A reexamination of the published literature shows that the testing of Ti-7 in a German Mg^{2+}-dominated brine[*] over a period of ~ 3.5 years exhibited no temperature dependence over the range 90 °C to 200 °C (Smailos et al 1987). At all temperatures the rate after this period of exposure was < 100 nm/year. Since this rate is consistent with the LTCTF database and the temperature range and aqueous environment covers the most aggressive condition anticipated within the repository we have retained our assumption that there will be no temperature dependence for the passive corrosion of the drip shield.

However, we have revised our model to incorporate a temperature dependence for the hydrogen absorption process leading to HIC. Our previous model for hydrogen absorption was very conservative since it assumed that all the hydrogen absorbed as a consequence of passive corrosion will remain in the residual wall thickness and will not be re-released as corrosion progresses. A credible case can be made, especially for temperatures < 80 °C, when hydrogen transport into the bulk of the metal will be slow (Schutz and Thomas 1987), that significant hydrogen levels will not accumulate in the bulk of the alloy, since its re-release will occur as passive corrosion progresses. However, evidence exists (Shibata and Zhu 1984, Noel 1999) demonstrating that oxide films on titanium restructure at higher temperatures, a process with the

---

[*] Q-brine (wt%) – 1.4 NaCl; 4.7 KCl; 26.8 $MgCl_2$; 1.4 $MgSO_4$, 65.7 H_2O (pH = 4.9 (at 25 °C))

potential to increase the absorption efficiency of hydrogen even though the corrosion rate itself does not appear to be affected (i.e., no temperature dependence is observed, as discussed above). This higher efficiency, coupled to a faster diffusion of hydrogen into the bulk of the alloy, could lead to a more rapid accumulation of hydrogen.

Consequently, we have incorporated a temperature dependence of the absorption efficiency into our revised model, Table 5-1. The selection of values reflects our opinion that our previous model overestimated the extent of hydrogen absorption at low temperatures, but could have underestimated it at the higher temperatures potentially achievable. It should be noted that our model remains conservative, since we retain the assumption that failure occurs as soon as the hydrogen content exceeds a critical value of 1000 ± 200 $\mu g.g^{-1}$. This value was adopted from the measurements of Ikeda and Quinn (1998) who found no influence of hydrogen on the fracture toughness of Ti-16 up to this concentration.[*] However, it ignores the observation of Clarke et al 1995 that the critical hydrogen concentration increases substantially with temperature. Unfortunately, ~~these measurements were only qualitative and no measured~~ dependence of H_{CRIT} on temperature presently exists.

sampling cover the range ?

Table 5-1
Variation of Hydrogen Absorption Efficiency (f_H) of Ti-7 with Temperature

Temperature Range (°C)	Hydrogen Absorption Efficiency (f_H)	Parameter Distribution
160 > T > 140	0.08 – 0.06	uniform
140 > T > 120	0.06-0.04	uniform
120 > T > 100	0.04 – 0.02	uniform
T ≤ 100	0.02 – 0	uniform

A final adjustment we have made to our model is the incorporation of an effect of fluoride ion in sensitivity calculations. To date, studies of ground water concentration processes have not yielded a firm value for the expected fluoride concentrations that could be achieved. Preliminary data suggests that high pH brines could contain around 1000 ppm, a substantial concentration (Gdowski LV, May 23, 2001). However, the presence of a significant concentration of Ca^{2+} would be expected to reduce this level significantly by precipitating CaF_2. Recent data suggests the influence of F^- on Ti-7 corrosion rates could be substantial (Cragnolino, 2001). Based on electrochemical measurements of dissolution currents in deaerated 1 $mol.L^{-1}$ NaCl (95 °C) containing various concentrations of F^-, the corrosion enhancement factors listed in Table 5-2 can be estimated.

---

[*] Ti-16 contains 0.06 wt% Pd compared to the ~0.2 wt% in Ti-7.

Table 5-2
Enhancement factor used to multiply passive corrosion rates (from Cragnolino 2001)

Fluoride Concentration (mol.L^{-1})	Enhancement Factor
0	1
10^{-4}	2
10^{-3}	1000
$\geq 10^{-2}$	4000

The sudden increase in rate over the concentration range 10^{-4} to 10^{-3} mol.L^{-1} suggests a loss of oxide passivity. Consequently, we would also anticipate that the rate would not retain the independence on temperature observed for passive conditions. In the absence of any measured value of activation energy we have assumed a value of 30 kJ/mol. This value is based on the expectation that the active corrosion of the alloy will occur beneath a surface layer of corrosion product. The accumulation of such a deposit is to be expected, since the solubility of dissolved titanium in the anticipated aqueous environments will be low. The presence of this layer is likely to make the active corrosion process at least partially transport-contolled, a feature reflected in the choice of activation energy.

The use of an activation energy coupled to the temperature-time curve for the drip shield is described below in section 5.3 on corrosion of the waste package. At these enhanced corrosion rates the rate of hydrogen absorption is likely to be slow, the majority of it being rapidly re-released as corrosion progresses. Thus when fluoride is present, we have adopted a low absorption efficiency (f_H) of 0 to 0.02 (uniformly distributed).

We are of the opinion that the calculations presented here, and in IMARC 5, encompass within their range of predictions the significant uncertainties in the processes of hydrogen absorption and fluoride-stimulated corrosion by the Ti-7 drip shield.

Failure by HIC is most likely to occur at sites subject to an impact (e.g., from collapsing tunnel sections). Without such an impact, failure would not necessarily occur even though the hydrogen content of the material had achieved the critical amount (H_{CRIT}). It should be recalled that the value of H_{CRIT} used in calculations is the lowest hydrogen level at which a decrease in fracture toughness can be detected. Consequently, a credible argument could be constructed that failure by HIC will be directly proportional to the number of impacts sustained by the drip shield, and that in the absence of such impacts much higher hydrogen contents could be tolerated before failure occurred.

The failure site induced could be quite large, but its location would not necessarily coincide with that of a seepage drip. And, hence, the consequences for the corrosion of the WP could be minor. The probability that a failure of the DS would influence the corrosion performance of the WP would then be proportional to the probability that the site of impact coincided with the site of seepage drips.

In the case of DS failure by fluoride-induced corrosion, however, the site of failure is likely to be closely linked to seepage drip sites. The size of the failure site will be related to the area of the DS influenced by the drip. Since corrosion is via a general process, the failure aperture would be expected to be quite large (possibly a few cm^2) and, assuming dripping continues at that site after failure, seepage water would then have direct access to the WP. Cosequently, the number of failure sites will be proportional to the number of drip sites, attenuated by the fraction of these sites which can produce enhanced fluoride concentrations.

5.3 Corrosion of the Waste Package

Within the last year two reviews, the NWTRB review (Sagues and DiBella, 2001) and the Peer Panel on Waste Package Performance review (Payer et al., 2001), have addressed the issue of waste package performance. Both these reviews concluded that, presently, no good case could be made to claim that the Alloy-22 would not be subject to localized corrosion, and that, despite the very low passive corrosion rates measured in the LTCTF at LLNL, additional attention should be paid to corrosion features that could increase these rates, and, hence, potentially shorten waste package lifetimes.

5.3.1 Localized Corrosion of the Waste Package

In IMARC 5 (EPRI, 2000) we included a model for the crevice corrosion of Alloy 22 on the assumption that this process could occur underneath saline deposits formed on the package as a consequence of the evaporative concentration of seepage drips. A review of the available literature up to that time suggested that crevice corrosion was a remote possibility providing the exposure environment was a mixed anion solution; i.e. the potentially high pH brine expected by concentration of local well waters. However, if near neutral Ca^{2+}/Mg^{2+} chloride-dominated brines occur, the probability of localized corrosion could be significantly increased. Thus crevice corrosion has been observed on Alloy 22 under electrochemically polarized conditions in chloride-dominated solutions (5.0 mol.L^{-1} LiCl + small concentrations of NO_3^- and SO_4^{2-}) at 95°C (Kehler et al 2001) and the repassivation potential for Alloy 22 has been shown to decrease substantially in concentrated chloride solutions especially for temperatures > 100 °C (Cragnolino, 2001).

Consequently, given the existing uncertainties surrounding the waste package exposure environment (section 5.1), we have retained a model for crevice corrosion. As in IMARC 5 we have used the accepted penetration growth law

$$d_{cc} = Bt^n \tag{5-2}$$

where d_{cc} is the maximum penetration depth due to crevice corrosion (µm/year), B is a crevice growth constant (µm/year^n), and n is the time exponent, expected to have a value of 0.5 if the penetration process is limited only by diffusive or resistive effects within the local corrosion site (EPRI, 2000). This growth law is then used in conjunction with two key temperatures;

(a) T_{CC}, the threshold value below which Alloy 22 is not susceptible to crevice corrosion;

and

(b) T_{AQ}, the temperature at which aqueous conditions are first established on the waste package.

The time period between these two temperatures ($T_{CC} - T_{AQ}$) then represents the window within which the waste package is potentially susceptible to the initiation of crevice corrosion. The two temperatures can then be used to establish a criterion for susceptibility of the waste package to under-deposit crevice corrosion:

(i) For $T_{AQ} > T_{CC}$, the initiation of crevice corrosion is assumed to occur and propagation would subsequently proceed indefinitely according to the growth law given in equation (5-2).

(ii) For $T_{AQ} < T_{CC}$, the waste package is assumed immune to crevice corrosion and only general passive corrosion is possible.

In IMARC 5 (EPRI, 2000) a considerable discussion was dedicated to the selection of these two temperature values. It is acknowledged that these two values are likely to be uniformly distributed, although this uncertainty is not incorporated into the present model. A value of T_{AQ} = 120 °C was adopted, based on the assumption that the most aggressive environment possible would be that formed by the evaporative concentration of typical well waters, such as J-13. As discussed above in section (5.1), the most hygroscopic solid within this mixed anion solution would be $NaNO_3$ with a deliquescence point capable of sustaining aqueous conditions at a temperature of 120 °C. We have retained this value in our base case calculations since such an environment remains the most probable. We assume that, in the absence of seepage drips, the environment produced on the waste package due to condensation of water vapour on/into dust and particulates deposited during ventilation, will not be sufficiently aggressive to initiate crevice corrosion. For this mixed anion environment our review of available localized corrosion data (EPRI, 2000) indicated a value of T_{CC} = 100 °C was appropriate.

However, if near-neutral Ca^{2+}/Mg^{2+} chloride dominated brines are possible then aqueous conditions are feasible at temperatures as high as 160 °C (section 5.2) and the probability of crevice corrosion would be significantly increased. Also, in concentrated chloride-dominated solutions, Kehler et al (2001) have shown that T_{CC} could be as low as 85 °C. Consequently, we have included in our sensitivity calculations this more aggressive scenario of T_{AQ} = 160 °C and T_{CC} = 85 °C. The adoption of this more aggressive scenario also forces us to adopt a temperature dependence for the propagation of crevice corrosion. In IMARC 5 (EPRI, 2000), when T_{AQ} = 120 °C and T_{CC} = 100 °C were very close, it was possible to ignore the possibility of a temperature dependence of the growth constant, B (equation 5-2) without compromising significantly the realistic nature of our model. Given the difference between T_{AQ} (= 160 °C) and T_{CC} (= 85 °C) possible in near neutral Ca^{2+}/Mg^{2+} chloride-dominated waters, this simplification is not as easy to justify. In our present calculations we adopt the same values of B (and an identical distribution) as used in IMARC 5 (EPRI, 2000), Table 5-3.

Table 5-3
Values of the growth constant, B (equation 5-2), used in the waste package crevice corrosion model.

B (µm/year^n)	Percentile
5	5
55	50
100	95

The temperature dependence of these values is then determined using the standard Arrhenius relationship

$$\frac{(B)_{T_1}}{(B)_{T_2}} = \exp\left\{\frac{E_A^{\ddagger}}{R}\left(\frac{1}{T_2} - \frac{1}{T_1}\right)\right\} \qquad (5\text{-}3)$$

In the absence of any measured value for Alloy 22, an activation energy, $E_A^{\ddagger}$ = 55 kJ.mol^{-1} was adopted from measurements made on the highly crevice corrosion susceptible alloy Grade-2 titanium (Shoesmith et al 1995). This is expected to be a conservative value since Grade-2 titanium has no propagation-arresting metallurgical features as is expected for Alloy-22. To investigate the influence of assuming such a high value, sensitivity calculations were performed over the range 30 to 55 kJ/mol. An activation energy value even lower than 30 kJ/mol is a distinct possibility, but the calculations (below) will show that any influence of temperature on localized corrosion is effectively eliminated for a value of 30 kJ/mol.

In the absence of measured values for Alloy 22, the B values in Table 5-3 are a composite set compiled from available test data (in 10% $FeCl_2$) for the alloys C-4 and C-276, with the data for the C-4 alloy being the primary source. For the parameter n (equation 2) a value uniformly distributed between 0.1 and 0.3 was adopted. Implicit in the adoption of this range of n values is the assumption that Alloy 22 possesses metallurgical features that will limit the propagation rate (controlled by B) and encourage repassivation. This assumption seems reasonable in view of the results of Kehler et al (2001) who showed that the electrochemically-driven propagation of crevice corrosion on Alloy 22 was limited in penetration depth. It is likely that this feature of the alloy is attributable to its high molybdenum content (Newman 1985, Clayton and Olefjord 1995), a hypothesis that remains to be demonstrated. Since C-4 and C-276 are not as resistant to localized corrosion as Alloy 22, the B values chosen may eventually prove conservative. However, the adoption of n values between 0.1 and 0.3 is likely to make model predictions relatively insensitive to the parameter B.

One major advantage of assuming corrosion processes were independent of temperature in IMARC 5 was that the corrosion performance of the waste package was connected to repository design features only through the two temperature points, T_{AQ} and T_{CC}. However, the adoption of an Arrhenius temperature dependence for our present calculations means we are obliged to calculate the evolution of rates as a function of temperature. To do this the temperature-time curves are fitted to yield polynomial expressions which can then be used to calculate the evolution of the growth parameter B with time. The fitted temperature-time relationships for three distinct waste packages with different initial heat output (3 kW, 7.4 kW and11.8 kW) are listed in Table 5-4. These are then subsequently mixed with a percentage of each based on a simplification of the information on the number of various types of waste packages and their initial heat output provided in Tables 5-6 and 5-7 of CRWMS M&O 2000e.

Table 5-4
Fits of Waste Package and Drip Shield Surface Temperature vs. Time (35-200,000 years)

EBS Component	Temperature (T in °C) vs. Time (t in years) Fits	R^2	% WPs	Cumulative WPs
3 kW WP	$T = 0.0742 ln(t)^4 - 2.6177 ln(t)^3 + 34.483 ln(t)^2 - 219.29 ln(t) + 674.52$	**0.9975**	**2.27%**	**2.27%**
7.4 kW WP	$T = 0.0760 ln(t)^4 - 2.6926 ln(t)^3 + 35.675 ln(t)^2 - 228.12 ln(t) + 700.83$	**0.9976**	**38.03%**	**40.30%**
11.8 kW WP	$T = 0.0755 ln(t)^4 - 2.6983 ln(t)^3 + 36.320 ln(t)^2 - 237.56 ln(t) + 741.71$	**0.9981**	**59.70%**	**100.00%**
Drip Shield	$T = 0.0708 ln(t)^4 - 2.4938 ln(t)^3 + 32.857 ln(t)^2 - 210.43 ln(t) + 658.10$	**0.9977**	**N/a**	**N/a**

Figure 5-2 shows the temperature-time profiles for the three distinct waste packages and for the drip shield from which the fits in Table 5-4 were generated. The profiles fitted are for a ventilation period of 25 years and a waste package spacing of 0.1 m.

With the incorporation of a temperature-dependence, our base case model is more closely linked to repository conditions than the IMARC 5 model. By incorporating the possible influence of Ca^{2+}/Mg^{2+}-dominated environments (i.e., reducing T_{CC} from 100°C to 85°C and increasing T_{AQ} from 120°C to 160°C), we believe our predictions are bounding for the possible influence of localized corrosion on the waste package performance.

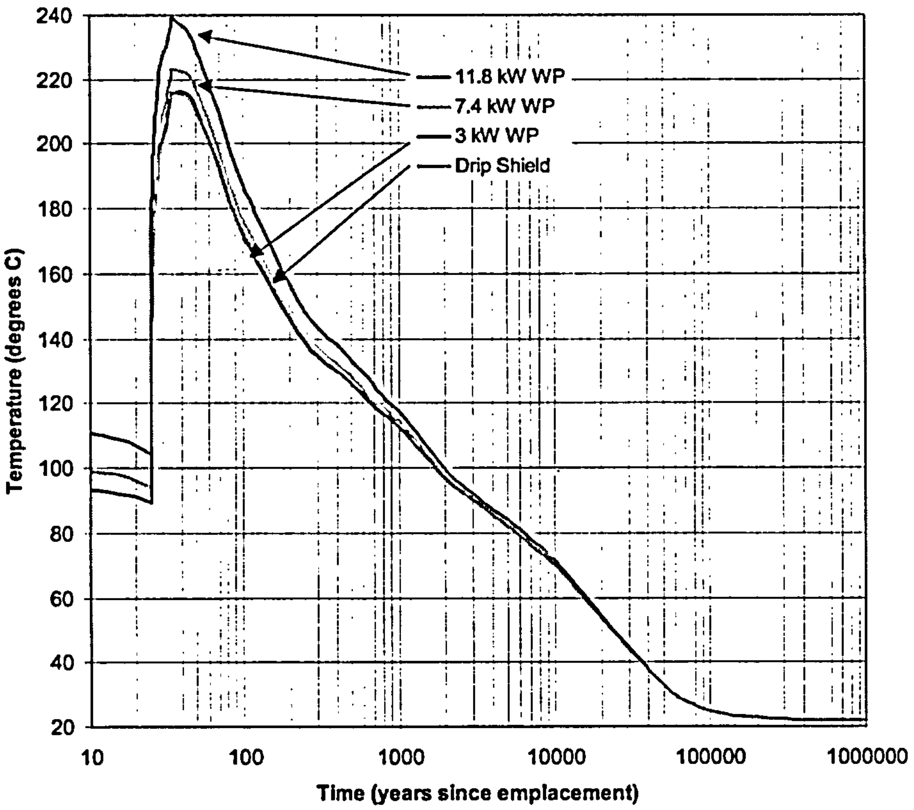

Figure 5-2
Waste Package and Drip Shield Temperature Histories

Compared to the USDOE model, our model is in some respects less conservative but in many other regards more conservative. As in our model, they assume that localized corrosion will only occur as a consequence of dripping directly onto the waste package through a failed drip shield. Their criterion for initiation is not based on a temperature threshold but an electrochemical potential threshold as commonly used in corrosion science (CRWMS M&O 1999a,b). Based on electrochemical potential measurements it is predicted that crevice corrosion is unlikely to initiate, a less conservative conclusion than used in our model. However, the recent NWTRB review concludes that electrochemical potentials could change significantly with time of exposure to the repository environment, and, hence, short-term measurements can not adequately determine the DS/WP susceptibilities to localized corrosion. This skepticism, the lack of a database of potential measurements over a sufficiently wide range of potential repository environments, and the absence of a justified model to predict the evolution of the corrosion potential make it difficult to presently define susceptibility to localized corrosion in potential terms. The USDOE model for crevice propagation, if it were to initiate, is extremely conservative. It is assumed that the penetration rate will be linear with time, equivalent to assuming a value of $n = 1$ in equation (5-2). Such a value ignores any ability of metallurgical features, or even diffusive or resistive effects, to slow propagation and reinforce repassivation. The values used could cause failure by crevice corrosion in terms of hundreds of years. By contrast, we have adopted (see above) an approach more closely aligned with published observations on localized corrosion processes by the use of the growth law given by equation 5-2.

5.3.2 General Corrosion of the Waste Package

The fear has been expressed that the passive general corrosion rates obtained from the LTCTF at LLNL are meaningless, since the weight change methodology used to obtain them is too insensitive to register meaningful changes. This is an unduly pessimistic viewpoint since independent techniques for measuring rates yield similar values. This has been particularly clearly shown in the case of the passive corrosion of titanium and its alloys (Shoesmith 2001). That measurements of rates in the nm/year range can be made is also supported by recent measurements made of rates in this range for iron in anoxic groundwaters using a barometric technique to measure hydrogen evolution (Smart et al. 2001). There appears to be no justifiable reason to dismiss the rates measured on specimens exposed in the LTCTF and we have continued to use them in our models.

In IMARC 5 (EPRI, 2000), a Weibull distribution ($\alpha = 40.381$, $\beta = 0.984$ and $\theta = 0$) fitted to the passive corrosion rates measured in the LTCTF at LLNL was used to calculate Alloy 22 general corrosion rates. The same database and distribution is assumed in the calculations presented here. As for Ti-7 the full database of available rates was used. Based on the absence of any temperature dependence in the LTCTF results (at 60 °C and 90 °C), and a minimal temperature dependence for general corrosion rates measured for the alloy C-4 in extremely aggressive saturated German brines (over the range 90 °C to 170 °C) (Accary 1985, Smailos 1986), we did not include any temperature dependence in our previous calculations.

Despite this experimental evidence, a great deal of skepticism has been expressed that passive corrosion rates can be independent of temperature, especially when exposed to aggressive saline conditions (i.e. Ca^{2+}/Mg^{2+} chloride-dominated solutions). Consequently, a considerable effort is being expended in attempts to verify whether passive corrosion rates are indeed independent of temperature over the range anticipated in the repository. Many of these efforts are based on attempts to measure the temperature-dependence of electrochemically measured passive current densities. Dunn et al (2000) found a temperature-dependence in low salinity solutions (0.028 $mol.L^{-1}$) but no temperature-dependence at higher salinities (4.0 $mol.L^{-1}$). Scully (quoted in CRWMS M&O 2001b) and Lloyd et al (2001) also measured passive dissolution currents and estimated activation energies of 36 kJ/mol (in 5 mol/L LiCl plus small amounts of SO_4^{2-} and NO_3^-) and 32 kJ/mol (in 1 mol/L NaCl plus 0.1 mol/L Na_2SO_4 (pH = 1)), respectively. In neither of these last two cases was steady-state achieved in the recorded values, and the estimated activation energies must, therefore, be considered suspect. Whether the values measured may over- or under-estimate the real steady-state value cannot be decided from the measurements made. Corrosion rates (from weight change measurements) of C-4 measured over a period of 3-5 years at temperatures in the range 90°C to 200°C in saturated Mg^{2+}-dominated brines yielded an activation energy of 19 $kJ\ mol^{-1}$ (Smailos et al 1987). This value may actually over-estimate the temperature-dependence since, on this alloy, pitting was also occurring and would have contributed to the weight loss on the basis of which the corrosion rates were estimated. Considering the duration of these last experiments, there is a good chance the rates measured are steady-state.

On the basis of this available data we have chosen an activation energy of 19 kJ/mol for our base case calculations of passive corrosion rates and use a value of 32 kJ/mol in sensitivity calculations. As with localized corrosion, the Arrhenuis relationship given in equation 5-3 and the T-t relationships in Table 5-4 were used to calculate temperature-dependent rates.

5.3.3 Stress Corrosion Cracking

In common with the USDOE model and our IMARC 5 model, we assume that SCC can only occur in the region of the waste package welds. Additionally, since all fabrication welds used in manufacturing the waste package can be fully annealed prior to emplacement of the waste, we agree that they will not be subject to residual stresses high enough for SCC to occur (CRWMS M&O 2000f, 2000g). Consequently, in common with the USDOE model, we assume that only the closure lid weld of the waste package can develop residual stresses high enough to cause SCC, since this weld must be made with the waste in place, a condition which disqualifies a subsequent full package anneal.

A very extensive discussion of SCC and those welding and fabrication features important in determining whether the waste package will be susceptible to this process was included in IMARC 5 (EPRI, 2000). Here, we will review briefly the form of our model and the conclusions reached based on IMARC 5 calculations, and the continuing measurements and tests which appear to be steadily confirming that SCC will not cause waste package failure.

Only those welds subject to seepage drips and, hence, evaporative concentration processes are assumed capable of developing an exposure environment sufficiently aggressive to sustain SCC. This is consistent with our general approach to localized corrosion on the waste package (above) in that it implicitly assumes that the dust and particulates deposited during ventilation cannot produce an SCC-sustaining environment when wetted with condensed water vapour. When subjected to drips, localized corrosion can start on the stress-relieved layer on the outside of the outer lid weld if $T_{AQ} > T_{CC}$, and corrosion will then proceed by both crevice propagation and general passive corrosion. If seepage drips do not contact the weld until $T_{AQ} < T_{CC}$, then only general passive corrosion occurs. The thickness of the stress-relieved outer layer on the weld is taken to be 12 ± 2 mm (IMARC 5) based on the calculations of stress distributions and stress intensity factors produced within the weld by the induction coil heating stress relief procedure (CRWMS M&O 2000f).

Conservative? stress

This 12 ± 2 mm stress-relieved layer must be removed before the conditions for susceptibility to SCC can be established. Since we assume the thickness of this layer is uniformly distributed, the time to remove it will be similarly distributed. Subsequently, the probability of instant penetration of the remaining 13 ± 2 mm of the weld thickness by SCC is the probability that a surface breaking flaw exists of sufficient depth to produce a stress intensity factor $K_I = 8$ MPa.m$^{1/2}$ at the tip of the flaw. The justification for choosing this value for K_I has been addressed elsewhere (section 5.4.3, EPRI, 2000). A description of the nature, size, distribution and alignment of weld flaws was included in IMARC 5, and a more extensive discussion published elsewhere (Massari and Shoesmith 2001).

Finally, we retain our assumption that the inner lid weld will not experience SCC because the three simultaneous criteria required for SCC to occur (metallurgical susceptibility, an aggressive environment, sufficient stress) will be extremely difficult to satisfy. This assumption is based on our calculation that failure of the outer lid will take so long that the subsequent development of an environment sufficiently aggressive to sustain SCC will not occur. This, coupled to the very low probability that both the inner and outer lids will possess a sufficiently large and correctly aligned flaw at adjacent sites, make failure of the inner lid by SCC extremely unlikely.

Since the publication of IMARC 5, the testing of Alloy 22 for SCC in a wide range of aggressive environments continues to support our opinion that, while no immunity to SCC can be claimed, waste package failure by this process is a very remote possibility (CRWMS M&O 2001a, Andresen 2001, Gordon 2001). Initially, in the absence of any measured data, a threshold stress of 20 to 40% of the alloy yield stress was selected by the USDOE for performance assessment calculations. On a smooth surface, the threshold stress for initiation has been found to exceed 170% of the yield stress when measured in a solution close in composition to the alkaline mixed anion environment anticipated in the respository. Similarly, initiation has not been observed in LTCTF tests, on U-bends exposed for > 1000 hours in boiling $MgCl_2$, or on constant load specimens exposed for over 4000 hours at stresses up to 96% of the Ultimate tensile stress in J-13 well water (7500 x) at 105 °C. On the basis of these results the threshold stress has been increased to 80 to 90% of the yield stress.

The USDOE chose to use the slip dissolution/film rupture model (SDM), developed originally for stainless steels (Ford and Andresen 1988, Andresen and Ford 1994), to calculate crack growth rates under simulated repository conditions. In the absence of measured data for Alloy 22 they selected values of the constants A and n based on available data for stainless steel. These two constants are obtained from electrochemical repassivation transients and define the crack growth rate (V_t) (usually measured in mm/s) in terms of the stress intensity factor (K_I in $MPa.m^{1/2}$) by the relationship,

$$V_t = \bar{A}(K_I)^{\bar{n}} \tag{5-4}$$

where $\bar{n} = 4n$, and n is a measure of the repassivation response of the crack in a specific exposure environment and

$$\bar{A} = A(4.1 \times 10^{-14})^n \tag{5-5}$$

As n increases, the rate of repassivation on film rupture becomes rapid and the crack growth rate decreases. The latest crack growth rates measured for Alloy 22 in a range of environments simulating anticipated repository conditions have yielded the lowest rates ever measured (~ 10^{-10} mm/s), and may only be sustainable in the presence of a small fatigue cycle. Since such a cycle will not be present in the waste package, this suggests that cracks may eventually arrest. These crack growth rates require a value of n > 1 to fit to equation (5-4). Such a high value of n indicates that, after film rupture to initiate crack growth at the crack tip, repassivation is very rapid, allowing very little opportunity for the development of the acidic environment necessary to sustain crack growth. Finally, the crack growth rates appear uninfluenced by the addition of 1000 ppm of lead (Andresen, 2001), suggesting that SCC will not be influenced by minor heavy metal concentrations which may be present in the repository exposure environment.

It is clear from these measurements that failure of the waste package by SCC is an unlikely occurrence.

5.4 Model Calculations

5.4.1 Base Case for the Model (Case A)

Based on the above discussion the base case for our model calculations can be specified as follows.

(1) Drip Shield

- For all conditions, the full database of passive corrosion rates from the LTCTF (LLNL) fitted to a Weibull distribution ($\alpha = 31.875$, $\beta = 0.807$ and $\theta = 6$, Figure 5-1) is used.
  - These rates were assumed independent of temperature
  - General passive corrosion starts when the drip shield temperature falls below 120°C (T_{AQ})

The hydrogen absorption factor (f_H) is assumed to be temperature dependent with the values given in Table 5-1. Only those values given for $T_{AQ} \leq 120°C$ are used.

A critical hydrogen concentration of 1000 ± 200 μg/g was used.

(2) Waste Package

(a) General Passive Corrosion

- For all conditions, the full database of passive corrosion rates from the LTCTF (LLNL) fitted to a Weibull distribution ($\alpha = 40.381$, $\beta = 0.984$ and $\theta = 0$), is used.
- These rates are assumed to have been measured at 75 °C and are taken to be temperature dependent with an activation energy, $E_A^{\ddagger}$, = 19 kJ/mol.
- Corrosion starts when $T_{AQ} = 120$ °C.

(b) Localized Corrosion

- The growth constant B values from IMARC 5 are used (Table 5-3).
- These values were assumed measured at 75 °C and are taken to be temperature-dependent, with an activation energy of 55 kJ/mol.
- The value of the time exponent n (equation 2) is uniformly distributed between 0.1 and 0.3.
- Localized corrosion starts only when the package is exposed to seepage drips and only when $T_{AQ} > T_{CC} = 100$ °C.
- The maximum value of T_{AQ} is 120 °C.

(c) SCC

- All the assumptions used in IMARC 5 (EPRI, 2000) apply.
- The thickness of the stress-relieved layer on the outer surface of the outer lid weld is 12 ± 2 mm of a total weld thickness of 25 mm.

5.4.2 Sensitivity Calculations

A series of sensitivity calculations were performed to determine the consequences of various drip shield and waste package scenarios.

(i) Drip Shield Only (Case A)

(a) To determine the sensitivity of the drip shield to the temperature at which aqueous conditions are first established, T_{AQ} was increased from 120 °C to 160 °C.

(b) To determine the possible influence of F^- on drip shield corrosion the base case calculation was repeated using the fluoride enhancement factors in Table 5-2 to multiply the passive general corrosion rates from the LTCTF and LLNL. In these calculations the hydrogen absorption efficiency was assumed independent of temperature and uniformly distributed between 0 and 0.02.

(ii) Drip Shield and Waste Package Together

(i) Case B. All parameter values were kept the same as the base case (Case A) except, T_{AQ} was increased from 120 °C to 160 °C for both Ti-7 and Alloy 22, and T_{CC} was reduced from 100 °C to 85 °C for Alloy 22.

(ii) Cases C-A and C-B. Both the base case calculation (case A) and the sensitivity case B were repeated for the drip shield model with 10^{-4} mol.L^{-1} fluoride present.

(iii) Cases D-A and D-B. Both the base case calculation (case A) and the sensitivity case B were repeated for the drip shield model with 10^{-3} mol/L fluoride present.

(iv) Case E-B. Case B was repeated with the activation energy for localized corrosion of the waste package reduced from 55 kJ/mol to 30 kJ/mol.

(v) Case E-C-B. Case B was repeated with the lower activation energy for localized corrosion (30 kJ/mol) of the waste package and the drip shield model with 10^{-4} mol/L fluoride present.

The parameter values used in each of these cases are summarized in Tables 5-5 and 5-6.

Table 5-5
Parameter Values used in Drip Shield Model Calculations

Case	R_1 (nm/year)	T_{AQ} (°C)	f_H	H_C (µg/g)	f_F	$(E_A^{\ddagger})_{Ti}$ (kJ/mol)
A	*LLNL database*	120	0.04-0	1000 ± 200	1	--
A'	"	160	0.08-0	"	0	--
B	"	160	0.08-0	"	1	--
C-A	"	120	0.02-0	"	2	30
C-B	"	160	0.02-0	"	2	30
D-A	"	120	0.02-0	"	1000	30
D-B	"	160	0.02-0	"	1000	30
E-B	"	160	0.08-0	"	1	--
E-C-B	"	160	0.08-0	"	1	--

R_1 – General passive corrosion rates (from LLNL database)
T_{AQ} – Temperature at which aqueous conditions established
f_H – Hydrogen absorption efficiency (Table 5-1)
H_C – Critical hydrogen concentration (Ikeda and Quinn 1998)
f_F – Corrosion rate enhancement factor due to the presence of fluoride (Table 5-2)
$(E_A^{\ddagger})_{Ti}$ – Activation energy for Ti-7 corrosion when fluoride is present.

Table 5-6
Parameter Values used in Waste Package Model Calculations

Case	R_2 (nm/year)	T_{AQ} (°C)	T_{CC} (°C)	B (µm/year^n)	n	$(E_A^{\ddagger})_{PC}$ (kJ/mol)	$(E_A^{\ddagger})_{LC}$ (kJ/mol)	d_w (mm)
A	LLNL database	120	100	Table 3	0.1-0.3	19	55	12 ± 2
B	"	160	85	"	"	"	"	"
C-A	"	120	100	"	"	"	"	"
C-B	"	160	85	"	"	"	"	"
D-A	"	120	100	"	"	"	"	"
D-B	"	160	85	"	"	"	"	"
E-B	"	160	85	"	"	"	30	"
E-C-B	"	160	85	"	"	"	30	"

R_2 – Passive corrosion rates of Alloy 22
T_{AQ} – The temperature at which aqueous conditions are first established.
T_{CC} – The threshold temperature below which Alloy 22 is not susceptible to crevice corrosion.
B – Growth constant for Alloy 22 crevice corrosion (Table 5-3 and equation 5-2)
n – Time exponent in the Alloy 22 crevice corrosion model (equation 5-2)
$(E_A^{\ddagger})_{PC}$ – Activation energy for the passive corrosion of Alloy 22
$(E_A^{\ddagger})_{LC}$ – Activation energy for the growth constant, B.
d_w – Thickness of the stress-relieved layer on the outer surface of the outer lid weld of the waste package.

5.5 Model Predictions

5.5.1 Model Predictions for the Drip Shield

Figure 5-3 shows the base case failure prediction for the drip shield. This figure enables us to assess the consequences of assuming a temperature-dependence for the hydrogen absorption efficiency, f_H (Table 5-1), by comparison to the failure distribution HICw/AGC in Figure 5-9 of IMARC 5, in which the acronym indicates identical conditions to those used here, but with a temperature-independent distribution (uniform) of f_H between 0 and 0.09. Using a cumulative probability of 10^{-4} (i.e. 1 in 10,000 drip shields) as the level of comparison, the first failures are predicted to occur in 3000 to 4000 years compared to 8000 years in the temperature independent case (IMARC 5). Using a cumulative probability of 0.5 as the level of comparison, the present model predicts 80,000 years as opposed to 200,000 years in our IMARC 5 results. If the assumption that the drip shield corrosion rate is independent of temperature is maintained, then this figure also shows that the consequences of forming aqueous conditions at 160 °C compared to 120 °C are minor.

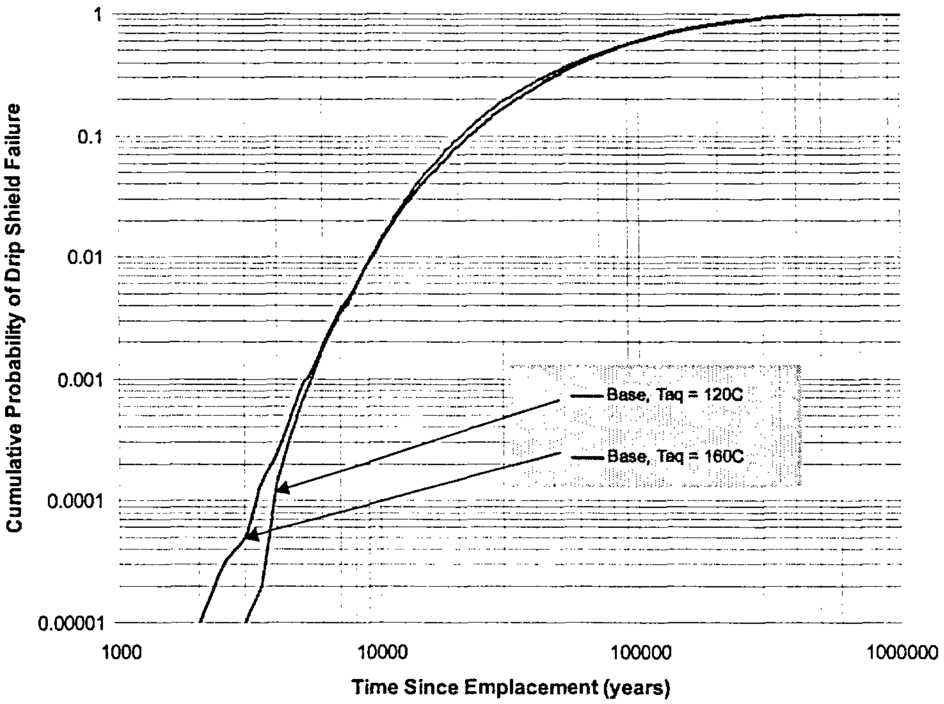

Figure 5-3
Cumulative probability of drip shield failure assuming aqueous conditions are established at either 160 °C or 120 °C.

The reason for the prediction of more rapid failures in the present model compared to that in IMARC 5 is the high values of f_H assumed above 100 °C (Table 5-1). This is confirmed in Figure 5-4, which shows the total fraction of failed drip shields due to HIC in our present model. Approximately 72% of the shields are predicted to fail by this process up to 100,000 years.

In the absence of experimental data it is difficult to assess whether our assumption of a high efficiency for hydrogen absorption for T > 100°C is conservative or not. What little data exists confirms that hydrogen absorption can be expected in concentrated brines, but no temperature-dependence was observed over the range 25°C to 110°C (Kim and Oriani, 1987). However, although the properties of oxide films on titanium alloys have been shown to change substantially above 100°C (Shoesmith and Ikeda, 1997), the influence of these changes on hydrogen absorption remains unknown. It is clear from the large differences in predicted DS lifetimes, with and without hydrogen absorption, that a clarification of the influence of hydrogen on corrosion performance of Ti-7 will significantly reduce the overall uncertainty in DS performance.

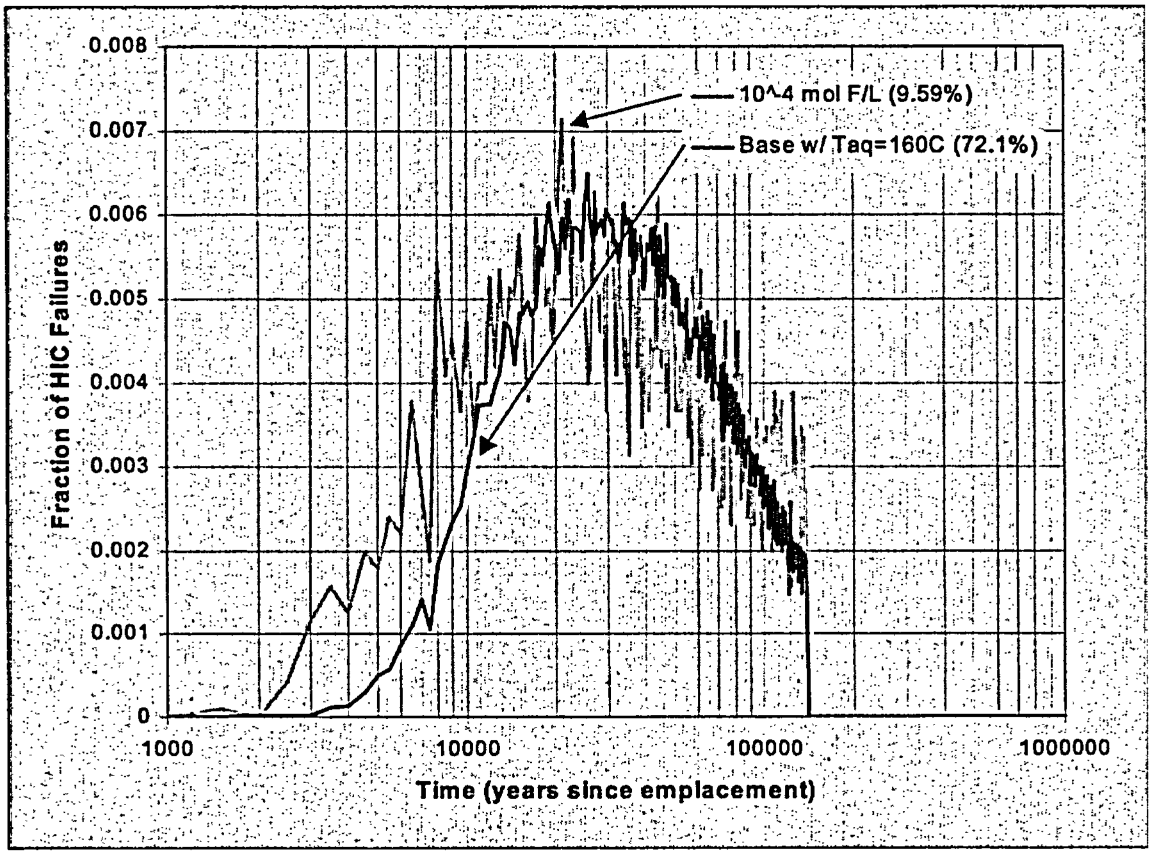

Figure 5-4
Total Fraction and Time Distribution of HIC Induced Drip Shield Failures for the base case calculation and for the case when exposure environment contains 10^{-4} mol/L of fluoride

Figure 5-5 shows the influence of groundwater fluoride concentration on predicted failure rates. For a low concentration of F^- (10^{-4} mol/L) the earliest failure (assumed to occur at a cumulative probability of 10^{-4}) is predicted to occur around 3000 years and to be only marginally influenced by whether T_{AQ} is taken equal to 160 °C or 120 °C. This early threshold is effectively the same as that for the base case. In the presence of fluoride, however, while these early failures may be attributable to HIC, the primary factor influencing early failure is the assumption that the corrosion rate will be temperature-dependent (with $E_A^{\ddagger} = 30$ kJ.mol^{-1}) in the presence of F^- as opposed to the assumption that the hydrogen absorption efficiency, f_H, is temperature-dependent.

The consequences of assuming no temperature-dependence for f_H are clearly indicated in the much wider long term distribution observed when fluoride is present and hydrogen absorption is minimal, Figure 5-5. When fluoride is present and f_H is temperature-independent, > 10^6 years are required to achieve a cumulative probability of failure of 0.5 compared to 80,000 years in the base case.

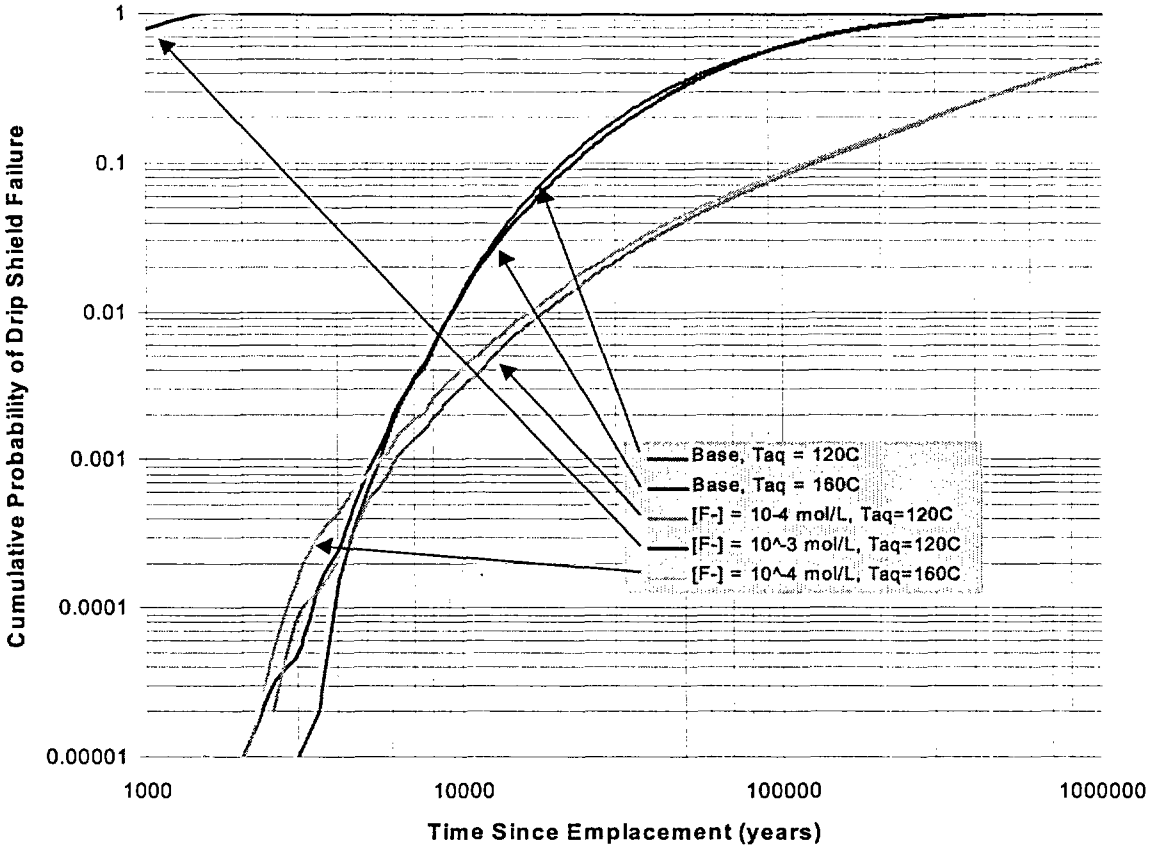

Figure 5-5
Cumulative probability of drip shield failure illustrating the influence of a change in the temperature on the establishment of aqueous conditions and the influence of fluoride in the exposure environment.

Based on the rate enhancement factors in Table 5-2 the influence on drip shield performance of an increase in fluoride concentration to 10^{-3} mol/L is major. All drip shields are predicted to fail in < 2000 years. While considerable caution should be exercised in interpreting these predictions, they clearly indicate the uncertainties introduced in drip shield performance by the inability to presently specify the fluoride content of the repository environment. In the tests conducted by Cragnolino et al. (2001), the influence of fluoride was determined in the presence of chloride and other anions, such as SO_4^{2-} and NO_3^-. These latter ions were found to have no effect on Ti-7 corrosion when F^- was present, in contrast to their ability to moderate the ability of Cl^- to cause passivity loss. However, the concentration of available F^- will be significantly reduced by precipitation (as CaF_2) when Ca^{2+} is present. Thus, the formation of Ca^{2+}/Mg^{2+}-

dominated brines with a high fluoride concentration, leading to aqueous environments at T > 120°C, will not occur. Whether or not the presence of species such as silicate will also moderate F^- concentrations also remains to be determined.

[illegible] to [illegible]

The implications of drip shield performance in the presence of a significant F^- concentration on the overall performance of the DS/WP combination will be dealt with in more detail below.

5.5.2 Drip Shield/Waste Package (DS/WP) Combined Failures

Figure 5-6 shows the base case failure scenario for the DS/WP combination. A number of key points are illustrated by these distributions.

(i) In the absence of seepage drips (i.e. when localized corrosion of the waste package cannot occur) the adoption of a temperature dependence for passive general corrosion in our present model leads to an improvement in DS/WP performance compared to the temperature-independent model used in IMARC 5. This improvement leads to a decrease in the predicted cumulative probability of failure at long times due to the decrease in passive corrosion rate as the surface temperature of the waste package decreases. This can best be seen by considering the cumulative probability after 10^5 years. In our present temperature-dependent case the cumulative probability is 0.004 compared to ~ 0.02 in the temperature-independent IMARC 5 case. This improvement at longer times is not achieved at the expense of a significantly increased short-term probability of failure.

(ii) When dripping is present, the difference in failure distribution when the DS is functioning to when it is not is small. This is an indication of how minor the influence of localized corrosion is (when aqueous conditions cannot be formed until T_{AQ} = 120 °C) despite the adoption of a conservatively large activation energy (55 kJ/mol) for its propagation. This similarity in failure distributions highlights two key points.

(a) A key feature determining the predicted localized corrosion behaviour is the adoption of a value of n (equation) between 0.1 and 0.3. This value acknowledges that the depth of crevice propagation on Alloy-22 should be limited (Kehler et al., 2001).

(b) The presence of the drip shield has only a minor influence on the overall performance of the waste package, at least in mixed anion environments when aqueous conditions are not established until the surface temperature falls to ≤120 C.

(iii) The distribution in Figure 5-6 for the WP failed at emplacement shows the much better corrosion performance of the WP compared to the DS. As discussed above, the primary reason for this discrepancy in performance of the two barriers is the HIC failure process incorporated into the DS model. If it were to be assumed that HIC of the drip shield would not occur then this discrepancy would be effectively eliminated[*]. However,

---

[*] It should be recalled that the drip shield is only 15 mm thick compared to a waste package thickness of 20 mm.

the predictions in Figure 5-6 clearly indicate that, despite the poorer predicted performance of the DS (due to the adoption of the temperature-dependence for HIC), the waste package remains robust enough for this poorer performance to have only minor consequences on the overall DS/WP performance.

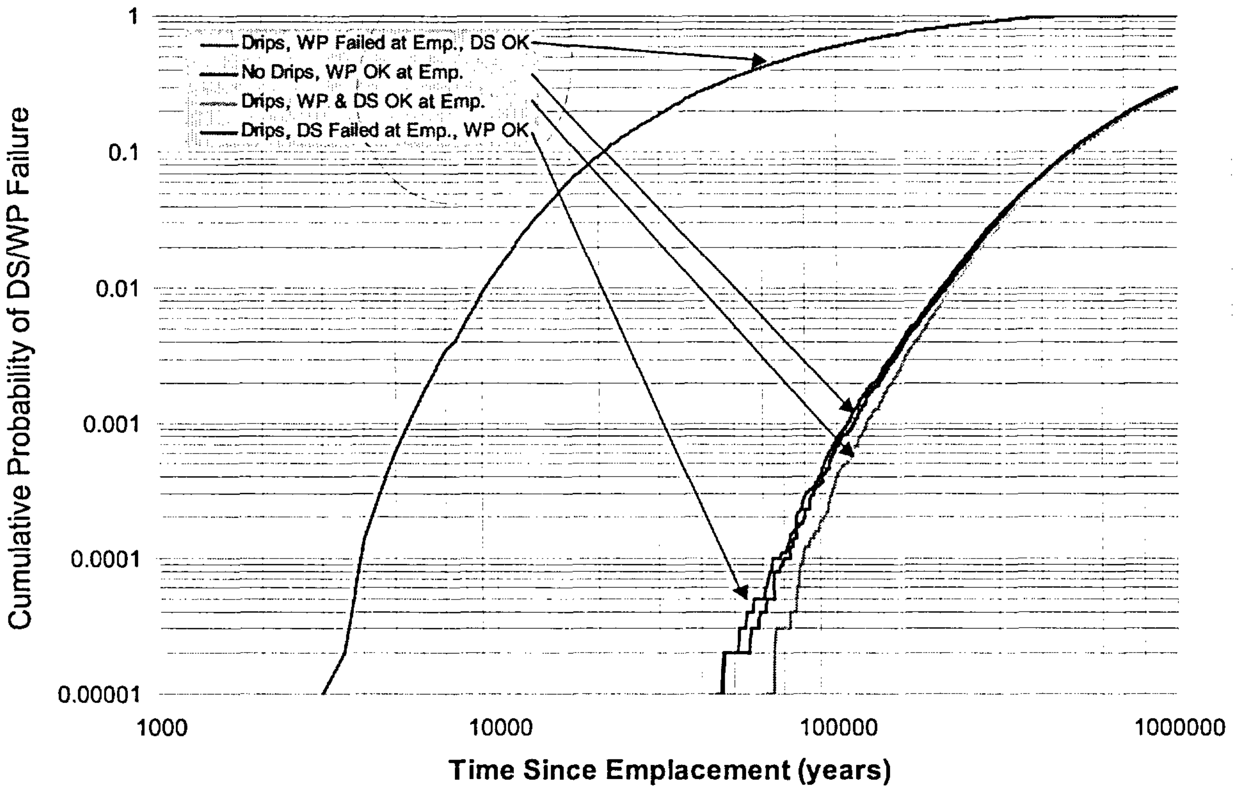

Figure 5-6
Cumulative failure probability for the drip shield/waste package combination according to the base case

5.5.3 Waste Package

Figure 5-7 shows the cumulative probabilities for waste package failure by general passive corrosion and general passive plus localized corrosion as a function of the activation energy for the general passive corrosion process. In these calculations the parameters in sensitivity case B (T_{AQ} = 160 °C and T_{CC} = 85 °C) were used in the localized corrosion model. These calculations represent the worst possible behaviour since the drip shield is assumed to be failed from emplacement. In the absence of localized corrosion, an increased temperature dependence for the general passive corrosion process (i.e., an increase is $E_A^‡$ from 19 kJ/mol to 32 kJ/mol) leads to increased waste package lifetimes. The cumulative probability of failure (using 10^{-4} as an indication when the first package failure might be expected) increases from 70,000 to 90,000 years. For a 0.1 cumulative probability of failure, the increase is from 500,000 to 10^6 years. This is attributable to the rapid decrease in temperature with time, Figure 5-2. The waste package temperature falls to below the value of 75 °C (the averaged value for the database of rates from the LTCTF) in under 10,000 years. Thus, the rates are suppressed to values less than the measured ones for the majority of the package lifetimes, leading to a much wider cumulative distribution at the higher activation energy.

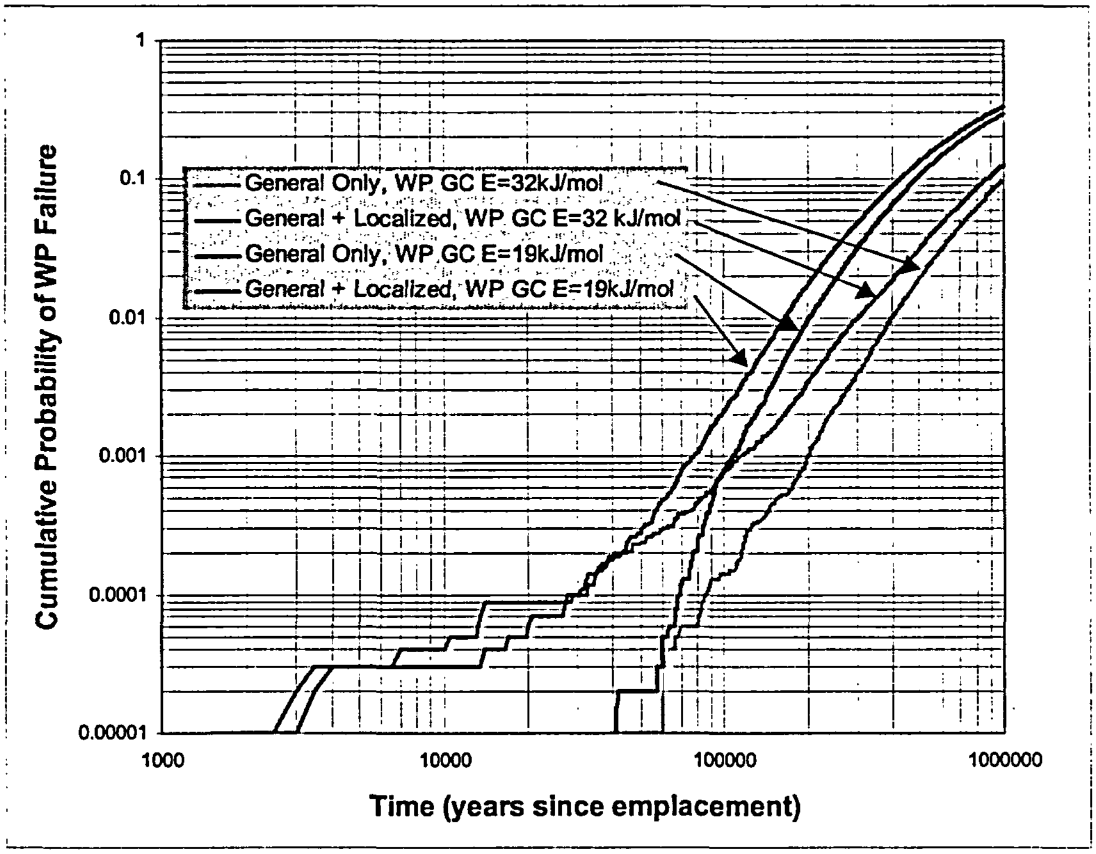

Figure 5-7
The influence of the temperature-dependence of the waste package general corrosion process on the cumulative distribution of failures in the absence of a drip shield.

Figure 5-7 also indicates the influence of localized corrosion coupled to general passive corrosion for both activation energies. In both cases localized corrosion introduces an increased cumulative probability of failure as expected in the absence of a DS. Again, using a cumulative probability of 10^{-4} as a reference point for the time of first package failure, this is predicted to be decreased from ~70,000 years to 30,000 years by localized corrosion ($E_A^{\ddagger}$ = 19 kJ/mol). For a cumulative probability of 0.1 the influence of localized corrosion is predicted to be marginal, the predicted lifetime decreasing from 500,000 years (no localized corrosion) to ~420,000 years. This long term insensitivity of the cumulative failure distribution reflects the short term nature of localized corrosion enforced by the form of equation (2) with an n value between 0.1 and 0.3.

Figure 5-8 shows the predicted performance of the DS/WP combination according to sensitivity case B; i.e. for the establishment of aqueous conditions for T_{AQ} = 160 °C and assuming a lower temperature threshold of susceptibility (T_{CC} = 85 °C) to crevice corrosion. The potential consequences of establishing such an aggressive environment can be appreciated by comparing the cumulative failure distributions assuming the drip shield is failed at emplacement for this environment to that for our base case (Figure 5-6). If a cumulative distribution of 10^{-4} is taken as an indication of the predicted time of first failure, then this failure would be around 25,000 years for the aggressive conditions (T_{AQ} = 160 °C, T_{CC} = 85 °C, Figure 5-8) compared to ~ 70,000 years for the base case (T_{AQ} = 120 °C, T_{CC} = 100 °C, Figure 5-6). The short term nature of the more aggressive conditions is clearly demonstrated by the prediction that the 0.5 cumulative probability of failure is > 10^6 years in both cases.

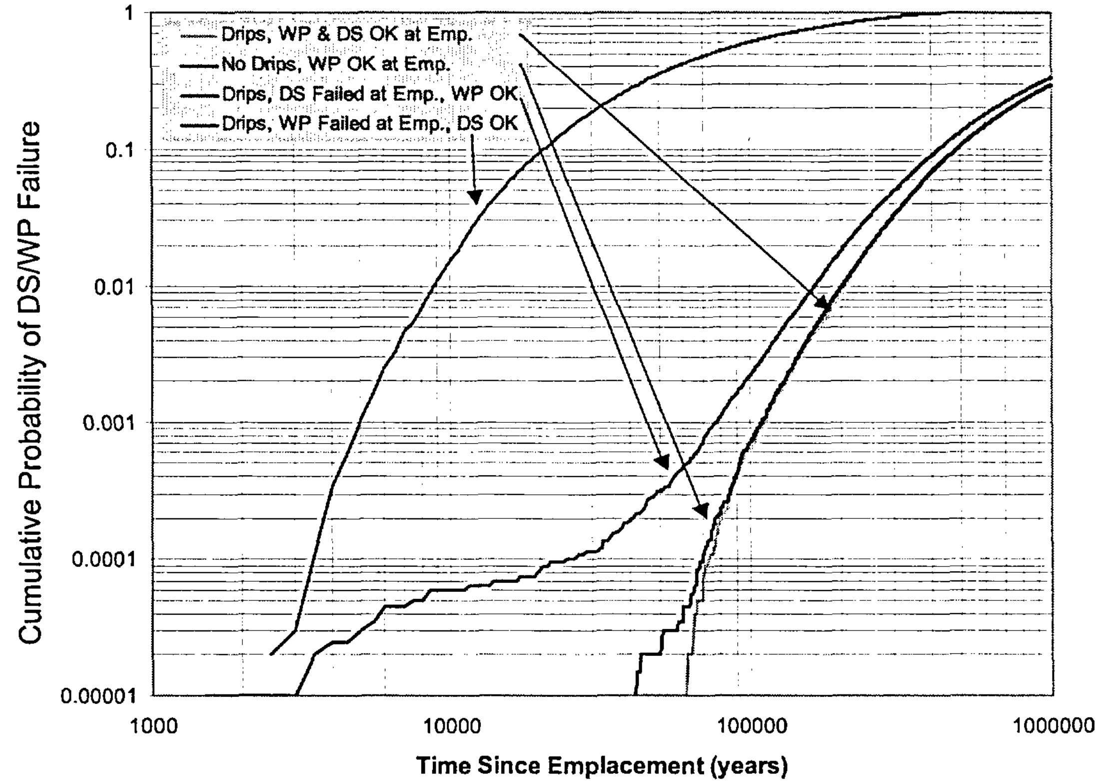

Figure 5-8
Cumulative distribution of failures for the DS/WP combination for the combination T_{AQ} = 160 °C and T_{CC} = 85 °C (Case B).

A second key feature of Figures 5-6 and 5-8 is that the proper function of the drip shield, even when evaluated by the present base case model involving the temperature-dependent absorption of hydrogen, effectively eliminates this increased probability of failure due to more aggressive localized corrosion conditions. This is clear from the marginal difference in the cumulative probability plots assuming the drip shield is working in the presence of drips, Figures 5-6 and 5-8 (Drips, WP & DS OK at Emp). This provides an essential demonstration of the drip shield's primary function; to protect the WP from the aggressive conditions which could prevail at short times when the WP surface temperature is high and localized corrosion possible.

If it is accepted that, once the surface temperature falls below 85°C, the waste package will no longer be susceptible to localized corrosion no matter what the exposure environment, then it is possible to define the period for which the DS must protect the WP from seepage drips. From the T-t curves in Figure 5-2 ~~this period can be defined as~~ between 3000 and 5000 years. The predictions of Figure 5-3 suggest this period of protection of the WP is achievable for all but a few WP (~1 in 1000; i.e., a cumulative probability of 0.0001) even assuming the potentially conservative model for HIC of the DS used in the calculations in this report. It can be concluded that the uncertainties in the DS performance due to the unknown influence of hydrogen are not a key issue in determining the overall performance of the DS/WP combination.

Figures 5-9 and 5-10 show sensitivity cases C-A and C-B and demonstrate that the combined DS/WP performance is only marginally influenced by the presence of a small concentration of fluoride. Of key importance is the prediction that the performance of the drip shield is still sufficient to effectively eliminate the short term localized corrosion of the WP in the more aggressive (T_{AQ} = 160 °C, T_{CC} = 85 °C) corrosion environment. This can be clearly seen by comparing the predicted distribution for a functioning drip shield to that for a failed drip shield in Figure 5-10.

If the fluoride concentration is increased in 10^{-3} mol/L then degradation of the drip shield is sufficiently rapid that it offers little protection against localized corrosion to the waste package. For case D-A (T_{AQ} = 120 °C, T_{CC} = 100 °C), this makes little difference to the waste package performance, Figure 5-11, since the influence of localized corrosion under dripping conditions is marginal anyway. For case D-B (T_{AQ} = 160 °C, T_{CC} = 85 °C) the WP would be exposed to the early influence of localized corrosion by the poor performance of the drip shield, Figure 5-12. However, as argued above (section 5.5.1), the coexistence of a Ca^{2+}/Mg^{2+}-dominated brine (required to enforce aqueous conditions at temperatures as high as 160°C) and a high F^- concentration are incompatible due to the insolubility of CaF_2. Thus, only the conditions used in Case D-A (Figure 5-11) would appear sustainable. Under these conditions, the waste package is sufficiently resistant to localized corrosion that the early failure of the drip shield with F^- present does not significantly influence the overall performance of the DS/WP combination.

In our model for localized corrosion of the waste package, we used an activation energy for the growth constant (B in Table 3) of 55 kJ/mol. This is a large activation energy taken from measurements of crevice propagation on the very susceptible Grade-2 titanium alloy, and is probably conservative for an alloy such as Alloy-22 designed with metallurgical features to limit the propagation of localized corrosion. To assess the significance of this assumption, we reduced the activation energy for the crevice corrosion growth constant to 30 kJ/mol, while retaining aggressive conditions (T_{AQ} = 160 °C, T_{CC} = 85 °C) (cases E-B and E-C-B). This decrease in activation energy effectively eliminates the influence of localized corrosion. This is apparent from the coincidence of all three cumulative distributions in Figures 5-13 and 5-14; i.e. the distributions are effectively insensitive to whether localized corrosion can, or cannot, occur and to whether the drip shield functions or not.

While it is impossible to be specific about the nature of the failure site in the waste package, a few general comments can be made. Localized corrosion failures are likely to involve failure at discrete small sites underneath the accumulated deposit necessary to form the crevice and initiate localized corrosion in the first place. Since failure by such a process involves the maintenance of acidic conditions within the propagating site, once failure occurs these conditions will be lost and repassivation should quickly follow failure. Subsequently, the widening of the failure aperture would occur by passive corrosion and would be slow. However, the number of failures predicted to occur by localized corrosion is small to negligible. More likely scenarios are that either an initial period of localized corrosion would occur but eventual failure would be by passive corrosion, or only passive corrosion would occur. Failure by both these processes is likely to lead to wider failure apertures, although again this site is likely to be choked by a combination of corrosion product debris and deposited silica. This would impede access of water to the inside of the failed package, but the delay is unlikely to be long.

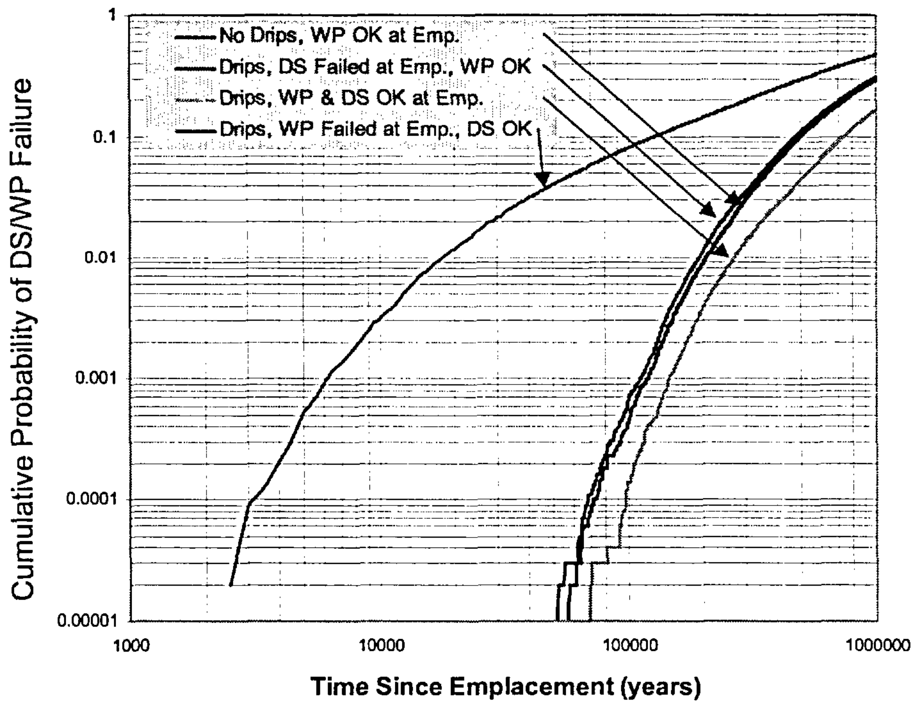

Figure 5-9
Cumulative probability of failure of the DS/WP combination with and without 10^{-4} mol/L fluoride in the aqueous environment. (Case C-A).

Although no credit is officially taken for the stainless steel liner within the waste package, it is worth considering whether this liner can provide any delay in access of water to the waste form. As for Alloy 22 the passive corrosion of stainless steel would be expected to be slow especially if it is protected for many thousands of years from the hot aqueous conditions anticipated at short emplacement times. Since waste package failures are not expected for t < 25,000 years or more, the surface temperature of the waste package would be around 55 to 50°C before stainless steel exposure occurred. Even at these temperatures stainless steel could be susceptible to localized corrosion in a sufficiently saline environment. However, failure of the stainless steel by processes such as pitting, crevice corrosion or SCC would lead only to a narrow aperture. Once created, the dimensions of this failure site would increase only slowly by passive corrosion. Consequently, irrespective of the mode of failure of the Alloy 22 WP, access of water to the waste form is likely to be severely restricted for a considerable period of time by the presence of the stainless steel liner.

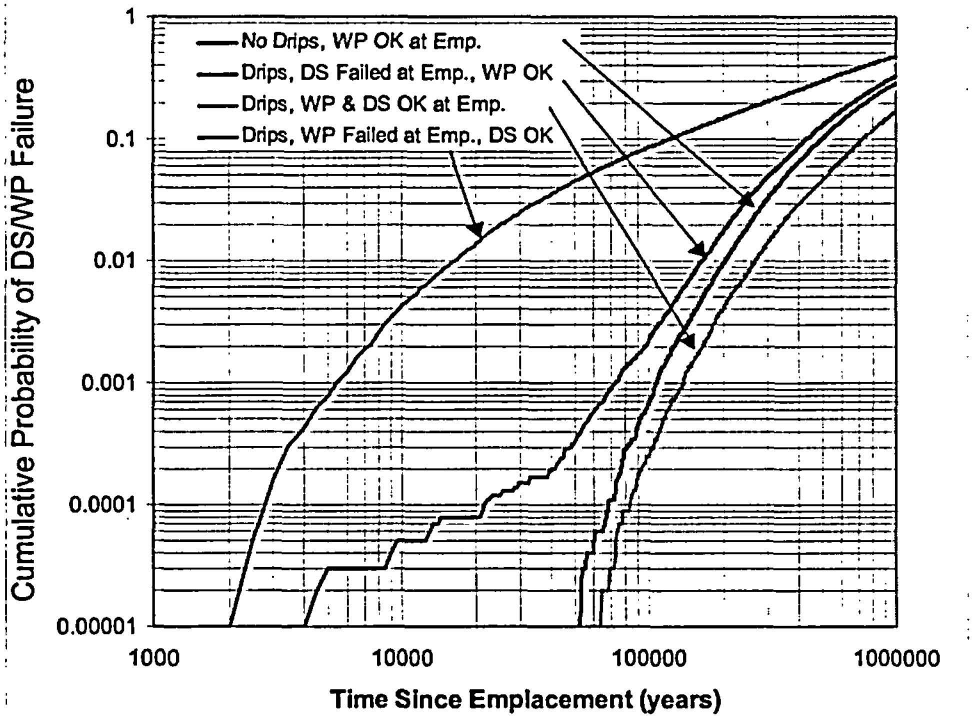

Figure 5-10
Cumulative probability of failure of the DS/WP combination with and without 10^{-4} mol/L fluoride in the aqueous environment. (Case C-B).

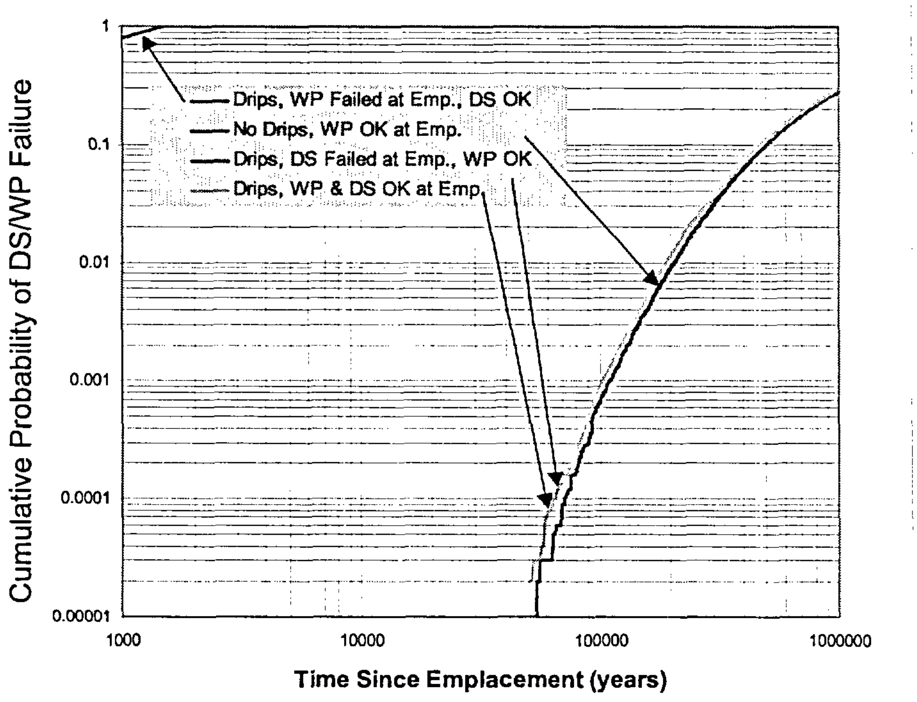

Figure 5-11
Cumulative probability of failure of the DS/WP combination with 10^{-3} mol/L fluoride in the aqueous environment (Case D-A).

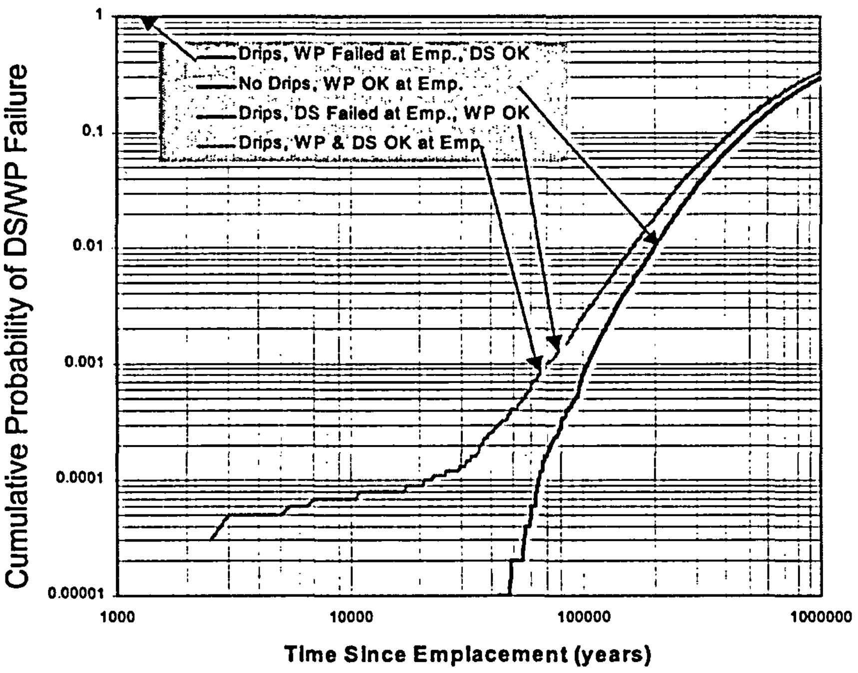

Figure 5-12
Cumulative probability of failure of the DS/WP combination with 10^{-3} mol/L fluoride in the aqueous environment (Case D-B).

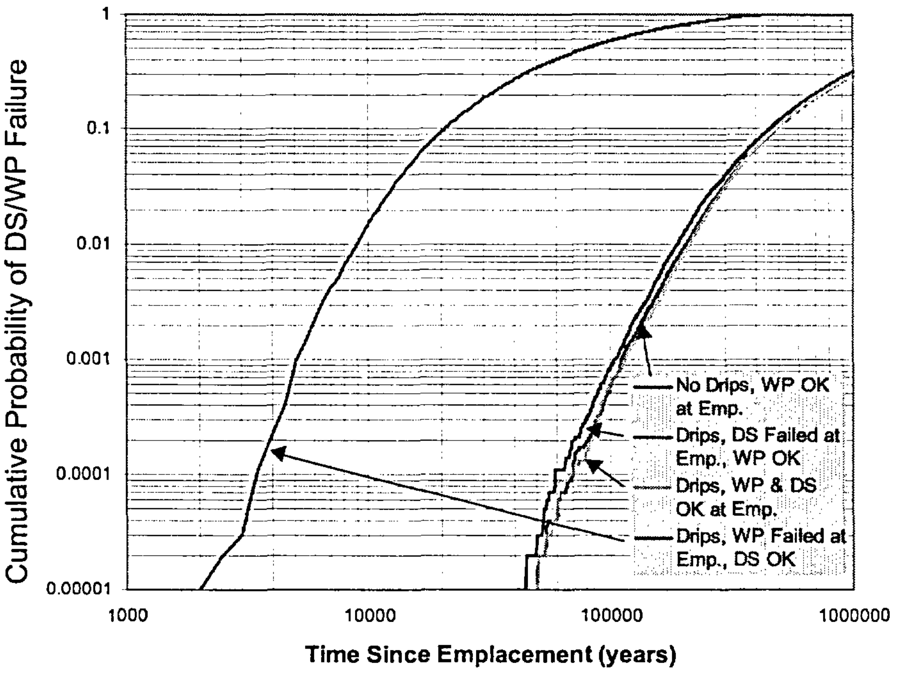

Figure 5-13
The influence on the cumulative probability of failure of the DS/WP combination of reducing the activation energy for localized corrosion of the waste package from 55 kJ/mol to 30 kJ/mol (Case E-B).

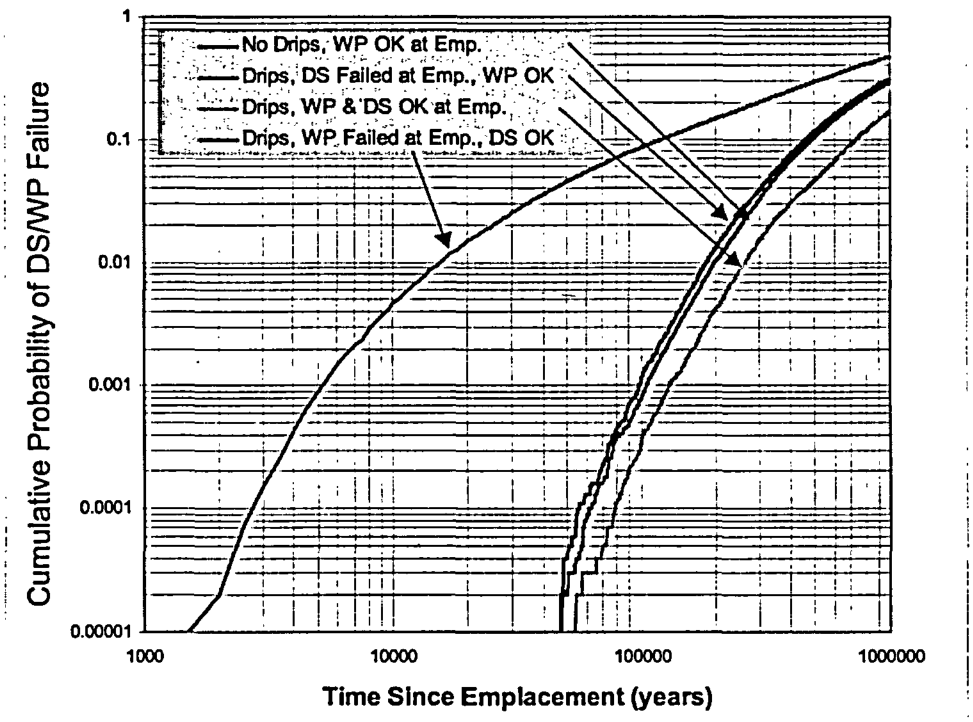

Figure 5-14
The influence of reducing the activation energy for localized corrosion of the waste package from 55 kJ/mol to 30 kJ/mol on the cumulative probability of failure of the DS/WP combination when the aqueous environment contains 10^{-4} mol/L fluoride (Case E-C-B).

5.6 Summary and Conclusions

aerosol

Based on the calculations performed a number of key points can be made.

1. If it is accepted that localized corrosion of the WP cannot occur in any environment providing its surface temperature is below 85°C, and can only occur if seepage drips contact the WP, then a performance criterion of 3000 to 5000 years can be defined for the DS.

2. The key process leading to drip shield failure could be HIC due to the absorption of hydrogen during passive corrosion. The uncertainties in defining the importance of this process have a major influence on predicted DS lifetimes, especially if aqueous conditions can be established at temperatures well above 100°C. If it can be demonstrated that the assumptions made in assessing the HIC performance of the DS are conservative, then a substantial performance margin (i.e., lifetimes well in excess of the performance criterion of 3000 to 5000 years) would be generated in the ability of the DS to provide its design function of protecting the WP from the potentially aggressive environments produced by contact of the package with seepage drips.

3. Predictions suggest that, for a sufficiently high fluoride concentration, the DS will not meet is design requirement. However, the coexistence of a Ca^{2+}/Mg^{2+}-dominated solution, capable of

establishing aqueous environments well above 120°C, and a high F$^-$ concentration is not feasible due to the insolubility of CaF_2. Under these circumstances, the WP remains sufficiently resistant to localized corrosion that the loss of protection from the DS has only a small influence on WP performance. Clearly, it is essential to determine the possible F$^-$ concentrations achievable in order to address this uncertainty.

4. The introduction of a temperature dependence for general passive corrosion of both the DS and the WP improves rather than degrades the long term performance of the waste package without significantly affecting its short term performance. Even if it is assumed that aggressive aqueous conditions can be established at very high temperatures (160 °C), the rates are slow enough, and the package wall thick enough, that the decrease in surface temperature with time reduces the corrosion rate to very low values long before wall penetration occurs.

5. Even if the exposure environment is chloride-dominated leading to the early establishment of very aggressive aqueous conditions (160 °C), the influence on the waste package failure times is not predicted to be major. This is a consequence of assuming that Alloy 22 possesses metallurgical features that will limit the extent of wall penetration by localized corrosion. This limitation in the extent of localized corrosion is a key feature that remains to be clearly demonstrated, but information presently published supports this optimism.

6. The model adopted for the localized corrosion of the waste package contains conservatively large temperature dependence and is very sensitive to this dependence. Thus, if this temperature-dependence is reduced slightly (i.e. the activation energy for propagation is decreased from 55 kJ/mol to 30 kJ/mol) then the influence of localized corrosion becomes negligible even if it is assumed that the drip shield is not present.

5.7 References

Accary, A. 1985. Corrosion Behaviour of Container Materials for Geological Disposal of High Level Radioactive Waste: Report of the Commission of European Communities, EUR 9836 EN.

Andresen, P. 2001. Waste Package Stress Corrosion Cracking Assessment and Strategy for Mitigation. Waste Package Materials Performance Peer Review Meeting, Las Vegas, NV, May 23, 2001.

Andresen, P.L. and F.P. Ford. 1994. Fundamental Modeling of Environment Cracking for Improved Design and Lifetime Evaluation in BWRs. *International Journal of Pressure Vessels and Piping* 59(1-3), 61-70.

Clarke, C.F., D. Hardie and B.M. Ikeda. 1995. Hydrogen Induced Cracking of Grade-2 Titanium. Atomic Energy of Canada Ltd Report, AECL-11284, COG-95-113.

Clayton, C.R. and I. Olefjord. 1995. Passivity of Austenitic Stainless Steels, *In* Corrosion Mechanisms in Theory and Practice, P. Marcus and J. Dudar (editors), Marcel Dekker Inc., New York, NY, 175-199.

Cragnolino, G. 2001. Corrosion Studies of HLW Engineered Barrier Materials. DOE Waste Package Materials Performance Peer Review Panel Meeting, Cleveland, OH, July 24, 2001.

CRWMS M&O 1999a. General Corrosion and Localized Corrosion of Waste Package Outer Barrier. ANL_EBS-MD-000003 REV 00.

CRWMS M&O 1999b. WAPDEG Analysis of Waste Package and Drip Shield Degradation. ANL-EBS-PA-000001 REV 00.

CRWMS M&O 1999c. 1999 Design Basis Waste Input Report for Commercial Spent Nuclear Fuel. B0000000-01717-5700-00041 REV 00.

CRWMS M&O 2000a. Environment on the Surfaces of the Drip Shield and Waste Package Outer Barrier. ANL-EBS-MD-000001 REV 00.

CRWMS M&O 2000b. Engineered Barrier System: Physical and Chemical Environment Model. ANL-EBS-MD-000033 REV 00.

CRWMS M&O 2000c. Analysis of Mechanisms for Early Waste Package Failure. ANL-EBS-MD-000023 REV 01.

CRWMS M&O 2000d. General Corrosion and Localized Corrosion of the Drip Shield. ANL-EBS-MD-00000 4 REV 00.

CRWMS M&O 2000e. Drift Scale Thermal Analysis. CAL-WIS-TH-000002 REV 00.

CRWMS M&O 2000f. Stress Corrosion Cracking of the Drip Shield, the Waste Package Outer Barrier, and the Stainless Steel Structural Material. ANL-EBS-MD-000005 REV 00.

CRWMS M&O 2000g. Abstraction of Models of Stress Corrosion Cracking of Drip Shield and Waste Package Outer Barrier and Hydrogen Induced Corrosion of Drip Shield. ANL-EBS-PA-000004 REV 00.

CRWMS M&O. 2001a. Yucca Mountain Science and Engineering Report. DOE/RW-0539.

EPRI, 2000, "Evaluation of the Candidate High-Level Radioactive Waste Repository at Yucca Mountain using Total System Performance Assessment", Phase 5, Report Number 10000802 (edited by J.H. Kessler), Electric Power Research Institute, Palo Alto, CA, November 2000, Chapter 5.

Ford, F.P. and P.L. Andresen. 1988. Development and Use of a Predictive Model of Crack Propagation in 304/316L, A533B/A508 and Inconel 600/182 Alloys in 288 °C water. *In* Proceedings of the Third International Symposium on Environmental Degradation of Materials in Nuclear Power Systems – Water Reactors. Traverse City, Michigan, August 30 – September 3, 1987. G.J. Theus and J.R. Weeks (editors), 798-800, NACE International, Houston, TX.

Gdowski, G.E. 2001. Environment on the Waste Package. Waste Package Materials Performance Review Meeting, Las Vegas, NV, May 23, 2001.

Gordon, G. 2001. Stress Corrosion Cracking. Waste Package Materials Performance Peer Review Meeting. Las Vegas, NV, September 25, 2001.

Ikeda, B.M. and M.J. Quinn. 1998. A Preliminary Examination of the Effects of Hydrogen on the Behaviour of Grade-16 Titanium at Room Temperature. Ontario Hydro Report No. 06819-REP-01200-0078-R00.

Kehler, B.A., G.O. Ilevbare and J.R. Scully. 2001. Crevice Corrosion Behaviour of Ni-Cr-Mo Alloys: Comparison of Alloys 625 and 22. *In* Localized Corrosion, NACE Research Topical Symposium, CORROSION 2001, NACE International, Houston, TX.

Massari, J.R. and D.W. Shoesmith. 2001. Effect of Weld Flaws on Waste Package Performance. Proceedings of the Nineth International High-Level Radioactive Waste Management Conference, American Nuclear Society, LaGrange Park, IL, USA, Paper E-7-2, May 2001.

NADP/NTN (National Atmospheric Deposition Program/National Trends Network 2001. National Atmospheric Deposition Program/NTN Annual/Seasonal Depositions, Seasonal Data for Site: NV00 (Red Rock Canyon), From January 22, 1985-October 3, 2000. Champaign, IL: National Atmospheric Deposition Program Office, Illinois State Water Survey.

Newman, R.C. 1985. The Dissolution and Passivation Kinetics of Stainless Alloys Containing Molybdenum, *Corrosion Science* 25(5), 331.

Noel, J.J. 1999. The Electrochemistry of Titanium Corrosion. Ph.D. Thesis, University of Manitoba, Manitoba, Canada.

Payer, J.H. ed., 2001. Waste Package Materials Performance Peer Review Panel: Interim Report. Bechtel SAIC Company, September.

Rosenberg, N.D., G.E. Gdowski and K.G. Knauss. 2000. Evaporative Chemical Evolution Of Natural Waters At Yucca Mountain, Nevada. UCRL-JC-137818. Lawrence Livermore National Laboratory.

Sagüés, A.A. and C.A. DiBella, eds., Proceedings from an International Workshop on Long-Term Passive Behaviour, July 19-20, 2001. Arlington, Virginia. 2001. U.S. Nuclear Waste Technical Review Board, December.

Schultz, R.W. and D.E. Thomas. 1987. Corrosion of Titanium and Titanium Alloys. *In* Metals Handbook, Nineth Edition, Volume 13, *Corrosion*, ASM International, Metals Park, OH, 669-706.

Shibata, T. and Y.-C. Zhu 1994. The Effect of Film Formation Temperature on the Stochastic Process of Pit Generation on Anodized Titanium. *Corrosion Science*, 36(10), 1735-1749.

Shoesmith, D.W. 2001. Titanium Drip Shield Issues, Waste Package Materials Performance Review Meeting, Las Vegas, NV, May 23, 2001.

Shoesmith, D.W., B.M. Ikeda, M.G. Bailey, M.J. Quinn and D.M. LeNeveu. 1995b. A Model for Predicting the Lifetimes of Grade-2 Titanium Nuclear Waste Containers. Atomic Energy of Canada Ltd. Report, AECL-10973, COG-94-558.

Smailos, E. and R. Koster. 1987. Corrosion Studies on Selected Packaging Materials for Disposal of High Level Wastes. *In* "Materials Reliability in the Back End of the Nuclear Fuel Cycle", IAEA, Vienna, Austria, IAEA-TECHDOC-421, 7-24.

Smailos, E., W. Schwartzkopf and R. Koster. 1986. Corrosion Behaviour of Container Materials for Disposal of High-Level Wastes in Rock Salt Formations. Nuclear Science and Technology, Commission of the European Communities, Luxembourg, EUR 10400 EN.

6

SOURCE TERM AND NEAR-FIELD PERFORMANCE

6.1 Introduction

This report contains the description of the model and analysis for the near field of a spent fuel repository located at Yucca Mountain. Recent documents published by the US Department of Energy's Yucca Mountain Project (YMP) are reviewed and updated with respect to inputs for the IMARC performance assessment code, as well as providing additional recommendations for possible future non-PA studies.

Section 6.2 presents an overview and update for the COMPASS source-term model used within IMARC. Section 6.3 assesses the conceptual models and data used by the USDOE in their modeling of colloidal transport of radionuclides within the near field and into the surrounding tuff host rock. Section 6.4 critically examines the near-field geochemistry modeling and interpretative results conducted by the USDOE. Finally, Section 6.5 presents an update of radioelement data for the near field, including radioelement data for Se-79 and Cl-36.

6.2 Review of Source Term and Near-Field Transport Models

This section reviews two of the Yucca Mountain Project's TSPA component models:

- Waste Form Degradation, and
- EBS Transport.

Review of these assessment studies is from a conceptual point of view. Conceptual comparison with the counterparts in EPRI IMARC is also conducted. Review of parameters and final assessment results are presented elsewhere. The primary reviewed material is the newly published S&ER (DOE 2001a) and SSPA (CRWMS M&O 2001). Some of the cited references are also briefly reviewed (CRWMS M&O, 2000a, b and c).

6.2.1 Source Term

6.2.1.1 Overview

In the YMP source term component, environmental parameters, such as the near-field chemistry, thermal development, and groundwater flow, are input to the model. Figure 6-1 shows the linkage and relationship between the source term model and other TSPA component models used by the YMP. The source term component calculates either release rates or concentrations of radionuclides that are used as boundary conditions to the EBS transport component.

As can be seen from Figure 6-1, this process model includes the following FEPs:

- Water contact with the waste form,
- Degradation of waste form,
- Radionuclide mobilization by dissolution (soluble, solubility-limited, and colloids),
- Inventory evolution due to radioactive decay and in-growth,
- Diffusive transport of radionuclides out of the waste package through small stress corrosion cracks (SCC) and/or larger corrosion patches, and
- Advective transport of radionuclides out of the package through corrosion patches.

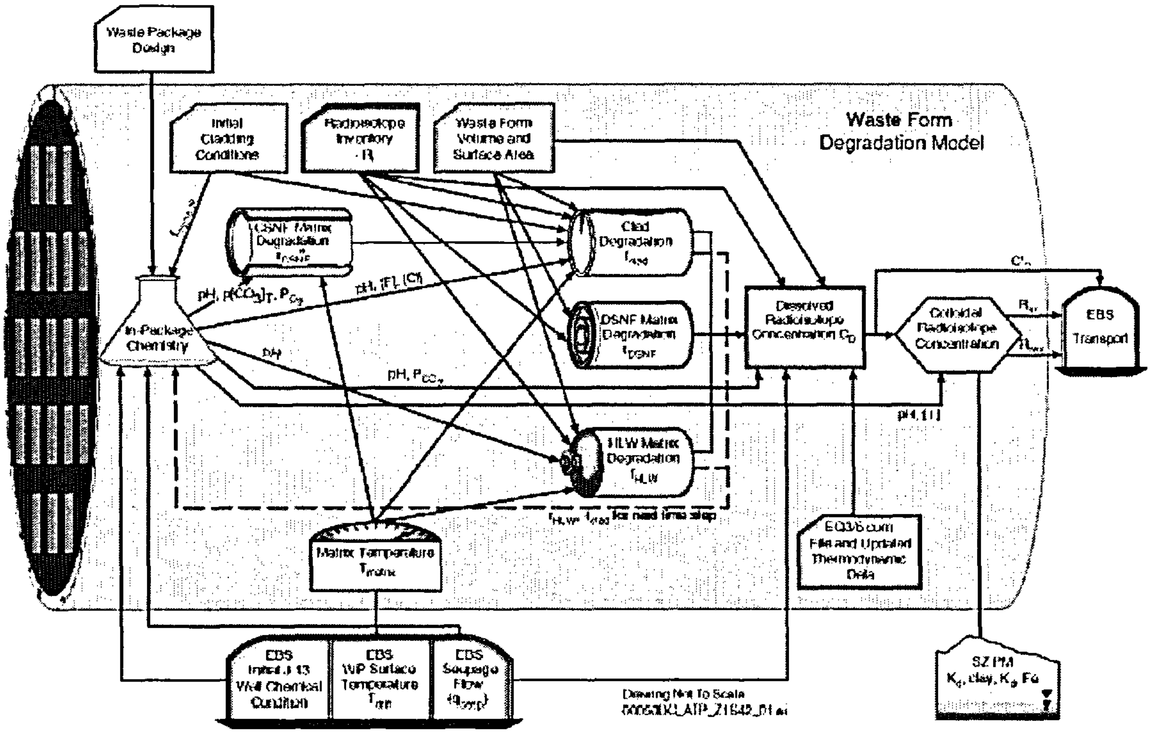

Figure 6-1
The YMP's source term components and linkages (S&ER, p.4-233).

Sub-process/system modeling parts, such as in-package chemistry, radionuclide inventories, waste form degradation, solubility, colloidal concentrations, etc, are parts of the YMP's source term study. Reviews of solubility, colloids, inventory, waste form degradation, near-field chemistry, etc., are described elsewhere. In this section, the focus is the approach used in calculating radionuclide release into the EBS.

6.2.1.2 Release from the Waste Package into the EBS

The release of radionuclides into the EBS is through advection and/or diffusion of aqueous concentrations of radionuclides inside the waste package. To determine the release rate, an approach adopted by EPRI IMARC (EPRI 1996) and programs of other countries (e.g., H12; SITE94) is to define a mixing cell and solve time-dependent radionuclide mass balance equations in the mixing cell. Usually, the void space next to the solid waste form is used as the mixing cell. In the unsaturated repository at Yucca Mountain, the mixing cell is defined as the void space inside the waste canister in both the YMP and EPRI IMARC.

Figure 6-2 illustrates the mass balance of a given radionuclide inside the mixing cell. Solution to the mass balance equation at a given time gives the release rates into the EBS at this time.

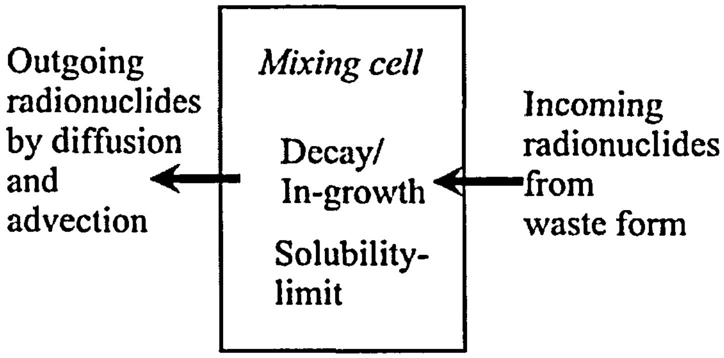

Figure 6-2
Conceptual model for calculating radionuclide release from the waste package into the EBS: mass balance in the aqueous volume next to the solid waste form.

Because evaluation of diffusion transport out of the mixing cell requires the concentration in the EBS in contact with the waste form, the mass balance equation inside the mixing cell is coupled with mass balance, or transport, equations in the EBS. Solutions to the system of mass balance equations are the radionuclide concentrations inside the waste package as well as in all the EBS components considered in the near field.

The YMP's model is conceptually the same as described above. The actual calculation, however, is not always consistent with the conceptual model.

It seems that the YMP actually determines the in-package concentration of a radionuclide by either the solubility or the waste matrix dissolution rate without considering mass depletion due to transport out of the waste package (CRWMS M&O 2000b). The potential conservatism is the overestimation of the in-package concentration if the transport out of the waste package is relatively fast. For example, when the near field is subject to a high advection flow rate, the near field may become an "empty house" after the completion of waste matrix alteration, i.e., concentrations (if sorption is reversible) in the waste package as well as in the EBS are all reduce to zero.

It is this in-package concentration of the given nuclide that is used as the boundary condition for the EBS transport (see the next sub-section). Furthermore, this treatment may cause errors in mass balance calculations. That is, the total amount of mass of a given nuclide in the waste package and in the EBS does not add up to the inventory at the given time.

This "baseline" approach was used in TSPA-SR. The concern over the absence of coupling (either directly or indirectly with appropriate assumptions) between the waste form and the EBS was raised by EPRI to the YMP's TSPA-SR report (EPRI 2000). In the SSPA report, this concern is addressed by the attempt to study diffusion from the waste package into the EBS. The effort, however, is focused on evaluation of water film formed on the pathway connecting the waste-form to the EBS. The study also considers potential falling film flow as a consequence of growing film thickness that could give rise to additional advection. Due to lack of information necessary for quantitative evaluation, the direct transport model between the waste package and the EBS is not pursued. Instead, the YMP proposes to study three-dimensional distributions of relative humidity and temperature, and interfacial processes that will produce the needed information for the film study. Therefore, the "baseline" approach is used in the S&ER.

Although the film distribution inside the canister is a potentially important parameter and deserves attention (see the next sub-section), the concern can be addressed more efficiently by solving coupled mass balance equations of the waste form and the EBS and treating the film thickness as a sensitivity parameter.

The YMP assumes that 87% of all waste packages is falling into "dry region" where there is no water flowing through the waste package and EBS, release of radionuclides from the waste form is assumed by diffusion through either SCC and/or larger corrosion patches. Hence, it is important to evaluate this process correctly and to state the solution procedure clearly. Conceptual model and mathematical implementation should be consistent.

6.2.1.3 The Amount of Water inside the Waste Package

The potentially important parameter in determining in-package concentrations is the amount of water inside the waste package. In the mixing-cell approach, the in-package concentration of a radionuclide is inversely proportional to the amount of water. Contrarily, the effective diffusion coefficient for radionuclide transport out of the waste package is proportional to this parameter. A previous sensitivity analysis demonstrated that release of solubility-limited radionuclides from the EBS could be sensitive to the amount of water inside the waste package (EPRI 2000). This study is based on the direct coupling of the waste form and the EBS.

In the YMP's model where the waste form and the EBS are not mathematically coupled, this parameter only affects the in-package concentrations of radionuclides for soluble nuclides. The potential conservatism is that if the amount of water inside the package void space is underestimated, the radionuclide concentrations become overestimated.

For waste packages experiencing "dry release", the YMP assumes that a thin film of water forms the continuous pathway for radionuclide diffusion from the waste form to the EBS. It is believed that the amount of water inside the waste package is based on the film thickness and the surface area. The film thickness used in the calculation, however, is unknown from the given information. In the previous TSPA-VA, the film thickness is assumed to be 1 mm. According to the preliminary study in the SSPA, this thickness would result in falling film flow and would be sustained only if continuous supply of water is guaranteed.

Evaporation of liquid film is not considered. Evaporation may reduce the film thickness even to zero, in which case, release of radionuclides from the waste package into the EBS may stop until continuous film is reestablished. Evaporation of liquid film can take place even when the drift is under isothermal and vapor saturated (relative humidity is 100%) conditions due to vapor pressure lower in the porous media (Zhou et al. 1992).

For the waste packages experiencing "flow-through release", the YMP assumes that the void space inside the canister is "filled with water" (CRWMS M&O, 2000a, p.3-13). The actual amount of water in the void space, however, is also unknown from the given information.

In the SSPA report, a model for evaluating the amount of water is presented. The purpose of the modeling, however, is to evaluate the in-package effective diffusion coefficient. The model assumes that the film on the interior surface of the waste package is formed by adsorption of water vapor. Numerical evaluation of the film distribution requires the surface area, which may vary by five orders of magnitude, and distribution of relative humidity. Although no results are generated from the model, the SSPA presents some ideas of effective water saturation, a parameter derived from the film distribution inside the waste package: depending on surface areas and relative humidity, the effective water saturation varies from 10^{-7} to 0.1. The reviewer considers that if the reliable numerical values on the effective water saturation inside the waste package are obtained, the results should be applied to calculate the in-package concentrations, as well as the effective diffusion coefficient for transport between the waste form and the EBS.

The SSPA attempts to address in-package diffusion that is considered more realistic than uniform concentrations in the mixing cell. The approach is to establish the pathway from the waste-form surface to the outer canister that is in contact with the invert. Corrosion products from the structural materials and canister are included in the pathway. In-package transport is assumed to occur by diffusion through the water film on the pathway. Hence, numerical evaluation of the in-package diffusion effect requires the film distribution, as discussed in the previous paragraph.

The reviewer considers that the mixing cell approach within the waste package is reasonable. There are too many uncertainties in evaluation of in-package transport due to heterogeneous processes and interactions of water contact, corrosion, spent-fuel grain boundary distribution, spent-fuel degradation, etc, which may eventually undermine the credibility of modeling results. The consideration of the role of corrosion products, however, is a right direction to go (see Section 6.2.2 for the EBS transport).

6.2.2 EBS Transport

6.2.2.1 Model Simplification

The YMP's EBS transport model and its connection with other TSPA component models are shown in Figure 6-3. This assessment component models transport of radionuclides released from the waste form to the unsaturated zone through the invert.

Near-field and in-drift thermo-hydrological modeling results are used to provide advection velocity through the invert as well as water saturation in the invert, including impact on the flow paths due to drift-shield conditions and flow diversion by backfill. The diffusion coefficient is calculated based on Archie's law and depends on porosity, water saturation, and tortuosity.[1]

FEPs considered in radionuclide transport are:

- Direct contact between the waste form and the invert,
- Diffusive transport, and
- Advective transport.

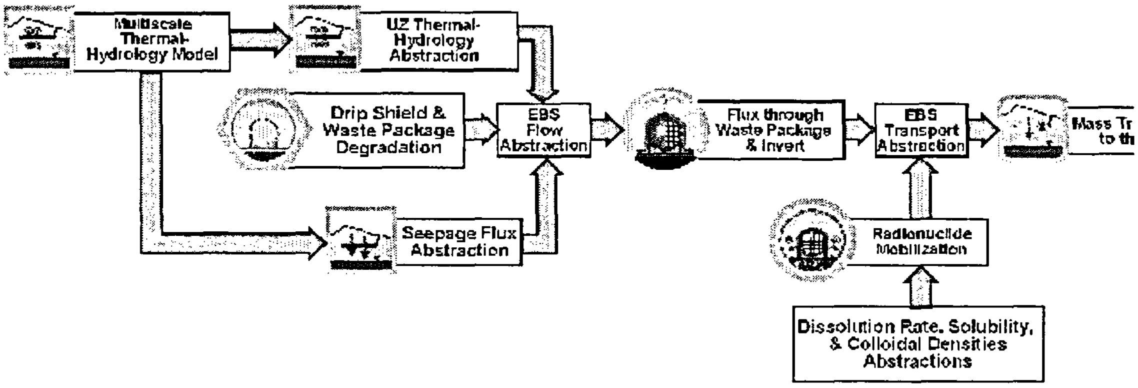

Figure 6-3
The YMP's EBS transport component model (S&ER).

Similar to TSPA-SR, the model is significantly simplified by ignoring the following FEPs:

- Barriers due to corrosion products formed from corrosion of structural materials and the canister (conservative because sorption and resistance to diffusion on corrosion products may retard radionuclide arrival at the invert),
- Sorption in the invert (conservative assumption since including it may cause further delay of some radionuclides exiting the EBS),

---

[1] The YMP has considered a departure from Archie's law to estimate diffusion coefficients at low values of matrix saturation. This lowers the estimate of the diffusion coefficient.

- Radioactive decay and in-growth (could be both conservative and non conservative depending on the radionuclide, but, on the whole, likely to be conservative), and
- Attenuation of colloids released from the waste form via filtration in the invert (conservative).

With all the conservative assumptions, the EBS radionuclide transport in the YMP is simplified to transport of a conservative tracer in the aqueous phase through the invert.

Critics on the conservatism were made to TSPA-SR (EPRI 2000). The YMP addresses the conservatism in the SSPA study, which quantifies sorption coefficients of radio-elements in the invert and corrosion products. These parameters are not used because no modeling of radionuclide EBS transport with sorption is conducted.

6.2.2.2 Solution Method

In the EBS radionuclide transport assessment study (CRWMS M&O 2000c), the YMP uses an existing analytical solution to evaluate the time-dependent diffusion and advection transport of an aqueous phase conservative tracer. The solution is for a transport system of advection and diffusion in one-dimensional, semi-infinite medium with a constant concentration at the boundary. Such a solution assumes the zero concentration at "infinite".

In the YMP's assessment calculation, the YMP used a different solution method to solve the problem of time-dependent diffusion and advection transport of an aqueous phase conservative tracer (TSPA-SR; CRWMS M&O 2000b). This method uses the in-package concentrations of radionuclides (discussed in Section 6.2.1.1) as the boundary condition at the top of the invert and a zero concentration at the bottom of the invert. A zero concentration right below the invert implies that radionuclides arriving at the end of the invert are rapidly removed due to fast flow in the rock below the invert. This assumption is applicable if flow at the bottom of the invert is relatively fast, but conservative if flow at the bottom of the invert is slow or absent.

For example, in the "dry release" cases, there is no flow through the waste package, the invert, and possibly the host rock right below the drift. Furthermore, the host rock below the invert is drier due to seepage diversion on the top of the drift, as shown in Figure 6-4. The S&ER has shown that due to capillary contrast between the rock and the drift, flow of seepage water is diverted to the sides of the drift, leaving a drier shadow zone in the host rock underneath the drift. This portion of rock has a lower saturation than the ambient and either is absent from, or has a very low rate of, flow. Transport of radionuclides in the shadow is controlled by diffusion. In this case, it is conservative to assume a fast sweep of arriving radionuclides at the bottom of the invert.

Overall, the S&ER used the "baseline" TSPA-SR approach in modeling the near field radionuclide release and transport. Addressing conservatism has been attempted, and some progress has been made. The effort, however, has been mostly focused on evaluation of parameters. No attempt has been made to model coupled waste form and EBS transport, and EBS transport in the invert with sorption, decay, and corrosion products included.

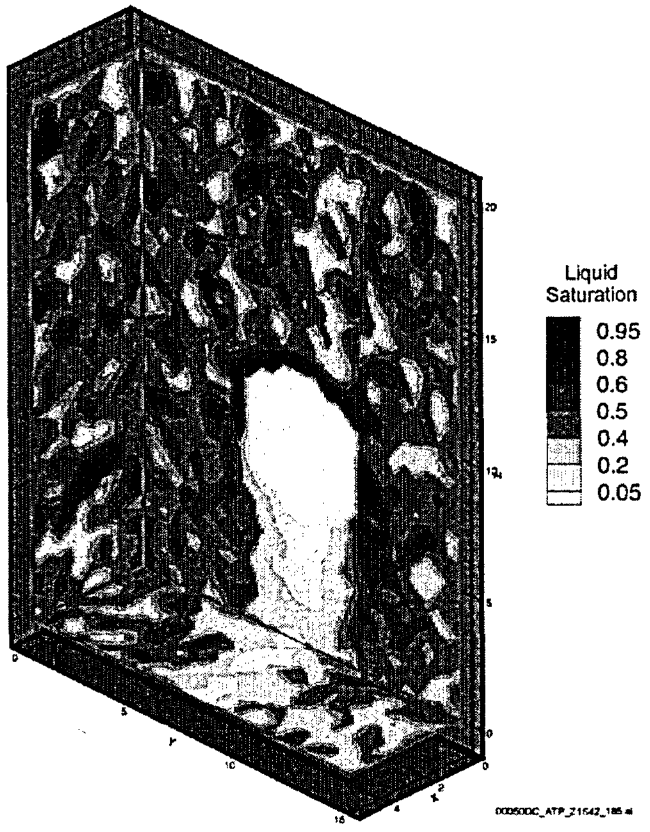

Figure 6-4
Saturation profiles around the drift showing a drier shadow zone below the drift (S&ER, p.4-291).

6.2.3 IMARC's Source-Term Model

6.2.3.1 Comparison with YMP's Model

IMARC's source-term model includes the waste form, EBS components, and a portion of near-field host rock as shown in Figure 6-5. FEPs considered in this system include:

- Water contact with the waste form,
- Degradation of waste form,
- Radionuclide mobilization by dissolution (soluble, solubility-limited, and colloids),
- Radioactive decay and in-growth,
- Transport by diffusion and advection,
- Solubility limit, and
- Sorption.

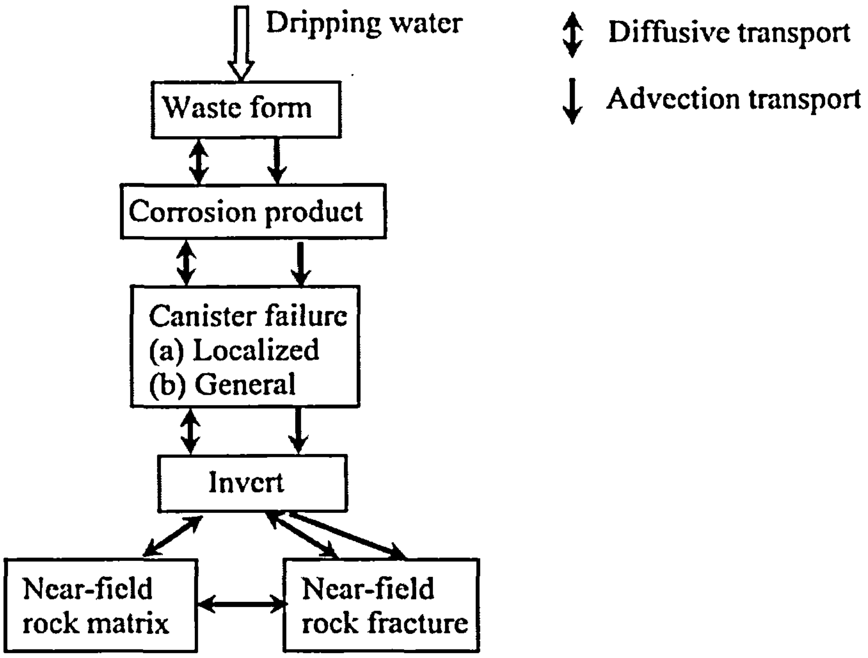

Figure 6-5
Schematic of Compartments within EPRI's IMARC Source-term and EBS Transport Model.

The following list highlights differences between the IMARC and the YMP's models:

- IMARC excludes colloid release from the waste package,
- IMARC uses a water saturation inside the waste package to calculate in-package concentrations and effective diffusion coefficient into the EBS,
- IMARC includes the following FEPs in the EBS transport:
  - Corrosion products,
  - Decay and in-growth in the EBS, and
  - Sorption in the EBS,
- IMARC includes a portion of host rock for the zero concentration boundary condition (the zero concentration is assumed to be held at the end of this portion of host rock),
- IMARC assumes a continuous pathway from the waste form all the way to the near-field host rock, and
- IMARC tracks the system mass balance at each given time (i.e., inventory, within the waste form, within the EBS, and out of the EBS) for a given nuclide.

Using the compartment approach (described in EPRI 1996), mass balance equations for a radionuclide in all the compartments shown in Figure 6-5 are solved simultaneously at each time-step. Concentration changes due to radioactive decay and in-growth are solved analytically at each time step. Transport equations featuring total concentrations of radionuclides after decay/in-growth in each compartment are then solved using the fully implicit method. The concentration is then partitioned into aqueous phase (responsible for transport between compartments), sorbed (reversible sorption is assumed), and precipitated (usually only in the waste form compartment, but included in other compartments). Use of compartment approach proves to be efficient and flexible because the method is able to capture important processes and features in the near field and adjust conceptual models corresponding to changes in design, parameters, or simply due to improved understanding. Complexity of the model and computation expense are usually controlled by the modeler by adjusting resolution and accuracy, etc.

At a given time, system mass balance of a radionuclide is tracked. The system mass balance includes the inventory at the given time, the amount of radionuclides in the waste form, in the EBS, and out of the EBS. For physically correct model with correct numerical implementation and programming, at any given time, the summation of the amount of radionuclides in the waste form, in the EBS, and out of the EBS should be equal to the inventory at this time with only small, tolerable truncation errors (set by the accuracy factor).

Compared with the YMP's model, the IMARC's model is less conservative, more detailed, but not complicated. This demonstrates that realistic assessment is not necessarily complicated, expensive, and unachievable.

6.2.3.2 Recent Revisions to the IMARC Source Term Model

EPRI's IMARC source-term and near-field transport models are covered by a single model code, COMPASS. COMPASS is upgraded in the following two aspects.

Time-Stepping Scheme

The time-stepping scheme for simulating the near-field system adopted by COMPASS is similar to a second order Runge-Kutta or modified midpoint method. By comparing solutions obtained at $t + \Delta t$ by taking a whole step Δt to those obtained from taking two half steps of length $\Delta t/2$, the solver detects behavior of the system at each time step, and thus decides whether to increase or decrease the next step, or abandon the current step and re-do calculation. This method is especially suitable for near-field systems that involve long time periods with coupled dissolution, transport, radioactive decay, and geochemical (solubility and sorption) processes.

The new time-stepping scheme adds an additional feature to the solver that is designed to take advantage of situations where the system approaches steady state. A decision is taken as to whether the two half steps are needed, thus increasing the computational efficiency. The feature is especially advantageous to calculating a system that has a fast transport rate (e.g., high advective flow rate). In this case, the near field becomes an "empty house" at a very early time. The newly implemented method is able to wind up computation rapidly once the "empty house" takes place.

It should be noted, however, for systems involving a large number of nuclides and time-varying parameters, computation may not take advantage of this added feature because such a system may not reach a steady state throughout the PA time period.

Incremental Cumulative Release

The previous version of COMPASS calculated instantaneous release rates of radionuclides at the near-field and far-field interface at a given output time. This treatment is consistent with flux continuity across the interface. In IMARC, however, output time intervals are generally large and release rates are converted into mixing-cell concentrations using numerical integration of instantaneous release rates and output time intervals. These treatments raise concerns of potential missing of peak release rates and any dramatic changes in release rates due to changes in input parameters. For example, using a time step of 1000 years will be difficult to capture the effect of waste-form alteration time of 500 years.

In order to accommodate IMARC's time-stepping approach, a feature is added to the new version of COMPASS, in which incremental cumulative release of radionuclides is output for the far-field model calculations.

Specifically, at time t_n, incremental cumulative release, R_n (mol), for a given nuclide is calculated as:

$$R_n = \int_{t_{n-1}}^{t_n} \dot{R}(t)dt \qquad (6\text{-}1)$$

where $\dot{R}$ is instantaneous release rate (mol/yr) for the given nuclide during Δt, $t_{n-1} = t_n - \Delta t$, Δt (yr) is the output time interval (note, it is different from simulation time step mentioned earlier), and dt (yr) is actually the simulation time step (generally, $\Delta t >> dt$).

The above equation means that numerical integration of instantaneous release rate is carried out using simulation steps that are much smaller than the output steps. This method is more accurate and is able to incorporate detailed histories of the system. Hence, this incremental cumulative release can be directly used in IMARC mixing-cell concentration calculation.

6.3 Colloidal Transport in the Near Field

The purpose of this section is to review the current Yucca Mountain TSPA model for generation and transport of colloids. The current TSPA model is the supplemental TSPA documented by DOE (2001a, 2001b). Aspects of the TSPA dealing with colloids have not been updated appreciably from the TSPA-SR (CRWMS M&O, 2000h).

The DOE TSPA colloid model is intended to evaluate colloids generated from the degradation of HLW glass, commercial SNF, and DOE SNF, and also colloidal transport of radionuclides sorbed on colloids. CRWMS M&O (2000h) states that the abundance of colloids in the waste package will depend on the extent of waste form alteration and the nature of the alteration products formed. Colloid abundance and stability also depend on many environmental factors, including the ionic strength, pH, cation concentrations, colloid content of groundwater entering the waste package from the drift, presence of fulvic and humic acids, and microbe fragments (DOE, 2001a).

Supporting documentation for the DOE TSPA-SR and SSPA reports recognize a large number of processes that should be accounted for in the colloid model. These include flocculation, filtration processes, and accumulation at air-water interfaces. However, in the TSPA-SR these processes were argued to be poorly understood and highly uncertain. The uncertainties were argued to be grouped as uncertainties in suspended colloid concentrations, uncertainties in the nature and extent of sorption to colloids, and uncertainties in colloid retardation. DOE (2001a, 2001b) acknowledges that in the TSPA-SR, uncertainties were addressed by following bounding approaches and choosing conservative inputs and conceptual models. This approach has been retained in the SSPA.

6.3.1 Amounts of Colloids Available

6.3.1.1 SNF Degradation

DOE (2001a, 2001b) briefly discuss the colloidal generation potential of DOE Spent Nuclear Fuel (SNF), Commercial SNF, and Defense SNF during degradation. They note that data are only available for Defense SNF, and state that experimental programs are underway for DOE and Commercial SNF. Preliminary unpublished results are stated to be inconclusive with respect to potential generation of true colloids from such other waste forms or to indicate generation of large numbers of particles, some of which are in the colloidal size range. Formal "generation" process-models for generating either true colloid dispersions or colloid-sized particles are not in the current YMP TSPA model. Consequently, there is the potential that new data might lead DOE to project larger (or smaller) numbers of colloids available for transport than are considered in the current TSPA. Hence, one cannot conclude whether colloid generation from SNF degradation is treated conservatively or not in the current YMP TSPA.

6.3.1.2 Sorbed Radionuclides

In the TSPA-SR, groundwater colloids flowing into the drift are assumed to behave like smectite; this approach is argued by DOE (2001a, 2001b) to be bounding, since smectite has a higher affinity for radionuclides than many other minerals. DOE (2001a) states that this assumption may overestimate colloidal uptake of radionuclides and be conservative. It is conservative only because their subsequent colloidal transport model has such colloids moving faster than solutes. It could be argued that colloidal transport is likely to be slower than that for solutes, so that assuming the colloids are all smectites would actually be non conservative. DOE (2001a) also states that information on colloid mineralogy collected from YMP-area wells may justify use of a mixture of mineralogies including less sorptive minerals, but this has not been done for the sake of conservatism.

DOE (2001a) states that distributions for plutonium irreversibly associated with waste form colloids are log-uniform distributions between

- 10^{-11} and 10^{-6} mol/L (for ionic strength less than or equal to 0.05 M) and
- 10^{-14} and 10^{-8} mol/L (for ionic strength greater than 0.05 M).

The upper range is roughly centered on the bounding concentration of 8x10^{-8} mol/L defined in CRWMS M&O (2001c). There is no discussion by DOE (2001a, 2001b) why the *bounding* value of the concentration identified by CRWMS M&O (2001c) was chosen as the *centerpoint* of the distribution. It could be because there are not enough measurements to state with confidence the highest concentration they have measured so far is, indeed, the very highest plausible concentration. Similarly, the lower range is centered on the minimum concentration measured experimentally, 10^{-11} mol/L (CRWMS M&O, 2001c). The minimum and maximum values of the higher ionic strength range are then plus-or-minus 3 orders of magnitude from 10^{-11} mol/L. Again, there is no discussion by DOE (2001a, 201b) for the basis for this distributionA preliminary review of data presented in Lu et al. (2000) suggests that while K_d values for plutonium and americium are generally higher for montmorillonite than silica, the difference is less than one order of magnitude. For TSPA to compare possible consequences of different colloids, it may be important that the different possible colloids are credibly modeled to capture the overall behavior of the system. The waste form and waste package degradation product colloids, and the uncertainty associated with their parameters (formation, abundance, and sorption), might outweigh any uncertainty in the groundwater colloid parameters.

DOE (2001a) states that corrosion of waste packages will generate large quantities of iron hydroxides that may constitute the most significant source of colloids with the capability of interacting with the radionuclides in solution as they are released from the waste forms. However, the data selected to represent sorption on colloids was not chosen to represent iron hydroxides. As discussed above, smectite was chosen as the representative colloid in terms of sorption.

Concentrations of iron-(hydr)oxide colloids are derived from the Morro de Ferro natural analogue site in Brazil. The measured concentration, 0.25 mg/L, is similar to concentrations of other inorganic colloids found in natural waters at other deep sites. The upper end of the range used in the TSPA, 1.0 mg/L, adopts a four-fold increase relative to the concentration observed at the analogue site.

6.3.1.3 Reversible Sorption on Colloids

In the current colloid model, plutonium and americium are treated as irreversibly attached to waste form colloids. These two radionuclides were considered the most significant radionuclides that could be subject to enhanced colloid-facilitated transport. In addition to plutonium and americium, two other radionuclides, protactinium and thorium, are considered for reversible attachment to waste form colloids and subsequent transport. The fractions of release from colloids associated with other dose-important radionuclides are considered insignificant relative to their dissolved concentrations (DOE, 2001a).

In the TSPA, uniform distributions for suspended colloid concentration were assigned to a combined population of groundwater and corrosion-derived colloids for two different ionic strength ranges. DOE (2001a) states that reasonable ranges for this combined colloid population are log-uniform distributions between

- 10^{-6} and 10^{-1} mg/L (for ionic strength less than or equal to 0.05) and
- 10^{-9} and 10^{-3} mg/L (for ionic strength greater than 0.05 M).

The basis by which these distributions are deemed to be reasonable is not referenced.

6.3.2 Transport Processes

6.3.2.1 Sorption and Adhesion to Solids

Colloid retardation by physical or chemical mechanisms in the waste package is ignored in the TSPA (DOE, 2001b). The same corrosion products that may form iron oxyhydroxides colloids may also effectively filter colloids, for example.

In the unsaturated zone, DOE (2001a) states that colloid filtration was limited to physical straining at tuff layer interfaces. Process model calculations treated colloid filtration as a linear retardation model, although the model itself is described only in rudimentary detail by CRWMS M&O (2000d) as

- accounting for partitioning between colloid and aqueous phases using a K_c model,
- accounting for partitioning of the colloids to the surface using an effective K_d model, and
- colloids are occluded from the matrix, so the colloid transport equations are applied only in the fractures.

Data sources for the retardation of colloids in the unsaturated zone are not fully referenced in any of the primary reference documents (CRWMS M&O, 2000d; DOE, 2001a; DOE, 2001b). In the saturated zone, DOE (2001a) states that colloid retention by the alluvium was modeled as a simple reversible retardation model, with values based on a simple K_c model for colloid sorption and a K_d model for radionuclide sorption. Sorption properties were derived from single-well tracer tests using microspheres. As microspheres can be expected to have significantly different sorption behavior than natural colloids, the technical basis for colloid sorption remains limited. In both unsaturated and saturated media, differing conceptual models of colloid-facilitated transport were implemented for irreversibly sorbed colloids and for reversibly sorbed colloids (DOE, 2001b).

DOE (2001a) describes consideration of three types of colloids: waste-form colloids, iron-(hydr)oxide colloids, and groundwater colloids. They state that in their model, waste-form colloids may have irreversibly attached or reversibly attached radionuclides. The iron-(hydr)oxide and groundwater colloids have only reversibly attached radionuclides. The irreversibly sorbed radionuclides are assumed to be generated only from DOE HLW glass (DOE, 2001b, p 3-37), with colloids from all other sources assumed to be associated with reversibly sorbed radionuclides. The majority of reversibly sorbed radionuclides on colloids are assumed to be generated from spent nuclear fuel.Irreversible colloids have the fastest transport in the base-case UZ transport model, with 50 percent of plutonium irreversible colloids reaching the water table in about 500 years for present-day climate (DOE, 2001b). In comparison, the reversible colloids have the slowest transport in the model, taking about 300,000 years to reach a 50-percent breakthrough for plutonium reversible colloids. This occurs despite the wetter glacial-transition climate is in effect for most of that period. Only 70 percent of the plutonium reversible colloids reach the water table within 1 million years (DOE, 2001b).

CRWMS M&O (2000e) states that the conceptual model for colloid-facilitated transport in the alluvium is essentially the same as in fractured tuffs. Colloids are assumed to transport only in advective water, and colloid attachment and detachment onto alluvial surfaces are described by first-order rate expressions. CRWMS M&O (2000e) also states that because no site-specific data for colloid transport in the alluvium are available, filtration theory and literature data were used to obtain distributions or bounds for attachment and detachment rate constants.

In the saturated zone, approximately 20 percent of all realizations have transport times of less than 1,000 years for irreversible colloids (DOE, 2001b). Reversibly sorbed colloids have longer travel times associated with the interchange on sorbed contaminants between colloid, aqueous, and solid phases.

6.3.2.2 Air-Water Interface Adhesion

Colloids adhere strongly to the interface between air and water (Abdel Fattah, 1997; DOE, 2001a). This process is omitted from the TSPA, with the argument that such omission is believed to be conservative. This belief stems from arguments that air-water interfaces are likely to be stagnant in field conditions, leading to an additional retardation mechanism. This assertion does not account for potential enhancement of mobility on gas bubbles, as discussed by Wan and Tokunaga (1999). While this phenomenon seems unlikely to have a dramatic effect on the overall transport results for the TSPA, the current justification for its omission is weak.

6.3.2.3 Microbial Effects

Microbial effects have been ignored. DOE (2001a) states that these effects might include (1) organic coatings on mineral colloids, which would tend to sorb radionuclides as well as destabilize the colloid suspension, and (2) development of colloids comprising monocellular microbes and fragments, which could sorb and transport radionuclides. Thus, either of two competing processes, one that encourages colloid mobilization, another that encourages colloid agglomeration and flocculation, may prevail (DOE, 2001a). It is uncertain which process would dominate at a particular location or point in time within the repository. Consequently, it is unclear whether the omission of microbial effects is conservative or not.. Inclusion of microbial effects on colloid transport seems unlikely to have a strong impact on the overall TSPA results, but the technical basis for their exclusion is currently weak, and needs improvement.

6.3.2.4 Thermal Effects

Thermal effects on colloidal transport are stated by DOE (2001a) to be unknown, but that colloid stability is generally expected to decrease with increasing temperature. DOE (2001a) also notes that actinide and metal sorption onto metal hydroxide colloids tends to increase with temperature. Sorption of uranium, neptunium, plutonium, and americium on hematite, montmorillonite, and silica increase roughly one order of magnitude as temperature increases from 20º to 80ºC in J-13 well water for 10-day runs (Lu et al. 2000). Thermal effects are omitted from the TSPA model.

6.3.3 Consequences of the Colloid Model

Irreversible colloids have the fastest transport in the base-case UZ transport model, with 50 percent of plutonium irreversible colloids reaching the water table in about 500 years for present-day climate (DOE, 2001b). In comparison, the reversible colloids have the slowest transport in the model, taking about 300,000 years to reach a 50-percent breakthrough for plutonium reversible colloids even though the wetter glacial-transition climate is in effect for most of that period; only 70 percent of the plutonium reversible colloids reach the water table within 1 million years (DOE, 2001b). This behavior is the result of interchanges of the reversibly sorbed radionuclides from the colloid to the surrounding water, and thence sorption on rocks and soils. That is, when radionuclides remain irreversibly bound to the colloid, they move at the speed of the colloid, but if they desorb from the colloid additional retardation mechanisms come into play.

The two radionuclides that represent greater than 70 percent of the annual dose in TSPA-SR are technetium-99 at earlier times and neptunium-237 at later times. Both of these radionuclides are transported as solute. Consequently, colloid modeling can only influence the remaining proportion of the dose curve. Consequently, the most effect that improved colloid modeling can have on the overall dose curve is to reduce it by 20-30 percent. On the other hand, at long times in the dose curves, when the mean dose rate is larger than at earlier times, this reduction is dose rate can potentially be a significant reduction in an absolute sense. Doses associated with colloid transport are only important in the nominal scenario, which produces limited doses in the first 10,000 years. After that time, significant (tens of mrem yr^{-1}) doses are obtained from the nominal scenario. Doses from colloidal radionuclides are not the highest in the analysis at any time. However, they represent a significant fraction of the total dose at all times. In the TSPA-SR model, at 100,000 years irreversibly bound Pu-239 produces a mean dose of about 70 mrem yr^{-1}. This is only deemed insignificant by DOE because it is exceeded by Np-237 doses at all times.

6.3.4 Summary

DOE has omitted most beneficial effects in transport phenomena from their colloid transport model. The result is likely an extremely conservative representation of the effect of colloids on doses from the Yucca Mountain repository. DOE justifies this conservatism by noting that colloidally transported radionuclides are not the dominant dose contributors in the TSPA-SR model or its successor. While the doses from colloidal radionuclides do not dominate the analysis, they are not insignificant, either. In the TSPA-SR model, at 100,000 years irreversibly bound Pu-239 produces a mean dose of about 70 mrem yr^{-1}. This is only deemed insignificant by DOE because it is exceeded by Np-237 doses by moderate amounts at all times. In their reassessment of neptunium solubility data, DOE has suggested lowering the effective solubility by 2-3 orders of magnitude. It would not take much additional reduction in neptunium doses to make colloid facilitated transport the dominating dose mechanism at long times.

The colloid model applies only to doses from the *nominal scenario*, which are only important after the 10,000-year time cutoff in 40 CFR 197. These doses may not be significant from a regulatory perspective. However, as the TSPA models and parameters evolve in future iterations of the work, it seems likely that colloid-facilitated transport will soon come to dominate the doses at long times, as the Np-237 doses decrease. The compounding conservatisms in the DOE's current colloid model should therefore receive more careful scrutiny.

6.4 In-Package Chemistry Modeling

This chapter focuses on processes leading to early corrosion of the drip shield and waste package. Failure of these EBS components must occur before water can access the waste form and waste-package internal structures (*e.g.*, canisters, baskets and heat conductors). The timing of eventual radionuclide releases to the geosphere thus depends on the time when corrosion of the drip shield and waste package begins and when the waste package fails. In our view, DOE's current estimate of this time may be overly conservative.

6.4.1 Environment on the Surface of the Drip Shield and Waste Package Outer Barrier

Estimates of the minimum post-closure time required for corrosion processes to begin are based on the evolution of temperature (*T*) and relative humidity (*RH*) at the surface of the drip shield (DS) and waste package outer barrier (WPOB). The *RH* is a principal descriptor of the chemical environment because it controls solution chemistry. Model predictions of *T* and *RH* evolution are shown in Figure 6-6 (CRWMS M&O 2000f). It is assumed that corrosion occurs when the *RH* evolves to 50%. This relative humidity corresponds to the deliquescence point of $NaNO_3$, which is assumed to be present on surfaces of the DS/WPOB as a result of earlier complete evaporation/boiling of water entering the drift, and/or dust settling onto the surface from unfiltered ventilation air.

This assumption is said to be conservative (CRWMS M&O 2000g) because it minimizes the time for corrosion to begin, and maximizes the temperature at that time (Figure 6-6). Here, we evaluate the reasonableness of conceptual models, assumptions, data and interpretations of calculated results supporting this assumption.

6.4.1.1 Interpretation of the Master Variable, Relative Humidity

DOE's explanation of how the temporal and spatial evolution of *RH* conditions in the repository controls the onset of corrosion is unclear. The explanation focuses on Figure 8 of CRWMS M&O (2000g), which is reproduced here as Figure 6-7. The relative humidity is treated somewhat differently in relation to the effects of temperature on pure water, and the deliquescence point and boiling point of saturated salt solutions. Our interpretation of these differences is summarized below. We assume for convenience that the total ambient pressure in the repository = 101.32 kPa (*i.e.*, conditions at sea level rather than at the repository elevation). This assumption does not affect any of the conclusions drawn below.

The relative humidity is given by (CRWMS M&O 2000g):

$$RH = \frac{p_{H_2O}}{\overset{o}{p}_{H_2O}}, \qquad (6\text{-}2)$$

where,

P_{H_2O} stands for the partial pressure of water vapor, and

$P^{o}_{H_2O}$ represents the equilibrium partial pressure of water vapor, *i.e.*, the equilibrium vapor pressure.

Equation (6-2) is used to calculate the relative humidity at the DS/WPOB surface (CRWMS M&O 2000g). In this case:

- P_{H_2O} refers to the actual vapor pressure at the surface, and
- $P^{o}_{H_2O}$ denotes the equilibrium vapor pressure of pure water at the temperature of the surface.

Equation (6-2) also determines the *RH* of various salts at their boiling point temperature. The boiling point temperature is the temperature at which the equilibrium vapor pressure of a solution equilibrated with the salt is equal to the total pressure. In this case:

- P_{H_2O} stands for the equilibrium vapor pressure of the saturated salt solution at the boiling point temperature and total pressure of interest, and
- $P^{o}_{H_2O}$ represents the equilibrium vapor pressure of pure water at the boiling-point temperature.

Equation (6-2) also determines the *RH* of various salts at their deliquescence point. The deliquescence point defines the minimum *RH* at which a salt will absorb water vapor to form a saturated solution. At the deliquescence point:

- P_{H_2O} denotes the equilibrium vapor pressure of the saturated salt solution at a given temperature and total pressure, and
- $P^{o}_{H_2O}$ stands for the equilibrium vapor pressure of pure water at the same temperature.

The different meanings attributed to *RH* noted above are consistent with one another if it is assumed that: 1) total pressure = 101.32 kPa at any location in the repository over the time period of interest, and 2) total pressure = P_{H_2O}. The *RH* at the DS/WPOB surface is then less than 1 if the surface temperature exceeds temperatures elsewhere in the repository (*e.g.*, 100°C, see below) because the equilibrium vapor pressure then exceeds 101.32 kPa. The curve representing such conditions is labeled in Figure 6-7 as "Max *RH* Boiling Point 100°C".

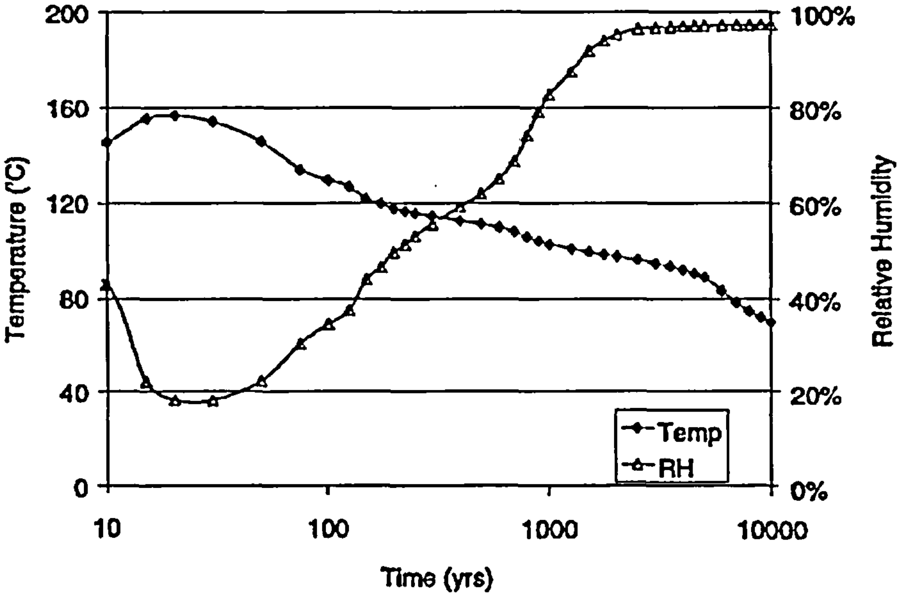

Figure 6-6
Predicted temporal evolution of temperature and relative humidity at the waste package surface (CRWMS M&O 2000f, p18).

The *RH* at the boiling point temperature is also constrained by the requirement P_{H_2O} = total pressure = 101.32 kPa. Relative humidities for several salts under these conditions are plotted in Figure 6-7. As can be seen, all the data lie on the *RH* curve for pure water. This indicates that the effect on *RH* of a highly concentrated salt solution is negligible compared to the effect of increasing temperature. In other words, the increase in equilibrium vapor pressure resulting from an increase in temperature is much greater than the reduction in vapor pressure caused by high electrolyte concentrations in a saturated salt solution at the same temperature. The *RH* at the boiling point is also the deliquescence point because the equilibrium vapor pressure of the salt solution is then equal to the total pressure at the salt's boiling point temperature. The deliquescence points shown in Figure 6-7 at temperatures other than the boiling point seem irrelevant to DOE's discussion.

The assumption that the total pressure in the repository is equal to the ambient nominal atmospheric pressure at the repository horizon (89.1 kPa, approximated in the above discussion as 101.32 kPa) is clearly stated by DOE (CRWMS M&O 2000g, p44). The associated assumption that the partial pressure of H_2O is equal to the total pressure is less clearly stated, however. This condition is noted in Section 6.2.3 of CRWMS M&O 2000g, p49), but not in the list of assumptions discussed in Section 6.5.5. It is also noted in Section 6.2.3 that the relative humidities shown in Figure 6-7 by the curve labeled "Max *RH* Boiling Point 100°C" are calculated assuming that the partial pressure of water vapor in the drift is no higher than the equilibrium water vapor at the temperature of the drift wall. This location apparently refers to the location of the 100°C isotherm.

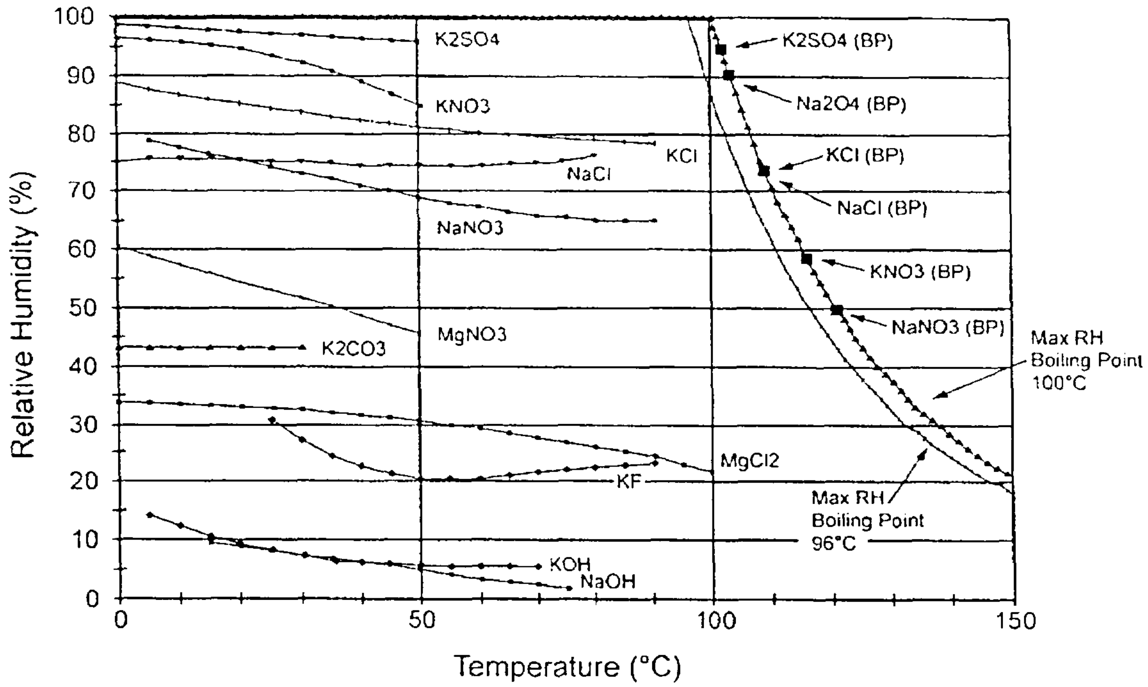

Figure 6-7
Plot illustrating the effect of temperature on the relative humidity of pure water (curves labeled "Max *RH* Boiling Point 100°C and "Max *RH* Boiling Point 96°C) and the deliquescence points and boiling points for several pure salts (CRWMS M&O 2000g, p57).

An alternative approach is to treat evaporation/boiling of water on the DS/WPOB surface as a diffusion-controlled process in which the partial pressure of water vapor in a volume of gas immediately adjacent to a droplet or film of water undergoing evaporation/boiling is controlled by the vaporization rate and the flux of water vapor toward cooler regions of the repository. Diffusion-film models of gas mass transfer across the liquid-gas interface (*e.g.*, Stumm and Morgan, 1996, p241) may be applicable under these conditions. It is assumed in such models that stagnant boundary layers of liquid and gas exist at the gas-liquid interface. The boundary layers lie between the gas-liquid interface and regions of the gas or liquid phase that are well mixed. Gas transfer across the interface is then controlled by chemical reaction (*e.g.*, vaporization) and diffusion through the boundary layer. In the present case, diffusion-film models may indicate that a gradient exists in the partial pressure of water vapor extending from the gas-liquid interface to the bulk gas phase. If so, a gradient in relative humidity would also exist with *RH* values equal to 1 at the interface and decreasing to values shown in Figure 6-7 at the boundary of the surface film and bulk phase. Scoping calculations are recommended to determine if this approach is more realistic than that used by DOE. If so, DOE's assumption that corrosion begins when the *RH* rises to 50% may be overly conservative.

6.4.1.2 Mineralogy of Precipitates/ Salts

The mineralogy of precipitates resulting from the evaporative concentration of perched groundwater and unsaturated-zone porewaters is an important constraint on the time when corrosion of the DS/WPOB can begin. Other salts entrained in ventilation air may also enter the repository. They are not considered here because filtration is a relatively simple engineering approach that could be used to ensure that such salts would not come into contact with the engineered barriers.

The chemical evolution and dissolution of salt assemblages is not well understood or easily predicted (CRWMS M&O 2000f, p31). Geochemical models using the Pitzer formalism for activity coefficients can be used to predict changes in mineralogy resulting from the evaporative concentration of aqueous solutions. Such models are limited, for conditions at Yucca Mountain, to relative humidities greater than about 85%, however (CRWMS M&O 2000f, p48). That is, evaporation of average J13 water to a water activity of 0.85 results in a concentrated solution with an ionic strength of about 10 molal, which represents the upper limit in ionic strength for application of the Pitzer model. For relative humidities in the range 85 % to about 18% (see Figure 4-1), DOE assumes that $NaNO_3$ and KNO_3 are the last minerals to precipitate. This assumption is based on the high solubilities and hygroscopic nature of these phases. The assumption is necessary because the evolution in solution compositions over this range of relative humidities cannot be simulated using existing geochemical models.

The assumption (*i.e.*, that $NaNO_3$ and KNO_3 would comprise part of the mineralogy of precipitates formed by the evaporative concentration of Yucca Mountain groundwater) may not be supported by recent experiments. Rosenberg *et al.* (2000) completely evaporated 30 *l* of synthetic groundwater approximating the composition of J13 water, and 30 *l* of a synthetic solution approximating the composition of pore waters from the unsaturated Paintbrush hydrostratigraphic unit. Two experiments were carried out at 85°C for each starting solution. One experiment contained only the solution of interest. The other included 10g of crushed Topopah Spring Tuff. The latter experiments simulate the interaction of evaporating solutions with particles of rock that may coexist with the solutions on the surface of engineered barriers.

Results from the experiments involving synthetic J13 water indicate that KNO_3 and a number of silicates, carbonates, sulfates and halite precipitate when this solution is completely evaporated. The mineralogy resulting from complete evaporation of J13 water in the presence of crushed Topopah Spring Tuff did not include $NaNO_3$ or KNO_3. Results from the experiments involving synthetic pore water from the unsaturated zone similarly indicate the absence of $NaNO_3$ or KNO_3 in precipitates formed by complete evaporation of these solutions. It should be noted that $NaNO_3$ and KNO_3 may have been present in all the precipitates, but in amounts that could not be detected by XRD (~ less than 5 weight percent), and that analysis of such hygroscopic phases is difficult. The experimental results do suggest, however, that $NaNO_3$ and/or KNO_3 will either not precipitate from evaporating solutions at Yucca Mountain, or that they will be present in trace amounts compared to other phases.

The conservative assumption by DOE that $NaNO_3$ and KNO_3 will be present in precipitates coating surfaces of the drip shield and waste package should be reconsidered in light of these experimental results. Alternative assumptions may increase the time required for corrosion of the engineered barriers to begin. If $NaNO_3$/KNO_3 are not present, for example, then a liquid phase should not appear until the *RH* evolves to the deliquescence point of halite (NaCl) (Figure 4-2). As can be seen in Figure 6-7, the *RH* is then about 73%. Referring to Figure 6-6, the *RH* would not rise to this value until about 800 years post-closure, or about 600 years later than is currently assumed by DOE.

If $NaNO_3/KNO_3$ are assumed to be present, but in trace amounts to other precipitates, then the effects of these other precipitates on the deliquescence behavior of the mixed salt system should be evaluated. Deliquescence can apparently occur at higher relative humidities for such systems than for the pure phases $NaNO_3/KNO_3$ (DOE, 2001c, page 4-166). If so, the deliquescence point of the mixture should lie closer to the deliquescence point of the predominant phase in the mixture than phases that occur in trace amounts. Although DOE asserts that selection of $NaNO_3/KNO_3$ in their model is conservative because *RH* values at the deliquescence point are then minimized, a review of recent research on the boiling point properties of mixed-salt systems could provide the basis for a more realistic and defensible model. It is anticipated that the more realistic model would raise the deliquescence point of the salt mixture, thus delaying the time when corrosion of the engineered barriers can occur .

6.4.2 Chemical Divides

The concept of chemical divides is used to estimate the compositions of brines that evolve from dilute solutions by evaporation (CRWMS M&O 2000g, p60). The concept is based on the observation that *"whenever a binary salt is precipitated during evaporation, and the effective ratio of the two ions in the salt is different from the ratio of the concentrations of these ions in solution, further evaporation will result in an increase in the concentration of the ion present in greater relative concentration in solution, and a decrease in the concentration of the ion present in lower relative concentration"* (Drever, 1982, p. 203.). Rosenberg *et al.* (2000) invoke this concept to explain how a Na-HCO_3-CO_3 alkaline brine could evolve by evaporation of J13 water (as observed in their experiments), and how a near-neutral Na-Ca-Mg-Cl brine could evolve by evaporation pore waters from the Paintbrush hydrostratigraphic unit (also as observed in their experiments). Although chemical divides probably oversimplify details of the chemical evolution of extremely concentrated solutions, they are useful in explaining the general trends in solution chemistry that result from extensive evaporation.

DOE's application of chemical divides to predict brine compositions generated by evaporation/boiling at the DS/WPOB surface may overlook some important processes that could affect brine chemistry. For example, if particles of host rock or "dust" (deposited from ventilation air) coexist with the brine, then ion-exchange reactions may remove some cations from solution. Such reactions are invoked to explain why potassium is almost always depleted relative to sodium in saline waters (Drever, 1986, p208). Although Rosenberg *et al.* (2000) did not observe the effects of ion-exchange in their experiments, these authors point out that such reactions may play a more prominent role over the longer term or at higher temperatures. Ion-exchange reactions involving potassium may thus be an important missing component of DOE's model because KNO_3 is assumed to precipitate during the final stages of evaporation, and the mass precipitated partially determines the amount of brine that forms when the relative humidity rises. In this regard, it should also be noted that when brine is re-generated due to an increase in relative humidity, other minerals that precipitated during the previous evaporation cycle would partially dissolve in the brine due to solubility constraints. The dissolution rate of some plausible minerals in such systems (*e.g.*, amorphous silica – see Rosenberg *et al.*, 2000) is slow, which suggests that the evolution of brine compositions could be kinetically controlled. These alternative models based on the concept of chemical divides should be evaluated more thoroughly.

6.4.3 Paragenesis of precipitates/salts

It is implicitly assumed that once highly soluble salts such as $NaNO_3$ and KNO_3 precipitate, subsequent dissolution of these phases is unimpeded by kinetic constraints or other factors (CWRMS M&O 2000f). Experimental investigations of relevant systems (*i.e.*, Rosenberg et al., 2000) indicate, however, that other minerals also precipitate during evaporation. It is conceivable that one or more of these minerals (*e.g.*, amorphous silica) could precipitate late in the paragenetic sequence of precipitated phases, possibly on the surfaces of $NaNO_3/KNO_3$. If so, $NaNO_3/KNO_3$ could be effectively isolated from contact with water vapor in the drift, in which case these salts would not deliquesce when the RH rises to appropriate levels. At present there is no experimental data characterizing the paragenetic sequence of minerals precipitated during complete evaporation of Yucca Mountain groundwater or pore waters. A review of the relevant literature of mineral paragenesis in evaporating systems could help shed light on whether soluble salts could be isolated from the environment by late-stage crystal growth on their surfaces.

6.4.4 Key Recommendation

Scoping calculations using alternative conceptual models of evaporation/boiling of water on the DS/WPOB surface are recommended because the results of such models may sensitively affect the container lifetime. The alternative models will be used in place of the overly conservative model adopted by DOE, which assumes that the partial pressure of water vapor is everywhere the same in the repository and is controlled by the equilibrium vapor pressure at 100°C. The alternative models will instead treat evaporation/ boiling as a coupled evaporative-diffusion process where the relative humidity at the DS/WPOB surface is controlled by the equilibrium vapor pressure at the higher surface temperature and the diffusive flux of water vapor outward to cooler regions of the repository. The objective of the calculations will be to evaluate whether the relative humidity in a layer of the gas phase immediately adjacent to liquid surfaces that is controlled by such coupled evaporation/diffusion processes is greater than the relative humidity predicted by DOE. If so, the relative humidity predicted by DOE may be overly conservative because it is too low, thus minimizing the time that corrosion can begin by deliquescence of $NaNO_3/KNO_3$ salts.

6.5 Source-term Data

Table 6-1 shows parameters and base case values for the COMPASS source-term code (see Section 6.2 of this report) that is utilized within IMARC. Most parameters used in IMARC's source-term code are to be kept unchanged. Recommended changes in a few parameters are explained below.

Table 6-1
Summary of EPRI Source-Term Code Parameters

Table 6-1(a) Physical Parameters

Component	**Porosity**	**Density $[\text{kg/m}^3]$**	**Water Saturation**	**Diffusion Coefficient $[\text{m}^2/\text{s}]$**
Waste form	0.239	0.0*	0.01	10^{-9}
Corrosion Product	0.42	5260	0.35	10^{-10}
Degraded Canister	0.42	3047	0.4	10^{-10}
Invert	0.545	2250	0.13	Derived**
Fracture	1.0	2250	0.05	5.35×10^{-10}
Matrix	0.12		0.88	5.35×10^{-11}

*: No sorption is considered in the waste-form compartment so density is not needed for this compartment.
**: Derived based on invert water saturation using empirical equation from Conca and Wright 1992 (Conca, J., and J. Wright, "Diffusion and Flow in Gravel, Soil, and Whole Rock", *Applied Hydrogeology*, Vol.1, No.1, 1992).

Table 6-1(b) Geometry Parameters

Parameter	Unit	Value
Waste-form volume	m^3	5.161
Corrosion-product volume	m^3	2.253
Inner canister radius	m	0.785
Outer canister radius	m	0.835
Canister length	m	5.276
Invert thickness	m	0.606
Near-field rock thickness	m	5
Near-field fracture aperture	m	0.00018
Near-field fracture spacing	m	0.31

Table 6-1(c) Nuclide Data

Nuclide	Daughter	Half Life [yr]	Inventory [mol]	Fraction in Gap
Se-79		1.13E6	1.10E-1	0.03
Tc-99		2.15E5	7.33E+1	0.002
I-129		1.59E7	1.30E+1	0.03
Cs-135		3.00E6	2.64E+1	0.03
Zr-93		1.50E6	8.20E+1	0.0
Nb-94		2.00E4	4.51E-1	0.0
Sn-126		1.00E5	1.93E+0	0.0
Pu-239	U-235	2.44E4	1.96E+2	0.0
U-235	Pa-231	7.10E8	3.92E+2	0.0
Pa-231		3.30E4	3.07E-9	0.0
Pu-240	U-236	6.58E3	8.11E+1	0.0
U-236	Th-232	2.34E7	1.78E+2	0.0
Th-232		1.4E10	8.3E-10	0.0
Am-241	Np-237	4.32E2	3.59E+1	0.0
Np-237	U-233	2.14E6	5.53E+1	0.0
U-233	Th-229	1.59E5	2.25E-4	0.0
Th-229		7.34E3	5.47E-8	0.0
Pu-242	U-238	3.79E5	1.59E+1	0.0
U-238	U-234	4.51E9	3.42E+4	0.0
U-234	Th-230	2.47E5	8.94E+0	0.0
Th-230	Ra-226	7.70E4	7.03E-4	0.0
Ra-226		1.60E3	8.54E-8	0.0
Cl-36		3.00E5	9.90E-2	0.0

Table 6-1(d) Sorption Coefficient*

Element	Near-field Rock K_d [m^3/kg]	Corrosion-Product K_d [m^3/kg]
Se	0	0
Tc	0	0
I	0	0
Cs	0.1	5.1e-1
Zr	1	1
Nb	1	1
Sn	1	1.1e-1
Pu	10	9.9e-2
U	1	2.0e-3
Pa	1	5.0e-2
Th	10	11
Am	10	11
Np	1e-3	9.7e-4
Ra	0.5	3.0e-1
Cl	0	0

*: no sorption credit is taken for the waste form and degraded canister.

Table 6-1(e) Infiltration Rate Data

Parameter	Unit	Value
Fraction of dripped canister top surface area	-	0.005
Infiltration Rate	[mm/yr]	See climate/infiltration chapter

Table 6-1(f) Containment Data

Parameter	Unit	Value
Inventory start time	yr	0
Failure time	yr	See containment chapter
Waste-form alteration time	yr	1000
Cladding failure history	Fraction vs. yr	See containment chapter

6.5.1 Physical Properties

The near-field rock matrix porosity has been revised by YMP from 0.08 to 0.15, based on a new value and supporting evidence as stated in DOE (2001c). To be consistent with the value used in IMARC's Unsaturated Zone flow and transport model, however, the matrix porosity of 0.12 is to be used in calculations.

For the same reason, values for the following parameters are adjusted in order to be consistent with values used in IMARC's Unsaturated Zone flow and transport model:

Near-field rock density: 2250 kg/m^3;

Near-field rock matrix diffusion coefficient: 3.2×10^{-11} m^2/s; and

Near-field rock matrix saturation: 0.88.

The near-field rock fracture saturation should be changed to 0.05 for the *flow-through scenario*, in which dripping water flows through the canister, invert, and the near-field rock. This value is derived from a process-modeling result published in DOE (2001c). As for the dry scenario, in which no water flows through the drift and the near-field rock below it, it is recommended that the minimum saturation in the fracture, 0.002, be used.

The presence of water within the canister is an important parameter, especially to solubility-limited nuclides. In the *dry-release scenario*(i.e., release only by diffusion, no advective transport), a small amount of water existing as a continuous film on solid surfaces is assumed to form inside the canister due to vapor condensation. In this case, a simple approach is adopted by assuming capillary equilibrium between porous materials inside the canister and the surrounding EBS and host rock. For this purpose, the fracture saturation in the *dry-release scenario*, 0.002, can be used as a reference value. Because porous materials inside the canister are likely to possess less capillary pressure than the fracture, a value of 0.001 is assumed for the saturation inside the canister.

In the *flow-through scenario* (i.e., release dominated by advective transport), water saturation inside the canister depends on water vapor condensation, dripping water flow rate, retention of dripping water due to surface physical and chemical effect of the materials inside the canister, chemistry of water flowing through the canister, etc. Again, without measured or calculated values for this parameter, the simple approach cited above is adopted. In this case, the value of 0.01 is assumed for water saturation inside the canister, based on the fracture saturation used in the same scenario, which is 0.05.

6.5.2 Radioelement Solubility

Figure 6-8 compares the solubility values previously used in IMARC (EPRI, 2000) with those recently derived for the YMP (CRWMS M&O, 2000h; DOE, 2001c). Each radioelement is discussed, and new recommended values (in some cases unchanged from previously recommended reasonable values) for "high", "medium" and "low" IMARC solubilities[2] are tabulated (Table 6-2).

Actinium

Actinium-227 has an unimportant inventory within spent fuel, but may be an important dose-contributing nuclide because of decay-chain ingrowth. Hence, its actual solubility at the fuel surface is probably unimportant to the magnitude of dose rate this nuclide may eventually contribute. A single value for this radioelement equal to the TSPA-SR "low" value, and within the range of previous EPRI values, is recommended.

Americium

Americum-241 and Am-243 are relatively short-lived (half-lives less than 500 years) nuclides initially present in the spent fuel. For containment times on the order of 5,000 years or more, the initial inventories for such nuclides will decay to effectively zero. Hence, these nuclides could be omitted in IMARC calculations for waste packages with containment times of 5,000 years or more, if this would make calculations more efficient. In any case, these nuclides are unlikely to ever represent a significant contributor to dose, even for early-failed waste packages. Therefore, a single solubility value equal to the "low" solubility value of TSPA-SR (and essentially equal to the "medium" value formerly used in IMARC calculations) is recommended.

Chlorine

Chlorine-36 (half life = 3×10^5 years) is an activation product of Cl-35 found as an impurity in zircaloy cladding and fuel matrix. Hence, the inventory of this nuclide is highly variable depending on assumptions regarding impurity level, burnup and fuel type. Chlorine is highly soluble in groundwater and no solubility limit is likely to be reached. Because of this, any relatively high solubility value (greater than 10 kg/m^3, for example) would be sufficient to represent the behavior of this nuclide. It is recommended to use the single TSPA-SR value, which is slightly lower than the previous IMARC values.

---

[2] It is important to remember that if a solubility limit for a radioelement is sufficiently high, the actual mechanism controlling the concentration of the radioelement at the spent-fuel surface may be the dissolution rate of the UO_2 matrix rather than the solubility limit.

Cesium

Cesium is an alkali element that is expected to undergo significant substitution in solubility-limiting mineral phases containing the more abundant alkali elements such as Na and K. TSPA-SR assumes a relatively high, single solubility value for Cs. The less conservative range, previously used in IMARC calculations, is suggested as a better and more likely representation of the behavior of this radioelement.

Iodine

Iodine is a highly soluble element in groundwater. As with Cl, there is no expectation of any solubility control on I, therefore, a single value equal to that of the TSPA-SR is recommended. This value is slightly less than the "low" value previously used in IMARC calculations, but this difference is irrelevant because the release of iodine from spent fuel will not be solubility limited for any of these values

Neptunium

Neptunium-237 is one of the key dose-contributing nuclides and its release rate may be controlled by solubility if it is sufficiently low. There is an enormous and continuing debate on the most reasonable value(s) for Np solubility to adopt for Yucca Mountain conditions. TSPA-SR cites values that essentially match the range of values formerly adopted in IMARC.

More recently, however, the Yucca Mountain Project has suggested that the actual solubility of Np may be much lower, by up to 3-4 orders of magnitude (see Figure 6-9). This supposition is based on Np concentration data obtained from "drip tests" conducted on spent fuel at Argonne National Laboratory. A full review of the ANL tests and interpretations is beyond the scope of this study. The important point is that concentrations from "drip tests" are not reversed solubility tests (i.e., bracketing Np solubility from both over-saturated and under-saturated conditions). Indeed, given the obvious scatter in the "drip tests" results (Figure 6-9), it is questionable whether such data even represent the lower bracket of a true solubility. Hence, it is highly speculative, perhaps even dubious, to identify such measurements as "solubility limits". It is more likely the ANL results indicate concentrations constrained by (1) the limited duration of tests, (2) the actual contact time between collected water and spent fuel, and (3) the surface area of the fuel specimen contacted by water, which may change during the course of the tests.

Nonetheless, Np solubility is one of the most important and sensitive parameters in performance assessment calculations. It is recommended, therefore, that the previous IMARC values for Np solubility (which are essentially identical to TSPA-SR values) continue to be used, and that a set of lower (by 3-4 orders of magnitude) values based on the ANL interpreted "solubility" values be used as a single sensitivity case.

Protactinium

Protactinium, as with Ac, has negligible initial inventory in spent fuel, and may be an important contributor to dose usually by the decay-chain ingrowth of Pa-231 from parent nuclides that have been released from spent fuel and are migrating through the site. The TSPA-SR range in solubilities closely matches the range previously used in IMARC calculations. Use of multiple values is probably unnecessary because the dose contribution for this nuclide will more likely be a function of the solubility of its parent actinides, rather than its own solubility limit. Therefore, a single solubility value equal to the former "medium" value used in IMARC calculations is recommended.

Lead

Lead isotopes represent the end members of the four actinide-decay chains; these isotopes have zero inventories initially in spent fuel. As such, their dose contribution will be constrained not by the elemental solubility of Pb, but the solubility and sorption behavior of the various actinide parents. The TSPA-SR range closely matches that formerly used in IMARC. It is recommended, therefore, that a single value for Pb solubility equal to that for the former "medium" value of IMARC be used.

Plutonium

There are several long-lived isotopes of Pu that need to be considered in safety assessments, hence, Pu solubility is a potentially key parameter. The TSPA-SR range encompasses that of the range formerly used in IMARC, although the TSPA-SR range extends to considerably higher values than thought previously by the YMP. Therefore, the range of solubilities for Pu previously adopted for IMARC calculations is still recommended.

Radium

Radium, like the other decay products radioelements, has a negligibly low initial inventory in spent fuel. Its dose contribution is more likely to be controlled by the solubility and sorption behavior of actinide parent nuclides than the elemental solubility of Ra itself. Therefore, it is recommended to use the single Ra solubility value adopted in TSPA-SR, and matching the value previously used in IMARC calculations.

Selenium

Selinium-79 is found to be a key dose-contributing radionuclide in many safety-assessment programs. Se is a highly soluble, non-sorbing radioelement with a revised half-life of 1.1×10^6 years. As such, its release behavior will follow that of I-129, having similar properties. TSPA-SR does not report solubility values for Se; previous Yucca Mountain references cited in EPRI (1996) indicate a range of values essentially the same as that used previously in IMARC calculations. Because solubility at the fuel surface is unlikely to be a key constraint on this highly soluble radioelement, it is suggested that a single value be used in IMARC calculations.

Technetium

Technetium is a highly redox-sensitive radioelement, with solubility values spanning 8-10 orders of magnitude depending on the redox potential (Eh) prevailing at the surface of spent fuel. For the unsaturated conditions at Yucca Mountain, the Yucca Mountain Project assumes highly oxidized Eh conditions, leading to extremely high solubility values for Tc. Accordingly, TSPA-

SR adopts only a single, high solubility value. Previous IMARC solubility values span a large range because of uncertainty regarding the actual Eh conditions. There has been no new evidence to support more reduced Eh conditions that might prevail within a waste package at Yucca Mountain. In the absence of any new, supporting evidence, it is recommended that the single TSPA-SR solubility value be adopted.

Thorium

The solubility of Th, like U, is important not only as a control on the release of its own isotope nuclides, but also as a potential limit on the dose contributions of decay daughters that will grow in from these Th isotopes. Unlike U, Th is not a redox-sensitive element. The Th solubility values cited in TSPA-SR are somewhat higher than the "high" value used in previous IMARC calculations, and also higher than previous estimates by the Yucca Mountain Project (EPRI, 1996). In absence of compelling evidence to raise the Th solubility, it is recommended to use the previous range of Th solubilities.

Uranium

Uranium solubility can act to limit the release of U isotopes, as well as many decay daughters that grow in as these U nuclides migrate through the repository. The TSPA-SR range of U solubilities closely matches that of the previous EPRI calculations. The somewhat narrower range in the TSPA-SR represents considerable analysis of thermodynamic data, and it is recommended that future IMARC calculations adopt this TSPA-SR range of U solubility values.

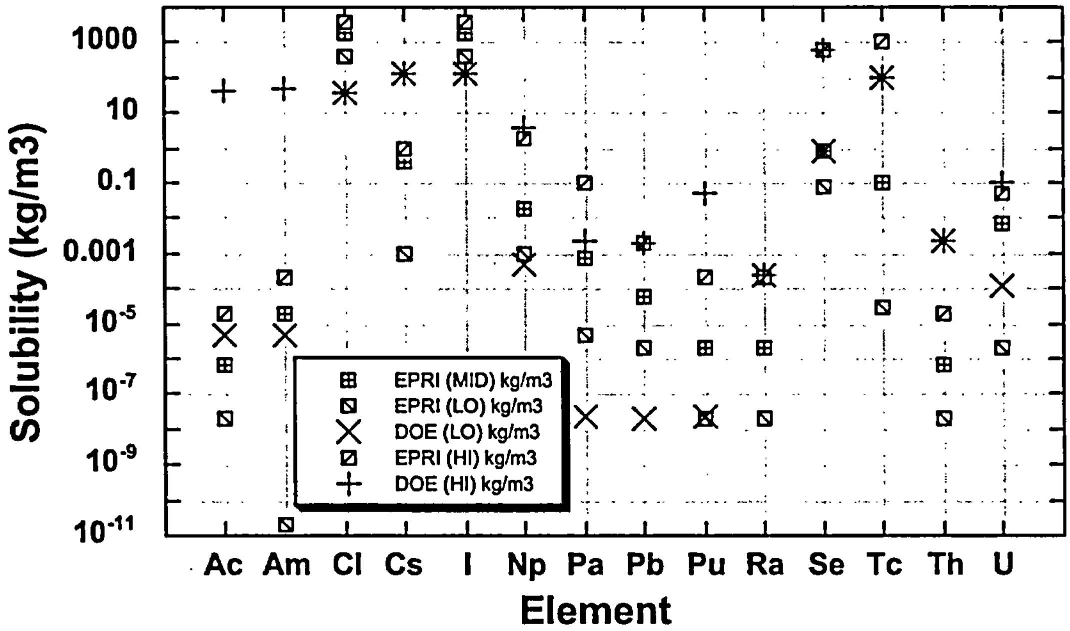

Figure 6-8
Plot of Solubility Ranges for Key Radioelements from TSPA-SR (DOE, 2001c) and Previous IMARC Calculations (EPRI, 2000).

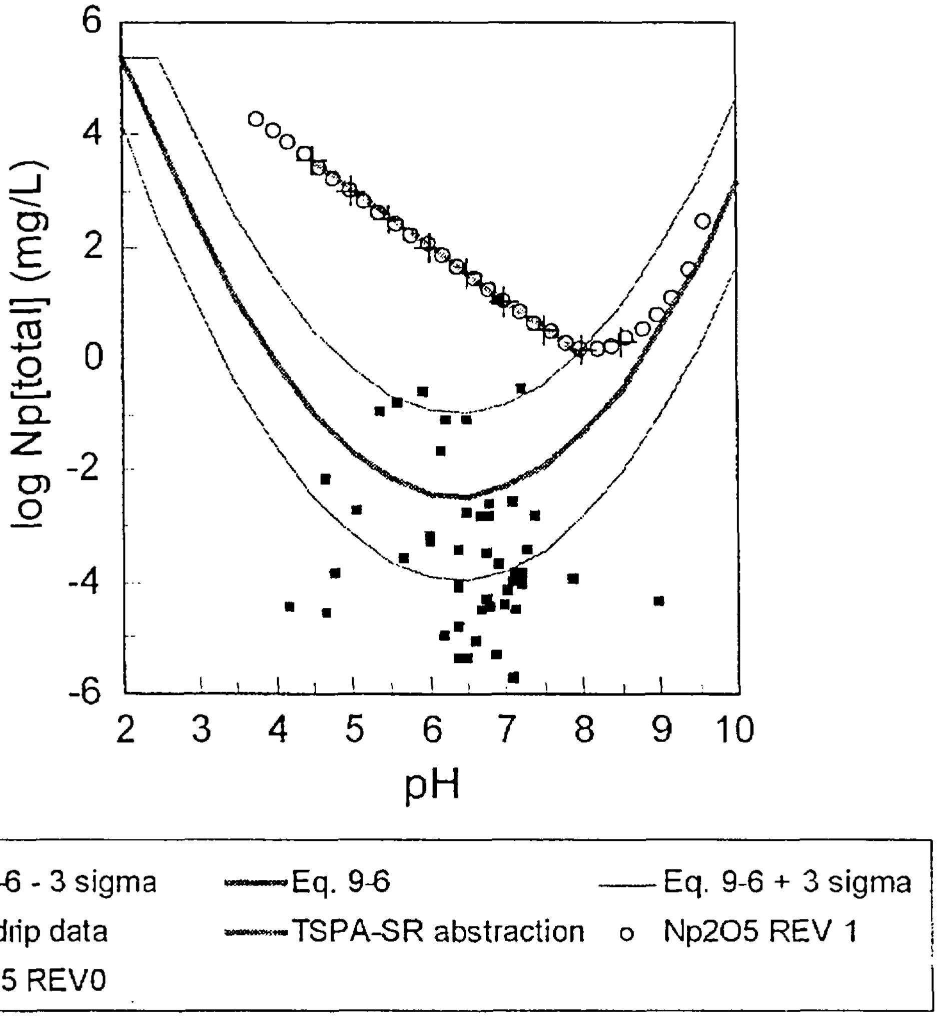

Source: Supplemental Science and Performance Analyses, Volume 1, Figure 9-6b.

Figure 6-9
Interpreted Neptunium Solubility Relationship to pH Derived from Un-reversed "Drip Tests" on Spent Fuel. Previous TSPA-SR (CRWMS M&O, 2000h) values shown for comparison.

Table 6-2
Recommended Ranges for Radioelement Solubilities (in moles/m^3).

Radioelement	High	Medium	Low
Ac*	2.2×10^{-5}	2.2×10^{-5}	2.2×10^{-6}
Am	2.1×10^{-5}	2.1×10^{-6}	2.1×10^{-5}
Cl‡	1.1×10^{3}	1.1×10^{3}	1.1×10^{3}
Cs	7.4×10^{0}	3.0×10^{0}	7.4×10^{-3}
I‡	7.8×10^{2}	7.8×10^{2}	7.8×10^{2}
Np	8.4×10^{0} (4.2×10^{-3})	8.4×10^{-2} (4.2×10^{-5})	4.2×10^{-3} (4.2×10^{-7})
Pa*	3.0×10^{-3}	3.0×10^{-3}	3.0×10^{-3}
Pb*	2.9×10^{-4}	2.9×10^{-4}	2.9×10^{-4}
Pu	8.3×10^{-4}	8.3×10^{-6}	8.3×10^{-8}
Ra*	8.8×10^{-4}	8.8×10^{-4}	8.8×10^{-4}
Se‡	1.0×10^{1}	1.0×10^{1}	1.0×10^{1}
Tc‡	1.0×10^{3}	1.0×10^{3}	1.0×10^{3}
Th	8.7×10^{-5}	3.0×10^{-6}	8.7×10^{-8}
U	2.1×10^{-1}	2.9×10^{-2}	4.2×10^{-4}

* Indicates radioelements whose dose-contributing nuclides are decay daughters, hence, their dose contribution probably is independent of their own radioelement solubility limit imposed at surface of spent fuel.

‡ Indicates radioelements that are expect to be highly soluble, without any actual solubility limit imposed at the surface of spent fuel.

6.5.3 Radioelement Sorption

The previously adopted radioelement sorption data, shown in Table 6-1d, is recommended for use. In addition, the sorption coefficients for Cl and Se with respect to all near-field materials (tuff, corrosion products, etc.) should be made equal to the range in values used for the other key anionic species, I.

6.5.4 Fuel-Matrix Alteration Time

The revised version of COMPASS now imbedded within IMARC can handle calculations of radionuclide release for extremely short (<1000 years) alteration times for the UO_2 matrix of spent fuel. It is recommended, therefore, that the previous "low" (i.e., long) and "medium" values previously assumed for fuel-matrix alteration time be kept. However, a new "high (i.e., short) fuel-matrix alteration time of 1000 years (minimum time step for the IMARC code)[3] is

---

[3] Newly upgraded IMARC source-term code is able to complement effect of IMARC timesteps on shorter alteration times.

recommended for use. This value is supported by EPRI's own fuel dissolution studies in France, and represents a value for which fuel-matrix alteration time (or its inverse, alteration rate) may have an important and demonstrable (albeit, adverse) impact on repository performance.

6.6 References

Abdel-Fattah, A., 1997, *Sorption Kinetics of Hydrophobic, Negatively Charged Microspheres onto a Stagnant Air-Liquid Interface*, Chemical and Nuclear Engineering, University of New Mexico, M. S. Thesis, Dec. 1997.

CRWMS M&O, 2000a, *Waste Form Degradation Process Model Report*, TDR-WIS-MD-000001 REV 00 ICN1, Las Vegas, Nevada.

CRWMS M&O, 2000b, *EBS Radionuclide Transport Abstraction*, ANL-WIS-PA-00001 REV 00 ICN02, Las Vegas, Nevada.

CRWMS M&O, 2000c, *EBS Radionuclide Transport Model*, ANL-EBS-MD-00034 REV 01, Las Vegas, Nevada.

CRWMS M&O, 2000d, *Unsaturated Zone Flow and Transport Model Process Model Report*, TDR-NBS-HS-000002 REV00, March 2000.

CRWMS M&O, 2000e, *Saturated Zone Flow and Transport Process Model Report*, TDR-NBS-HS-000001 REV 00, April 2000.

CRWMS M&O, 2000f, *In-drift Precipitates/salts Analysis*, ANL-EBS-MD-000045 REV 00. Las Vegas, Nevada: CRWMS M&O. ACC: Mol.20000512.0062.

CRWMS M&O, 2000g, *Environment on the Drip Shield and Waste Package Outer Barrier*. ANL-EBS-MD-000001 REV 00. Las Vegas, Nevada: CRWMS M&O. ACC: Mol. 20000328.0590.

CRWMS M&O, 2000h, *Total System Performance Assessment for the Site Recommendation*. TDR-WIS-PA-000001 REV 00. Las Vegas, Nevada: CRWMS M&O. ACC: Mol. 20001220.0045.

CRWMS M&O, 2001, *FY01 Supplemental Science and Performance Analysis*, TDR-MGR-MD-000007, REV 00, Las Vegas, Nevada.

CRWMS M&O, 2001, *Waste Form Colloid-Associated Concentrations Limits: Abstraction and Summary*. ANL-WIS-MD-000012 REV 00 ICN 01. Las Vegas, Nevada: CRWMS M&O. ACC: MOL.20010130.0002.

DOE (2001a), *Yucca Mountain Science and Engineering Report*, DOE/RW-0539, Department of Energy, USA.

DOE, 2001a, *Supplemental Science and Performance Analyses*, Volume 1 Scientific Bases and Analyses" TDR-MGR-MD-000007 REV 00, 2001a.

DOE, 2001b, *Supplemental Science and Performance Analyses*, Volume 2 Performance Analyses" TDR-MGR-MD-000001 REV 00, 2001b.

DOE, 2001c, *Yucca Mountain Science and Engineering Report*, DIRS 153849, Department of Energy, USA.

Drever, J. I., 1982, *The Geochemistry of Natural Waters*. Prentice-Hall, Engelwood Cliffs, N. J., 388p.

EPRI, 2000, *Evaluation of the Candidate High-Level Radioactive Waste Repository at Yucca Mountain Using Total System Performance Assessment, Phase 5*, Electric Power Research Institute, Palo Alto, California.

Lu, N.; Conca, J.; Parker, G.R.; Leonard, P.A.; Moore, B.; Strietelmeier, B.; and Triay, I.R., 2000, *Adsorption of Actinides Onto Colloids as a Function of Time, Temperature, Ionic Strength, and Colloid Concentration*, Waste Form Colloids Report for Yucca Mountain Program (Colloid Data Summary from 1999 to 2000 Research). LA-UR-00-5121. Los Alamos, New Mexico: Los Alamos National Laboratory.

Rosenberg, N. D., Gdowski, G. E. and Knauss, K. G., 2000, "Evaporative chemical evolution of natural waters at Yucca Mountain, Nevada," *Appl. Geochem.*, 16, 1231-1240.

Stumm, W. and Morgan, J. J., 1996, *Aquatic Chemistry*, 3rd ed. Wiley Interscience, New York, 1022p.

Wan, J., and T.K. Tokunaga, 1999, *Sorption of Colloids, Organics, and Metals onto Gas - Water, Interfaces: Transport Processes and Potential Remediation Technology*, DOE research publication, Grant Number: DE-AC03-76SF-00098.

Zhou, W., P. L. Chambré, T. H. Pigford, W. W.-L. Lee, "Evaporation Analysis in Nuclear Waste Boreholes in Unsaturated Tuff," *Scientific Basis for Nuclear Waste Management, a Material Research Society Symposium Proceeding, 1992.*

7

UNSATURATED ZONE AND SATURATED ZONE FLOW AND TRANSPORT

Unsaturated zone (UZ) and saturated zone (SZ) transport are potential natural barriers to radionuclides released from the planned repository. These barriers operate to reduce a potential dose by delaying the release, enabling radioactive decay to operate on short-lived radionuclides, and by diluting the radionuclide concentrations through various dispersion processes. This section of the report examines issues with respect to the conceptualization of the UZ and SZ, and how these issues bear on the selection of transport parameters for IMARC. A theme that will continue here from previous EPRI reports (EPRI, 1998; EPRI, 2000) is our opinion that the current conceptualization of the SZ by the Yucca Mountain Project (YMP) is conservative.

7.1 Yucca Mountain Project Conceptualization of UZ and SZ Transport

Through TSPA-SR (CRWS M&O, 2000a) and SSPA, the YMP has established a conceptual model that yields relative rapid migration of radionuclides through the UZ and SZ. For a nonsorbing species (e.g., ^{99}Tc), initial breakthrough (defined as 5% of the initial concentration) at the water table occurs only a few years after a release from the potential repository in the YMP model, with 50-percent breakthrough between a few hundred and a few thousand years. This fast transport through the UZ occurs because contaminants leaving the engineered barrier system (EBS) enter the fracture network directly. Non-sorbed contaminants are transported to the water table subject to minor interaction with the rock blocks. Mass that experiences some transport through rock matrix moves much more slowly. Thus, nuclide breakthrough at the water table would be bimodal with an early mass arrival related to fast flow in the matrix and a later mass arrival reflecting matrix transport.

There are also indications that the relatively rapid transport of some radionuclides through the UZ is related to the modeling approach. Indications are that the particle-tracking version of the FEHM code, used by the YMP in Total System Performance Assessment-Site Recommendation (TSPA-SR) is conservative – especially for radionuclides that sorb onto tuff minerals, such as neptunium. Travel time for neptunium through the UZ (between the repository horizon and the saturated zone – some 300 meters below the repository) may be one to two orders–of- magnitude longer than that predicted using the existing particle tracking code in FEHM, such that UZ travel time is significant (compared to 10,000 years). The particle-tracking algorithm in the FEHM code needs to be modified to model the interaction between fractures and the matrix in the UZ more rigorously or replaced by another particle tracking code.

In the SZ, transport along a 20 km flow path for a non-sorbed contaminant might occur in as little as 100 years in the YMP model, with a calculated mean transport time of 600 years for the present climate. This relatively rapid transport through the SZ comes from routing flow through widely spaced flowing intervals that provide for minimal attenuation from matrix diffusion or other processes. Thus, for non-sorbing nuclides, the geologic barriers appear to be relatively ineffective in delaying their migration. With radionuclides that sorb (e.g., ^{237}Np), transport times through the UZ and SZ are expected to be considerably larger. For example, ^{237}Np transport through the SZ was calculated to require thousands, to tens-of-thousands of years (BSC, 2001; Vol 2).

The pathway for radionuclide transport through the SZ consists of fractured volcanic rock and likely a limited and, as yet undetermined, leg through alluvium. Generally, flow in the volcanic rock is considered to occur through flowing intervals, which represent a relatively small proportion of the rock volume. This focusing of flow coupled with the small effective porosities, typically assigned to the unit in stochastic simulations, provide rapid mass transport through the fractured volcanic rock (CRWMS M&O, 2000b). Because the alluvium is treated as a porous medium, flow velocities are lower than the fractured volcanic rock. Most simulations involve quite small transverse vertical dispersion, which minimizes dispersion.

The SZ modeling approach treats flowing intervals as effective fractures. This treatment, coupled with the relatively large distance between flowing intervals, means that matrix diffusion will not occur. Overall, then, the combination of relatively large advective fluxes and minimal matrix diffusion, and dispersion means that simulated plumes move quickly with large nuclide concentrations.

7.1.1 Analysis of Changes to the YMP Conceptual Model

One of the interesting features of the SSPA report is an analysis of how changes in the conceptual model might impact UZ/SZ transport. Here, we review the M&O analyses (BSC, 2001; Vol. 2) concerned with (1) effects of a drift shadow zone, (2) no matrix diffusion in the SZ, (3) increased matrix diffusion in the SZ, and (4) minimum flow-path length in the alluvium. In all cases, the stochastic output for the base case in TSPA-SR is compared with a nearly identical simulation in which one process or parameter is altered (i.e., "one off" analyses).

The shadow zone could develop beneath individual waste-emplacement drifts because of the diversion of water around drifts. This zone would be drier than ambient conditions for the host rock with less flow. The impact of this zone on transport is not accounted for in the UZ component of the TSPA model. Radionuclides moving out of the EBS are released directly into the fracture network. This treatment is viewed as conservative because not considering the shadow zone leads to faster releases.

An analysis examined the effect of the shadow zone in performance assessment. This effect was simulated by adding diffusive releases from the EBS into the matrix instead of the fracture network[1]. In effect, the bulk of the releases are required to migrate through the matrix, which increases transport times substantially. The simulation results showed that breakthrough of the mean annual dose was delayed by about 10,000 years and the peak dose was diminished by a

---

[1] The current YMP model assumes that 100% of the radionuclide mass exiting the EBS is added directly to the fracture network.

factor of about two (BSC, 2001; Vol. 2, Figure 3.2.9-1), as compared to the base case. These reductions are attributed to the importance of diffusion in tempering the rate of mass release into the UZ.

An analysis was undertaken to show what effect matrix diffusion was playing in SZ transport. For the SZ, Setting the diffusion coefficient for the rock blocks 10 orders-of-magnitude lower than the base case effectively shut off matrix diffusion. There was no discernable difference between the two sets of results. Essentially, matrix diffusion is not an important process with the conceptual model for flow SZ developed in TSPA-SR. This was an issue recognized in the previous EPRI analysis (EPRI, 2000). With the large parameter ranges in the stochastic simulations, there are many realizations where matrix diffusion would be essentially inoperative. Thus, actually shutting off the process does not change the result.

Another analysis studied how adding matrix diffusion would impact dose calculations. Essentially, the simulation involved reducing the flow interval spacing by a factor of 100. Such interval spacing is comparable to those of the EPRI (2000) analysis. The result was a slight (20%) decrease in the dose as determined in the stochastic simulation (BCS 2001; Volume 2). This result was cited as an example of how a change in a sub-component model can have impact in that model but not on the total system.

The YMP results are different than our previous analyses that showed than matrix diffusion was effective in changing the dose rate and delaying the plume arrival by a factor of two or more in the best situation. In effect, the YMP simulation approach only biased one variable out of several that control matrix diffusion. Changing the statistics on the flowing-interval spacing does not necessarily "turn on" matrix diffusion. Realizations with relatively large ground-water fluxes, low diffusion coefficients, and relatively small ^{237}Np sorption coefficient mostly override the effect of a reduced flowing interval spacing at least for the calculation of the mean annual dose (BSC 2001; Vol. 2). Thus, the sensitivities of matrix remain diluted by many realizations the process is still essentially inactive. In our simulations, many fewer parameters are allowed to vary stochastically. Thus, when matrix diffusion is operative, its impact is felt in all realizations, and thus, more obviously affects model outputs.

The final sensitivity analysis examined the mean annual dose for the TSPA-SR base case compared with the mean annual dose with minimal alluvium along the flow path. The case was meant to examine a situation where there was virtually no alluvium along the travel path. In general, the minimum alluvium case produced a dose that was approximately 10 percent higher and very slightly earlier.

Of all the processes or parameters considered in the YMP model, only the presence of the drift shadow zone appears to influence dose and transport time significantly. Results were apparently not sensitive to the presence/absence of matrix diffusion, the size of the flowing-interval spacing, or the absence of alluvium. In the following section, we question the meaning of this kind of sensitivity analysis.

7.1.2 Discussion of Stochastic Sensitivity Analysis

The previous section discussed the results of the stochastic sensitivity analyses involving changes to the UZ/SZ conceptual model. Beyond the drift shadow zone, it appeared that none of the other (e.g., matrix diffusion) had a significant impact on dose. This result is in contrast to EPRI simulation experiments (EPRI, 2000) that showed generally that transport times in the SZ were sensitive to the extent to which matrix diffusion was operational. The difference in the results occurs because the simulation approaches are quite different from one another. In the EPRI model, most parameter values are fixed as compared to the YMP approach where many more variables are uncertain and allowed to vary stochastically. With this a wide range of parameter values, the relative importance of transport processes like matrix diffusion can be quite different in every realization. In the EPRI modeling the relative importance of parameters is generally fixed by our conceptualization of the system.

Stochastic sensitivity analysis used by YMP could conceal significant sensitivities because finding no sensitivity in risk space does not guarantee that sensitivities are evident in some subset of the realizations. Thus, one must be cautious in the way sensitivities are presented because the realizations are all quite different from one another. It is not clear that one could simply answer the question is matrix diffusion important in controlling doses. The manner in which simulations are run (with a one-off parameter adjustment) does not necessarily "turn on" matrix diffusion in a controllable and quantifiable manner. For example, with matrix diffusion, reducing the flowing interval spacing will not control matrix diffusion if diffusion coefficients are so low that diffusion is not operative or if by chance that diffusion coefficients are so high that no more diffusion is possible irrespective of block size. Thus, reducing the block size by itself is not the same as providing for enhanced matrix diffusion.

Fundamentally, the conceptual model that is developed by YMP for the SZ minimizes the role of matrix diffusion as a process. In the stochastic analysis, many of the realizations would exhibit this behavior because block sizes are large, diffusion coefficients are small, or residence times in the flow system are small. Thus, it is not surprising that with diffusion turned off that there was little difference between the mean annual dose calculated in the TSPA-SR and that calculated without matrix diffusion. With matrix diffusion favored by reducing the flowing interval spacing, we would expect some realizations where matrix diffusion is beneficial and sensitivities exist. One might expect that repository behavior is determined not by ensemble behavior but as one of the individual realizations. A better way to examine sensitivities would be to determine what proportion of the individual realizations were sensitive to the parameter.

7.2 Geochemical Studies

There have been extensive geochemical studies of water in the UZ and SZ. These studies typically involve major ions, stable isotopes, particularly ^{18}O and D, and radiogenic isotopes, tritium, ^{14}C and ^{36}Cl. In studies of the UZ, geochemical information, particularly with respect to the isotopes, has been instrumental in elucidating infiltration and unsaturated flow processes. Geochemical data are also important in assessing the viability of mathematical models developed for the UZ (CRWMS M&O, 2000c).

SZ studies have also made use of geochemical data, but to a much more limited extent than was the case with the UZ. CRWMS M&O (2001; Vol. 1) describes how geochemical data provided evidence of a flow path from Yucca Mountain toward the Amargosa Desert (Figure 7-1). More specifically, this flow path traces groundwater from the proposed repository and Ghost Dance fault southeastward along Dune Wash and southward to the site-model boundary (Figure 7-1).

Many parameters of interest in the geochemical investigations provide direct or indirect age dates on the water but these do not appear to have been utilized in SZ modeling. The following section reviews key geochemical investigations particularly with respect to the age of the water in the SZ.

7.2.1 Key Geochemical Investigations

The framework of geochemical investigations at Yucca Mountain and the Nevada Test Site (NTS) is reviewed in detail in CRWMS M&O (2001). It is beyond the scope of this review to discuss all the papers in detail. However, here we will concentrate on those concerned particularly with the origin of recharge to the SZ, estimates of water age, and calculated groundwater velocities. The work of Claassen (1985) represents one of the early assessments of geochemical data. In looking at both ion and isotopic data in the west central Amargosa Desert, Claassen (1985) concluded that the alluvial aquifer was recharged by the overland flow of snowmelt in or near present-day stream channels, rather than by subsurface flow from highland recharge areas to the north. Much of the recharge was also thought to have occurred during the late Wisconsin time, older than ~ 11,000 years ago).

A study by White and Chuma (1987) interpret much the same data in a different manner. They concluded that ground water in the upper end of the Amargosa Desert originated principally as water in tuffs underlying Fortymile Canyon. They also determined that groundwater in the alluvium was old. Accounting for the effects of reactions on ^{14}C dates, they estimated actual flow velocities of between 3 and 30 m/yr between J-13 and the north central Amargosa Desert (Figure 7-2). These velocities describe the movement of the ground-water along the most permeable pathways.

Chapman et al. (1995) used chemical and isotopic data to define flow paths at the Nevada test site and to estimate ground-water velocities for these flow paths. One of the flow paths at Fortymile Wash is relevant to Yucca Mountain (Figure 7-2). NETPATH modeling determined that the travel time from J-12 to Lathrop Wells was 6875 years and 7589 years from J-13 to Lathrop wells. Although the results are slightly ambiguous, they imply flow velocities of 1.9 to 2.4 m/yr in the fractured volcanic aquifer beneath lower Fortymile Wash. These values compare with the approximate range of 6 to $6x10^4$ m/yr or more that could be generated in M&O simulations, given the range in effective porosity. In the YMP analyses, flow velocities in the fractured volcanic aquifer are determined by the combination of values of recharge and specific discharge. Generally, estimates of specific discharge are still based on the SZ expert elicitations. The large uncertainties in these estimates are considered by considering three discrete cases of high (10x higher), low (10x lower) and medium flux, with the calibrated SZ corresponding to the mean flux case. In the unquantified uncertainty analyses (BSC, 2001; Vol. 2), the range of uncertainty was reduced to a factor of three higher and lower with virtually no change from the previous analyses.

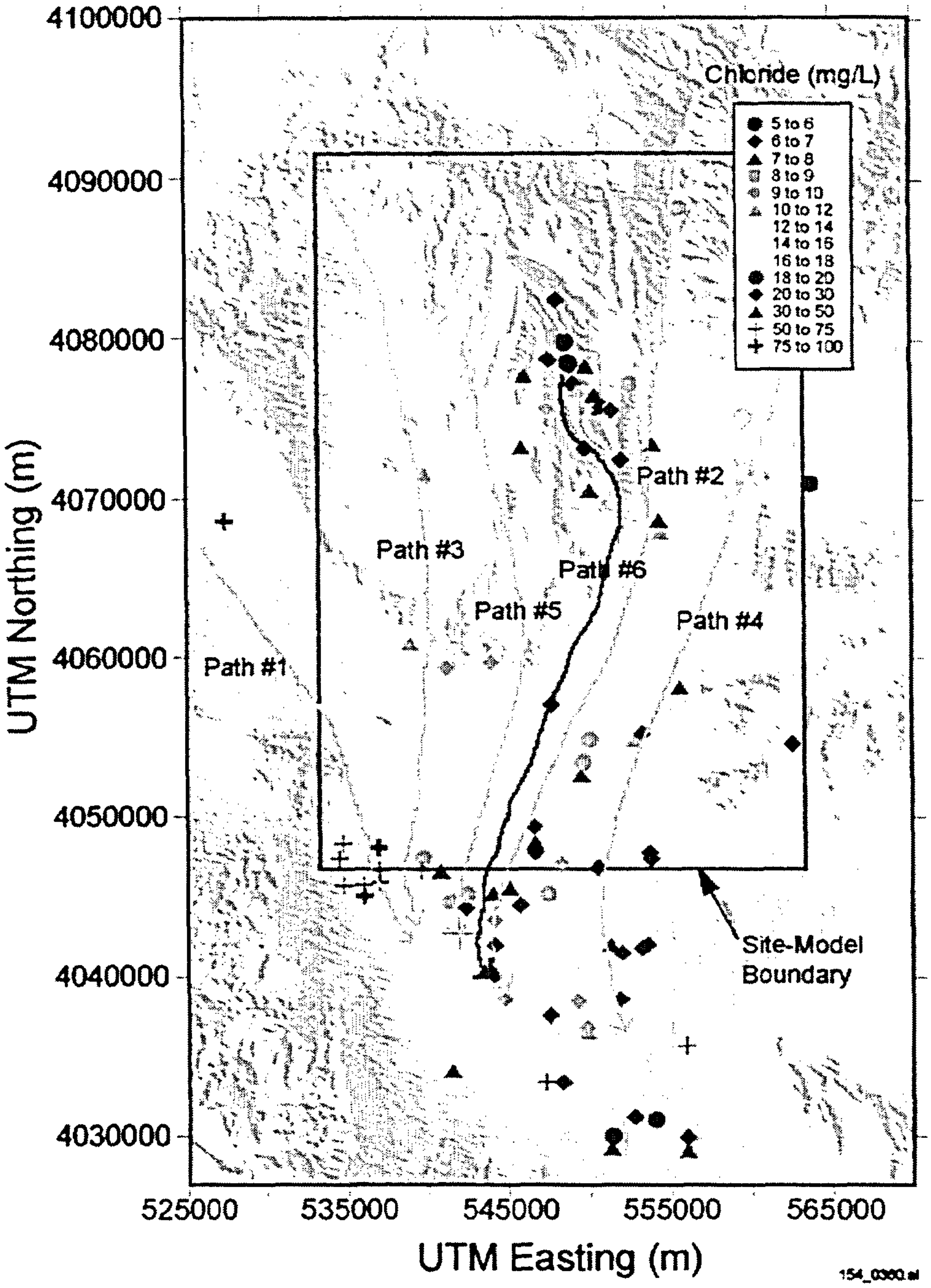

Figure 7-1
Flow paths indicated by geochemical data. Flow path #2 is thought representative of the path followed by a potential plume.

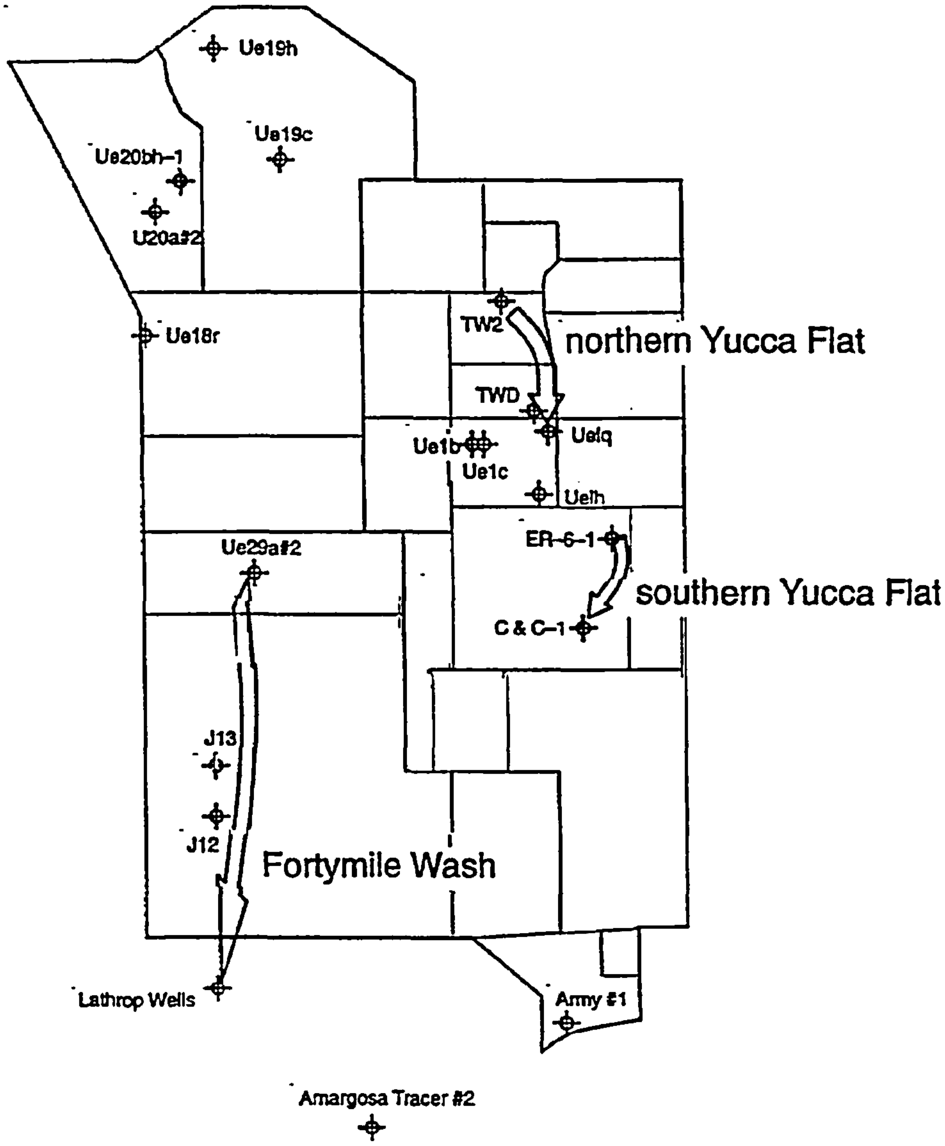

Figure 7-2
Chapman et al. (1995) determined an estimate of flow velocities from J-13 to Lathrop Wells.

CRWMS M&O (2001) presents a comprehensive review and analysis of chemical and isotopic data collected through the years. Of interest in this report is the evaluation of ^{14}C data from Yucca Mountain, Fortymile Wash and Amargosa Valley. The data suggest that ground water in the vicinity of Yucca Mountain was recharged between 10,000 to 19,000 years ago. The report, however, suggests that the wells might not have been located appropriately to provide samples of younger water. The ^{18}O and D data support this conclusion, pointing to recharge during colder climates.

The ages of water samples from along Fortymile Wash generally falls in a range range from 0 to 10,000 years. The youngest samples come from the northern end of the wash (i.e., north of J-12 and J-13). In the Amargosa Desert, south of Highway 95, samples suggest water ages around 10,000 years. The ^{18}O and D data indicate a cooler and more humid climate than present, which is also consistent with this interpretation. In this area also, there are no age trends evident in the direction of flow suggesting that water originated farther upstream (CRWMS M&O, 2001). Thus, in the Amargosa Desert patterns of recharge could have been similar to the conceptual model of Claassen (1985).

Indications are that ground water in the Amargosa Desert was likely recharged in the late Pleistocene, or early Holocene (8,000 to 11,000 years BP), at the latest. The absence of ^{14}C ages less than 9,000 years BP supports the contention that recharge has not been important in the Amargosa Desert near Fortymile Wash during the Holocene.

In general, the geochemical data as presently analyzed are not generally helpful in proving parameter estimates beyond advective velocities. There, however, is some hope that transport modeling coupled with regional ground-water flow modeling would be helpful in evaluating preliminary interpretations from geochemical data and providing other parameter values, like dispersivity. For example, inspection of the data in Figure 1 suggests that transverse dispersion is not particularly efficient in mixing water normal to the direction of ground-water flow. The current EPRI conceptualization of transport in the SZ has limited transverse dispersion, particularly in relation to the length of the plume.

7.2.2 Evaluation of Geochemical Data

A preliminary examination of the isotopic data suggests a different conceptual model than is presently driving near all performance assessment codes. Particularly in the SZ, it difficult to conceive of how a plume of contaminated water could flow through 10,000-year-old water and reach the 18-kilometer boundary in only several thousand years. For example, along Flow Path #2, water at Yucca Mountain appears to be older than water down stream in the Amargosa Desert.

Overall, flow systems appear to be sluggish to the extent that post-Pleistocene recharge has yet to be evident in wells in the north central part of the Amargosa Desert. In other words, the fast transport pathway away from Yucca Mountain southward remains unappreciated or that mixing with older ground water is more complete than current conceptualizations of dispersion would admit. We think that the conceptual models of the SZ require modification to fit age relationships implicit with isotopic data. In the absence of information, the geochemical data could be more reliable than the results of the expert elicitation, which still drives the current conceptualization.

A revised conceptual model could have these implications:

1. Flow velocities would be much lower than current expectations. Exactly why this might be the case is uncertain. One possibility is poor communication among the flowing intervals. Cross sections in CRWMS, M&O (2000b) indicate broad variability in the occurrence of flowing interval with respect to depth and or stratigraphic unit. Another possibility is structural disruption in the continuity of layers in the tuff units due to displacement along

normal faults could provide. East-west cross sections across Yucca Mountain show large numbers of major and minor faults that disrupt the lateral continuity of units. Finally, the major fracture systems might lead to three-dimensional flow effects to an extent that remains undiscovered because of the scarcity of present hydraulic information. In effect, enhancement of vertical flow would create lower net-horizontal velocities, while still allowing for the relatively flat hydraulic gradients found downstream.

2. The heterogeneity in water ^{14}C ages at Yucca Mountain suggests that the likely pattern of future plume migration will be much more complicated in the SZ than is presently represented by flow tube and similar models. The origin of this heterogeneity may be related to variability in recharge rates accompanied by limited dispersive mixing, or complexity in the transport related to a heterogeneous hydraulic conductivity field. Moreover, sampling generally has not discovered a body of post-Pleistocene water at Yucca Mountain. One possibility is that modern recharge could be getting lost at the scale of sampling because (1) fast fracture flow is a small fraction of all recharge and (2) in the zone of saturation, this new water would form a relatively thin wedge on top of older ground water. Thus, modern recharge is not displacing the old ground water but mixing in a narrow zone near the water table.

3. During pluvial events, there is likely more recharge to the alluvial aquifer along Fortymile Wash than occurs currently. The much more limited present-day recharge along Fortymile Wash is gradually displacing the older Pleistocene/Late Holocene waters southward.

4. Under present climatic conditions, potential plumes from Yucca Mountain should not impact major pumping areas south of Highway 95 for many thousands of years. Under the present climatic regime, modern recharge is not evident in the SZ. If pumping continued through a period of climate change, then conditions could change. While more recharge would be available at Yucca Mountain, there would be some component of local, uncontaminated water available to wells.

7.3 Simulation Parameters for IMARC Runs

This section presents the simulation parameters used for the base-case runs with IMARC. The unsaturated flow parameters are summarized in EPRI (1998). The parameter set for the SZ (Table 7-1; 7-2) is similar to the parameter set used in EPRI (2000). One important change is a reduction in the specific discharge to 0.15 m/yr and an increase in the effective porosity to 0.06. Both values lie in the range of uncertainty for these parameters as utilized in YMP (CRWMS, M&O, 2000b). However, the selected specific discharge is lower than their medium flux case (0.6 m/yr), and the selected effective porosity is toward the high end of their range (10^{-5} to 10^{-1}). Overall, these changes and other assumptions provide a linear ground water velocity of 10 m/yr at the upstream side boundary. The reduction in this advective velocity is justified on the basis of isotopic data (White and Chuma, 1987; Chapman et al., 1995). Recharge through the top of the flow system increases the flow velocity down stream in the system. At the minimum velocity, transport times for an unretarded contaminant would be of the order of 1800 years in the SZ. Later, sensitivity analyses with IMARC will examine even slower flow velocities.

As has been the case with previous analyses with IMARC, dispersivity values in the longitudinal and horizontal transverse directions are relatively small. Where we differ from other interpretations is in considering the possibility for the vertical transverse dispersivity to take on a comparatively high value that facilitates significant vertical mixing. The most recent justification of these values is provided in EPRI (1998).

Table 7-1
Summary of base hydraulic and transport parameters for the SZ, October 10/01

Parameter Type	Parameters	Volcanic Rocks	Alluvium
Matrix	Effective Porosity	0.19	0.15
	Bulk density (kg/m^3)	1940	1910
	Diffusion Coefficient (m^2/s)	3.2×10^{-11}	0
	Radius Matrix Block (m)	0.75	--
Flowing Interval	Effective Porosity	1.5×10^{-2} or $6.0 \times 10^{-2}/4$[a]	--
	Diffusion Coefficient (m^2/s)	5×10^{-10}	--
	Bulk Hydraulic Conductivity (m/s)	1×10^{-4}	1×10^{-4}
Transport	Specific Discharge (m/yr)	0.15	0.15
	Approximate Linear Ground-Water Velocity (m/yr)	10	1.0
	Longitudinal Disp. (m)	20	20
	Transverse Disp. (m)	5	5

[a] Reflects flow only in ¼ of the cross-section available for flow.

Another minor change involves the K_d parameters for volcanic rocks and alluvium in the SZ. Values have been modified to conform to more recent measurements, described in BSC (2001; Vol. 1). The most significant change is that K_d values for ^{99}Tc and ^{129}I are set to zero for alluvium. Previous non-zero values provided an advantage in performance.

Table 7-2
Summary of K_d and dimensionless K_d values for volcanic units and alluvium in SZ, October 10/01

Radionuclide	K_{dv} (volcanics) (mL/g)	K_{dv} x $_b$ (dimensionless)	K_{da} x c (alluv.) (mL/g)	K_{da} x $_b$ x c (dimensionless)
Np	1.0	1.94	5	9.5
I	0.0	0.0	0.0	0.0
U	2.0	3.9	5	9.5
Tc	0.0	0.0	0.0	0.0
C	0.0	0.0	0.0	0.0
Am, Pu, Pa,Th	50	97	25.5	49
Cs, Sr	25	49	12.8	24
Se	2.0	3.9	2.0	3.8

$_{bv} = 1.94$ g/cm^3
$_{ba} = 1.91$ g/cm^3
$c = \frac{\theta_e}{\theta_T} = \frac{0.15}{0.3} = 0.50$; Rationale for correction described in CRWMS, M&O (2000b)

7.4 Concluding Comments

This chapter presented a brief review of geochemical and isotopic data from wells in the vicinity of Yucca Mountain. The stable and radiogenic isotopes in particular suggest that flow systems are sluggish. The wells in the North Central Amargosa Desert appear to be pumping water that was recharged during the late Pleistocene or early Holocene. Even after 10,000 years, this water has yet to be flushed by modern recharge. Moreover, it is difficult to even find modern water in the system. The picture painted by these actual data are inconsistent with performance assessment models that have thick large plumes sweeping down from Yucca Mountain in one or two thousand years.

It is likely that much of the water moving south along Fortymile Wash originated further upstream in the wash or even locally as Claassen (1985) suggests. It is possible that flow in the immediate vicinity of Yucca Mountain may be much more controlled structurally than present thinking would suggest. The present monitoring system is deficient in its ability to measure vertical gradients, and has not characterized flow along major fault systems.

As was the case in the UZ, geochemical data can play an important role in elucidating flow systems and rates of flow. Present PA models need to incorporate these data much more extensively than is presently the case. In addition, additional work using the geochemical data could yield an understanding of flow in the SZ.

7.5 References

BSC (Bechtel SAIC Company), 2001. FY 01 Supplemental Science and Performance Analyses - Volume 1 Scientific Bases and Analyses. TDR-MGR-MD-000007, Las Vegas, Nevada: Bechtel SAIC Company.

Chapman, J.B., R.L. Hershey, and B.F. Lyles, 1995. Groundwater Velocities at the Nevada Test Site: ^{14}Carbon-based Estimates. DOE/NV/11508-03, UC-703.

Claassen, H.C., 1985. Sources and Mechanisms of Recharge for Ground Water in the West-Central Amargosa Desert, Nevada – A Geochemical Interpretation. U.S. Geological Survey, Professional Paper 712-F.

CRWMS M&O, 2000a. Total Performance Assessment for the Site Recommendation. TDR-WIS-PA-00001. Las Vegas, Nevada: CRWMS M&O.

CRWMS, M&O, 2000b. Uncertainty Distribution for Stochastic Parameters. ANL-NBS-MD-000011. Las Vegas Nevada: CRWMS M&O.

CRWMS M&O, 2000c. Unsaturated Flow and Transport Model Process Model Report. TDR-NBS-HS-000002. Las Vegas, Nevada: CRWMS M&O.

CRWMS M&O, 2000d. Input and Results of the Base Case Saturated Zone Flow and Transport Model for TSPA. ANL-NBS-HS-000030. Las Vegas Nevada: CRWMS M&O.

CRWMS M&O, 2001. Geochemical and Isotopic Constraints on Groundwater Flow Directions, Mixing, and Recharge at Yucca Mountain, Nevada. ANL-NBS-HS—000021. Las Vegas, Nevada: CRWMS M&O.

EPRI, 1998. Alternative Approaches to Assessing the Performance and Suitability of Yucca Mountain for Spent Fuel Disposal. EPRI TR-108732, 18 Chapters.

White, A.F., and N.J. Chuma, 1987. Carbon and isotopic mass balance models of Oasis Valley—Fortymile Canyon groundwater basin, southern Nevada. Water Resour. Res., 23(4), 571-582.

8
BIOSPHERE MODELING AND DOSE ASSESSMENT

8.1 Introduction

This report provides updated values for Biosphere Dose Conversion Factors (BDCFs) for use in EPRI's Total System Performance Assessment (TSPA) of the candidate used nuclear fuel and high-level radioactive waste (HLW) disposal at Yucca Mountain. The BDCFs are values of annual individual effective dose[1], mrem/y, arising to an assumed critical group making domestic and agricultural use of well water containing unit concentrations, mole/m3, of each of a set of relevant radionuclides. The values of BDCF may be multiplied by radionuclide concentrations in abstracted groundwater, calculated in other parts of the TSPA, to provide estimates of dose to the average member of the critical group. The term 'critical group' is used to describe a set of individuals who, because of their location and commonality in their behaviour and habits, were amongst the most highly exposed to releases from a nuclear facility [IAEA, 1999]. This concept is used by BIOMASS and the international community and is similar to the RMEI concept EPA requires for Yucca Mountain. The work builds on biosphere assessment work reported in EPRI TR-107190 [EPRI, 1996] and methodology development which has taken place within Theme 1 of the International Atomic Energy project, BIOMASS [IAEA, 2001].

The main updates and revisions made compared with EPRI [1996] include:

- use of the current ICRP dose coefficients given in ICRP Publication 72 [ICRP, 1999],
- review and revision of the model for uptake of radionuclides into fruit,
- addition of Cl-36 in the list of radionuclides,
- improvement in the model for interception and uptake of radionuclides in groundwater by crops, adapted from the model provided by the BIOMASS project [IAEA, 2001], and
- reference to the BIOMASS methodology for model development.

In addition, brief consideration is given to the implications for BDCFs for a volcanic release scenario, and ideas are presented for biosphere research and related activities which could be included in a programme of performance confirmation.

---

[1] Hereafter referred to as dose.

8.1.1 References for Section 8.1

EPRI (1996). Biosphere Modelling and Dose Assessment for Yucca Mountain. EPRI TR-107190. Electric Power Research Institute, Palo Alto, CA.

IAEA (1999). Guidance on the Definition of Critical and Other Hypothetical Exposed Groups for Solid Radioactive Waste Disposal, BIOMASS/T1/WD03, IAEA, Vienna

IAEA (2001). BIOsphere Modelling and ASSessment BIOMASS Programme Working Documents 1-10, April 1998-June 2001, International Atomic Energy Agency, Vienna, (Reproduced on CD by the IAEA, February 2001).

ICRP (1999). Age-dependent Doses to members of the Public from Intake of Radionuclides: Part 5. International Commission on Radiological Protection, ICRP 72, Pergamon Press.

8.2 Groundwater Release Via Irrigation Well

Each of the subsections that follows corresponds with the steps in the BIOMASS Reference Biospheres methodology [IAEA, 2001].

8.2.1 Assessment Context

The Assessment Context can be summarised as follows:

Purpose:	Support EPRI TSPA Demonstrate compliance with regulatory requirements. Contribute to the confidence of policy makers, the scientific community and the public. Guide later stages of repository development. Guide research priorities.
Assessment Endpoint:	Annual individual effective dose.
Assessment Philosophy:	'Equitable' (similar to "realistic" or "best estimate"), except with respect the critical group definition, for which a 'cautious' (similar to "conservative") approach is adopted
Repository Type:	Yucca Mountain HLW repository.
Site Context:	Amargosa valley. Sub-tropical arid (desert climate), ZBIII in the classification of Walker [1984].

Geosphere/Biosphere Interface:	Well intruding into aquifer plume with abstraction at a rate consistent with domestic and agricultural use.
Source Term:	Constant unit concentration in abstracted water maintained indefinitely for each of a set of relevant radionuclides, see Table 2.1.
Societal Assumptions:	Agricultural community, adopting modern practices (machinery and methods) for cultivation and animal husbandry.
Time Frame:	Up to 1 million years. Release via well continues continuously for long enough for concentrations to reach steady state in the assumed constant biosphere.

Table 8-1
Radionuclides Considered

Cl-36	Pa-231	Pb-210	Np-237
Se-79	Th-232	Ra-226	U-238
Nb-94	U-233	Ac-227	Pu-239
Tc-99	Pa-233	Th-228	Pu-240
I-129	U-234	Ra-228	Pu-242
Cs-135	U-235	Th-229	Am-243
Po-210	U-236	Th-230	

Each of the above components of the assessment context is considered in turn in order to discuss its potential implications for model development.

Assessment Purpose

The biosphere assessment will support the EPRI TSPA by supporting the demonstration of compliance with regulatory requirements, contributing to the confidence of policy makers, the scientific community and the general public. The results are intended to guide the later stages of repository development and research priorities. The model described and implemented will provide a mechanism for estimating the radiological significance of potential future discharges of radionuclides.

Assessment Endpoints

This report provides BDCFs in units of mrem y^{-1} per mole m^{-3} of each radionuclide in the groundwater from which well water is abstracted. Consideration is restricted to the calculation of annual individual effective dose to adult members of the 'modified AMCG' (ArMagosa valley Critical Group) characterised by behaviour determined from Amagosa Valley survey data supplied via staff on the DOE Yucca Mountain Project [Wasiolek, 2001].

Assessment Philosophy

The assessment philosophy provides a broad indication of how it is presumed that irreducible uncertainties should be addressed through basic assessment assumptions and hypotheses. As far as components of the assessment model other than the definition of the critical group are concerned, the assumption made here is that an 'equitable' assessment philosophy is adopted. This is taken to imply that parameter value selection for the representation of contaminant transfer pathways in the biosphere model should be based on the assumption of realistic, rather than extreme values. (See discussion in IAEA [1999a].) More generally, equitable refers to "realistic" or "best estimate" values.

By contrast, the identification and description of potentially relevant critical group exposure pathways is assumed here to require a more cautious approach. A cautious philosophy tends to result in the use of generally conservative assumptions in order to ensure that, within the overall constraints imposed on the assessment, the results are unlikely to underestimate the corresponding dose that would arise for the release and exposure mechanisms considered. For example, whereas a contaminated well may be just one of several possible sources of water available to a community, a cautious approach to description of the hypothetical critical group dictates that calculations need be undertaken for those individuals for whom the well is the primary source of water used for drinking and other purposes. Cautious (or conservative) assumptions are used therefore in relation to the use of the well water and the exposure to critical group members who interact with contaminated foodstuffs and other environmental media.

Repository Type

The proposed HLW repository at Yucca Mountain is assumed. This has implications for the potential radioactive source term to biosphere, both in terms of radionuclides and the nature of the geosphere-biosphere interface. These are considered in other components of the EPRI TSPA.

Site Context

As a matter of practicality, the assumed location of any well needs to be such that the contaminated aquifer is at a reasonably accessible depth, based on the presumed habits and technology of the inhabitants of the local region. As a general rule, information concerning the assumed depth and location of the well would be consistent with past or current, potential or actual practice. It is assumed that assumptions regarding abstraction rates in the biosphere system description and aquifer capacity in the geosphere model are consistent.

Geosphere/Biosphere Interface

It is assumed that all calculations (e.g. flow and transport effects, dilution arising as a result of pumping and other changes within the well itself) that may be required to determine concentrations of radionuclides in water delivered at the well head are supplied externally to the biosphere calculation.

Source Term

The concentration of each radionuclide in well water is assumed to be constant over the time frame of the assessment and within each year. Hence the results of the biosphere calculations will provide 'conversion factors' for annual individual effective dose per unit concentration in water at the well head. Radioactive progeny with relatively short half-lives are assumed to be in secular equilibrium with their parents. The definition of short half-life depends on rates of change in the system under consideration, and is taken to be 25 days for the current biosphere system at Amargosa Valley. This is why, for example, Pb-210 and Po-210 are considered explicitly in the biosphere calculations although they are not in the geosphere modelling.

Societal Assumptions

In order to avoid endless speculation regarding the technology, physiology and socio-economic structures of future communities, the primary assumption is made that the activities and characteristics of the population exploiting the well water are similar to those of present-day communities. This is consistent with the IAEA's general principle of ensuring that predicted impacts on the health of future generations will not be greater that the relevant levels of impact that are acceptable today [IAEA, 1995].

The assumed assessment context dictates consideration of an agricultural community. Consideration of the range of potential exposure pathways involved in the production and consumption of these foodstuffs implies a need to take into account various aspects of the migration and accumulation of radionuclides as well as the specific aspects of accumulation in the foodchain.

Time Frame

It is not intended to imply that the biosphere will remain constant for a period of one million years; only that the results should be applicable to any geosphere release within that period.

8.2.2 Biosphere System Identificaton and Justification

The biosphere system is not fully defined by the assessment context and so the relevant components of the biosphere system must be identified and justified. The identification and justification process is based on the classification scheme presented in IAEA [1999c]. This assessment is for a specific site and the assessment context requires assumptions of present day conditions. Therefore it is relatively straightforward to justify assumptions. However, not all site characterisation data is available that could be obtained, at least for this assessment.

One of the more important factors determining the identification of components of the biosphere system is the assumed degree of control or management by the local human community. There is no explicit guidance on this matter in the assessment context given above. However, given that a present day agricultural community is to be assumed (societal context) and that the primary route of contamination of the biosphere system is via the use of well water (geosphere/biosphere interface), it is appropriate to focus attention on a highly controlled ecosystem.

This decision does not suggest that there can be no possible interest in the potential radiological implications of contamination of natural and/or seminatural ecosystems via other types of geosphere/biosphere interface, resulting in contamination of different environmental and possibilities for other types of human exposure via a range of different pathways. For example, consideration was given to direct discharge of contaminated groundwater to the biosphere in EPRI [1999]. The following principal components of the biosphere system are identified.

Climate

The climate type assumed is sub-tropical arid (desert climate), ZBIII in the classification of Walker [1984].

Topography and Geographical Extent

The following topographical characteristics (selected from Table TI in IAEA [1999c]) of the biosphere system in the region exploited by the local community can be identified, consistent with the assessment context:

Geographical context: **inland** – as specified;

Altitude: **lowland** – circa 3000 feet;

Landform: **plain** – this is the alternative most consistent with the use of irrigation water for agricultural purposes;

Localised erosion: **limited localised erosion** – most consistent with the choice of the land for agricultural purposes and the absence of significant surface water courses.

Human Community

The human community is taken to be the present day community at Amargosa Valley. This includes residents, some of whom produce some food in gardens and yards as well as some farms.

Near-surface Lithostratigraphy

The underlying rock type is only of secondary relevance, since the way in which the geosphere/biosphere interface is described means that there is no need describe the regional aquifer as part of the biosphere system. The surface soil is assumed to be naturally sandy with low organic content, but to be significantly modified by farming practice in the areas irrigated.

Water Bodies

There are no natural, permanent surface water bodies, though there may be storage facilities. The aquifer providing the source term needs to be capable of supplying the amoutn of water assumed to be abstracted.

Biota

Consistent with the underlying assessment context, it is possible to identify a managed, cultivated ecosystem as being consistent with the overall assessment context.

All surface water bodies (other than the well and water storage and distribution system) have been excluded from the identified biosphere system. The only managed aquatic ecosystems that are relevant to describing biotic communities are therefore those associated with man-made reservoirs. In addition, given the assessment context and the various arguments developed above, all managed terrestrial ecosystems can be excluded with the exception of:

- field crops/cultivated land, and
- residential gardens and yards.

The assessment context specifies that biosphere system change need not be considered. A constant biosphere system based on the different components identified above can therefore be assumed. Therefore the model assumes that the biosphere system is in a steady state and the model is run until the concentrations of radionuclides in the biosphere system comes into steady state too.

8.2.3 Biosphere System Description

Screening of System Characteristics

The first step of the biosphere description procedure is to identify those characteristics and properties of each component of the biosphere system identified above that are relevant to providing an assessment-oriented description of the system. This is achieved by working through a checklist of common general characteristics, descriptive of potentially relevant features for each Principal Component, and selecting specific items for their relevance to the overall assessment objective according to the assessment context and any additional assumptions invoked in the preceding system identification.

More detail is required to construct a model, based on the BIOMASS methodology. Further description of the Principal Components of the Biosphere System is provided in Appendix D.

8.2.4 Exposure Group Definition

The systems description given above allows consideration of how humans might interact with that system, consistent with the assessment context and receive exposure by it. Table 2.2 lists activities relevant to the potentially contaminated source or environmental medium [IAEA, 1999a]. The Table below lists the exposure modes, routes and activities that are considered in the conceptual biosphere system. A more comprehensive table that details all potential exposure modes, routes and activities can be found in Appendix E.

Table 8-2
Conceptual Exposure modes, exposure routes and examples of typical activities.

Source/ medium	Exposure mode	Example exposure route	Examples of typical activities	Assumed parameters
	inhalation	*gaseous release to air*	*outdoor activities,*	A, B, E
		resuspension of soil particulates	*ploughing, walking, misc. outdoor activities, indoor exposure resulting from soil brought inside*	A, B, E
	ingestion	*incidental soil ingestion*	*gardening, fresh fruit and veg. consumption, recreational activities, occupational activities*	A, B, H
	external	*external radiation exposure*	*activities over/near contaminated soil, including dermal contact,*	A, C, F, G
Water	inhalation	*spray/aerosols/volatiles*	*spray (irrigation,), recreation, domestic (showering, sauna, cooking),*	A, B, E
	ingestion	*deliberate water intake*	*drinking, as a component of diet in other foods (cooking)*	B
	external	*external exposure from water bodies*	*Immersion during bathing, recreation*	A, C, F, G
Plants and plant products	inhalation	*particulates from combustion, from plant processing*	*burning of plant material (, stubble,*	A, B, E
	ingestion	*food consumption*	*eating, drinking plant material as part of the diet, root veg. , green veg, cereals, fruit, etc.*	B
	external	*exposure from plants and plant products*	*Working/ recreation in fields, storage of plants, wearing clothes derived from plants,*	A, C, F, G
Animals and animal products	ingestion	*food consumption*	*animal products consumed include meat, milk, offal, eggs, dairy products, other products (e.g., gelatin)*	B
	external	*exposure from animals and animal products*	*animal husbandry, processing/storage of animal products and materials*	A, C, F, G

Legend:
A - Exposure duration (hours a^{-1})
B - Rate of intake (kg a^{-1})
C - Shielding of source (yes/no, shielding factor)
D - Deposition rate (kg m^{-2} a^{-1})
E - Resuspension/release rate [(kg soil) $(m^3 \text{ air})^{-1}$, m^{-1}, kg $hour^{-1}$, etc.]
F - Source geometry (infinite plane, line, sphere, semi-infinite cloud, etc.)
G - Relation to source (distance, orientation – above, beside, below, immersed, etc.)
H - Age specific information relevant

8.2.5 Model Development

8.2.5.1 Conceptual Model for Radionuclide Transfer

As a starting point, consideration was first given to the nature of the endpoint(s) under consideration; in this case individual radiation doses to members of potential exposure groups.

Such radiation doses can occur via any of four principal radiation exposure modes: ingestion, inhalation, external irradiation, and by transfer of radionuclides through the skin, by puncture or absorption. Provisionally, all four modes should be considered, but the fourth one is not considered further here on the basis of its probable low significance [BIOMOVS II, 1996].

The following Conceptual Model Objects have been identified from the biosphere system description:

Aquifer, as the source of contamination.

Water Storage and Distribution System, representing the means by which water is made available throughout the year for domestic use, animal watering and crop irrigation.

Atmosphere, including the open air and confined spaces.

Cultivated Soil, including all managed farmland.

Food and Fodder Crops, grown in the cultivated soil, which are assumed to be irrigated by contaminated water.

Farm Animals, including poultry, which may be watered from the contaminated source or eat contaminated fodder crops grown on irrigated land.

Farm Product Storage, Distribution and Processing System, representing an important link in the chain of contamination to human exposure.

Sinks, representing losses of radioactive contamination from the biosphere system resulting from processes such as radioactive decay, downward percolation of contaminated water, consumption in food and atmospheric transport.

From the perspective of describing radionuclide movement from one part of the biosphere system to another, the presence of people is of comparatively limited importance compared with the objects identified above. People might potentially be included as part of the transfer pathway from foodstuffs to soil (via sewage), or perhaps as a secondary contaminant transfer pathway associated with the movement of soil attached to clothing. Overall, however, it was considered that such pathways of 'transfer via humans' would not represent a significant contribution to the overall environmental distribution of radionuclides within the biosphere system.

Nevertheless, it should be noted that the role of human activities in the distribution of radionuclides (e.g. via ploughing and irrigation) is implicit in the transfer processes between other different components of the biosphere system. Moreover, human behaviour leading to exposure, and corresponding exposure groups, are explicitly incorporated at a later stage in the development of conceptual models for radiological exposure.

The principal elements of the conceptualised biosphere system were then included in an Interaction Matrix. An Interaction Matrix represents the conceptual model for contaminant transport in a biosphere system. The Leading Diagonal Elements (LDEs) are normally Features, and the Off Diagonal Elements (ODEs) are the Events and Processes that when read clockwise provide the interaction between Features. Each LDE influences the one below it. These matricies allow potential radionuclide transfer pathways to be investigated by representing them as off-diagonal elements of the matrix. An Interaction Matrix for the biosphere system of Yucca Mountain is illustrated in Table 8-3.

Auditing the Radionuclide Transfer Interaction Matrix

Comparison with the Biosphere System Description

Those components of the Biosphere System Description previously considered to be relevant to the assessment model (i.e. those marked 'Y' in column 3 of Tables in Appendix D) are listed separately in Table 8-4. This Table classifies the components as 'implicit' or 'explicit', depending on whether they are associated with, respectively, leading diagonal elements or off-diagonal elements of the Radionuclide Transfer Interaction Matrix.

For the most part, all the relevant components appear in the Interaction Matrix, with a significant number being implicitly associated with that part of the model corresponding to radionuclide behaviour in cultivated soil. In developing the corresponding mathematical model of radionuclide transfer, it is necessary to ensure that all relevant FEPs, whether implicit or explicit in the Matrix, are appropriately addressed.

Comparison with Independent FEP List

The International FEP list (as presented in [BIOMASS, 2001]) was next examined. All FEPs listed before Item 3.1.3 in the list (Cycling and Distribution of Materials in Living Components) are concerned with, and accommodated within, system identification and description (Appendix D). The remaining FEPs within the list are addressed in the Radionuclide Transfer Interaction Matrix as described in Table 8-5.

Table 8-3
Radionuclide Transfer Interaction Matrix

	1	2	3	4	5	6	7	8	9
1	Aquifer	Water abstraction	x	x	x	x	x	Ingestion	x
2	x	Water Storage and Distribution System	Volatilisation Degassing	Irrigation Sediment transfer	Irrigation and interception	Drinking Water Sediment consumption	x	x	Decay Human consumption
3	x	x	Atmosphere (external &\ internal)	Vapour / aerosol deposition	Vapour / aerosol deposition	Vapour / aerosol inhalation	x	Vapour / aerosol inhalation	Decay Advecti n
4	x	x	*Suspension* Volatilisation Gas	Cultivated Soil	Root uptakeSoil splash	*Consumption of* soil on fodder crops	Transfer of soil on crops	Ingestion	Decay Leaching / Percolation Erosion
5	x	x		WeatheringLeaf litterPloughed in detritus	Food and Fodder Crops	Ingestion of fodder	Harvesting	Ingestion	Decay
6	x	x		Manuring	x	Farm Animals	SlaughteringMilkingEgg collect	Ingestion	Decay
7	x	x	Volatilisation	Green manuring / composting	x	Consumption of stored fodder	Farm product storage distribution & processing	x	Consumption Decay Silage leachate
8	x	x	Respiration	Excretion	x	x	x	Human Cummunity	x
9	x (Recharge)	x	x	x	x	x	x	x	Sinks

Notes on the Radionuclide Transfer Interaction Matrix

'x' = not relevant

Leading diagonal elements

Water Storage (2,2) incorporates: Evaporation, Sorption, Sedimentation, Precipitation and Dissolution

Atmosphere (3,3) incorporates: Filtration, Controlled Ventilation

Cultivated Soil (4,4) incorporates: Sorption, Ploughing, Bioturbation, Water Balance (Infiltration, Macropore Flow, Capillary Rise)

Food and Fodder Crops (5,5) incorporates: Translocation

Farm Animals (6,6) incorporates: Metabolism

Farm Product Storage, Distribution and Processing System (7,7) incorporates: Food Processing

Off diagonal elements

'Sediment' in (4,2) and (6,2) relate to accumulated sediment in tanks and ponds.

Transfer from stored crops to atmosphere (7,3) is likely to be low by comparison with standing crop / bare soil owing to low surface area for release.

Potential loss/transfer of radionuclides to atmosphere from crops (5,3) and animals (6,3) is assumed not to be significant for the radionuclides considered. It could be important for ^{14}C and is excluded by the assessment context.

Transfer from animals to crops (6,5) would be potentially relevant if pasture were included, however, this practice does not occur currently at Amargosa Valley.

Green manuring (7,4) is the use of silage leachate or excess crops for fertilisation and soil improvement.

Table 8-4
Components of the Biosphere System Description included in the Conceptual Model

Biosphere System Component	Descriptive Class	How included in the model
Climate Characteristics	Temperature Precipitation	Secondary characteristics affecting evaporation, transpiration, the required amount of irrigation, etc.
Temporal variability of climate	Diurnal Seasonal	Secondary characteristics affecting evaporation, transpiration, the required amount of irrigation, etc.
Consolidated/ Solid Geology	Lithostratigraphy Fracture systems Degree of Weathering Erodability Deposition rates Mineralogy	Secondary characteristics that are relevant insofar as they affect soil parameters
Unconsolidated/ Drift Geology	Lithostratigraphy Fracture systems Degree of Weathering Erodability Deposition rates Mineralogy	Secondary characteristics that are relevant insofar as they affect soil parameters
Soil	Stratification (e.g. soil horizons) Composition (organic content, mineralogy) Texture Areal variation	Soil is a primary element of the conceptual model (4,4). Individual characteristics listed here affect soil-related parameters used in the model.
Human Activities	*Recycling and mixing of bulk materials*	
	Ploughing	Affects soil properties (4,4)
	Well	Incorporated under abstraction from well (1,2)
	Irrigation	Explicit in matrix (2,4) and (2,5)
	Recycling of bulk solid materials	Explicit in matrix (6,4) and (7,4)
	Controlled ventilation	Affects mixing of atmosphere (3,3)
	Redistribution of trace materials	
	Waste water treatment and use in manuring	Subsumed within recycling (6,4) and (7,4)
	Air filtration	Affects atmosphere concentrations (3,3)
	Food processing	Affects food concentrations (7,7)
Water Bodies	Basal characteristics	Represented in storage system (2,2)
	Suspended sediments	Represented in storage system (2,2)
	Hydrochemistry Major ions Minor ions Organic compounds Colloids Sorption Precipitation / dissolution Mineralisation pH and Eh	Characteristics affecting parameters radionuclide distribution, uptake and metabolism
Water Balance	Precipitation	Characteristic affecting irrigation requirements (2,5)
	Irrigation	Explicit in matrix (2,4) (2,5)
	Evaporation	Represented in soil water balance (4,4)
	Transpiration	Represented in soil water balance (4,4); also (5,3)
Land surface	Infiltration Porous medium Macropore flow	Affect soil water balance (4,4)
Land surface	Interflow (throughflow) = storage	Affect soil water balance and irrigation requirements (4,4) (2,5)

NOTE: MATRIX ELEMENTS IN THIS TABLE REFER TO TABLE 8-3.

Table 8-5
Checklist for appearance of FEPs from the INDEPENDENT FEP list in the Radionuclide Transfer Interaction Matrix (Table 8-8)

FEP [BIOMASS, 2001]	Where Included in Table 2.3
Root uptake (3.1.3.1.1)	Soil to plant transfer (4,5)
Respiration (3.1.3.1.2)	Plant to atmosphere (5,3)
Transpiration (3.1.3.1.3)	Plant to atmosphere (5,3); Soil water balance (4,4)
Intake by Fauna (3.1.3.1.4)	Consumption / inhalation (2,6) (3,6) (4,6) (5,6)
Interception (3.1.3.1.5)	Irrigation (2,5); Aerosol deposition (3,5)
Weathering (3.1.3.1.6)	Plant to soil transfer (5,4)
Bioturbation (3.1.3.1.7)	Soil process (4,4)
Translocation (3.1.3.2.1)	Fodder crop models (5,5)
Animal metabolism (3.1.3.2.2)	Animal models (6,6)
Evaporation (3.1.4.1.1)	Soil water balance (4,4); Stored water (2,2)
Gas transport (3.1.4.1.2)	Atmosphere (3,3) (3,8); also (4,3) (5,3) (6,3)
Aerosol transport (3.1.4.1.3)	Soil to atmosphere (4,3) (3,3) (3,8)
Precipitation (3.1.4.1.4)	Input to infiltration => soil water balance (4,4)
Wet/dry deposition (3.1.4.1.5/6)	Atmosphere to soil/plant (3,4) (3,5)
Infiltration (3.1.4.2.1)	Soil process (4,4)
Percolation (3.1.4.2.2)	Soil process (4,4)
Capillary rise (3.1.4.2.3)	Soil process (4,4)
Erosion (3.1.4.2.10)	In this model represents a transfer to sink (4,9)
Sedimentation (3.1.4.3.2)	Stored water process (2,2)
Suspension (3.1.4.3.3)	Stored water process (2,2)
Rain splash (3.1.4.3.4)	Soil splash (4,5)

Discussion and Iterative

The following discussion reviews the conceptual model implicit in Tables 8-3 through 8-5 and justifies simplifying assumptions (i.e., elimination of FEPs) for what should be carried forward into the mathematical model.

Water Supply

All the elements of the Radionuclide Transfer Interaction Matrix can be cross-referenced to the System Description output. Therefore the Interaction should contain all the FEPs identified as being relevant to a model description of radionuclide transfer.

A variety of FEPs have been identified in the conceptual model that could potentially change the concentration of radionuclides in the water supply, compared with that in the abstracted well water. These include evaporation of the water, sorption onto sediments or other surfaces, sedimentation, precipitation and dissolution.

Evaporation of water during storage and distribution might give rise to a small increase in concentration of those radionuclides remaining in solution. However, total water losses via this route are considered unlikely to be significant, in an arid (ZB III [Walker, 1984]) environment, and the process is not included in the model.

Although suspended sediment may be present within the water supply, the total sediment load must be low enough for the water to remain potable (since no deliberate water treatment is assumed to take place). Sorption onto suspended sediment, and subsequent sedimentation, may occur over time; however, the overall effect of this will only be to reduce radionuclide concentrations in bulk water supplied at the point of delivery. The periodic removal of accumulated sediments from cisterns and other parts of the storage and distribution system could potentially give rise to a transient 'spike' in water concentration resulting from the remobilization of radionuclides. This might possibly be relevant if the focus of interest were the dose from exposure with a specific year; over a longer period, however, the average concentration in the water supply will not exceed that delivered at the well head. Furthermore, any transfer of radionuclides associated with the possible removal to soil of accumulated sediment from within the water distribution system is unlikely to be significant, since the volumes involved will be comparatively small. Moreover, if the material is suitable for spreading on the land, sorption coefficients are unlikely to be significantly different from those for the irrigated soil itself. The effects of sorption and sedimentation in modelling radionuclide transfer within the water distribution system can therefore be ignored.

Precipitation and/or dissolution of radionuclides associated with changes to water chemistry (e.g. because of microbial action) may possibly affect concentrations in bulk water. Again, however, their net effect can only be to reduce radionuclide concentrations in bulk water compared with that delivered at the well head. Provided that the radionuclide concentration in bulk water (i.e. including suspended solids) is specified at the geosphere-biosphere interface (or can be calculated), it will therefore be cautious to ignore the effects of precipitation and dissolution in the radionuclide transfer model.

Potential exposures linked to contact with contaminated sediments and other surfaces within the water supply system are considered negligible compared with those associated with other media. This might be less easy to justify for an 'industrial' or 'commercial' biosphere system, in which maintenance of water storage, distribution and supply systems could potentially constitute a specialised job. However, the present assessment context excludes consideration of large-scale commercial/industrial activities. Hence, sorption and sedimentation within the water storage and distribution system can also be ignored in the context of evaluating radiological exposures. Decay and in-growth of radionuclides would also be negligible compared with geosphere processes and processes occurring at the well head. For modelling purposes, it is assumed that the water supply to other parts of the biosphere system is provided at the same bulk concentration as that delivered at the well head, as calculated in the geosphere model within the TSPA.

Atmosphere

Concentrations of dust or trace materials in the atmosphere can vary rapidly over a considerable range according to local meteorological conditions (atmospheric pressure, wind speed, precipitation etc) as well as factors such as artificial disturbance (e.g. dusts generated by ploughing). The processes involved are complex; however, a significant proportion of the locally-generated transfer of aerosol and vapour will typically remain within a near-surface atmospheric boundary layer and not travel very far before being deposited again. Nevertheless, over time, such transport can lead to losses of radionuclides from the biosphere system; at the same time, other material will be brought into the system from outside by atmospheric processes. Because such transfers are expected to be small compared with, for example, irrigation and percolation in groundwater, it is considered appropriately cautious, without being excessively so, to make the simplifying modelling assumption that their effect can be ignored.

Such simplifications mean that there is no need for an explicit representation of atmospheric transfer processes, and no atmosphere compartment is therefore incorporated in the assessment model. However, radioactive vapour, gas or aerosol within the atmosphere can represent an inhalation hazard, which can potentially be a significant exposure pathway for some radionuclides. It is therefore appropriate to evaluate radionuclide concentrations in the near-surface atmospheric boundary layer, or in indoor atmospheres that may receive releases of gas or vapour. Standard practice is to represent the long-term equilibrium relationship between average atmospheric concentrations and those in soils, plants and other environmental media using empirical correlations.

Arable Crops

Crops will become contaminated due to direct deposition of irrigation water. A fraction can be retained on the plant surface and another fraction can be transferred within the plant, particularly to edible parts. Weathering of plant surfaces results in transfer of intercepted radionuclides to soil. Crops may then become contaminated by root uptake. Soil splash may result in further crop contamination. Although seasonal factors can substantially influence details of what could happen within any one year, given the nature of the time frames of interest as discussed above, all the above processes can be modelled on the basis of equilibrium between the concentration in the irrigation water and the concentration in crops, or between the soil and crops. Models, for this set of processes with the same type of context, commonly use this approach [BIOMOVS II, 1996].

EPRI [1996] identified fruit consumption as an important pathway for some radionuclides. BIOMASS [IAEA, 2001] included a special working group to consider this process and the results are reviewed here (Appendix C) for significance to this assessment. While the IAEA [2001] work has some implications for model parameter values, no changes to the EPRI [1996] model itself are suggested. This does not mean that changes should not be made in future if better information becomes available.

Animals

The same equilibrium approach is adopted for animal product contamination, with concentrations being directly related to concentrations in the irrigation water (for consumption of water but also contribution via crop contamination) or in soil (for contribution via crop contamination or direct ingestion).

Cultivated Soil

Cultivated soil is assumed to be ploughed or dug over, if not every year then every few years. Given the time frames under consideration this means that detailed soil structure is not to be modelled. A "well mixed" layer is assumed associated with typical ploughing depths and to the dominant region in the profile for root uptake by crops and other biotic activity. Processes within the soil result in downward movement, primarily due to infiltration of water. Loss from soil sue to erosion is identified in the matrix, however, noting the sensitivity studies in IAEA [2001], this process is ignored due to low significance compared with infiltration. Cropping is assumed to effectively remove activity from soil though this may also be of low significance for most radionuclides.

Farm Products in Storage, Distribution and Processing Systems

Radionuclide behaviour in stores is not considered to be of great interest only producing a minor decay effect. However these assumptions for storage etc can affect how food is distributed (diluted) before consumption. Processing may result in changed concentrations in the foods/fodder.

Radiation Exposure Pathways

It should be noted that, in the case of exposure assessment, the items of interest correspond to a particular contaminated medium, rather than a physical location. Thus, for example, exposure to contaminated soil might arise from material that has been transferred on clothing from the land into the domestic environment. Based on the Radionuclide Transfer Interaction Matrix (Table 8-3), and the corresponding definitions for each leading diagonal elements, the following media can be identified as qualitatively distinct sources of radiation exposure:

- Water (for domestic use, animal watering and irrigation)
- Atmosphere (indoor and outdoor)
- Arable Crops (in field and storage)
- Animals (in field or barn)
- Cultivated Soil
- Farm Products in the Storage, Distribution and Processing System

Noting the table of conceptual exposure pathways (Table 8-2) and the above discussion, the following exposure pathways are carried forward for consideration in the mathematical model.

Table 8-6
Exposure Pathways

Source	Pathway
Domestic Water	Ingestion– included Spray Inhalation– omitted, low significance Immersion (bathing) - included External (exposure to storage/distribution system) – omitted, low significance
Irrigation Water	Spray Inhalation – omitted, low significance
Atmosphere	Suspended soil and other dust, vapour/gas – omitted, low significance
Cultivated Soil	Ingestion, with food product, and direct ingestion – included External exposure - included
Crops in Field and Storage	External exposure– omitted, low significance
Animal in Field/Barn	External exposure– omitted, low significance
Food Products	External (eg silage clamp) – omitted, low significance Ingestion - included

8.2.5.2 Mathematical Model

Intercompartmental Transfer Processes

The mathematical representation of the intercompartment transfer processes takes the form of a matrix of transfer coefficients that allow the compartmental inventories to be represented as a set of first-order, linear differential equations. Generally, for the *i*th compartment, the rate at which the compartment inventory changes with time is given by:

$$\frac{dN_i}{dt} = \left(\sum_{j\neq i} \lambda_{ji} N_j + \lambda_N M_i + S_i(t)\right) - \left(\sum_{j\neq i} \lambda_{ij} N_i + \lambda_N N_i\right) \tag{8-1}$$

where:

N_i is the activity of radionuclide N in biosphere compartment i, Bq,

N_j is the activity of radionuclide N in biosphere compartment j, Bq,

M_i is the amount of radionuclide M in biosphere compartment i (M is the precursor radionuclide of N in a decay chain), Bq,

$S_i(t)$ is an external source term of radionuclide N to compartment i, Bq y^{-1},

λ_N is the decay constant for radionuclide N, y^{-1},

λ_{ji} is a set of transfer coefficients inputs to compartment i from the other j ($\neq i$) compartments in the system, y^{-1},

λ_{ij} is the set of transfer coefficients representing the loss terms of N from compartment i to the other j $(\neq i)$ compartments of the system and to sinks.

The intercompartment transfer rate coefficients (λ_{ij}) are the mathematical representation of the transfer processes identified in the conceptual model.

The processes included dynamically in the conceptual model are shown in Figure 8-1. The calculations are made on the basis of irrigation of unit area (1 m^2), avoiding the need to quantify the areas irrigated on the assumption that enough water is available to irrigate sufficient land to support the needs of the candidate critical groups. Only one soil in considered, even though soil concentrations may vary with crop type. This is because some rotation of crops is assumed in the long term. There are a number of loss mechanisms from this soil, as well as radioactive decay and in-growth, to calculate.

8.2.5.2.1 Process representation in the dynamic model

Irrigation source term

Irrigation water is assumed to be applied to cultivated soil at a rate V_{irr} m^3 y^{-1}. This volume rate is that applied to 1 m^2 of soil. Although a fraction of irrigation water is intercepted by crops, all the activity in the water is assumed to enter the soil immediately[2]. The relatively minor delay before weathering removes intercepted activity to the soil is ignored so far as the concentration in soil calculation is concerned. Similarly, the proportion of intercepted activity which is absorbed by the crop is also ignored so far as calculation of this concentration is concerned. It is assumed that plant material, excluding the cropped fraction, is recycled and incorporated into the soil. Changes in irrigation water concentrations from the well head to the soil surface are also ignored.

Thus, the source term to the soil due to irrigation, S, Bq y^{-1}, is given by:

$$S = V_{irr} C_w \tag{8-2}$$

where C_w is the radionuclide concentration in the well water, Bq m^{-3}.

Leaching (and other downward losses) from cultivated soil

The rate coefficient for the transfer of radionuclides out of cultivated soil due to leaching, λ_{1l}, y^{-1}, is given by:

$$\lambda_{1l} = \frac{I}{R \, \theta \, d} \tag{8-3}$$

---

[2] Concentrations of radionulcides in crops due to interception of irrigation water are assessed assuming equilibrium with concentrations in the irrigation water, see below.

where:

I is the net annual infiltration/recharge rate, m y^{-1},

R is the retardation coefficient for the cultivated soil compartment,

θ is the water filled porosity of the cultivated soil compartment,

d is the thickness of the cultivated soil compartment, m.

The R term is calculated using the following equation:

$$R = 1 + \frac{(1-\theta_t)\rho}{\theta} K_d \tag{8-4}$$

where:

θ_t is the total porosity of the cultivated soil compartment,

ρ is the grain density of the cultivated soil compartment, kg m^{-3},

K_d is the linear, reversible sorption coefficient of the cultivated soil compartment, m^3 kg^{-1}.

It is noted that better data may be available for R than for K_d and related parameters. Furthermore, K_d's determined from column experiments are usually more relevant than batch experiments, being more likely to represent fully the effect of water moving through the soil.

Cropping

In circumstances of high uptake of radionuclides from soils into growing plants, the concentration in soils would be modified. The activity in that proportion of plants not returned to soil through plant decay, i.e. the proportion removed in cropping, would be lost from the system. It is recognised that this process is only significant for those radionuclides that are significantly taken up into crops. The crops are assumed to be grown in rotation on the unit area of land, and so the loss rate is taken to be the average associated with the 5 crops considered. The rate constant for removal from the soil, λ_{1C} y^{-1}, is given by:

$$\lambda_{1C} = \frac{\sum_{crop} \frac{1}{5}(CF_{crop} + S_{crop})Y_{crop}}{(1-\theta_t)\rho d} \tag{8-5}$$

where:

CF_{crop} is the concentration factor from root uptake for the crop, Bq kg^{-1} (fresh weight of crop)/Bq kg^{-1} (dry weight of soil),

S_{crop} is the soil contamination on the crop, kg (dry weight soil) kg^{-1} (fresh weight of crop),

Y_{crop} is the wet weight biomass of the crop, kg $m^{-2} y^{-1}$, obtained at harvest from the unit area irrigated.

Thus, the conceptual model of radionuclide transfer processes is illustrated in Figure 8-1 and the equation for the radionuclide concentration in the bulk cultivated soil compartment, C_s, for radionuclide N, Bq m^{-3}, is:

$$\frac{dC_s}{dt} = - (\lambda_N + \lambda_{1C} + \lambda_{1I})C_s + V_{irr} C_w \qquad (8\text{-}6)$$

Losses due to wind and water erosion are ignored on the basis that either they are not significant compared to the other transfers or they are so slow as to require the consideration of biosphere change before it would make have a significant affect on the radionuclide concentration of the soil compartment (see Appendix E).

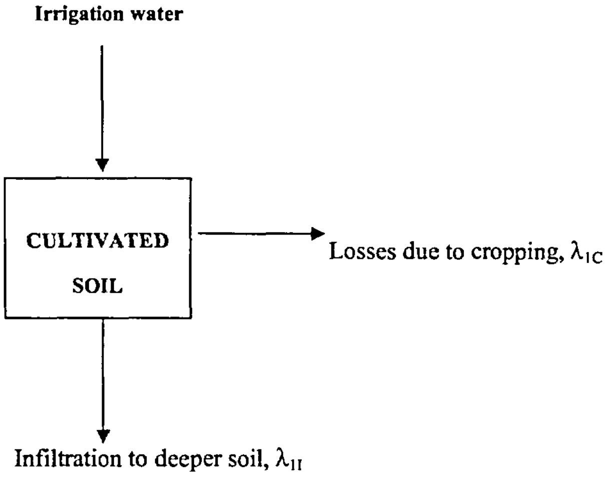

Figure 8-1
Conceptual Model of Radionuclide Transfer Processes

8.2.5.2.2 Dose equations

Doses have been assessed for the pathways indicated as included in Table 8-6.

Consumption of Drinking Water

The annual individual dose from the consumption of unfiltered drinking water from the well is given by:

$$D_w = ING_w \, DC_{ing} \, C_w \qquad (8\text{-}7)$$

where:

D_w is the individual dose from consumption of well water, mrem y^{-1},

ING_w is the individual ingestion rate of well water, m^3 y^{-1},

DC_{ing} is the dose coefficient for ingestion, mrem Bq^{-1}.

Consumption of Agricultural Crops

The annual individual dose from the consumption of agricultural crops is given by:

$$D_{crop} = ING_{crop}\, DC_{ing}\, C_{crop} \tag{8-8}$$

where:

D_{crop} is the individual dose from consumption of the crop, mrem y^{-1},

ING_{crop} is the individual ingestion rate of the crop, kg y^{-1},

C_{crop} is the radionuclide concentration in the edible part of the crop, Bq kg^{-1} (fresh weight of crop).

The C_{crop} term is calculated using the following equation:

$$C_{crop} = \frac{(F_{p2}CF_{crop} + F_{p1}S_{crop})C_s}{(1-\theta_t)\rho} + I_{crop}V_{irr}C_w\left(\frac{(1-F_{abs})e^{-WT}F_{p3}}{Y} + \frac{F_{abs}F_{p2}F_{trans}}{Y}\right) \tag{8-9}$$

where:

I_{crop} is the fraction of radionuclide in spray irrigation water that is initially deposited on standing biomass,

F_{trans} is the fraction of absorbed activity that is translocated to the edible portion of the plant by the time of harvest (translocation fraction),

F_{abs} is the fraction of intercepted radionuclide initially deposited onto the plant surface that is absorbed from external surfaces into plant tissues,

F_{p1} is the fraction of external soil contamination on the edible part of the crop retained after food processing,

F_{p2} is the fraction of the internal contamination associated with the edible part of the plant at harvest that is retained after food processing has occurred,

F_{p3} is the fraction of external contamination from interception that is retained on the edible part of the crop after food processing,

W is the removal rate of radionuclide deposited on plant surface by irrigation by weathering processes (weathering rate) including mechanical weathering, wash-off and leaf fall, y^{-1},

T is the interval between irrigation and harvest, y.

It should be noted that it is assumed that the crop can be contaminated due to:

- internal uptake of contaminants from the cultivated soil compartment into the crop via the roots (represented by the $\frac{CF_{crop}C_s}{(1-\theta_t)\rho}$ term);
- external contamination of the crop due to deposition of re-suspended sediment from the surface soil compartment (represented by the $\frac{S_{crop}C_s}{(1-\theta_t)\rho}$ term);
- irrigation (represented by the $I_{crop}V_{irr}C_w$ term).

It is assumed that contamination can be lost due to:

- food preparation (represented by F_{p1}, F_{p2} and F_{p3} terms);
- weathering of the external contamination to the soil (represented by the e^{-WT} term).

An alternative to the e^{-WT} formulation is applied for pasture, see below. This averages out processes on-going through the year, and is more appropriate in the case of pasture since cropping by cows or sheep would be continuous. Using e^{-WT} allows the investigation of alternative assumptions for T, potentially more significant for crops directly consumed by humans.

Consumption of Animal Produce

The annual individual dose from the consumption of animal produce is given by:

$$D_{prod} = ING_{prod}\ DC_{ing}\ C_{prod} \tag{8-10}$$

where:

D_{prod} is the individual dose from consumption of the animal product, mrem y^{-1},

ING_{prod} is the individual consumption rate of the animal product, kg y^{-1},

C_{prod} is the radionuclide concentration in the animal product, Bq kg^{-1}.

The C_{prod} term is calculated using the following equation:

$$C_{prod} = TF_{proding}\left(C_{fodd} ING_{fodd} + C_w ING_{wa} + \frac{C_s \; ING_{sa}}{(1-\theta_t)\rho + \theta\rho_w} \right) + (BR_a O_{an} C_{airs}) TF_{prodinh} \qquad (8\text{-}11)$$

where:

$TF_{proding}$ is the transfer factor for ingestion for the animal product, d kg^{-1} (fresh weight of product),

C_{fodd} is the radionuclide concentration in the animal fodder, Bq kg^{-1} (fresh weight of fodder),

$TF_{prodinh}$ is the transfer factor for inhalation for the animal product, d kg^{-1} (fresh weight of product),

ING_{fodd} is the consumption rate of fodder by the animal, kg (fresh weight) d^{-1},

C_w is the radionuclide concentration in the well water, Bq m^{-3},

ING_{wa} is the consumption rate of water by the animal, m^3 d^{-1},

ING_{sa} is the consumption rate of soil from the cultivated soil compartment by the animal, kg (wet weight of soil) d^{-1},

ρ_w is the density of water, kg m^{-3},

BR_a is the breathing rate of the animal, m^3 h^{-1},

O_{an} is the occupancy time of the animal in the cultivated soil compartment, h d^{-1},

C_{airs} is the radionuclide concentration in the air above the cultivated soil compartment, Bq m^{-3}.

The C_{airs} term is calculated using the following equation:

$$C_{airs} = \frac{C_s}{(1-\theta_t)\,\rho} \, \frac{(R \;\; - 1)}{R} \, dust_s \qquad (8\text{-}12)$$

where:

$dust_s$ is the soil derived dust level in the air above the cultivated soil compartment, kg m^{-3}.

The $TF_{prodinh}$ term is calculated using the following equation:

$$TF_{prodinh} = TF_{proding} \frac{f_L + f_C \, f_1(inh)}{f_1(ing)} \qquad (8\text{-}13)$$

where:

f_L is the fraction of inhaled activity reaching the systemic circulation following transfer across the lung lining,

f_C is the fraction of inhaled activity that is cleared to the gastrointestinal tract, and

$f_l(inh)$ is the fraction of inhaled activity, cleared to the gastrointestinal tract, that is transferred to the systemic circulation.

$f_l(ing)$ is the fraction of ingested activity reaching the body fluids in man.

The nature of the fodder consumed by the animal depends on the type of animal. In this example, one animal type is considered, cows. It is assumed that the cows consume fodder grown on irrigated land. The C_{fodd} term, Bq m^{-3}, is calculated using the following equation:

$$C_{fodd} = \frac{(CF_{past} + S_{past})C_s}{(1-\theta_t)\rho} + \frac{I_{past} V_{irr} C_w}{SB_{past} W_{past} + 365\, ING_{fodd} SD} \tag{8-14}$$

where:

CF_{past} is the concentration factor for pasture, Bq kg^{-1} (fresh weight of pasture)/Bq kg^{-1} (dry weight of soil)

S_{past} is the soil contamination on pasture, kg (dry weight soil)/kg (fresh weight of pasture),

I_{past} is the interception fraction for irrigation water on pasture,

SB_{past} is the standing yield of pasture, kg,

W_{past} is the removal rate of irrigation water from pasture by weathering (weathering rate), y^{-1},

SD is the number of animals per unit area,

ING_{Fodd} here, cf Eqn 8-11, has to be multiplied by 365 to convert to intake as kg fw y^{-1},

The following points should be noted.

It is assumed that the animal can be contaminated due to:

- consumption of contaminated fodder (represented by the $C_{fodd}\, ING_{fodd}$ term);
- consumption of contaminated water (represented by the $C_w\, ING_{wa}$ term);
- consumption of contaminated soil (represented by the $\dfrac{C_s ING_{sa}}{(1-\theta_t)\rho + \theta\rho_w}$ term);
- inhalation of contaminated soil (represented by the $BR_a\, O_{an}\, C_{airs}$ term).

Consumption of Soil

Apart from inadvertent consumption due to soil contamination of crops, soil can be consumed by humans both inadvertently and deliberately. The annual individual dose to humans from this type of soil consumption is given by:

$$D_{soil} = ING_{soil} DC_{ing} \frac{C_s}{(1-\theta_t)\rho + \theta\rho_w} \tag{8-15}$$

where:

D_{soil} is the individual dose from consumption of the soil, mrem y^{-1},

ING_{soil} is the individual consumption rate of the soil, kg y^{-1}, wet weight.

External Irradiation from Soil

The annual individual dose to humans from external irradiation from soil/sediment, during occupancy of the soil compartment, is given by:

$$D_{exsoil} = \frac{O_s DC_{exts} C_s}{(1-\theta_t)\rho + \theta\rho_w} \tag{8-16}$$

where:

D_{exsoil} is the individual dose from external irradiation from the soil, mrem y^{-1},

O_s is the individual occupancy in the soil compartment, h y^{-1},

DC_{exts} is the dose factor for external irradiation from soil, mrem h^{-1}/Bq kg^{-1}.

External Irradiation from Immersion in Water

The annual individual dose to humans from external irradiation from immersion in water is given by:

$$D_{imwat} = O_{wat}\ DC_{imw}\ C_w \tag{8-17}$$

where:

D_{imwat} is the individual dose from external irradiation from immersion in the water, mrem y^{-1},

O_{wat} is the individual occupancy in the water, h y^{-1},

DC_{immw} is the dose coefficient for external irradiation from immersion in water, mrem h^{-1} / Bq m^{-3}.

Inhalation of Dust

The annual individual dose to humans from the inhalation of dust, during occupancy of the soil compartment, is given by:

$$D_{dust} = DC_{inh} BR \; O_s C_{airs} \tag{8-18}$$

where:

D_{dust} is the individual dose from the inhalation of dust, mrem y^{-1},

DC_{inh} is the dose coefficient for inhalation, mrem Bq^{-1},

BR is the breathing rate of the human in the soil compartment, m^3 h^{-1}.

Inhalation of Aerosols/Spray in irrigation activities

The annual individual dose to humans from the inhalation of aerosols in water spray is given by:

$$D_{aero} = DC_{inh} BR \; AIR_{aero} O_{aero} C_w \tag{8-19}$$

where:

D_{aero} is the individual dose from the inhalation of aerosols, mrem y^{-1},

Air_{aero} is the aerosol level in the air in the area affected by aerosols/spray, m^3 m^{-3},

O_{aero} is the individual occupancy in the area affected by aerosols, h y^{-1}.

8.2.5.3. Quantitative description of exposure groups

Assumptions are required for consumption of the following foods and water, assumed to be consumed:

- root vegetables;
- green vegetables;
- grain;
- fruit;

- cow meat;
- chicken meat;
- eggs; and
- water.

These foods are chosen because of their correspondence to the system description and to habit survey data for Amargosa Valley residents. In addition, inadvertent ingestion of soil is included. Consumption data for these relevant to Amargosa Valley were provided by Wasiolek [2001]. These are mean values allowing for the proportion of food derived from uncontaminated sources. A nominal 1 kg y^{-1} consumption of cow liver is also assumed because of high uptake potential [EPRI, 1996]; [BIOMOVS II, 1996].

Occupancy times and breathing rates are also required for inhalation and external irradiation pathways. Data are provided by Wasiolek [2001]; however, the occupancy for inhalation of dust from soil is split into two values, one at low dust level for most of the year and low breathing rate and the other at a raised dust level (associated with working/recreation with the soil itself) and high breathing rate, but only for a small proportion of the year. That is, it is assumed here that the critical group member spends some time doing activities which involve creation of dust, but most of the time not doing so. Data values and sources are discussed below.

8.2.6 Provision of Data

Element-independent data are provided in Table 8-7; radionuclide-specific data are in Table 8-8 and element dependent data are provided in Tables 8-9 – 8-24. Single values of parameters to be used in calculations are provided, with references. This approach relies upon justifying the selection of parameters from previous modelling experience, notably IAEA [2001]. It is difficult to identify critical but uncertain parameters until a real source term is applied. However, several examples of potentially important data deficiencies are identified in IAEA [2001].

The data used were substantially taken from the BIOMASS Example 2A [IAEA, 2000a]. Where the data in this model were clearly not suitable for this assessment, data were found in alternative literature, e.g. with more relevant parameter values for the arid climate of Yucca Mountain. For example, where available, sorption coefficients in soil were used for sandy soils likely to be prevalent in Amargosa Valley. It is suggested here, however, that information is generally lacking for many radionuclides, especially as regards correlations, e.g. soil type to sorption and root uptake.

Table 8-7
Element-Independent Data

Parameter	Value	Units	Justification and Comments – references are at end of table.
Irrigation rate, V_{irr}	2.0E-1	$m^3 y^{-1}$	Irrigation rates will vary from crop to crop. Garden producers may use less water than commercial growers. The value adopted is an assumed average over the crop and producer type. Note that the consumption rate assumptions relate to the proportion of food type associated with local produce, which may be dominated by gardeners or small producers in Amargosa Valley.
Infiltration rate, I	1.0E-1	$m y^{-1}$	
Wet soil porosity, θ	2.0E-1	-	
Total soil porosity, θ_t	5.0E-1	-	
Cultivated soil thickness, d	3.0E-1	m	Ploughing/tilling depths
Soil grain density,	2.65E3	$kg m^{-3}$	
Groundwater ingestion rate humans, ING_w	7.9E-1	$m^3 y^{-1}$	Wasiolek [2001]
Locally-produced crop ingestion rate human, ING_{crop}		$kg y^{-1}$	
- Root veg	8.5E0		Wasiolek [2001] Consumption rates are for locally-produced crops, not the total consumption rates.
- Green veg	7.0E0		
- Grain	6E-1		
- Fruit	2.31E1		
Crop soil contamination, S_{crop}		kg dw soil per kg fw crop	

- Root veg	2.0E-4		Chosen from consideration of data in BIOMOVS II [1996], Müller and Prohl [1993], Ashton and Sumerling [1988], EPRI [1996] and Brown and Simmonds [1995]
- Green veg	2.0E-4		
- Grain	2.0E-4		
- Pasture	2.0E-3		
- Fruit	2.0E-4		
Crop annual yield, Y		kg fw y^{-1}	Values are all per m^2 of soil area
- Root veg	3.0E0		Chosen from consideration of data in BIOMOVS II [1996], Müller and Prohl [1993], Ashton and Sumerling [1988], EPRI [1996] and Brown and Simmonds [1995]
- Green veg	3.0E0		
- Grain	4.0E-1		
- Pasture, Y_{past}	5.0E0		
- Fruit	7E-1		
Standing yield of fodder, SB_{past}	8.3E-1	kg	Assumes the annual yield is grazed six times
Locally-produced animal product consumption rate, ING_{prod}		kg y^{-1}	
- Cow meat	3.3E0		Wasiolek, [2001]
- Cow liver	1.0E0		Nominal value to illustrate partial significance
- Milk	4.2E0		Wasiolek, [2001]
- Chicken meat	6E-1		
- Chicken eggs	8.9E0		

Animal consumption rate, fodder ING_{fodd}		kg d^{-1} fw	
- Cow	6E1		EPRI [1996]
- Chicken	3E-1		EPRI [1996]
Animal groundwater consumption rate, ING_{wa}		m^3 d^{-1}	
- Cow	6E-2		EPRI [1996]
- Chicken	5E-4		EPRI [1996]
Animal soil consumption rate, ING_{sa}		kg d^{-1} wet soil	
- Cow	6E-1		EPRI [1996]
- Chicken	2E-2		EPRI [1996]
Water density, ρ_w	1.0E3	kg m^{-3}	Lide [2000]
Animal breathing rate, BR_a		m^3 h^{-1}	
-cow	5.4E0		Brown and Simmonds [1995]
-chicken	1E-2		EPRI [1996]
Animal occupancy, O_{an}	2.4E1	h d^{-1}	
Dust in air, $dust_s$ value for normal activity value for physical working in dry soil conditions	 1.0E-7 5.0E-6	kg m^{-3}	BIOMASS [2000
Number of animals in area of interest, SD		-	
- Cow	4.3E-4		EPRI [1996]

- Chicken	3E0		EPRI [1996]
Inadvertant soil consumption, human, ING_{soil} (adults)	1.8E-2	kg y^{-1} fw	Wasiolek [2001]
Soil occupancy, human O_s	3.4E3	h y^{-1}	Wasiolek [2001]
Inhalation occupancy, human O_{inh}		h y^{-1}	Wasiolek [2001] for total but ratio between the two activities as per IAEA [2001]
value for normal activity	5.5E3		
value for hard physical activity in dry soil conditions	6.1E2		
Bathing occupancy, O_{wout}	3.65E2	h y^{-1}	BIOMASS [2001]
Human Adult Breathing rate, BR		m^3 h^{-1}	BIOMASS [2000]
value for normal activity	1.2E0		
value for physical working in dry soil conditions	1.7E0		
Time from irrigation to harvest, T		y	
- Root veg	4.0E-2		Typical farming practice as suggested by personal communication from Prohl and Coughtrey.
- Green veg	2.0E-2		
- Grain	7.5E-2		
- Pasture	2.0E-2		
- Fruit	2.0E-2		

Table 8-7 References

Ashton J and Sumerling T J (1988). Biosphere database for assessments of radioactive waste disposals. UKDoE Report No. DoE/RW/88.083.

BIOMOVS (1990). Scenario B6. Transport of Radionuclides to Root-zone Soil from Contaminated Groundwater. BIOMOVS Phase 1 Technical Report 9. Swedish Radiation Protection Institute, Stockholm.

Brown J and Simmonds J R (1995). FARMLAND, A Dynamic Model for the Transfer of Radionuclides through Terrestrial Foodchains, NRPB-R273.

EPRI (1996). Biosphere Modelling and Dose Assessment for Yucca Mountain. EPRI Report TR-107190, Electric Power Research Institute, Palo Alto CA.

IAEA (2001). BIOsphere Modelling and ASSessment BIOMASS Programme Version 2, Working Material CD, Reproduced by the IAEA, February 2001. International Atomic Energy Agency, Vienna

Müller H and Prohl G (1993). ECOSYS.87: A Dynamic Model for Assessing Radiological Consequences of Nuclear Accidents, Health Physics, Vol 64, No 3.

Wasiolek M (2001). Data supplied as personal communication by the Yucca Mountain Project Biosphere Assessment team.

Radionuclide-Specific Data

Table 8-8
Half-life and Dose Coefficient Data

[Includes contributors from short-lived daughters assumed to be in equilibrium.]

Radionuclide	Half life [1]	Ingestion Dose coefficient [3]	Ingestion Dose coefficient[†]	Inhalation Dose Coefficient [3]	Inhalation Dose Coefficient[†]	External Irradiation from soil [4]	External Irradiation from Water [4]
	Years	Sv/Bq	mrem/mol	Sv/Bq	mrem/mol	(mrem/h)/(mol/kg)	(mrem/h)/ (mol/m3)
Cl-36	3.01E5	9.3E-10	4.1E-4	7.3E-9	3.2E-3	0	0
Se-79 [2]	1.136	2.9E-9	3.4E-4	6.8E-9	8.0E-4	0	1.9E-1
Nb-94	2.03E4	1.7E-9	1.1E-2	4.9E-8	3.2E-1	2.0E7	3.9E4
Tc-99	2.13E5	6.4E-10	4.0E-4	1.3E-8	8.1E-3	0	1.5E0
I-129	1.57E7	1.1E-7	9.3E-4	3.6E-8	3.0E-4	4.1E1	3.1E-1
Cs-135	2.30E6	7.9E-10	4.5E-5	8.6E-9	4.6E-4	0	7.1E-2
Pb-210	2.23E1	6.9E-7	4.1E3	5.6E-6	3.3E4	4.5E6	4.2E4
Po-210	3.79E1	1.2E-6	4.2E5	4.3E-6	1.5E6	6.0E6	1.2E4
Ra-226	1.60E3	2.8E-7	2.3E1	9.5E-6	7.9E2	2.0E8	5.6E5
Ac-227	2.18E1	1.1E-6	6.7E3	5.5E-4	3.3E6	2.3E9	9.1E6
Ra-228	5.75E0	6.9E-7	1.6E4	1.6E-5	3.7E5	3.0E10	7.8E7
Th-228	1.91E0	7.2E-7	5.0E4	4.0E-5	2.8E6	6.3E10	3.9E8
Th-229	7.34E3	4.9E-7	8.8E0	2.4E-4	4.3E3	5.2E6	2.3E4
Th-230	7.70E4	2.1E-7	3.6E-1	1.0E-4	1.7E2	1.0E2	3.2E0
Pa-231	3.28E4	7.1E-7	2.9E0	1.4E-4	5.7E2	6.9E4	4.4E2
Th-232	1.41E10	2.3E-7	2.2E-6	1.1E-4	1.0E-3	2.9E-4	9.3E-6
Pa-233	7.39E-2	8.7E-10	1.6E3	3.9E-9	7.0E3	5.6E11	1.3E9
U-233	1.59E5	5.1E-8	4.3E-2	9.6E-6	8.0E0	4.2E1	2.1E-1
U-234	2.45E5	4.9E-8	2.7E-2	9.4E-6	5.1E0	2.1E1	4.7E-1
U-235	7.04E8	4.7E-8	8.8E-6	8.5E-6	1.6E-3	1.9E1	1.2E-1
U-236	2.34E7	4.7E-8	2.7E-4	8.7E-6	4.9E-2	1.8E-1	3.2E-3
Np-237	2.14E6	1.1E-7	6.8E-3	5.0E-5	3.1E0	8.7E3	5.0E1
U-238	4.47E9	4.5E-8	1.3E-6	8.0E-6	2.4E-4	7.7E-1	3.9E-3
Pu-239	2.41E4	2.5E-7	1.4E0	1.2E-4	6.6E2	9.3E1	2.4E0
Pu-240	6.54E3	2.5E-7	5.1E0	1.2E-4	2.4E3	9.7E2	1.1E1
Pu-242	3.76E5	2.4E-7	8.4E-2	4.8E-5	1.7E1	1.3E1	1.5E-1
Am-243	7.38E3	2.0E-7	3.6E0	9.6E-5	1.7E3	7.9E5	3.2E3

[†] The mrem/Mol values were obtained by converting Sv/Bq to moles according to the half life of the radionuclide

References for Table 8-8

[1] ICRP (1983). ICRP Publication 38, Radionuclide Transformations: Energy and Intensity of Emissions, Annals of ICRP 11-13. International Commission on Radiological Protection, Pergamon Press.

[2] Nuclear Instruments and Methods in Phyisics Research, 1997, Series B, Vol 123 P405-4-9

[3] ICRP (1999). ICRP Publication 72, Age-dependent Doses to members of the Public from Intake of Radionuclides: Part 5. International Commission on Radiological Protection, Pergamon Press.

[4] Ashton J and Sumerling T J (1988). Biosphere Database for Assessments of Radioactive Waste Disposals. UK Department of the Environment Report DoE/RW/88/083.

Table 8-9
Element Dependent Data: Actinium

Parameter	Value	Units	Justification – references are at end of table.
Sorption coefficient soil, K_d	4.5E-1	$m^3\ kg^{-1}$ dw	EPRI [1996]
Crop concentration factor, CF_{crop}		Bq kg^{-1} fw per Bq kg^{-1} dw	
- Root veg	1.0E-3		EPRI [1996]
- Green veg	1.0E-3		EPRI [1996]
- Grain	1.0E-3		EPRI [1996]
- Pasture	1.0E-3		EPRI [1996]
- Fruit	5.0E-4		Appendix C
Interception factor for crop, I_{crop}	3.0E-1		EPRI [1996]
External interception fraction retained after food processing, F_{p3}		-	
- Root veg	1.0E-1		BIOMASS Example 2A [IAEA, 2001]
- Green veg	1.0E-1		BIOMASS Example 2A [IAEA, 2001]
- Grain	0.0E0		BIOMASS Example 2A [IAEA, 2001]
- Fruit	1.0E0		Appendix C
Internal food processing retained fraction, F_{p2}	1.0E0		BIOMASS Example 2A [IAEA, 2001]
External contamination due to soil, food processing retained fraction, F_{p1}	1.0E-1	-	
- Root veg	1.0E-1		BIOMASS EXAMPLE 2A [IAEA, 2001]
- Green veg	1.0E-1		BIOMASS EXAMPLE 2A [IAEA, 2001]

Parameter	Value	Units	Justification – references are at end of table.
- Grain	1.0E-1		BIOMASS EXAMPLE 2A [IAEA, 2001]
- Fruit	1.0E-1		Appendix C
Absorbed fraction, external to internal, F_{abs}		-	BIOMASS Example 2A [IAEA, 2001]
- Fruit	4.8E-1		Appendix C
- Others	5.0E-1		BIOMASS EXAMPLE 2A [IAEA, 2001]
Translocation factor, F_{trans}		-	
- Root veg	2.9E-1		EPRI [1996]
- Green veg	4.5E-1		EPRI [1996]
- Grain	2.0E-1		EPRI [1996]
-Fruit	1.0E0		Appendix C
Weathering rate, W		y^{-1}	
- Root veg	1.8E1		EPRI [1996]
- Green veg	1.8E1		EPRI [1996]
- Grain	8.4E0		EPRI [1996]
- Pasture	1.8E1		EPRI [1996]
- Fruit	1.8E1		Appendix C
Animal product transfer factor, $TF_{proding}$		$d\ kg^{-1}$	
- Cow Meat	1.6E-3		EPRI [1996]
- Cow Liver	1.4E-2		EPRI [1996]
- Cow Milk	4.0E-7	$d\ l^{-1}$	EPRI [1996]
-Chicken Meat	6.6E-3		EPRI [1996]

Parameter	**Value**	**Units**	**Justification – references are at end of table.**
-Chicken Egg	1.6E-2		EPRI [1996]
Animal product transfer factor from inhalation, $T_{fprodinh}$		d kg^{-1}	
- Cow Meat	1.6E-3		EPRI [1996]
- Cow Liver	1.4E-2		EPRI [1996]
- Cow Milk	4.0E-7	d l^{-1}	EPRI [1996]
-Chicken Meat	6.6E-3		EPRI [1996]
-Chicken Egg	1.6E-2		EPRI [1996]

References for Table 8-9

EPRI (1996). Biosphere Modelling and Dose Assessment for Yucca Mountain. EPRI Report TR-107190, Electric Power Research Institute, Palo Alto CA.

IAEA (2001). BIOsphere Modelling and ASSessment BIOMASS Programme Version 2, Working Material CD, Reproduced by the IAEA, February 2001. International Atomic Energy Agency, Vienna.

Table 8-10
Element Dependent Data, Americium

Parameter	Value	Units	Justification –references are at end of table.
Sorption coefficient soil, K_d	2.0E0	$m^3\ kg^{-1}$ dw	EPRI [1996]
Crop concentration factor, CF_{crop}		Bq kg^{-1} fw per Bq kg^{-1} dw	
- Root veg	1.0E-3		EPRI [1996]
- Green veg	1.0E-3		EPRI [1996]
- Grain	1.0E-5		EPRI [1996]
- Pasture	5.0E-3		EPRI [1996]
- Fruit	1.0E-3		Appendix C
Interception factor for crop, I_{crop}	3.0E-1		EPRI [1996]
External interception fraction retained after food processing, F_{p3}		-	
- Root veg	1.0E-1		BIOMASS Example 2A [IAEA, 2001]
- Green veg	1.0E-1		BIOMASS Example 2A [IAEA, 2001]
- Grain	0.0E0		BIOMASS Example 2A [IAEA, 2001]
- Fruit	1.0E0		Appendix C
Internal food processing retained fraction, F_{p2}	1.0E0		BIOMASS Example 2A [IAEA, 2001]
External contamination due to soil, food processing retained fraction, F_{p1}	1.0E-1	-	
- Root veg	1.0E-1		BIOMASS Example 2A [IAEA, 2001]
- Green veg	1.0E-1		BIOMASS Example 2A [IAEA, 2001]

Parameter	Value	Units	Justification –references are at end of table.
- Grain	1.0E-1		BIOMASS Example 2A [IAEA, 2001]
- Fruit	1.0E-1		Appendix C
Absorbed fraction, external to internal, F_{abs}		-	
- Fruit	4.8E-1		Appendix C
- Others	5.0E-1		BIOMASS Example 2A [IAEA, 2001]
Translocation factor, F_{trans}		-	
- Root veg	2.9E-1		EPRI [1996]
- Green veg	2.8E-1		EPRI [1996]
- Grain	1.3E-1		EPRI [1996]
-Fruit	1.0E0		Appendix C
Weathering rate, W		y^{-1}	
- Root veg	1.8E1		EPRI [1996]
- Green veg	5.1E1		EPRI [1996]
- Grain	5.1E1		EPRI [1996]
- Pasture	1.8E1		EPRI [1996]
- Fruit	1.8E1		EPRI [1996]
Animal product transfer factor, TFproding		d kg^{-1}	
- Cow Meat	4.0E-4		EPRI [1996]
- Cow Liver	6.8E-2		EPRI [1996]
- Cow Milk	5.0E-6	d l^{-1}	EPRI [1996]
-Chicken Meat	1.0E-1		EPRI [1996]

Parameter	Value	Units	Justification –references are at end of table.
-Chicken Egg	3.9E-3		EPRI [1996]
Animal product transfer factor from inhalation, TFprodinh		d kg^{-1}	
- Cow Meat	4.0E-4		EPRI [1996]
- Cow Liver	6.8E-2		EPRI [1996]
- Cow Milk	5.0E-6	d l^{-1}	EPRI [1996]
-Chicken Meat	1.0E-1		EPRI [1996]
-Chicken Egg	3.9E-3		EPRI [1996]

References for Table 8-10

BIOMASS (2001). Contributions to the documentation of Critical and other Exposure Groups for ERB2A & ERB2B. BIOMASS Theme 1, Task Group 1, Note 1, Version 2.0, February 2001.

EPRI (1996). Biosphere Modelling and Dose Assessment for Yucca Mountain. EPRI Report TR-107190, Electric Power Research Institute, Palo Alto CA.

Table 8-11
Element Dependent Data: Cesium

Parameter	Value	Units	Justification –references are at end of table.
Sorption coefficient soil, K_d	2.7E-1	$m^3\ kg^{-1}$ dw	EPRI [1996]
Crop concentration factor, CF_{crop}		Bq kg^{-1} fw per Bq kg^{-1} dw	
- Root veg	3.0E-2		EPRI [1996]
- Green veg	3.0E-2		EPRI [1996]
- Grain	2.0E-2		EPRI [1996]
- Pasture	3.0E-2		EPRI [1996]
- Fruit	5.0E-2		Appendix C
Interception factor for crop, I_{crop}	3.0E-1		EPRI [1996]
External interception fraction retained after food processing, F_{p3}		-	
- Root veg	1.0E-1		BIOMASS Example 2A [IAEA, 2001]
- Green veg	1.0E-1		BIOMASS Example 2A [IAEA, 2001]
- Grain	0.0E0		BIOMASS Example 2A [IAEA, 2001]
- Fruit	1.0E0		Appendix C
Internal food processing retained fraction, F_{p2}	1.0E0		BIOMASS Example 2A [IAEA, 2001]
External contamination due to soil, food processing retained fraction, F_{p1}	1.0E-1	-	
- Root veg	1.0E-1		BIOMASS Example 2A [IAEA, 2001]

Parameter	**Value**	**Units**	**Justification –references are at end of table.**
- Green veg	1.0E-1		BIOMASS Example 2A [IAEA, 2001]
- Grain	1.0E-1		BIOMASS Example 2A [IAEA, 2001]
- Fruit	1.0E-1		Appendix C
Absorbed fraction, external to internal, F_{abs}		-	
- Fruit	4.8E-1		Appendix C
- Others	5.0E-1		BIOMASS Example 2A [IAEA, 2001]
Translocation factor, F_{trans}		-	
- Root veg	3.0E-1		EPRI [1996]
- Green veg	1.9E-1		EPRI [1996]
- Grain	8.8E-2		EPRI [1996]
-Fruit	1.0E0		EPRI [1996]
Weathering rate, W		y^{-1}	
- Root veg	1.8E1		EPRI [1996]
- Green veg	1.8E1		EPRI [1996]
- Grain	8.4E0		EPRI [1996]
- Pasture	1.8E1		EPRI [1996]
- Fruit	1.8E1		EPRI [1996]
Animal product transfer factor, Tfproding		d kg^{-1}	
- Cow Meat	5.0E-2		EPRI [1996]
- Cow Liver	3.1E-2		EPRI [1996]

Parameter	**Value**	**Units**	**Justification –references are at end of table.**
- Cow Milk	8.0E-3	d l^{-1}	EPRI [1996]
-Chicken Meat	1.2E1		EPRI [1996]
-Chicken Egg	4.0E-1		EPRI [1996]
Animal product transfer factor from inhalation, TFprodinh		d kg^{-1}	
- Cow Meat	5.0E-2		EPRI [1996]
- Cow Liver	3.1E-2		EPRI [1996]
- Cow Milk	8.0E-3	d l^{-1}	EPRI [1996]
-Chicken Meat	1.2E1		EPRI [1996]
-Chicken Egg	4.0E-1		EPRI [1996]

References for Table 8-11

BIOMASS (2001). Contributions to the documentation of Critical and other Exposure Groups for ERB2A & ERB2B. BIOMASS Theme 1, Task Group 1, Note 1, Version 2.0, February 2001.

EPRI (1996). Biosphere Modelling and Dose Assessment for Yucca Mountain. EPRI Report TR-107190, Electric Power Research Institute, Palo Alto CA.

Table 8-12
Element Dependent Data, Chlorine

Parameter	Value	Units	References
Sorption coefficient soil, K_d	8.0E-4 (1)	$m^3\ kg^{-1}$ dw	[1]
Crop concentration factor, CF_{crop}		Bq kg^{-1} fw per Bq kg^{-1} dw	
- Root veg	5.0E+0		[2], [3]
- Green veg	5.0E+0		[2], [3]
- Grain	5.0E+0		[2], [3]
- Pasture	5.0E+0		[2], [3]
- Fruit	5.0E+0		[2], [3]
Interception factor for crop, I_{crop}	3.0E-1		In the absence of data for chlorine, using data for Iodine [1], [5]
External interception fraction retained after food processing, F_{p3}		-	
- Root veg	0		[5] used in absence of specific data
- Green veg	1.0E-1		[5] used in absence of specific data
- Grain	1.0E-2		[5] used in absence of specific data
- Fruit	1.0E+0		Appendix C
Internal food processing retained fraction, F_{p2}	1.0E+0		[4]
External contamination due to soil, food processing retained fraction, F_{p1}		-	
- Root veg	1.0E-1		[5] data used in absence of specific data

Parameter	Value	Units	References
- Green veg	1.0E-1		[5] data used in absence of specific data
- Grain	1.0E-1		[5] data used in absence of specific data
- Fruit	1.0E-1		Appendix C
Absorbed fraction, external to internal, F_{abs}	5.0E-1	-	[5] data used in the absence of specific data
Translocation factor, F_{trans}		-	
- Root veg	1.0E-1		[5] data for iodine used in the absence of specific data
- Green veg	1.0E+0		[5] data for iodine used in the absence of specific data
- Grain	1.0E-1		[5] data for iodine used in the absence of specific data
-Fruit	1.0E+0		Data for iodine [4]
Weathering rate, W		y^{-1}	
- Root veg	1.8E1		[5]
- Green veg	1.8E1		[5]
- Grain	1.8E1		[5]
- Pasture	1.8E1		[5]
- Fruit	3.2E1		Data for iodine [4]
Animal product transfer factor, TFproding		d kg^{-1}	
- Cow Meat	4.3E-2		[1], [2]
- Cow Liver	4.3E-2		[1], [2]
- Cow Milk	1.7E-2	d l^{-1}	[1], [2], [6]

Parameter	Value	Units	References
-Chicken Meat	8.7E+0		[1]
-Chicken Egg	8.7E+0		[1]
Animal product transfer factor from inhalation, TFprodinh		d kg^{-1}	
- Cow Meat	4.3E-2		[1], [2]
- Cow Liver	4.3E-2		[1], [2]
- Cow Milk	1.7E-2	d l^{-1}	[1], [2], [6]
-Chicken Meat	8.7E+0		[1]
-Chicken Egg	8.7E+0		[1]

References for Table 8-12

[1] Reference to Coughtrey et al [1983], suggest that chlorine (Cl -) is highly mobile within a soil environment and moved rapidly by leaching. It can be assumed that when chlorine radioisotopes enter soil as soluble compounds, the majority of the added activity will remain present as chloride ions, either in soil solutions or weakly ion exchanged.

[2] Smith G M, Fearn H S, Smith K R, Davis J P and Klos R (1988). Assessment of the radiological impact of disposal of solid radioactive waste at Drigg. National Radiological Protection Board, NRPB-M148, Chilton, UK

[3] Coughtrey P J, Jackson D, Thorne M C (1983-85). Radionuclide Distribution and Transport in Terrestrial and Aquatic Ecosystems. Volumes 1-6. AA Balkema, Rotterdam.

[4] Appendix C of this report.

[5] IAEA (2001). BIOsphere Modelling and ASSessment BIOMASS Programme Version 2, Working Material CD, Reproduced by the IAEA, February 2001. International Atomic Energy Agency, Vienna.

[6] Dickson J M (19930. Derivation of a quality assured database for BIOS. Nirex Safety Studies Report NSS/B106

Table 8-13
Element Dependent Data, Iodine

Parameter	**Value**	**Units**	**Reference**
Sorption coefficient soil, K_d	1.0E-3	$m^3 kg^{-1}$ dw	[1], [2], [3], [4]
Crop concentration factor, CF_{crop}		Bq kg^{-1} fw per bq kg^{-1} dw	
- Root veg	1.0E-1		[1], [2], [5],[6], [7], [8], [10]
- Green veg	1.0E-1		[1], [2], [5],[6], [7], [8], [10]
- Grain	1.0E-1		[1], [2], [5],[6], [7], [8], [10]
- Pasture	1.0E-1		[1], [2], [5],[6], [7], [8], [10]
- Fruit	1.0E-2		[9]
Interception factor for crop, I_{crop}	3.0E-1	-	[1], [10]
External food processing retained fraction, F_{p3}		-	
- Root veg	0		[10]
- Green veg	1.0E-1		[10]
- Grain	1.0E-2		[10]
- Fruit	1.0E+0		[9]
Internal food processing retained fraction, F_{p2}	1.0E+0	-	[10]
External contamination due to soil, food processing retained fraction, F_{p1}			
- Root veg	1.0E-1		[10]

Parameter	Value	Units	Reference
- Green veg	1.0E-1		[10]
- Grain	1.0E-1		[10]
- Fruit	1.0E-1		[10]
Absorbed fraction, external to internal, F_{abs}	5.0E-1		[10]
Translocation factor, F_{trans}		-	
- Root veg	1.0E-1		[10]
- Green veg	1.0E+0		[10]
- Grain	1.0E-1		[10]
-Fruit	1.0E+0		[9]
Weathering rate, W		y^{-1}	
- Root veg	1.8E+1		[10]
- Green veg	1.8E+1		[10]
- Grain	8.4E0		[10]
- Pasture	1.8E+1		[10]
- Fruit	3.2E+1		[9]
Animal product transfer factor, Tfproding		d kg^{-1}f.w.	
- Cow Meat	3.0E-3		[1], [2], [8], [11], [14], [15]
- Cow Liver	2.0E-3		[2], [10]
- Cow Milk	3.0E-3	d l^{-1}	[2], [5], [10], [11], [12], [15]
- Chicken Meat	2.0E-1		[1], [14]

Parameter	Value	Units	Reference
- Chicken Eggs	1.6E+0		[1], [13]
Animal product transfer factor from inhalation, TFprodinh		d kg^{-1}f.w.	
- Cow Meat	3.0E-3		[1], [2], [8], [11], [14], [15]
- Cow Liver	2.0E-3		[2], [10]
- Cow Milk	3.0E-3	d l^{-1}	[2], [5], [10], [11], [12], [15]
- Chicken Meat	2.0E-1		[1], [14]
- Chicken Eggs	1.6E+0		[1], [13]

References for Table 8-13

[1] Ashton J and Sumerling T J (1988). Biosphere Database for Assessments of Radioactive Waste Disposals. UK Department of the Environment Report DoE/RW/88/083.

[2] Smith G M, Fearn H S, Smith K R, Davis J P and Klos R (1988). Assessment of the radiological impact of disposal of solid radioactive waste at Drigg. National Radiological Protection Board, NRPB-M148, Chilton, UK

[3] Pinner A V, Hemming C R and Hill M D (1984). An assessment of the radiological protection aspects of shallow land burial of radioactive waste. U.K. National Radiological Protection Board, NRPB-R161, Chilton, UK

[4] Sheppard M I, Beals D I, Thibault D H and O'Connor P (1984). Soil nuclide distribution coefficients and their statistical distributions. Atomic Energy of Canada Limited Report AECL-8364.

[5] Coughtrey P J, Jackson D, Thorne M C (1983-85). Radionuclide Distribution and Transport in Terrestrial and Aquatic Ecosystems. Volumes 1-6. AA Balkema, Rotterdam.

[6] Klos R A, Smith K R, Smith G M (1989). Calculations of the Radiological Impact of Unit Releases of Radionuclides to the Biosphere from Solid Waste Disposal Facilities. National Radiological Protection Board, NRPB-M150, Chilton, UK

[7] IAEA (1995). Generic Models and Parameters for Assessing the Environmental Transfer of Radionuclides from Routine Release Safety Series No 57 (draft). IAEA, Vienna

[8] Simmonds J R and Crick M J (1982). Transfer parameters for use in terrestrial foodchain models. NRPB report No M63

[9] Appendix C of this report

[10] IAEA (2001). BIOsphere Modelling and ASSessment BIOMASS Programme Version 2, Working Material CD, Reproduced by the IAEA, February 2001. International Atomic Energy Agency, Vienna.

[11] Dickson J M (1993). Derivation of a quality assured database for BIOS. Nirex Safety Studies Report NSS/B106

[12] Bishop G P, Beetham C J and Cuff Y S (1989). Review of literature for chlorine, technetium, iodine and neptunium. Nirex Safety Studies Report NSS/R193

[13] Ng Y C, Colsher C S and Thompson S E (1982). Transfer coefficients for assessing the dose from radionuclides in meat and eggs. NUREG/CR-2976.

[14] Ng Y C (1982). A review of transfer factors for assessing the dose from radionuclides in agricultural products. Nuclear Safety, Vol 23, No 1, pp57.

[15] IAEA (1994). Handbook of Parameter Values for the Prediction of Radionuclide Transfer in Temperate Environments. Technical Reports Series No 364. IAEA, Vienna.

Table 8-14
Element Dependent Data, Lead

Element Dependent Data, Lead			
Parameter	**Value**	**Units**	**Justification –references are at end of table.**
Sorption coefficient soil, K_d	2.7E-1	$m^3\ kg^{-1}$ dw	EPRI [1996]
Crop concentration factor, CF_{crop}		Bq kg^{-1} fw per Bq kg^{-1} dw	
- Root veg	1.0E-2		EPRI [1996]
- Green veg	1.0E-2		EPRI [1996]
- Grain	1.0E-2		EPRI [1996]
- Pasture	1.0E-2		EPRI [1996]
- Fruit	1.0E-2		Appendix C
Interception factor for crop, I_{crop}	3.0E-1		EPRI [1996]
External interception fraction retained after food processing, F_{p3}		-	
- Root veg	1.0E-1		BIOMASS Example 2A [IAEA, 2001]
- Green veg	1.0E-1		BIOMASS Example 2A [IAEA, 2001]
- Grain	1.0E-2		BIOMASS Example 2A [IAEA, 2001]
- Fruit	1.0E0		Appendix C
Internal food processing retained fraction, F_{p2}	1.0E0		BIOMASS Example 2A [IAEA, 2001]

Element Dependent Data, Lead			
Parameter	**Value**	**Units**	**Justification –references are at end of table.**
External contamination due to soil, food processing retained fraction, F_{p1}	1.0E-1	-	
- Root veg	1.0E-1		BIOMASS Example 2A [IAEA, 2001]
- Green veg	1.0E-1		BIOMASS Example 2A [IAEA, 2001]
- Grain	1.0E-1		BIOMASS Example 2A [IAEA, 2001]
- Fruit	1.0E-1		Appendix C
Absorbed fraction, external to internal, F_{abs}		-	
- Fruit	4.8E-1		BIOMASS Example 2A [IAEA, 2001]
- Others	5.0E-1		BIOMASS Example 2A [IAEA, 2001]
Translocation factor, F_{trans}		-	
- Root veg	2.2E-1		EPRI [1996]
- Green veg	2.2E-1		EPRI [1996]
- Grain	1.0E-1		EPRI [1996]
-Fruit	1.0E0		Appendix C
Weathering rate, W		y^{-1}	
- Root veg	1.8E1		EPRI [1996]
- Green veg	1.8E1		EPRI [1996]
- Grain	8.4E0		EPRI [1996]
- Pasture	1.8E1		EPRI [1996]

Element Dependent Data, Lead			
Parameter	Value	Units	Justification –references are at end of table.
- Fruit	1.8E1		Appendix C
Animal product transfer factor, Tfproding		d kg^{-1}	
- Cow Meat	1.0E-2		EPRI [1996]
- Cow Liver	1.3E0		EPRI [1996]
- Cow Milk	3.0E-4	d l^{-1}	EPRI [1996]
-Chicken Meat	1.2E0		EPRI [1996]
-Chicken Egg	1.2E0		EPRI [1996]
Animal product transfer factor from inhalation, Tfprodinh		d kg^{-1}	
- Cow Meat	1.0E-2		EPRI [1996]
- Cow Liver	1.3E0		EPRI [1996]
- Cow Milk	3.0E-4	d l^{-1}	EPRI [1996]
-Chicken Meat	1.2E0		EPRI [1996]
-Chicken Egg	1.2E0		EPRI [1996]

References for Table 8-14

EPRI (1996). Biosphere Modelling and Dose Assessment for Yucca Mountain. EPRI Report TR-107190, Electric Power Research Institute, Palo Alto CA.

IAEA (2001). BIOsphere Modelling and ASSessment BIOMASS Programme Version 2, Working Material CD, Reproduced by the IAEA, February 2001. International Atomic Energy Agency, Vienna.

Table 8-15
Element Dependent Data, Neptunium

Element Dependent Data, Neptunium			
Parameter	Value	Units	References
Sorption coefficient soil, K_d	5.0E-3	$m^3\ kg^{-1}$ dw	[1], [2], [3], [4]
Crop concentration factor, CF_{crop}		Bq kg^{-1} fw per bq kg^{-1} dw	
- Root veg	5.0E-3		[1], [2], [5], [6], [7], [8]
- Green veg	5.0E-3		[1], [2], [5], [6], [7], [8]
- Grain	2.0E-3		[1], [2], [5], [6], [7], [8]
- Pasture	5.0E-3		[1], [2], [5], [6], [7], [8]
- Fruit	1.0E-3		[9]
Interception factor for crop, I_{crop}	5.0E-1		[1], [10]
External interception fraction retained after food processing, F_{p3}		-	
- Root veg	0		[10]
- Green veg	1.0E-1		[10]
- Grain	1.0E-2		[10]
- Fruit	1.0E+0		[9]
Internal food processing retained fraction, F_{p2}	1.0E+0	-	[10]
External contamination due to soil, food processing retained fraction, F_{p1}		-	
- Root veg	1.0E-1		[10]

Element Dependent Data, Neptunium			
Parameter	Value	Units	References
- Green veg	1.0E-1		[10]
- Grain	1.0E-1		[10]
- Fruit	1.0E-1		[9]
Absorbed fraction, external to internal, F_{abs}	5.0E-1	-	[10]
Translocation factor, F_{trans}			
- Root veg	2.1E-1		[10]
- Green veg	1.0E+0		[10]
- Grain	1.0E-2		[10]
- Fruit	1E+0		[9]
Weathering rate, W		y^{-1}	
- Root veg	1.8E+1		[10]
- Green veg	1.8E+1		[10]
- Grain	1.8E+1		[10]
- Pasture	1.8E+1		[10]
- Fruit	3.2E+1		[9]
Animal product transfer factor, Tfproding		d kg^{-1} fw	
- Cow Meat	1.2E-4		[2], [8] [10], [11],
- Cow Liver	2.0E-2		[1], [2], [10]
- Cow Milk	5E-6	d l^{-1}	[2], [5], [14]
- Chicken Meat	1.7E-3		[1]

Element Dependent Data, Neptunium			
Parameter	Value	Units	References
- Chicken Eggs	1.7E-2		[1]
Animal product transfer factor from inhalation, Tfprodinh		d kg^{-1} fw	
- Cow Meat	1.2E-4		[2], [8] [10], [11],
- Cow Liver	1.0E-4		[1], [2], [10]
- Cow Milk	1.0E-4	d l^{-1}	[2], [5], [14]
- Chicken Meat	1.7E-3		[1]
- Chicken Eggs	1.7E-2		[1]

References for Table 8-15

[1] Ashton J and Sumerling T J (1988). Biosphere Database for Assessments of Radioactive Waste Disposals. UK Department of the Environment Report DoE/RW/88/083.

[2] Smith G M, Fearn H S, Smith K R, Davis J P and Klos R (1988). Assessment of the radiological impact of disposal of solid radioactive waste at Drigg. National Radiological Protection Board, NRPB-M148, Chilton, UK

[3] Pinner A V, Hemming C R and Hill M D (1984). An assessment of the radiological protection aspects of shallow land burial of radioactive waste. U.K. National Radiological Protection Board, NRPB-R161, Chilton, UK

[4] Sheppard M I, Beals D I, Thibault D H and O'Connor P (1984). Soil nuclide distribution coefficients and their statistical distributions. Atomic Energy of Canada Limited Report AECL-8364.

[5] Coughtrey P J, Jackson D, Thorne M C (1983-85). Radionuclide Distribution and Transport in Terrestrial and Aquatic Ecosystems. Volumes 1-6. AA Balkema, Rotterdam.

[6] Klos R A, Smith K R, Smith G M (1989). Calculations of the Radiological Impact of Unit Releases of Radionuclides to the Biosphere from Solid Waste Disposal Facilities. National Radiological Protection Board, NRPB-M150, Chilton, UK

[7] IAEA (1995). Generic Models and Parameters for Assessing the Environmental Transfer of Radionuclides from Routine Release Safety Series No 57 (draft). IAEA, Vienna

[8] Simmonds J R and Crick M J (1982). Transfer parameters for use in terrestrial foodchain models. NRPB report No M63

[9] Appendix C of this report.

[10] BIOMASS (2001a) ERB2A revised mathematical model and results. BIOMASS Theme 1, Task Group 6, Note 5, Version 2. February 2001. IAEA, Vienna.

[11] Dickson J M (19930. Derivation of a quality assured database for BIOS. Nirex Safety Studies Report NSS/B106

[12] Bishop G P, Beetham C J and Cuff Y S (1989). Review of literature for chlorine, technetium, iodine and neptunium. Nirex Safety Studies Report NSS/R193

[13] Ng Y C, Colsher C S and Thompson S E (1982). Transfer coefficients for assessing the dose from radionuclides in meat and eggs. NUREG/CR-2976.

[14] Ng Y C (1982). A review of transfer factors for assessing the dose from radionuclides in agricultural products. Nuclear Safety, Vol 23, No 1, pp57.

Table 8-16
Element Dependent Data, Niobium

Element Dependent Data, Niobium			
Parameter	**Value**	**Units**	**Justification –references are at end of table.**
Sorption coefficient soil, K_d	3.0E-1	$m^3\ kg^{-1}$ dw	EPRI [1996]
Crop concentration factor, CF_{crop}		Bq kg^{-1} fw per Bq kg^{-1} dw	
- Root veg	1.0E-2		EPRI [1996]
- Green veg	1.0E-2		EPRI [1996]
- Grain	1.0E-2		EPRI [1996]
- Pasture	1.0E-2		EPRI [1996]
- Fruit	5.0E-3		EPRI [1996]
Interception factor for crop, I_{crop}	3.0E-1		EPRI [1996]
External interception fraction retained after food processing, F_{p3}		-	
- Root veg	1.0E-1		BIOMASS Example 2A [IAEA, 2001]
- Green veg	1.0E-1		BIOMASS Example 2A [IAEA, 2001]
- Grain	0.0E0		BIOMASS Example 2A [IAEA, 2001]
- Fruit	1.0E0		BIOMASS Example 2A [IAEA, 2001]
Internal food processing retained fraction, F_{p2}	1.0E0		BIOMASS Example 2A [IAEA, 2001]
External contamination due to soil, food processing retained fraction, F_{p1}	1.0E-1	-	
- Root veg	1.0E-1		BIOMASS Example 2A [IAEA, 2001]

Element Dependent Data, Niobium			
Parameter	**Value**	**Units**	**Justification –references are at end of table.**
- Green veg	1.0E-1		BIOMASS Example 2A [IAEA, 2001]
- Grain	1.0E-1		BIOMASS Example 2A [IAEA, 2001]
- Fruit	1.0E-1		BIOMASS Example 2A [IAEA, 2001]
Absorbed fraction, external to internal, F_{abs}		-	
- Fruit	4.8E-1		BIOMASS Example 2A [IAEA, 2001]
- Others	5.0E-1		BIOMASS Example 2A [IAEA, 2001]
Translocation factor, F_{trans}		-	
- Root veg	5.3E-1		EPRI [1996]
- Green veg	5.2E-1		EPRI [1996]
- Grain	5.6E-2		EPRI [1996]
-Fruit	1.0E0		Appendix C
Weathering rate, W		y^{-1}	
- Root veg	1.8E1		EPRI [1996]
- Green veg	1.8E1		EPRI [1996]
- Grain	8.4E0		EPRI [1996]
- Pasture	1.8E1		EPRI [1996]
- Fruit	1.8E1		Appendix C
Animal product transfer factor, Tfproding		d kg^{-1}	
- Cow Meat	2.0E-4		EPRI [1996]
- Cow Liver	1.7E-4		EPRI [1996]

Element Dependent Data, Niobium			
Parameter	Value	Units	Justification –references are at end of table.
- Cow Milk	4.0E-7	d l^{-1}	EPRI [1996]
-Chicken Meat	4.0E-2		EPRI [1996]
-Chicken Egg	2.2E-2		EPRI [1996]
Animal product transfer factor from inhalation, TFprodinh		d kg^{-1}	
- Cow Meat	2.0E-4		EPRI [1996]
- Cow Liver	1.7E-4		EPRI [1996]
- Cow Milk	4.0E-7	d l^{-1}	EPRI [1996]
-Chicken Meat	4.0E-2		EPRI [1996]
-Chicken Egg	2.2E-2		EPRI [1996]

References for Table 8-16

EPRI (1996). Biosphere Modelling and Dose Assessment for Yucca Mountain. EPRI Report TR-107190, Electric Power Research Institute, Palo Alto CA.

IAEA (2001). BIOsphere Modelling and ASSessment BIOMASS Programme Version 2, Working Material CD, Reproduced by the IAEA, February 2001. International Atomic Energy Agency, Vienna.

Table 8-17
Element Dependent Data, Plutonium

Element Dependent Data, Plutonium			
Parameter	**Value**	**Units**	**Justification –references are at end of table.**
Sorption coefficient soil, K_d	**5.4E-1**	$m^3\ kg^{-1}$ dw	EPRI [1996]
Crop concentration factor, CF_{crop}	3.0E-005	Bq kg^{-1} fw per Bq kg^{-1} dw	
- Root veg	**1.0E-3**		EPRI [1996]
- Green veg	1.0E-4		EPRI [1996]
- Grain	3.0E-5		EPRI [1996]
- Pasture	1.0E-3		EPRI [1996]
- Fruit	1.0E04		Appendix C
Interception factor for crop, I_{crop}	3.0E-1		EPRI [1996]
External interception fraction retained after food processing, F_{p3}		-	
- Root veg	1.0E-1		BIOMASS Example 2A [IAEA, 2001]
- Green veg	1.0E-1		BIOMASS Example 2A [IAEA, 2001]
- Grain	0.0E0		BIOMASS Example 2A [IAEA, 2001]
- Fruit	1.0E0		Appendix C
Internal food processing retained fraction, F_{p2}	1.0E0		BIOMASS Example 2A [IAEA, 2001]
External contamination due to soil, food processing retained fraction, F_{p1}	1.0E-1	-	
- Root veg	1.0E-1		BIOMASS Example 2A [IAEA, 2001]

Element Dependent Data, Plutonium			
Parameter	**Value**	**Units**	**Justification –references are at end of table.**
- Green veg	1.0E-1		BIOMASS Example 2A [IAEA, 2001]
- Grain	1.0E-1		BIOMASS Example 2A [IAEA, 2001]
- Fruit	1.0E-1		Appendix C
Absorbed fraction, external to internal, F_{abs}		-	
- Fruit	4.8E-1		BIOMASS Example 2A [IAEA, 2001]
- Others	5.0E-1		BIOMASS Example 2A [IAEA, 2001]
Translocation factor, F_{trans}		-	
- Root veg	4.3E-2		EPRI [1996]
- Green veg	3.6E-1		EPRI [1996]
- Grain	1.6E-1		EPRI [1996]
-Fruit	1.9E-1		Appendix C
Weathering rate, W		y^{-1}	
- Root veg	1.8E1		EPRI [1996]
- Green veg	5.1E1		EPRI [1996]
- Grain	5.1E1		EPRI [1996]
- Pasture	1.8E1		EPRI [1996]
- Fruit	1.8E1		Appendix C
Animal product transfer factor, from ingestion, TFproding		d kg^{-1} fw	
- Cow Meat	2.0E-4		EPRI [1996]

Element Dependent Data, Plutonium			
Parameter	**Value**	**Units**	**Justification –references are at end of table.**
- Cow Liver	6.8E-2		EPRI [1996]
- Cow Milk	5.0E-006	d l^{-1}	EPRI [1996]
-Chicken Meat	1.0E-1		EPRI [1996]
-Chicken Egg	8.0E-3		EPRI [1996]
Animal product transfer factor from inhalation, TFprodinh		d kg^{-1}	
- Cow Meat	2.0E-4		EPRI [1996]
- Cow Liver	6.8E-2		EPRI [1996]
- Cow Milk	5.0E-006	d l^{-1}	EPRI [1996]
-Chicken Meat	1.0E-1		EPRI [1996]
-Chicken Egg	8.0E-3		EPRI [1996]

References for Table 8-17

EPRI (1996). Biosphere Modelling and Dose Assessment for Yucca Mountain. EPRI Report TR-107190, Electric Power Research Institute, Palo Alto CA.

IAEA (2001). BIOsphere Modelling and ASSessment BIOMASS Programme Version 2, Working Material CD, Reproduced by the IAEA, February 2001. International Atomic Energy Agency, Vienna.

Table 8-18
Element Dependent Data, Polonium

Element Dependent Data, Polonium			
Parameter	**Value**	**Units**	**Justification –references are at end of table.**
Sorption coefficient soil, K_d	**1.5E-1**	$m^3\ kg^{-1}$ dw	EPRI [1996]
Crop concentration factor, CF_{crop}		Bq kg^{-1} fw per Bq kg^{-1} dw	
- Root veg	**2.0E-4**		EPRI [1996]
- Green veg	2.0E-4		EPRI [1996]
- Grain	2.0E-4		EPRI [1996]
- Pasture	2.0E-4		EPRI [1996]
- Fruit	2.0E-4		Appendix C
Interception factor for crop, I_{crop}	3.0E-1		EPRI [1996]
External food processing retained fraction, F_{p3}		-	
- Root veg	1.0E-1		EPRI [1996]
- Green veg	1.0E-1		EPRI [1996]
- Grain	0.0E0		EPRI [1996]
- Fruit	1.0E0		Appendix C
Internal food processing retained fraction, F_{p2}	1.0E0		
External contamination due to soil, food processing retained fraction, F_{p1}	1.0E-1	-	
- Root veg	1.0E-1		BIOMASS Example 2A [IAEA, 2001]
- Green veg	1.0E-1		BIOMASS Example 2A [IAEA, 2001]

Element Dependent Data, Polonium			
Parameter	**Value**	**Units**	**Justification –references are at end of table.**
- Grain	1.0E-1		BIOMASS Example 2A [IAEA, 2001]
- Fruit	1.0E-1		Appendix C
Absorbed fraction, external to internal, F_{abs}		-	
- Fruit	4.8E-1		BIOMASS Example 2A [IAEA, 2001]
- Others	5.0E-1		BIOMASS Example 2A [IAEA, 2001]
Translocation factor, F_{trans}		-	
- Root veg	2.2E-1		EPRI [1996]
- Green veg	2.2E-1		EPRI [1996]
- Grain	1.0E-1		EPRI [1996]
-Fruit	1.0E0		Appendix C
Weathering rate, W		y^{-1}	
- Root veg	1.8E1		EPRI [1996]
- Green veg	1.8E1		EPRI [1996]
- Grain	8.4E0		EPRI [1996]
- Pasture	1.8E1		EPRI [1996]
- Fruit	1.8E1		Appendix C
Animal product transfer factor, TFproding		d kg^{-1}	
- Cow Meat	4.0E-3		EPRI [1996]
- Cow Liver	4.0E-3		EPRI [1996]
- Cow Milk	3.0E-4	d l^{-1}	EPRI [1996]

Element Dependent Data, Polonium			
Parameter	**Value**	**Units**	**Justification –references are at end of table.**
-Chicken Meat	1.2E0		EPRI [1996]
-Chicken Egg	1.2E0		EPRI [1996]
Animal product transfer factor from inhalation, TFprodinh		d kg^{-1}	
- Cow Meat	4.0E-3		EPRI [1996]
- Cow Liver	4.0E-3		EPRI [1996]
- Cow Milk	3.0E-4	d l^{-1}	EPRI [1996]
-Chicken Meat	1.2E0		EPRI [1996]
-Chicken Egg	1.2E0		EPRI [1996]

References for Table 8-18

EPRI (1996). Biosphere Modelling and Dose Assessment for Yucca Mountain. EPRI Report TR-107190, Electric Power Research Institute, Palo Alto CA.

IAEA (2001). BIOsphere Modelling and ASSessment BIOMASS Programme Version 2, Working Material CD, Reproduced by the IAEA, February 2001. International Atomic Energy Agency, Vienna.

Table 8-19
Element Dependent Data, Protactinium

Element Dependent Data, Protactinium			
Parameter	**Value**	**Units**	**Justification –references are at end of table.**
Sorption coefficient soil, K_d	**5.4E-1**	$m^3\ kg^{-1}$	Ashton and Sumerling [1998], generic soil
Crop concentration factor, CF_{crop}		Bq kg^{-1} fw per Bq kg^{-1} dw	
- Root veg	4.0E-2		EPRI [1996]
- Green veg	4.0E-2		EPRI [1996]
- Grain	4.0E-2		EPRI [1996]
- Pasture	4.0E-2		EPRI [1996]
- Fruit			Appendix C
Interception factor for crop, I_{crop}	3.0E-1		Ashton and Sumerling [1998].
External interception fraction retained after food processing, F_{p3}		-	
- Root veg	1.0E-1		BIOMASS Example 2A [IAEA, 2001]
- Green veg	1.0E-1		BIOMASS Example 2A [IAEA, 2001]
- Grain	0.0E0		BIOMASS Example 2A [IAEA, 2001]
- Fruit	1.0E0		Appendix C
Internal food processing retained fraction, F_{p2}	1.0E0		BIOMASS Example 2A [IAEA, 2001]
External contamination due to soil, food processing retained fraction, F_{p1}	1.0E-1	-	
- Root veg	1.0E-1		BIOMASS Example 2A [IAEA, 2001]

Element Dependent Data, Protactinium			
Parameter	**Value**	**Units**	**Justification –references are at end of table.**
- Green veg	1.0E-1		BIOMASS Example 2A [IAEA, 2001]
- Grain	1.0E-1		BIOMASS Example 2A [IAEA, 2001]
- Fruit	1.0E-1		Appendix C
Absorbed fraction, external to internal, F_{abs}		-	
- Fruit	4.8E-1		BIOMASS Example 2A [IAEA, 2001]
- Others	5.0E-1		BIOMASS Example 2A [IAEA, 2001]
Translocation factor, F_{trans}		-	
- Root veg	2.9E-1		BIOMASS Example 2A [IAEA, 2001]
- Green veg	4.5E-1		BIOMASS Example 2A [IAEA, 2001]
- Grain	2.0E-1		BIOMASS Example 2A [IAEA, 2001]
-Fruit	1.0E0		Appendix C
Weathering rate, W		y^{-1}	
- Root veg	1.8E1		BIOMASS Example 2A [IAEA, 2001]
- Green veg	1.8E1		BIOMASS Example 2A [IAEA, 2001]
- Grain	8.4E0		BIOMASS Example 2A [IAEA, 2001]
- Pasture	1.8E1		BIOMASS Example 2A [IAEA, 2001]
- Fruit	1.8E1		Appendix C
Animal product transfer factor, from ingestion, TFproding		d kg^{-1}	
- Cow Meat	5E-005		EPRI [1996]

Element Dependent Data, Protactinium			
Parameter	**Value**	**Units**	**Justification –references are at end of table.**
- Cow Liver	1.1E-3		EPRI [1996]
- Cow Milk	5E-006	d l^{-1}	EPRI [1996]
-Chicken Meat	4.1E-3		EPRI [1996]
-Chicken Egg	4.1E-3		
Animal product transfer factor from inhalation, TFprodinh		d kg^{-1}	
- Cow Meat	5E-005		EPRI [1996]
- Cow Liver	1.1E-3		EPRI [1996]
- Cow Milk	5E-006	d l^{-1}	EPRI [1996]
-Chicken Meat	4.1E-3		EPRI [1996]
-Chicken Egg	4.1E-3		EPRI [1996]

References for Table 8-19

Ashton J and Sumerling T J (1988). Biosphere database for assessments of radioactive waste disposals. UKDoE Report No. DoE/RW/88.083.

EPRI (1996). Biosphere Modelling and Dose Assessment for Yucca Mountain. EPRI Report TR-107190, Electric Power Research Institute, Palo Alto CA.

IAEA (2001). BIOsphere Modelling and ASSessment BIOMASS Programme Version 2, Working Material CD, Reproduced by the IAEA, February 2001. International Atomic Energy Agency, Vienna.

Table 8-20
Element Dependent Data, Radium

Element Dependent Data, Radium			
Parameter	**Value**	**Units**	**Justification –references are at end of table.**
Sorption coefficient soil, K_d	**4.9E-1**	$m^3\ kg^{-1}$ dw	EPRI [1996]
Crop concentration factor, CF_{crop}		Bq kg^{-1} fw per Bq kg^{-1} dw	
- Root veg	**4.0E-2**		EPRI [1996]
- Green veg	**4.0E-2**		EPRI [1996]
- Grain	**4.0E-2**		EPRI [1996]
- Pasture	**4.0E-2**		EPRI [1996]
- Fruit	**4.0E-2**		Appendix C
Interception factor for crop, I_{crop}	3.0E-1		EPRI [1996]
External interception fraction retained after food processing, F_{p3}		-	
- Root veg	1.0E-1		BIOMASS Example 2A [IAEA, 2001]
- Green veg	1.0E-1		BIOMASS Example 2A [IAEA, 2001]
- Grain	0.0E0		BIOMASS Example 2A [IAEA, 2001]
- Fruit	1.0E0		Appendix C
Internal food processing retained fraction, F_{p2}	1.0E0		BIOMASS Example 2A [IAEA, 2001]
External contamination due to soil, food processing retained fraction, F_{p1}	1.0E-1	-	
- Root veg	1.0E-1		BIOMASS Example 2A [IAEA, 2001]

Element Dependent Data, Radium

Parameter	Value	Units	Justification –references are at end of table.
- Green veg	1.0E-1		BIOMASS Example 2A [IAEA, 2001]
- Grain	1.0E-1		BIOMASS Example 2A [IAEA, 2001]
- Fruit	1.0E-1		Appendix C
Absorbed fraction, external to internal, F_{abs}		-	
- Fruit	4.8E-1		BIOMASS Example 2A [IAEA, 2001]
- Others	5.0E-1		BIOMASS Example 2A [IAEA, 2001]
Translocation factor, F_{trans}		-	
- Root veg	9.9E-2		EPRI [1996]
- Green veg	1.8E-1		EPRI [1996]
- Grain	8.0E-2		EPRI [1996]
- Fruit	1.0E0		EPRI [1996]
Weathering rate, W		y^{-1}	
- Root veg	1.8E1		EPRI [1996]
- Green veg	1.8E1		EPRI [1996]
- Grain	8.4E0		EPRI [1996]
- Pasture	1.8E1		EPRI [1996]
- Fruit	1.8E1		EPRI [1996]
Animal product transfer factor, Tfproding		d kg^{-1}	
- Cow Meat	1.3E-3		EPRI [1996]
- Cow Liver	1.9E-2		EPRI [1996]

Element Dependent Data, Radium			
Parameter	**Value**	**Units**	**Justification –references are at end of table.**
- Cow Milk	1.3E-3	d l^{-1}	EPRI [1996]
-Chicken Meat	4.8E-1		EPRI [1996]
-Chicken Egg	2.5E-1		EPRI [1996]
Animal product transfer factor from inhalation, TFprodinh		d kg^{-1}	
- Cow Meat	1.3E-3		EPRI [1996]
- Cow Liver	1.9E-2		EPRI [1996]
- Cow Milk	1.3E-3	d l^{-1}	EPRI [1996]
-Chicken Meat	4.8E-1		EPRI [1996]
-Chicken Egg	2.8E-1		EPRI [1996]

References for Table 8-20

EPRI (1996). Biosphere Modelling and Dose Assessment for Yucca Mountain. EPRI Report TR-107190, Electric Power Research Institute, Palo Alto CA.

IAEA (2001). BIOsphere Modelling and ASSessment BIOMASS Programme Version 2, Working Material CD, Reproduced by the IAEA, February 2001. International Atomic Energy Agency, Vienna.

Table 8-21
Element Dependent Data, Selenium

Element Dependent Data, Selenium			
Parameter	**Value**	**Units**	**Justification – references are at end of table.**
Sorption coefficient soil, K_d	1.5E-1	$m^3 kg^{-1}$ dw	[1], [2], [3], [4], [11]
Crop concentration factor, CF_{crop}		Bq kg^{-1} fw per bq kg^{-1} dw	
- Root veg	1.0E0		[2]
- Green veg	1.0E0		[2]
- Grain	1.0E0		[2]
- Pasture	1.0E0		[2]
- Fruit	1.0E0		[7]
Interception factor for crop, I_{crop}	5.0E-1 (1)		[1]
External interception fraction retained after food processing, F_{p3}		-	
- Root veg	0		[8] used in the absence of specific data, assuming that root veg are peeled or scrubbed before consumption.
- Green veg	1.0E-1		[8] used in the absence of specific data,
- Grain	1.0E-2		[8] used in the absence of specific data,
- Fruit	1.0E+0		[8] used in the absence of specific data,
Internal food processing retained fraction, F_{p2}	1.0E+0	-	[8]

Element Dependent Data, Selenium

Parameter	Value	Units	Justification – references are at end of table.
External contamination due to soil, food processing retained fraction, F_{p1}		-	
- Root veg	1.0E-1		[8] data used in absence of specific data
- Green veg	1.0E-1		[8] used in the absence of specific data,
- Grain	1.0E-1		[8] used in the absence of specific data,
- Fruit	1.0E-1		[7]
Absorbed fraction, external to internal, F_{abs}	5.0E-1		[8]
Translocation factor, F_{trans}			
- Root veg	6.8E-2		[1], [6]
- Green veg	3.0E-1		[1], [5]
- Grain	1.3E-1		[1], [5]
-Fruit	1.0E0		[7]
Weathering rate, W		y^{-1}	
- Root veg	1.8E+1		[8]
- Green veg	1.8E+1		[8]
- Grain	8.4E0		[8]
- Pasture	1.8E+1		[8]
- Fruit	3.2E+1		[7]
Animal product transfer factor, TFproding		d kg^{-1}f.w	
- Cow Meat	5.4E-1		[1], [2]

Element Dependent Data, Selenium			
Parameter	**Value**	**Units**	**Justification – references are at end of table.**
- Cow Liver	1.0E0		[1], [2], [6], [9]
- Cow Milk	4.0E-3	$d\ l^{-1}$	[1], [2], [5]
-Chicken Meat	8.3E+0		[1], [10]
-Chicken Eggs	8.3E+0		[1], [10]
Animal product transfer factor from inhalation, TFprodinh		$d\ kg^{-1}$f.w	
- Cow Meat	5.4E-1		[1], [2]
- Cow Liver	1.0E1		[1], [2], [6], [9]
- Cow Milk	4.0E-3	$d\ l^{-1}$	[1], [2], [5]
-Chicken Meat	8.3E+0		[1], [10]
-Chicken Eggs	8.3E+0		[1], [10]

References for Table 8-21

[1] Ashton J and Sumerling T J (1988). Biosphere Database for Assessments of Radioactive Waste Disposals. UK Department of the Environment Report DoE/RW/88/083.

[2] Smith G M, Fearn H S, Smith K R, Davis J P and Klos R (1988). Assessment of the radiological impact of disposal of solid radioactive waste at Drigg. National Radiological Protection Board, NRPB-M148, Chilton, UK

[3] Pinner A V, Hemming C R and Hill M D (1984). An assessment of the radiological protection aspects of shallow land burial of radioactive waste. U.K. National Radiological Protection Board, NRPB-R161, Chilton, UK

[4] Sheppard M I, Beals D I, Thibault D H and O'Connor P (1984). Soil nuclide distribution coefficients and their statistical distributions. Atomic Energy of Canada Limited Report AECL-8364.

[5] Coughtrey P J, Jackson D, Thorne M C (1983-85). Radionuclide Distribution and Transport in Terrestrial and Aquatic Ecosystems. Volumes 1-6. AA Balkema, Rotterdam.

[6] Simmonds J R and Crick M J (1982). Transfer parameters for use in terrestrial foodchain models. NRPB report No M63

[7] Appendix C of this report.

[8] IAEA (2001). BIOsphere Modelling and ASSessment BIOMASS Programme Version 2, Working Material CD, Reproduced by the IAEA, February 2001. International Atomic Energy Agency, Vienna

[9] Dickson J M (19930. Derivation of a quality assured database for BIOS. Nirex Safety Studies Report NSS/B106

[10] Ng Y C, Colsher C S and Thompson S E (1982). Transfer coefficients for assessing the dose from radionuclides in meat and eggs. NUREG/CR-2976.

[11] IAEA (1994). Handbook of Parameter Values for the Prediction of Radionuclide Transfer in Temperate Environments. Technical Reports Series No 364. IAEA, Vienna

Table 8-22
Element Dependent Data, Tecnetium

Element Dependent Data, Technetium			
Parameter	Value	Units	Reference
Sorption coefficient soil, K_d	1.0E-4	m^3 kg^{-1} dw	[1], [2], [3], [4]
Crop concentration factor, CF_{crop}		Bq kg^{-1} fw per bq kg^{-1} dw	
- Root veg	1.0E+1		[1], [2], [5], [6], [7], [8]
- Green veg	1.0E+1		[1], [2], [5], [6], [7], [8]
- Grain	1.0E+1		[1], [2], [5], [6], [7], [8]
- Pasture	1.0E+1		[1], [2], [5], [6], [7], [8]
- Fruit	1.0E+1		[9]
Interception factor for crop, I_{crop}	1.0E-1		[1], [10]
External interception fraction retained after food processing, F_{p3}			
- Root veg	0		[10]
- Green veg	1.0E-1		[10]
- Grain	1.0E-2		[10]
- Fruit	1.0E+0		[9]
Internal food processing retained fraction, F_{p2}	1.0E+0		[10]
External contamination due to soil, food processing retained fraction, F_{p1}		-	
- Root veg	1.0E-1		[10]

Element Dependent Data, Technetium

Parameter	Value	Units	Reference
- Green veg	1.0E-1		[10]
- Grain	1.0E-1		[10]
- Fruit	1.0E-1		[9]
Absorbed fraction, external to internal, F_{abs}	5.0E-1	-	[10]
Translocation factor, F_{trans}		-	
- Root veg	1.0E-1		[10]
- Green veg	1.0E+0		[10]
- Grain	1.0E-1		[10]
-Fruit	1.0E+0		[9]
Weathering rate, W		y^{-1}	
- Root veg	1.8E+1		[9], [10]
- Green veg	1.8E+1		[9], [10]
- Grain	8.4E0		[9], [10]
- Pasture	1.8E+1		[9], [10]
- Fruit	3.2E+1		[9]
Animal product transfer factor, TFproding		d kg^{-1}f.w.	
- Cow Meat	*6.0E-3*		[8], [10], [11]
- Cow Liver	2.1E-2		[1], [2], [11]
- Cow Milk	7.5E-3	d l^{-1}	[1], [2], [10], [11], [12]
- Chicken Meat	1.2E+0		[1], [13]

Element Dependent Data, Technetium			
Parameter	Value	Units	Reference
-Chicken Egg	1.2E+0		[13].
Animal product transfer factor from inhalation, TFprodinh		d kg^{-1} f.w.	
- Cow Meat	5.0E-4		[8], [10] [11]
- Cow Liver	2.1E-2		[1], [2], [11]
- Cow Milk	1.0E-4	d l^{-1}	[1], [2], [10], [11], [12]
- Chicken Meat	1.2E+0		[1], [14]
-Chicken Egg	1.2E+0		[13]

References for Table 8-22

[1] Ashton J and Sumerling T J (1988). Biosphere Database for Assessments of Radioactive Waste Disposals. UK Department of the Environment Report DoE/RW/88/083.

[2] Smith G M, Fearn H S, Smith K R, Davis J P and Klos R (1988). Assessment of the radiological impact of disposal of solid radioactive waste at Drigg. National Radiological Protection Board, NRPB-M148, Chilton, UK

[3] Pinner A V, Hemming C R and Hill M D (1984). An assessment of the radiological protection aspects of shallow land burial of radioactive waste. U.K. National Radiological Protection Board, NRPB-R161, Chilton, UK

[4] Sheppard M I, Beals D I, Thibault D H and O'Connor P (1984). Soil nuclide distribution coefficients and their statistical distributions. Atomic Energy of Canada Limited Report AECL-8364.

[5] Coughtrey P J, Jackson D, Thorne M C (1983-85). Radionuclide Distribution and Transport in Terrestrial and Aquatic Ecosystems. Volumes 1-6. AA Balkema, Rotterdam.

[6] Klos R A, Smith K R, Smith G M (1989). Calculations of the Radiological Impact of Unit Releases of Radionuclides to the Biosphere from Solid Waste Disposal Facilities. National Radiological Protection Board, NRPB-M150, Chilton, UK

[7] IAEA (1995). Generic Models and Parameters for Assessing the Environmental Transfer of Radionuclides from Routine Release Safety Series No 57 (draft). IAEA, Vienna

[8] Simmonds J R and Crick M J (1982). Transfer parameters for use in terrestrial foodchain models. NRPB report No M63

[9] Appendix C of this report.

[10] IAEA (2001). BIOsphere Modelling and ASSessment BIOMASS Programme Version 2, Working Material CD, Reproduced by the IAEA, February 2001. International Atomic Energy Agency, Vienna [9] Dickson J M (19930. Derivation of a quality assured database for BIOS. Nirex Safety Studies Report NSS/B106

[11] Dickson J M (19930. Derivation of a quality assured database for BIOS. Nirex Safety Studies Report NSS/B106

[12] Bishop G P, Beetham C J and Cuff Y S (1989). Review of literature for chlorine, technetium, iodine and neptunium. Nirex Safety Studies Report NSS/R193

[13] Ng Y C, Colsher C S and Thompson S E (1982). Transfer coefficients for assessing the dose from radionuclides in meat and eggs. NUREG/CR-2976.

[14] Ng Y C (1982). A review of transfer factors for assessing the dose from radionuclides in agricultural products. Nuclear Safety, Vol 23, No 1, pp57.

Table 8-23
Element Dependent Data, Thorium

Element Dependent Data, Thorium			
Parameter	Value	Units	Justification – references are at end of table.
Sorption coefficient soil, K_d	3.0E0	$m^3\ kg^{-1}$ dw	EPRI [1996]
Crop concentration factor, CF_{crop}		Bq kg^{-1} fw per Bq kg^{-1} dw	
- Root veg	5.0E-4		EPRI [1996]
- Green veg	5.0E-4		EPRI [1996]
- Grain	5.0E-4		EPRI [1996]
- Pasture	5.0E-4		EPRI [1996]
- Fruit	5.0E-4		Appendix C
Interception factor for crop, I_{crop}	3.0E-1		EPRI [1996]
External interception fraction retained after food processing, F_{p3}		-	
- Root veg	1.0E-1		BIOMASS Example 2A [IAEA, 2001]
- Green veg	1.0E-1		BIOMASS Example 2A [IAEA, 2001]
- Grain	0.0E0		BIOMASS Example 2A [IAEA, 2001]
- Fruit	1.0E0		Appendix C
Internal food processing retained fraction, F_{p2}	1.0E0		BIOMASS Example 2A [IAEA, 2001]
External contamination due to soil, food processing retained fraction, F_{p1}	1.0E-1	-	
- Root veg	1.0E-1		BIOMASS Example 2A [IAEA, 2001]

Element Dependent Data, Thorium			
Parameter	Value	Units	Justification – references are at end of table.
- Green veg	1.0E-1		BIOMASS Example 2A [IAEA, 2001]
- Grain	1.0E-1		BIOMASS Example 2A [IAEA, 2001]
- Fruit	1.0E-1		Appendix C
Absorbed fraction, external to internal, F_{abs}		-	
- Fruit	4.8E-1		BIOMASS Example 2A [IAEA, 2001]
- Others	5.0E-1		BIOMASS Example 2A [IAEA, 2001]
Translocation factor, F_{trans}		-	
- Root veg	2.9E-1		EPRI [1996]
- Green veg	3.8E-2		EPRI [1996]
- Grain	1.3E-1		EPRI [1996]
- Fruit	1.3E-1		Appendix C
Weathering rate, W		y^{-1}	
- Root veg	1.8E1		EPRI [1996]
- Green veg	1.8E1		EPRI [1996]
- Grain	8.4E0		EPRI [1996]
- Pasture	1.8E1		EPRI [1996]
- Fruit	1.8E1		Appendix C
Animal product transfer factor, from ingestion, TFproding		d kg^{-1}	
- Cow Meat	2.7E-3		EPRI [1996]

Element Dependent Data, Thorium			
Parameter	Value	Units	Justification – references are at end of table.
- Cow Liver	6.3E-2		EPRI [1996]
- Cow Milk	5.0E-006	d l^{-1}	EPRI [1996]
-Chicken Meat	1.8E-1		EPRI [1996]
-Chicken Egg	1.8E-1		EPRI [1996]
Animal product transfer factor from inhalation, TFprodinh		d kg^{-1}	
- Cow Meat	2.7E-3		EPRI [1996]
- Cow Liver	6.3E-2		EPRI [1996]
- Cow Milk	5.0E-006	d l^{-1}	EPRI [1996]
-Chicken Meat	1.8E-1		EPRI [1996]
-Chicken Egg	1.8E-1		EPRI [1996]

References for Table 8-23

EPRI (1996). Biosphere Modelling and Dose Assessment for Yucca Mountain. EPRI Report TR-107190, Electric Power Research Institute, Palo Alto CA.

IAEA (2001). BIOsphere Modelling and ASSessment BIOMASS Programme Version 2, Working Material CD, Reproduced by the IAEA, February 2001. International Atomic Energy Agency, Vienna [9] Dickson J M (19930. Derivation of a quality assured database for BIOS. Nirex Safety Studies Report NSS/B106

Table 8-24
Element Dependent Data, Uranium

Element Dependent Data, Uranium			
Parameter	Value	Units	Justification – references are at end of table.
Crop concentration factor, CF_{crop}		Bq kg^{-1} fw per Bq kg^{-1} dw	
- Root veg	1.0E-4		EPRI [1996]
- Green veg	1.0E-3		EPRI [1996]
- Grain	1.0E-3		EPRI [1996]
- Pasture	1.0E-3		EPRI [1996]
- Fruit	1.0E-4		Appendix C
Interception factor for crop, I_{crop}	3.0E-1		EPRI [1996]
External interception fraction retained after food processing, F_{p3}		-	
- Root veg	1.0E-1		BIOMASS Example 2A [IAEA, 2001]
- Green veg	1.0E-1		BIOMASS Example 2A [IAEA, 2001]
- Grain	0.0E0		BIOMASS Example 2A [IAEA, 2001]
- Fruit	1.0E0		Appendix C
Internal food processing retained fraction, F_{p2}	1.0E0		BIOMASS Example 2A [IAEA, 2001]
External contamination due to soil, food processing retained fraction, F_{p1}	1.0E-1	-	
- Root veg	1.0E-1		BIOMASS Example 2A [IAEA, 2001]
- Green veg	1.0E-1		BIOMASS Example 2A [IAEA, 2001]

Element Dependent Data, Uranium			
Parameter	Value	Units	Justification – references are at end of table.
- Grain	1.0E-1		BIOMASS Example 2A [IAEA, 2001]
- Fruit	1.0E-1		Appendix C
Absorbed fraction, external to internal, F_{abs}		-	BIOMASS Example 2A [IAEA, 2001]
- Fruit	4.8E-1		BIOMASS Example 2A [IAEA, 2001]
- Others	5.0E-1		BIOMASS Example 2A [IAEA, 2001]
Translocation factor, F_{trans}		-	
- Root veg	4.3E-2		EPRI [1996]
- Green veg	3.6E-2		EPRI [1996]
- Grain	1.6E-1		EPRI [1996]
- Fruit	1.9E-1		Appendix C
Weathering rate, W		y^{-1}	
- Root veg	1.8E1		EPRI [1996]
- Green veg	1.8E1		EPRI [1996]
- Grain	8.4E0		EPRI [1996]
- Pasture	1.8E1		EPRI [1996]
- Fruit	1.8E1		Appendix C
Animal product transfer factor, from ingestion, TFproding		d kg^{-1}	
- Cow Meat	6.9E-4		EPRI [1996]
- Cow Liver	6.9E-4		EPRI [1996]

Element Dependent Data, Uranium			
Parameter	Value	Units	Justification – references are at end of table.
- Cow Milk	4.0E-4	d l^{-1}	EPRI [1996]
-Chicken Meat	1.0E-1		EPRI [1996]
-Chicken Egg	1.0E-1		EPRI [1996]
Animal product transfer factor from inhalation, TFprodinh		d kg^{-1}	
- Cow Meat	6.9E-4		EPRI [1996]
- Cow Liver	6.9E-4		EPRI [1996]
- Cow Milk	4.0E-4	d l^{-1}	EPRI [1996]
- Chicken Meat	1.0E-1		EPRI [1996]
- Chicken Egg	1.0E-1		EPRI [1996]

References for Table 8-24

EPRI (1996). Biosphere Modelling and Dose Assessment for Yucca Mountain. EPRI Report TR-107190, Electric Power Research Institute, Palo Alto CA.

IAEA (2001). BIOsphere Modelling and ASSessment BIOMASS Programme Version 2, Working Material CD, Reproduced by the IAEA, February 2001. International Atomic Energy Agency, Vienna [9] Dickson J M (19930. Derivation of a quality assured database for BIOS. Nirex Safety Studies Report NSS/B106

8.2.7 Deterministic Results

Table 8-25 gives results for BDCFs (mrem y^{-1} per mole m^{-3}) to average members of the critical group via each pathway for each radionuclide. The total summed over all pathways for each radionuclide is also given. These doses are the doses due to the presence of one mole $m^{-3}$of the specified radionuclide being in the abstracted groundwater. They include the effects of daughter radionuclides which grow in after release into the biosphere. For example the Th-230 dose values includes contributions to dose from Ra-226 which grows in from decay of th-230 accumulating in soil.

The results for each radionuclide assessed in the geosphere part of the TSPA are included. Thus the total dose summed over all radionuclides for a particular geosphere calculation are obtained by summing the products of the molar concentration for each radionuclide in the groundwater abstracted via the well (calculated within the geosphere model) and the corresponding BDCF in Table 8-25.

Some relatively short-lived radionuclides are not modelled explicitly in the geosphere part of the assessment. They are assumed to be in secular equilibrium with their parents in all parts of the geosphere. However, because of the relatively fast rate of biosphere processes in the biosphere, they do require explicit dynamic representation in the biosphere model. These radionuclides are Ac-227, Pa-233, Th-228, Ra-228, Pb-210 and Po-210. Since no geosphere calculation is made of their concentration in the groundwater, their contribution to BDCFs is added in with the respective parents, on the assumption that the daughters are in secular equilibrium with their parents at the well head. This may not be true, especially if the parents and daughters are differently mobile in that environment. The total BDCF including these daughter contributions is also provided in table 8-25 for the relevant radionuclides.

Finally, some even shorter-lived radionuclides are not modelled dynamically even in the biosphere. Their radiation effects have been included in with their parents, assuming secular equilibrium in all parts of the environment; e.g. their contribution to dose coefficients is included in Table 8-8.

The main changes and reasons for change compared with previous results [EPRI, 1996] are as follows.

A variety of generic factors apply to all radionuclides but do not affect them all to the same extent. Firstly, consumption rates for most foodstuffs have been reduced significantly compared with assumptions in EPRI [1996]. The previous assumptions were based on the idea that the critical group would be determined by conservative assumptions with respond to a particular pathway, e.g. obtaining all foods from local production sources. Since a single individual would be unlikely, for example, to consume significantly more than average amounts of all foodstuffs, it would be inappropriate, according to that approach, to sum over all pathways at higher than average rates of consumption to determine the critical group dose. The US EPA has now noted that it feels the Reasonably Maximally Exposed Individual (RMEI) is defined as being "Maximally Exposed" by location alone. Furthermore, for additional EPA policy reasons, EPA requires DOE to assume the majority of their drinking water is consumed from local, contaminated sources. That is, the RMEI is assumed to be located in the region of highest groundwater contamination; they are not further specified as having exceptional behaviour leading to different exposure, but are to be assumed to have average behaviour. To further assume that the RMEI consumes 100% of their food needs from local sources (when the survey shows to be far from the case) is no longer "Reasonable". In this case, however, it is reasonable to sum over exposure pathways.

Water consumption has not changed significantly, so this pathway and inhalation and external irradiation pathways are all relatively more significant.

The model for interception of irrigation water, weathering and uptake of radionuclides into crops has been updated according to the model suggested in IAEA [2001]. This model includes more mechanistic features, but it can be argued that the data are not always available to justify this level of detailed treatment, e.g. for translocation of radionulcides from leaves to the fruiting body in the case of fruit.. The assumptions for degree absorption of radionuclides on the surface of leaves into the body of the plant is conservative, especially for crops for which only a small proportion of the plant is edible. This may have tended to increase BDCFs for radionuclides for which foodchain doses dominate.

The effect of using the ICRP 72 dose coefficients is small.

The effect of ignoring erosion is very small, eg given the results of sensitivity analyses given in IAEA [2001].

A number of element dependent parameter values have been changed are likely to be important in some cases, but comparison given the model changes for interception, weathering and absorption, make it difficult to differentiate the significance of parametric assumptions.

Cl-36

This radionuclide was not considered previously. It has some similarities in behaviour but a lower dose coefficient for ingestion than I-129.

Se-79

The BDCF is much reduced because of a combination of factors, including a significantly reduced assumption for uptake into liver, a reduced consumption rate for liver, lower consumption rates for other foods, and an increased half-life[3].

Nb-94

The BDCF is still substantially dominated by external irradiation from the soil.

---

[3] Since the units are per mol m^{-3}, the number of Bq m^{-3} is reduced because of the increase in half-life from 6.5E4 y to 1.13E6 y. The cow liver dose is still about 25% of the total dose when just 1 kg is consumed per year.

Tc-99

Reduced interception factor, reduced root uptake by fruit (previously the highest contributor to dose) and lower food consumption have combined to reduce the BDCF by about a factor of three.

I-129

BDCF is not significantly changed. Reductions in food consumption are off-set by the potentially conservative treatment of absorption.

Cs-135

A combination of factors associated primarily with revised assumptions for plant uptake has increased the BDCF by a factor of 7.

Ra-226 (in combination with Pb-210 and Po-210)

Results for the BDCF for Ra-226 and all its daughters in assumed secular equilibrium in the well[4] are similar to before, but with a greater contribution from external irradiation.

Th-232 (in combination with Th-228 and Ra-228)

The BDCF for Th-232 and all its daughters in assumed secular equilibrium in the well is significantly higher, with an increased proportion of the dose due to inhalation. This increase is partly due to an assumed higher dust concentration in air associated with some activities linked to use of the soil. The inhalation dose arises from accumulation of activity in the soil given assumed continued irrigation of the same area of land over many years. This may not be considered unrealistic, but in any event, is not subject to resolution by survey of present day behaviour.

Other long-lived alpha emitters

The general picture is the same as for Th-232, with higher BDCFs due to more significant inhalation doses. In all these cases, there are outstanding questions to be asked about the distribution of activity among the suspended particles, and the relative distribution of activity within the bulk soil compared with the suspendable fraction. The answers to these questions may in turn depend on the process giving rise to the suspension of dust, whether this is by man or some other process. These may be capable of resolution by survey of Amargosa habits and activities.

The above results imply further consideration of the critical group definition. Surveys have been carried out to determine local foodstuff consumption. Corresponding surveys may need to be carried out to achieve the same level of understanding of how, and how long, Amargosa Valley

---

[4] It is not obvious that the daughters would be in secular equilibrium.

residents spend their time interacting with the soil. This could include collecting information about the amounts, rates and types of irrigation that are used by gardeners, as opposed to farmers for whom commercial practice is relatively well understood. For example, some crop types may be more commonly drip irrigated than by spray, which would result in significantly lower BDCFs for some radionuclides. While local surveys may provide useful information in this respect, some caution may be appropriate in that such habits may change quite rapidly, so that future surveys may point to different behaviour and so different results. Such surveys might also usefully address the question of how the local environment might be exploited rather than focus on precise details of what is occurring, almost literally, today.

Table 8-25
Deterministic Results for BDCF's (mrem y^{-1} per mole m^{-3})

All data is in
(mrem/yr)/(mol/m^3)

Pathway	Cl-36	Se-79	Nb-94	Tc-99	I-129	Cs-135	Pb-210	Po-210	Ra-226
Root vegetable	2.3E6	2.1E6	4.6E7	2.9E6	5.5E6	1.9E5	1.0E12	7.8E13	8.4E10
green vegetable consumption	2.2E6	1.8E6	3.9E7	2.1E6	5.2E6	1.6E5	1.1E12	8.5E13	7.1E10
grain	1.8E5	1.8E5	3.2E6	1.7E5	4.3E5	1.0E4	2.4E11	2.0E13	6.7E9
fruit	1.2E7	8.5E6	2.4E8	2.0E6	1.5E7	1.4E6	8.2E13	7.0E15	6.1E11
dust inhalation	2.1E3	3.3E3	8.2E7	1.3E3	1.1E4	4.6E4	6.0E10	7.0E10	4.8E10
external soil	0	0	2.5E11	0	8.4E4	0	4.0E8	1.3E7	2.1E12
chicken meat	4.4E5	3.9E5	2.5E5	6.2E4	3.8E4	1.4E5	4.2E10	1.7E12	2.1E9
cow meat	2.4E6	2.8E7	4.2E5	3.4E5	4.4E5	3.0E5	4.0E11	1.2E13	3.3E9
cow milk	1.2E6	2.6E5	1.1E3	5.4E5	5.6E5	6.2E4	1.5E10	1.1E12	4.3E9
cow liver	7.4E5	1.6E7	1.1E5	3.6E5	8.9E4	5.7E4	1.6E13	3.5E12	1.5E10
eggs	6.5E6	5.7E6	2.0E6	9.2E5	4.5E6	7.0E4	6.2E11	2.5E13	1.6E10
soil	8.6E2	3.8E3	7.7E6	4.4E2	1.0E5	1.2E4	2.4E10	5.3E10	3.8E9
external water	0	6.8E1	1.4E7	5.4E2	1.1E2	2.6E1	1.5E7	4.2E6	2.08
water consumption	3.2E6	2.9E6	8.8E7	3.1E6	7.3E6	2.7E5	3.9E13	3.3E15	1.8E11
Total	**3.2E7**	**6.5E7**	**2.5E11**	**1.2E7**	**4.0E7**	**2.8E6**	**1.4E14**	**1.1E16**	**3.1E12**
Total including daughters not modelled in the geosphere, assuming secular equilibrium with their parents in well water.									**7.6E12** **Pb-210 and Po-210**

All data is in (mrem/yr)/(mol/m^3)

Pathway	Ra-228	Ac-227	Th-228	Th-229	Th-230	Th-232	Pa-231	Pa-233	U-233	U-234
Root vegetable	1.6E12	1.7E12	1.2E13	5.0E9	5.7E8	4.9E3	1.6E10	3.9E1	2.7E7	9.7E6
green vegetable	3.0E12	2.4E12	3.8E12	3.0E9	4.3E8	3.8E3	1.3E10	5.7E11	1.9E8	6.9E7
grain	6.3E11	6.2E11	3.0E12	7.4E8	5.7E7	4.4E2	1.3E9	1.4E11	1.9E7	7.2E6
fruit	2.7E14	1.1E14	8.3E14	1.6E11	7.5E9	4.8E4	8.8E10	2.6E13	7.8E8	4.6E8
dust inhalation	9.0E10	3.3E12	4.5E11	1.8E12	3.1E11	2.8E6	5.0E10	2.2E7	2.8E10	9.6E9
external soil	3.7E11	1.1E11	5.1E11	1.1E11	9.1E6	3.9E1	3.1E8	8.8E10	7.4E6	2.0E6
chicken meat	3.1E10	2.3E8	3.2E10	1.3E9	2.1E8	1.9E3	3.2E6	2.1E7	2.8E7	9.4E6
cow meat	1.5E11	7.8E10	9.3E11	4.0E9	6.6E8	5.9E3	2.3E7	5.4E8	4.0E7	1.4E7
cow milk	1.9E11	2.5E7	2.2E9	9.4E6	1.6E6	1.4E1	2.9E6	6.8E7	3.0E7	1.0E7
cow liver	6.7E11	2.1E11	6.6E12	2.8E10	4.7E9	4.2E4	1.5E8	3.6E9	1.2E7	4.2E6
eggs	2.4E11	8.2E9	4.8E11	1.9E10	3.2E9	2.9E4	4.8E7	3.2E8	4.1E8	1.4E8
soil	1.1E10	1.8E10	2.2E10	1.0E10	1.7E9	1.6E4	6.9E8	1.3E7	4.0E8	1.4E8
external water	2.9E10	3.3E9	1.4E11	8.5E6	1.2E3	3.4E3	1.6E5	4.8E11	7.6E1	1.7E2
water consumption	1.3E14	5.3E13	3.9E14	7.0E10	2.9E9	1.7E4	2.8E10	1.2E13	3.4E8	2.1E8
Total	**4.0E14**	**1.7E14**	**1.3E15**	**2.6E12**	**3.3E11**	**3.0E6**	**1.9E11**	**4.0E13**	**3.0E10**	**1.1E10**
Total including daughters not modelled in the geosphere, assuming secular equilibrium with their parents in well water.						**3.3E6** **Ra-228 and Th-228**	**3.1E11** **Ac-227**			

All data is in (mrem/yr)/(mol/m3)

Pathway	U-235	U-236	U-238	Np-237	Pu-239	Pu-240	Pu-242	Am-243
Root vegetable	8.3E3	2.1E5	6.5E2	3.7E7	2.6E9	2.1E9	2.6E8	2.2E9
green vegetable	5.8E4	1.5E6	4.6E3	3.6E7	6.3E8	1.6E9	4.8E7	1.9E9
grain	5.4E3	1.4E5	4.6E2	1.0E6	1.1E8	3.7E8	7.0E6	2.1E8
fruit	1.7E5	5.0E6	2.4E4	1.9E8	2.4E10	8.5E10	1.5E9	6.3E10
dust inhalation	8.2E6	2.1E8	6.2E5	2.1E9	8.4E11	6.1E11	3.5E10	4.2E11
external soil	4.9E6	4.0E4	1.0E6	3.0E8	6.0E6	1.2E7	1.4E6	9.7E9
chicken meat	8.5E3	2.2E5	6.5E2	1.6E4	3.2E8	2.4E8	3.3E7	1.8E8
cow meat	1.3E4	3.2E5	9.5E2	3.6E5	1.4E8	1.1E8	1.4E7	2.0E8
cow milk	9.2E3	2.3E5	7.0E2	1.9E4	4.4E6	3.4E6	4.4E5	3.1E6
cow liver	3.8E3	9.6E4	2.9E2	1.8E7	1.4E10	1.1E10	1.4E9	1.0E10
eggs	1.3E5	3.2E6	9.6E3	2.4E6	3.9E8	2.8E8	3.9E7	1.0E8
soil	1.2E5	3.1E6	9.4E3	1.3E7	4.7E9	3.4E9	4.7E8	2.4E9
external water	4.3E1	1.2E0	1.4E0	1.8E4	8.6E2	4.1E3	5.5E1	1.2E6
water consumption	7.0E4	2.1E6	1.1E4	5.4E7	1.1E10	4.0E10	6.7E8	2.8E10
Total	**1.4E7**	**2.3E8**	**1.7E6**	**2.7E9**	**9.0E11**	**7.5E11**	**3.9E10**	**5.4E11**
Total including daughters not modelled in the geosphere, assuming secular equilibrium with their parents in well water.				**2.7E9** **Pa-233**				

8.2.8 References for Section 8.2

BIOMOVS II (1996). Development of a Reference Biospheres Methodology for Radioactive Waste Disposal. BIOMOVS II Technical Report No. 6, published on behalf of the BIOMOVS II Steering Committee. ISBN 91-972134-5-4, Swedish Radiation Protection Institute, Stockholm.

EPRI (1996). Biosphere Modelling and Dose Assessment for Yucca Mountain, TR-107190, Final Report, Prepared by QuantiSci Inc, UK. Electric Power Research Institute, Palo Alto.

EPRI (1998). Alternative Approaches to Assessing the Performance and Suitability of Yucca Mountain for Spent Fuel Disposal, EPRI TR-108732. Electric Power Research Institute, Palo Alto.

IAEA (1995). The Principles of Radioactive Waste Management. IAEA Safety Series No.111-F, Vienna.

IAEA (1999a). Guidance on the Definition of Critical and Other Hypothetical Exposed Groups for Solid Radioactive Waste Disposal, BIOMASS/T1/WD03, IAEA Working Material, Vienna

IAEA (1999b). BIOMASS Example Reference Biosphere 1: Drinking Water Well, BIOMASS/T1/WD05, IAEA Working Material, Vienna.

IAEA (1999c). Biosphere System Identification and Justification, BIOMASS/T1/WD06, IAEA Working Material, Vienna

IAEA (2000a), Example Reference Biosphere 2A: Agricultural Well, Constant Biosphere, BIOMASS/T1/WD08, IAEA Working Material, Vienna.

IAEA (2001). BIOsphere Modelling and ASSessment BIOMASS Programme Version 2, Working Material CD, Reproduced by the IAEA, February 2001. International Atomic Energy Agency, Vienna.

WALTER (1984). Vegetation of the Earth and Ecological Systems of the Geo-Biosphere. Eugene Ulmer Verlag, Stuttgart.

Wasiolek M (2001). Data supplied as personal communication by the Yucca Mountain Project Biosphere Assessment team.

9
INTEGRATION OF SUBSYSTEM MODELS TO ESTIMATE CONCENTRATIONS AND DOSES IN IMARC-6

9.1 Introduction

The IMARC-6 implementation uses a methodology similar to previous applications of the IMARC code to estimate radionuclide concentrations and doses to potential future populations in the vicinity of the Yucca Mountain. The methodology is based on a "logic tree" approach that represents uncertainties in models and parameters with nodes and branches, each branch representing an alternative model or parameter with an associated probability. The family of end branches therefore represents a set of assumptions on models and parameters, with an associated composite probability, that can be used to calculate concentrations and doses. The composite probability is calculated as the product of probabilities on branches leading to that end branch. The family of end branches and the associated calculations of concentrations and doses leads to a *distribution* of concentrations and doses reflecting uncertainties in models and parameters.

The logic tree methodology is best used in an evolutionary fashion, expanding the analyses (and nodes) that are most critical to calculations, and contracting the analyses (and nodes) that are least critical. These expansions and contractions have gone on through all phases of the IMARC effort. The current logic tree reflects the models, parameters and assumptions that we have found to be most critical. Thus the IMARC-6 code represents a high-level analysis tool, rather than a performance assessment code that grinds through uncertainties in all phases of the analysis. The most critical models and parameters, represented in the IMARC-6 logic tree, have been described in previous chapters and are summarized below.

The results of the IMARC-6 analysis are primarily presented as mean concentrations and doses. The reason is that we believe mean results to be the most appropriate for comparison to other natural and man-made risks (e.g. the risk of latent cancers). Distributions of the major models and parameters are maintained in the logic tree and in individual model distributions, for example of waste container failure, because calculating mean concentrations and doses vs. time requires such distributions. We cannot calculate mean system response using mean model and parameter assumptions, because of the nonlinear response of concentrations and doses to those assumptions.

9.2 Discussion of IMARC-6 Implementation

Four nodes are used in the IMARC-6 analysis, representing the four sets of models and assumptions found to be most influential in previous analyses. These nodes and branches result in 54 end branches (54 sets of assumptions), for which concentrations and doses are calculated. Figure 9-1 illustrates the logic tree used in IMARC-6. Input values of infiltration rate, focused flow factor, solubility and alteration time, and species retardation are documented in previous sections and are summarized below.

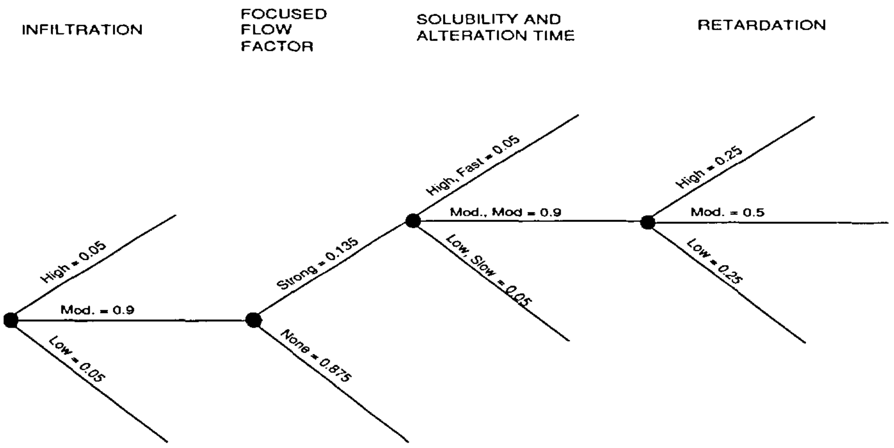

Figure 9-1
Logic tree for IMARC-6, shown simplified. There are 54 end branches in the full logic tree.

9.2.1 Future Climate Change and Net Infiltration

The assumptions on future climate and net infiltration for IMARC-6 are the same as for the previous release (IMARC-5). To summarize, we estimate low, moderate, and high values of net infiltration for three climate periods: a greenhouse climate, an interglacial climate, and a full-glacial-maximum climate. The greenhouse and interglacial climates are expected to last 100 years each, followed by the onset of a full-glacial-maximum climate in year 2000 (after present). This full-glacial-maximum climate continues for the remainder of the million year analysis. The first two climates have very little effect on dose calculations, because of the robust waste container designs being considered. We continue to model the two early climates in the event of possible future refinement of the climate node. The net infiltration rates (in mm/yr) used for each climate, and for the three infiltration branches of the logic tree, are listed below.

	Low	Moderate	High
Greenhouse (1000 years)	1.1	11.3	19.2
Interglacial (1000 years)	1.1	7.2	9.6
Full glacial maximum (remainder)	6.8	19.6	35.4

9.2.2 Focused Flow Factors

Modeling of focused flow in the unsaturated zone of Yucca Mountain has been an important part of recent IMARC applications. In the current version, we model two scenarios of flow focusing with the logic tree. The first alternative represents no flow focusing, where the percolation flux throughout the repository is uniform. This branch never produces release since none of the infiltration scenarios are high enough to initiate dripping according to CRWMS M&O (2001). The second alternative represents focused flow, with a factor of four increase in percolation flux occurring in 25% of the repository. Within this area, under the moderate or high infiltration scenarios, 5% of the drifts experience dripping, hence 1.25% of the repository is capable of releasing waste. In the remainder of the repository, waste containers are not dripped on, so they remain dry and are assumed to never release. The first alternative is given a credibility of 86.5%, the second 13.5%.

9.2.3 Solubility and Alteration Rate

Alternative solubilities for each radionuclide are summarized in Table 9-1; values are discussed in Section 6. The alteration time of the waste form is also assumed to be uncertain, with values of 1000 years (probability 0.05), 3000 years (probability 0.9), and 5000 years (probability 0.05). These are the same alteration times used in the previous version of IMARC. Values of alteration times are linked to values of solubilities (fast alteration is linked to high solubility, and so on) because any specific radionuclide's concentration in groundwater is generally governed by one or the other, not both. Previous sensitivity studies have shown that we do not need to model combinations of fast alteration and low solubility, and slow alteration with high solubility.

9.2.4 Saturated zone flow

The unsaturated zone model and retardation values are unchanged from previous versions of IMARC. The saturated zone model has been updated to use revised interpretations available from the Yucca Mountain project. A summary of hydraulic and transport parameters for the saturated zone are shown in Table 9-2.

Retardation values in the saturated zone were modified to reflect K_d values for neptunium in the volcanic and alluvium layers, and revised K_d values for other radionuclides in the alluvium. A listing of all K_d values is given in Table 9-3.

Table 9-1
Radioelement solubilities (in moles/liter)

Radioelement	High solubility	Moderate solubility	Low solubility
Am	=	2.1E-8	=
Cl**	=	1.1E0	=
Cs	7.4E-3	3E-3	7.4E-6
I**	=	7.8E-1	=
Np	8.4E-3 (4.2E-6)+	8.4E-5 (4.2E-8)+	4.2E-6 (4.2E-10)+
Pa*	=	3.0E-6	=
Pu	8.3E-7	8.3E-9	8.3E-11
Ra*	=	8.8E-7	=
Se**	=	1.0E-2	=
Tc**	=	1.0E0	=
Th	8.7E-8	3.0E-9	8.7E-11
U	2.1E-4	2.9E-5	4.2E-7

* Radioelements whose dose-contributing nuclides are decay daughters, so their dose contribution is probably independent of the solubility limit at the surface of spent fuel.

** Radioelements that are expected to be highly soluble, without any actual solubility limit imposed at the surface of spent fuel.

\+ Alternate values based on results by Argonne National Lab.

= Assigned values are identical to "moderate solubility" value.

Table 9-2
Summary of hydraulic and transport parameters of the saturated zone.

Parameter type	Parameter	Volcanic tuff	Alluvium
Matrix	Effective Porosity	0.19	0.15
	Bulk density (kg/m^3)	1940	1910
	Diffusion coefficient (m^3/day)	2.8E-6	0
	Radius matrix block (m)	0.75	--
Flowing interval	Effective porosity	1.5E-2	--
	Diffusion coefficient (m^2/day)	4.3E-5	--
	Bulk hydraulic conductivity (m/day)	8.64	8.64
Transport	Specific discharge (m/day)	4.1E-4	4.1E-4
	Appr. linear groundwater vel. (m/yr)	2.7E-2	2.7E-2
	Longitudinal dispersivity (m)	20	20
	Transverse dispersitivity (m)	5	5

Table 9-3
K_d values for sorption in tuff and alluvium in the saturated zone

Radionuclide	K_{dv} (volcanics) (mL/g)	$K_{dv} x \rho_b$ (dimensionless)	K_{da} (alluvium) (mL/g)	$K_{da} x \rho_b x c$ (dimensionless)
Np	1.0	1.94	5	9.5
I	0	0	0	0
U	2.0	3.9	5	9.5
Tc	0	0	0	0
C	0	0	0	0
Am, Pu, Pa, Th	50	97	25.5	49
Cs, Sr	25	49	12.8	24
Se	2.0	3.9	2	3.8

ρ_b for volcanic tuff is 1.94 g/cm^3
ρ_b for alluvium is 1.91 g/cm^3
$c = \theta_c/\theta_T = 0.15/0.3 = 0.5$, as described in CRWMS, M&O (2000a)

9.2.5 Waste container failures

As in the previous version of IMARC, three barriers must all fail before water is assumed to contact the waste form. The titanium drip shield must first fail, so that flowing groundwater can contact the waste package itself. Corrosion processes requiring flowing groundwater are assumed to start on the waste package surface once the drip shield has failed.

The third barrier is the fuel cladding. A small fraction of cladding is assumed to have failed at the time of emplacement, thus being exposed to water and available for transport immediately. The remainder of the intact cladding is assumed to fail over time in the presence of groundwater according to a failure model, once groundwater contacts the cladding.

The waste container model is represented by third failure curves. The first is applied to a 0.0001 fraction of all waste containers, and assumes that the drip shield has failed on emplacement but the waste packages are intact. The second is applied to a 0.0001 fraction of all waste containers, and assumes that the drip shield is intact on emplacement, but that the waste packages have failed. The third failure curve, applied to the remaining 0.9998 fraction, assumes that both the drip shields and waste containers are intact on emplacement. The analysis using all three failure modes includes the failure of cladding as part of the overall failure model, as discussed above.

General corrosion is the mechanism by which waste containers are assumed to fail, once the drip shield has failed. Dissolution of radionuclides begins once more than 0.001 of a container fails in a given time step. In this way the time of release depends on the fraction of the repository that is wet, which in turn depends on infiltration and flow focusing scenarios. The low infiltration scenario never produces a source, since no dripping water is anticipated for this case and diffusive transport is not considered for these calculations.

Figure 9-2 compares the failure curves for the three cases discussed above (combinations of drip shields and waste containers failing or not failing). Having the drip shield intact does not significantly delay the failure of waste container, presumably because if water is available to corrode the drip shield, it will also be available in the same location to corrode the waste container.

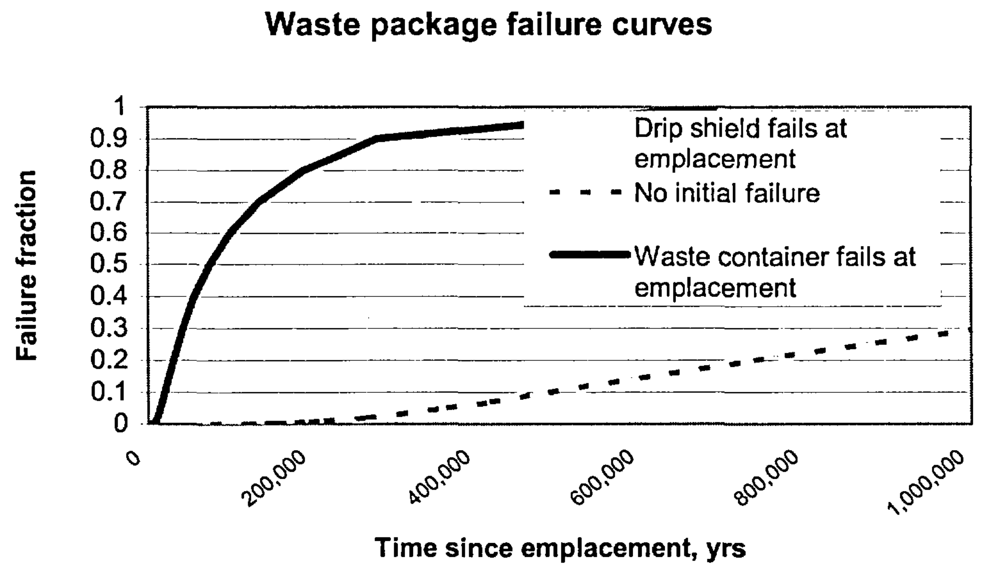

Figure 9-2
Waste package failure curves.

9.2.6 Fractions of repository wet

The "fraction wet" is the fraction of waste containers above which liquid water is assumed to be dripping into the drifts. We assume that dripping is required to initiate dissolution of radionuclides into groundwater. The fraction wet was taken from CRWMS M&O (2001), and a summary is included in Table 9-4. These fractions depend on the degree of flow focusing and on the infiltration rate. Climate conditions are included in the table but have a negligible effect on the fraction wet, since the climate model anticipates the onset of a continuous glacial period after the first 2000 years. Thermal conditions are expected to persist for the first 1000 years, during which the repository is assumed to remain dry.

Table 9-4
Fractions of waste packages that are wet

		Infiltration rate		
	Climate	Low	Medium	High
Unfocused flow (area=1, F=1, prob.=0.865)	All	0	0	0
Focused flow (area=0.2, F=4, prob.=0.135)	Thermal	0 (0)	0 (0)	0 (0)
	Current	0 (5)	0 (29)	0 (38)
	Glacial	0 (27)	0.05 (78)	0.05 (142)

Note: numbers in parentheses are local percolation fluxes in mm/yr.

9.2.7 Source term

Radionuclides in the waste package are released immediately after the container fails. All water dripping on a failed waste package is allowed to enter the container and thereby is made available for waste dissolution. The amount of available water was estimated by interpolation of the "Uncertainty in Seepage Parameters as a Function of Percolation" table from CWRMS M&O (2001). After exiting the waste container, radionuclides in solution are mixed with all water flowing through the repository before being transported through the unsaturated zone.

It is assumed that any failed containers in the "dry" zones within the repository (where no active dripping of groundwater into the drifts occur) do not release anything. This neglects the possible contribution to release made by diffusion from those failed containers in the "dry" zones. Separate analyses suggest that neglecting diffusive release does not significantly affect the overall dose rate estimates, although it is likely that dose rates due to ^{99}Tc and ^{129}I may be underestimated by approximately an order of magnitude.

9.2.8 Repository Configuration

Dimensions of the repository are modeled as 2500m in the dimension perpendicular to groundwater flow, and 700m in the dimension parallel to groundwater flow. On average 1.25% of the repository is considered wet, with wet areas occurring in isolated locations. The unsaturated zone (UZ) model in IMARC-6 is one-dimensional, so a vertical column through the UZ was defined to accommodate alternatives for the fraction of the repository plan area considered wet. To represent widely dispersed failed containers, this column was allowed to extend over the entire 2500m width of the repository (see Figure 9-3). This orientation is optimistic (with respect to calculated doses) at early times when the possibility exists for a single container to fail directly upstream from an abstraction well. As modeled, the plume from a single container will be dispersed over the 2500m wide column, making the dose to the average member of the critical group from that single container failure lower than otherwise would be. Results presented in IMARC-5 indicate that this is not a large source of conservatism. Over longer periods of time, when multiple failures are occurring over the entire repository, and when average concentrations and doses are calculated, failures over the entire width of the repository are reasonably represented.

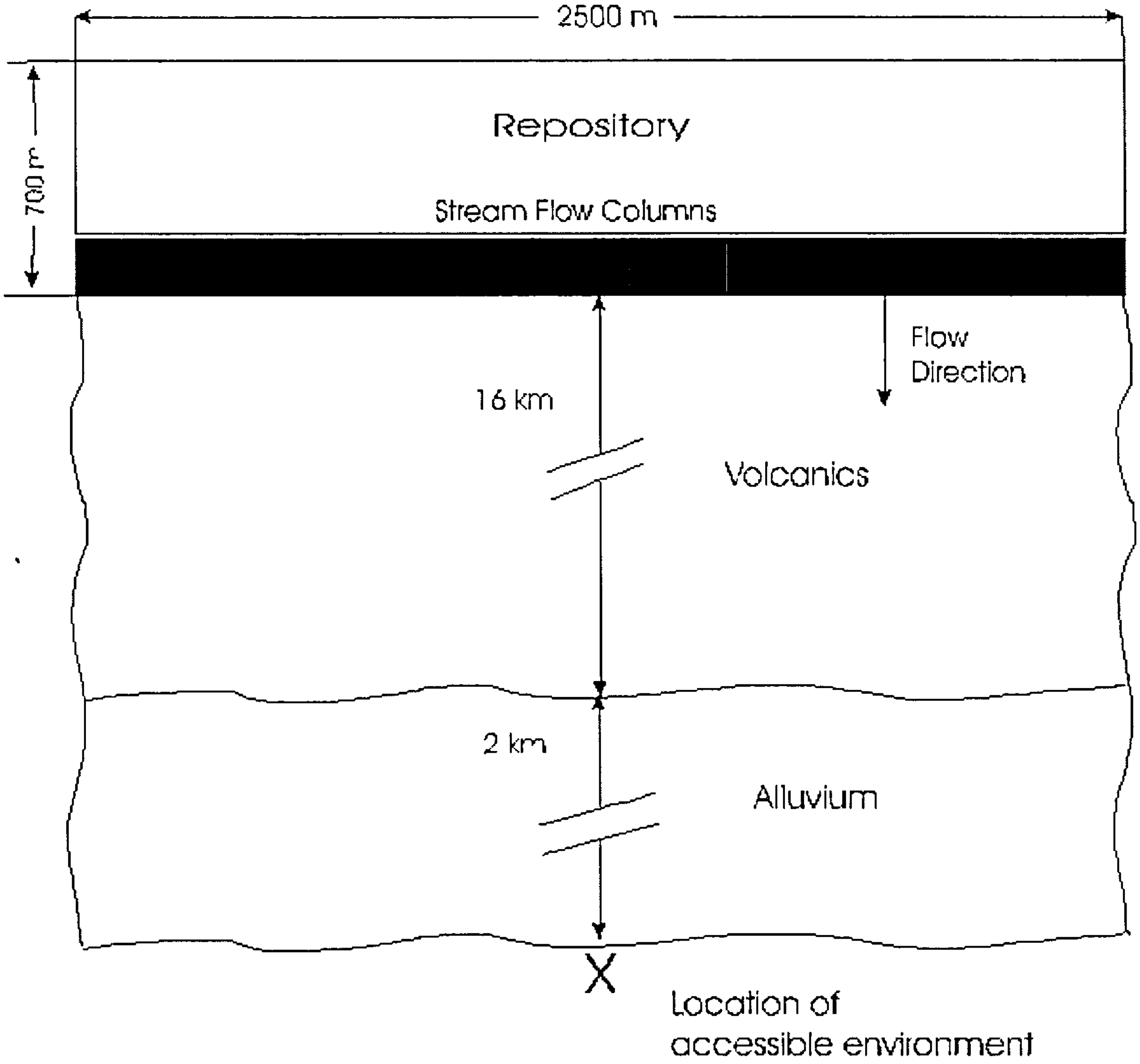

Figure 9-3
Configuration of vertical flow columns and flow through the unsaturated zone.

9.2.9 Dose factors

Dose factors were reviewed and revised for IMARC-6, as discussed in Section 8. They are summarized in Table 9-5.

Table 9-5
Dose factors for water consumption and for all pathways [(mrem/yr)/(mol/m^3)]

Radionuclide	Water consumption only	All pathways
^{36}Cl	3.24E6	3.17E7
^{79}Se	2.69E6	6.47E7
^{94}Nb	8.78E7	2.53E11
^{99}Tc	3.14E6	1.20E7
^{129}I	7.33E6	3.96E7
^{135}Cs	2.75E5	2.75E6
^{226}Ra	1.84E11	3.12E12
^{229}Th	6.99E10	2.25E12
^{230}Th	2.91E9	3.28E11
^{231}Pa	2.27E10	1.92E11 (3.07E11*)
^{233}U	3.35E8	2.99E10
^{234}U	2.09E8	1.07E10
^{235}U	6.99E4	1.37E7
^{238}U	2.10E6	2.30E8
^{237}Np	1.05E4	1.68E6
^{239}Pu	5.38E7	2.71E9 (2.71E9*)
^{240}Pu	4.00E10	7.51E11
^{242}Pu	6.68E8	3.93E10
^{241}Am	9.26E9	

*** value includes dose from daughter products**

10

IMARC-6 RESULTS AND SENSITIVITY STUDIES

Performance assessments use calculations of radionuclide release and dose to evaluate a repository's performance, using several formats. The calculations presented in this Section concentrate on estimating dose to the reasonably maximally exposed individual (RMEI) located 18 km downstream from the repository boundary (i.e., 18 km from the edge of the "accessible environment"). Most of these results and sensitivity studies are presented as doses to the RMEI for transport pathways considering water as the only means of ingestion; others present results for all pathways to ingestion.

10.1 Results Using All IMARC Branches

The first set of results is for calculations made using all 54 branches of the logic tree. Figure 10-1 is the probability-weighted mean annual dose contributed by the ten radionuclides that contribute the most to dose from all exposure pathways considered in the biosphere model – the "base case".[1] This figure shows the annual dose from all pathways. Dose rates prior to 10,000 years are significantly lower than 10^{-6} mrem/yr – more than ten million times lower than the 15-mrem/yr limit in 10 CFR Part 63 [NRC, 2001].

Peak annual doses from all pathways occur at about 600,000 years and are on the order of 10^{-1} mrem. The general character of the dose curves shown in Figure 10-1 is as follows: the ^{237}Np decay chain (^{237}Np, ^{233}U, and ^{229}Th) dominates RMEI doses at all times considered because ^{237}Np is available in adequate inventories, dose conversion factors for the chain are relatively high, and it is not significantly retarded in geologic units during transport. It was necessary to have the vertical axis on this plot start at an extremely small annual dose to show even the earliest breakthrough at 18 km before 100,000 years. This very long delay is caused by the very long combined lifetime of the engineered barriers considered in this model: the drip shield, container, and cladding. Delay is also caused by the relatively long travel times through the unsaturated zone (UZ) and the saturated zone (SZ).

As discussed in Chapter 9, diffusive release from containers in "dry" zones (zones with no active dripping of groundwater into the drifts) has been neglected. Separate analyses indicate that, by neglecting diffusive releases from the dry zones, the dose rates due to ^{99}Tc and ^{129}I have been underestimated by about an order of magnitude. This does not significantly affect the total dose rate.

---

[1] The U-236 curve does not appear on this figure because it lies directly under the U-238 curve. It so happens that the product of the ratio of the number of moles of each radionuclide times the ratio of the dose conversion factors for these two radionuclides [Ci/mole] is very nearly one.

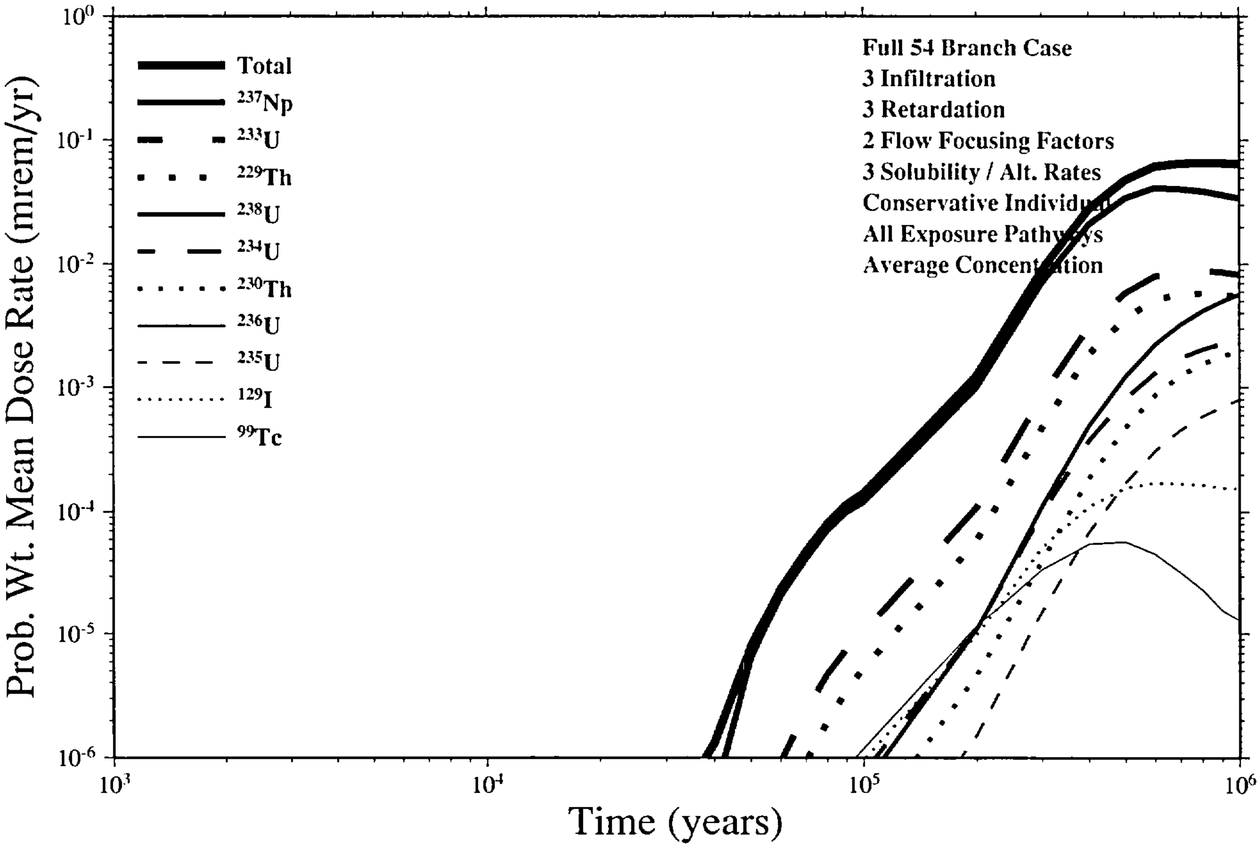

Figure 10-1
Probability-Weighted Mean Annual Dose Versus Time 18 km Downstream, All Exposure Pathways

In previous IMARC analyses ("IMARC-5") [EPRI, 2000], the dominant radionuclides at the earliest times were ^{79}Se, ^{99}Tc and ^{129}I. This is no longer the case due primarily to a reduction in the estimated Np sorption coefficient in the saturated zone, and to changes in the dose conversion factors from our previous analyses. Also, there was an error in the way the dose for ^{79}Se was calculated in IMARC-5 such that its dose rate was overestimated by a factor of approximately 20. The combination of changes in the way dose conversion factors are determined (see Chapter 8), along with this factor of 20 error, results in ^{79}Se no longer being one of the "top ten" dose contributors. Thus, ^{79}Se is not shown in this figure.

While there are no regulatory requirements limiting RMEI dose rates beyond 10,000 years, a potential, subjective "figure of merit" could be a comparison to natural background dose rates. This is because the RMEI is meant to represent those few individuals who, due to location and habit, are among those most exposed to any radionuclides moving downstream into the accessible environment. If the RMEI dose were comparable to or lower than natural background levels (on the order of 10^2 mrem/yr in the Amargosa Valley region), then this should provide additional confidence that the combination of repository natural and engineered systems are providing a high level of protection to individuals who might be living in the Amargosa Valley region in the far future.

Figure 10-2 provides a linear plot of probability-weighted mean dose rate versus time after repository closure from the ten major radionuclides contributing to dose from all exposure pathways. Natural background levels are in the 100 to 300 mrem per year range. The estimated mean dose rate is indistinguishable from zero at this scale.

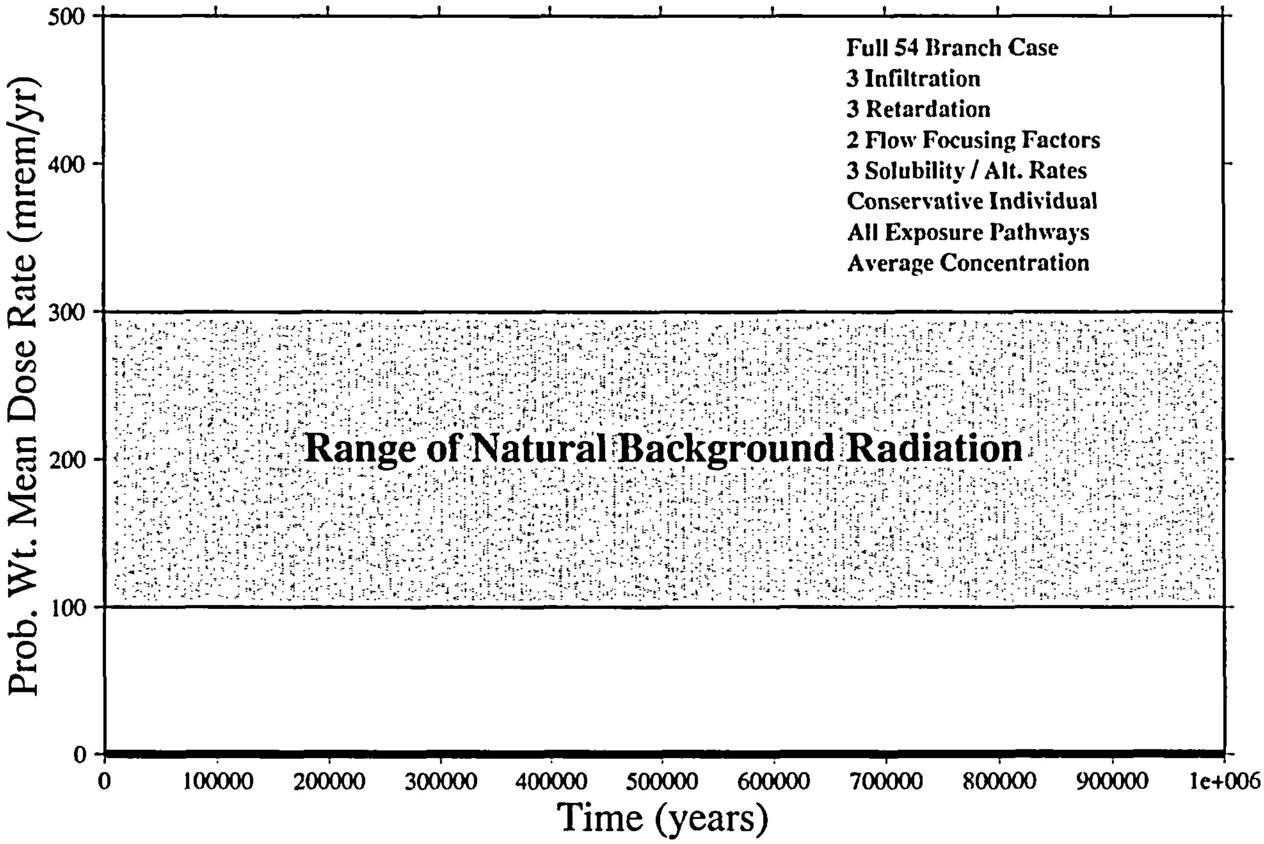

Figure 10-2
Probability-Weighted Mean Annual Dose Versus Time 18 km Downstream, All Exposure Pathways

Figure 10-3 is the same plot with the vertical scale expanded by a factor of ten (i.e., instead of the scale being zero to 500 mrem/yr it is now from zero to 50 mrem/yr). For this figure, the natural background range is off the top of the scale. Instead, the regulatory limit of 15 mrem/yr is shown, although it only applies for the first 10,000 years. Again, the estimated dose rate even at this scale is indistinguishable from zero.

The next expansion of ten in the vertical scale (now from zero to just 5 mrem/yr) is shown in Figure 10-4. For this figure, the estimated dose rate versus time curve finally appears to rise a very small distance off of the zero line.

The next expansion of ten in the vertical scale (now from zero to just 0.5 mrem/yr) is shown in Figure 10-5. The dose rate curve is now clearer, but still has not risen very far toward the top of the figure.

The final expansion is a factor of five in the vertical scale (from zero to only 0.1 mrem/yr) is shown in Figure 10-6. For this curve, it can be seen that the dose rate rises above zero at about 200,000 years. To put that amount of time in perspective, 200,000 years ago is about 20 times longer than the earliest recorded human history, and is several times longer ago than when the cave paintings in Europe were painted. Furthermore, it has taken more than three expansions of ten (or a factor of more than one thousand) from the natural background curve to clearly distinguish the probability-weighted dose rate curve, as summarized in Figure 10-7. This means that, for the "normal" release scenario envisioned for the Yucca Mountain repository system, the probability-weighted mean dose to a reasonably maximally exposed individual living downstream of the Yucca Mountain repository would add less than one part in one thousand more to the dose they would receive annually from natural radiation sources in the Yucca Mountain vicinity. In other words, one would multiply the natural background dose by just 1.001 to get the dose to the reasonably maximally exposed individual that includes both natural radiation and that due to the "normal" release scenario from Yucca Mountain.

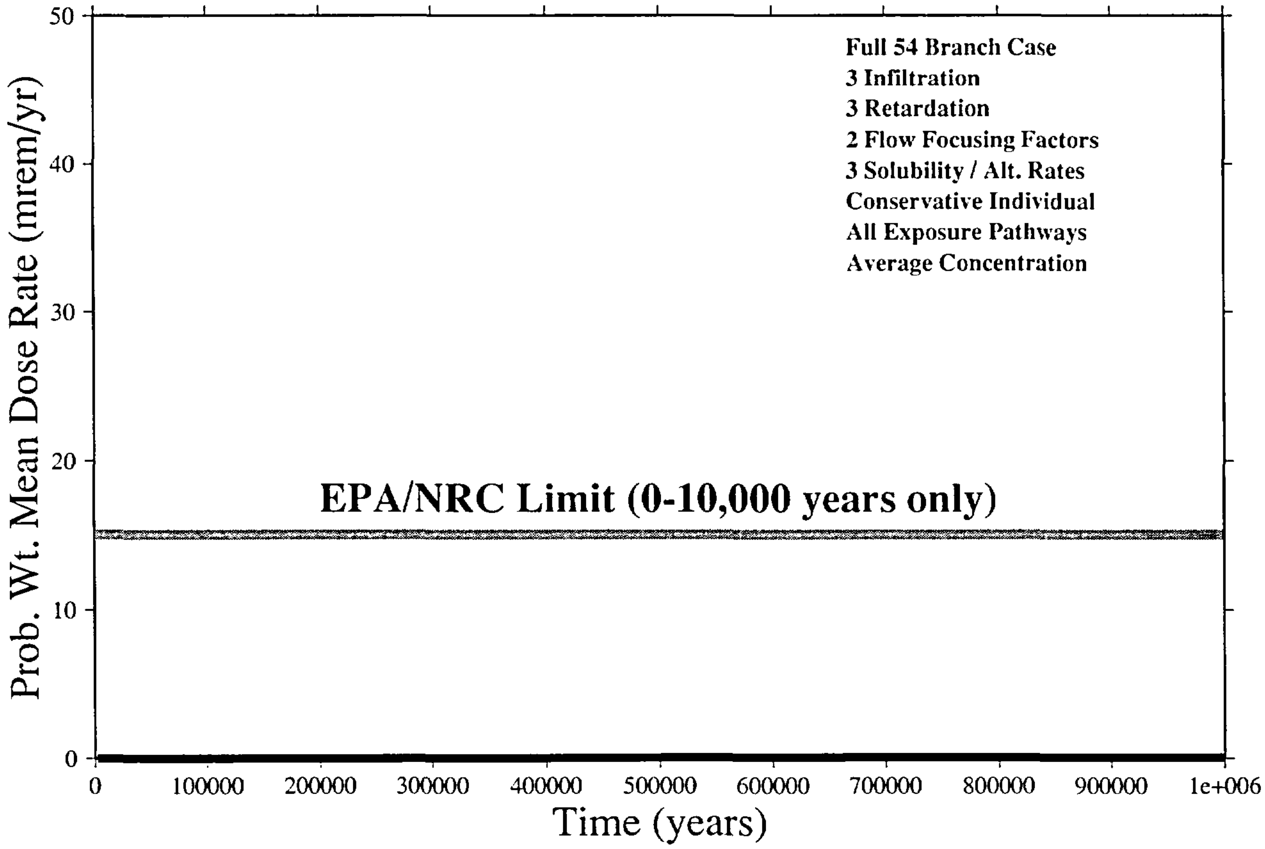

Figure 10-3
Probability-Weighted Mean Annual Dose Versus Time 18 km Downstream, All Exposure Pathways

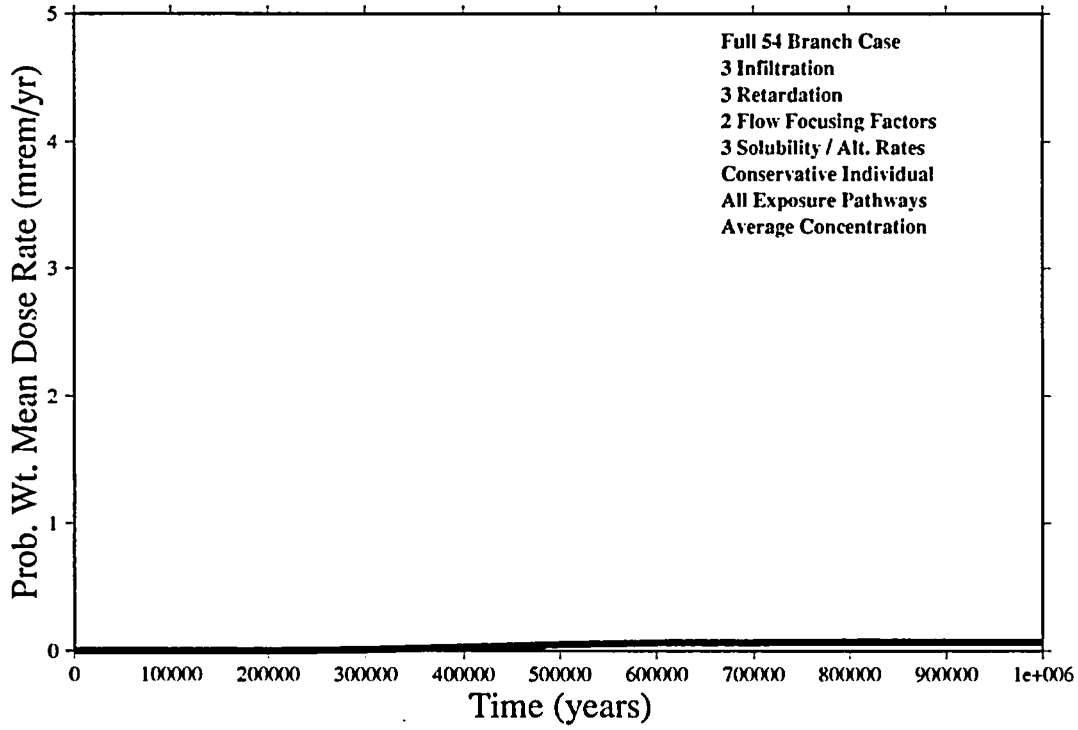

Figure 10-4
Probability-Weighted Mean Annual Dose Versus Time 18 km Downstream, All Exposure Pathways

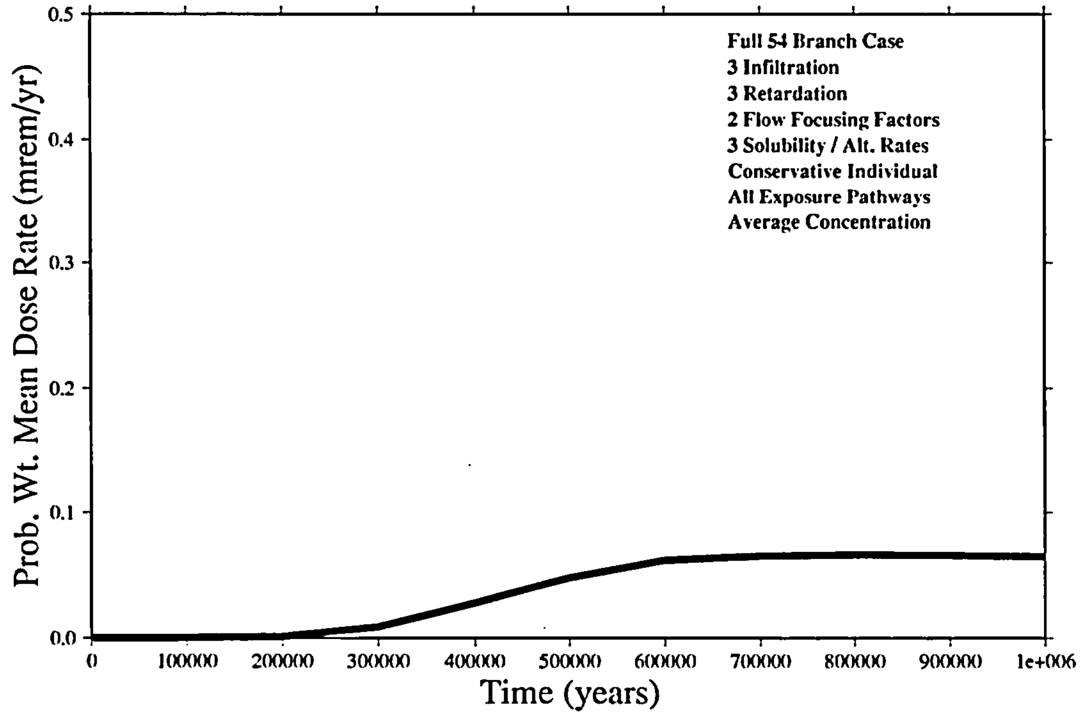

Figure 10-5
Probability-Weighted Mean Annual Dose Versus Time 18 km Downstream, All Exposure Pathways

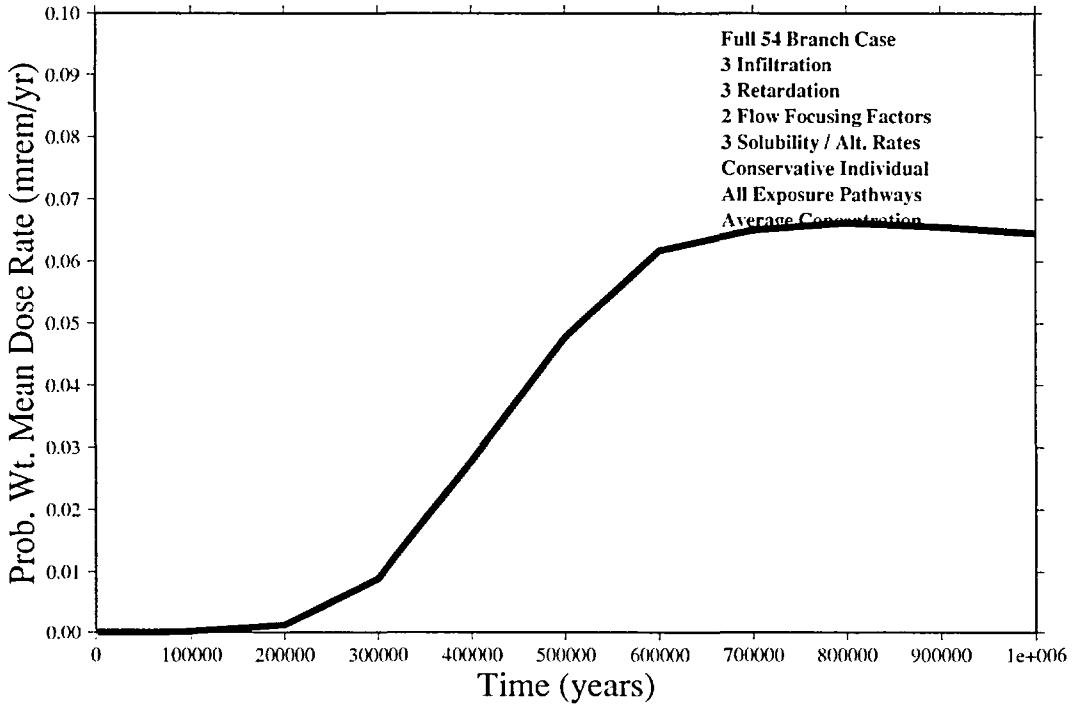

Figure 10-6
Probability-Weighted Mean Annual Dose Versus Time 18 km Downstream, All Exposure Pathways

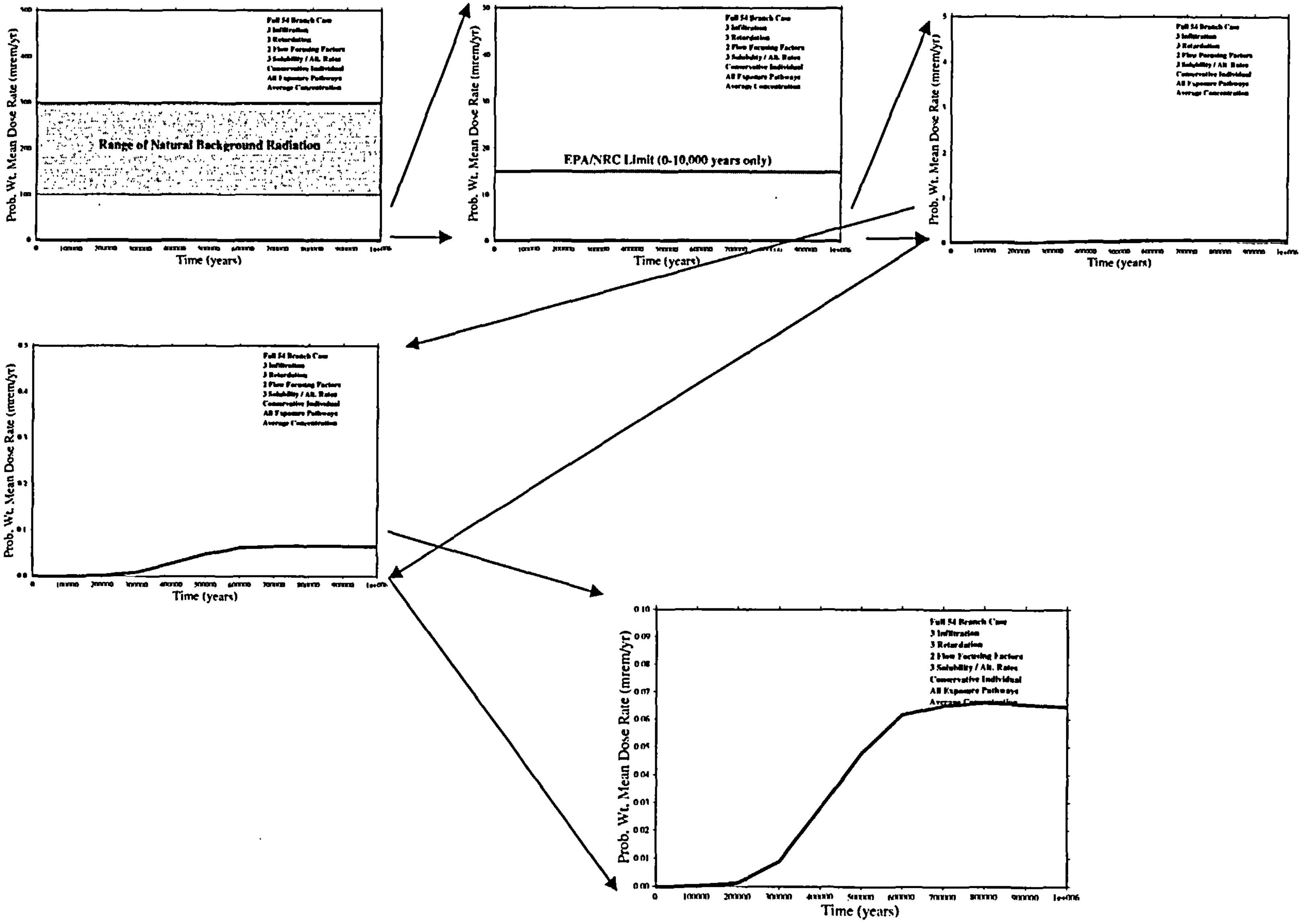

Figure 10-7
Expansion of Vertical Axes From Figure 10-2 through 10-6. Arrows indicate expansion of axes from the previous figure.

Figure 10-8 shows the same "base case" annual dose versus time, but for just the drinking water pathway, rather than for all exposure pathway as shown in Figure 10-1. When just the drinking water pathway is considered, the peak annual dose to the RMEI is approximately 10^{-3} millirem – about 10^{2} times lower than the peak annual dose from all exposure pathways. The major contributors to peak dose for the drinking water pathway are essentially the same as those for all exposure pathways.

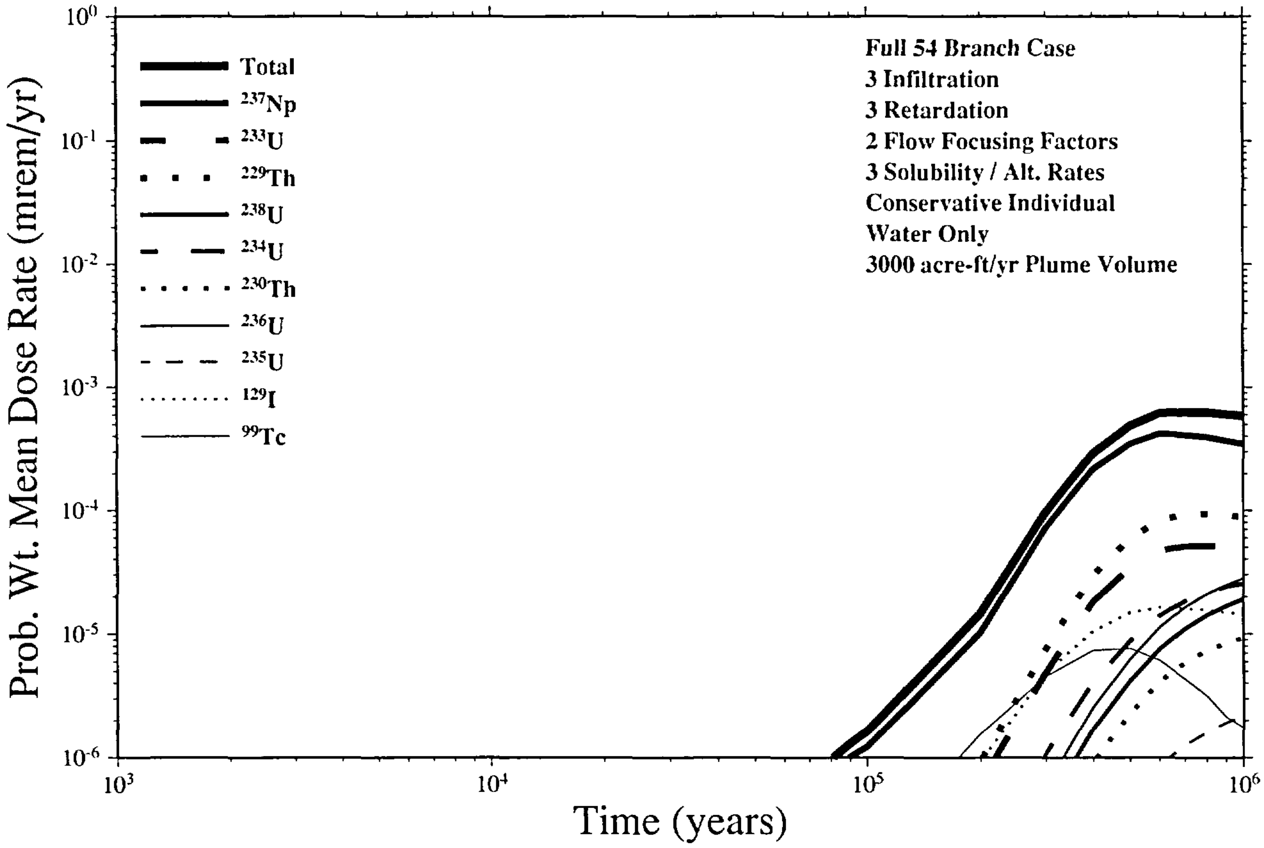

Figure 10-8
Probability-Weighted Mean Annual Dose Versus Time 18 km Downstream, Drinking Water Pathway Only

Figure 10-8 shows that, for the regulatory time period of compliance, the drinking water dose rate is well below 10^{-6} mrem/yr. Since the individual drinking water dose rate limit in 10 CFR 63 is 4 mrem/yr, this suggests that well over six orders of magnitude of margin exist below this limit. Even at the time of peak individual dose rate, nearly four orders of magnitude of margin exist below 4 mrem/yr. While not shown here, the maximum concentration limits in 10 CFR Part 63 are also met with significant margin.

Two factors contribute to the lower dose rates for the drinking water-only pathway. The dose factors for the drinking water pathway are significantly lower than for all exposure pathways. For example, the drinking water dose factor for ^{237}Np is about 50 times lower than that for all exposure pathways. The other factor is the radionuclide concentration in the groundwater. For the all exposure pathway case (Figure 10-1), the size of the plume at 18 km is such that the groundwater flux within the plume is approximately 750 acre-ft/yr.[2] For the drinking water-only case (Figure 10- 8), the assumed groundwater flux within the plume is 3 000 acre-ft/yr, which is four times less than that assumed for the all exposure pathways case. We chose 3 000 acre-ft/yr for the drinking water-only case per the regulatory subsystem requirements for groundwater protection [NRC, 2001]. The fact that we used an effective plume groundwater flux four times larger for the drinking water-only case means that the effective radionuclide concentrations are four times lower. Thus, these two factors provide an effective dose reduction on the order of 10^2.

The logic tree format facilitates sensitivity studies on uncertainties included directly into the IMARC logic tree. Figures 10-9 through 10-16 explore the individual sensitivities to the sets of IMARC branches for ^{129}I, ^{237}Np, and ^{238}U. Figure 10-9 shows the sensitivity to the infiltration rate of individual dose due to ^{129}I from all pathways. Roughly only a factor of two in annual dose can be seen between the 'high' and 'moderate' infiltration rates.[3] The dependence on alteration rate is demonstrated by the fact that the curve for the high infiltration rate is lower than that for the moderate infiltration rate. Since alteration rate of the used fuel waste form matrix is assumed to be independent of infiltration rate, a higher infiltration rate results in more dilution of the solubility-unlimited radionuclides like ^{129}I.

Figure 10-10 shows the sensitivity to infiltration rate for ^{237}Np. In the case of ^{237}Np, a somewhat different sensitivity to infiltration rate than that for ^{129}I can be seen at early times. The initial breakthrough is found to be earlier for the "high" infiltration than for the "moderate", although the order of the peaks is the same as that for ^{129}I. The reversal of order for the initial breakthrough is caused by a small reduction in the groundwater travel time for the "high" infiltration rate compared to the "moderate" rate. As for ^{129}I, the highest peak dose rate is for the "moderate" infiltration rate. This suggests that the release of neptunium is also limited by the alteration rate of the used fuel waste form rather than solubility limits.

Figure 10-11 shows the sensitivity to infiltration rate for ^{238}U. A different behavior is shown for this radionuclide. In this case, the highest peak dose is for the 'high' infiltration rate. This suggests that uranium is somewhat solubility-limited since a higher infiltration rate causes a greater release of uranium into solution.

---

[2] The edge of the plume was defined as the location where the concentration was 1% of the highest concentration (at the plume center). The radionuclide concentration was the flow-weighted average: the total number of moles of each radionuclide passing the 18km downstream position divided by the plume annual groundwater flux (~750 acre-ft/yr).

[3] The "low" infiltration rate curve does not appear in the figure since none of the scenarios with the "low" rate leads to active dripping anywhere in the repository.

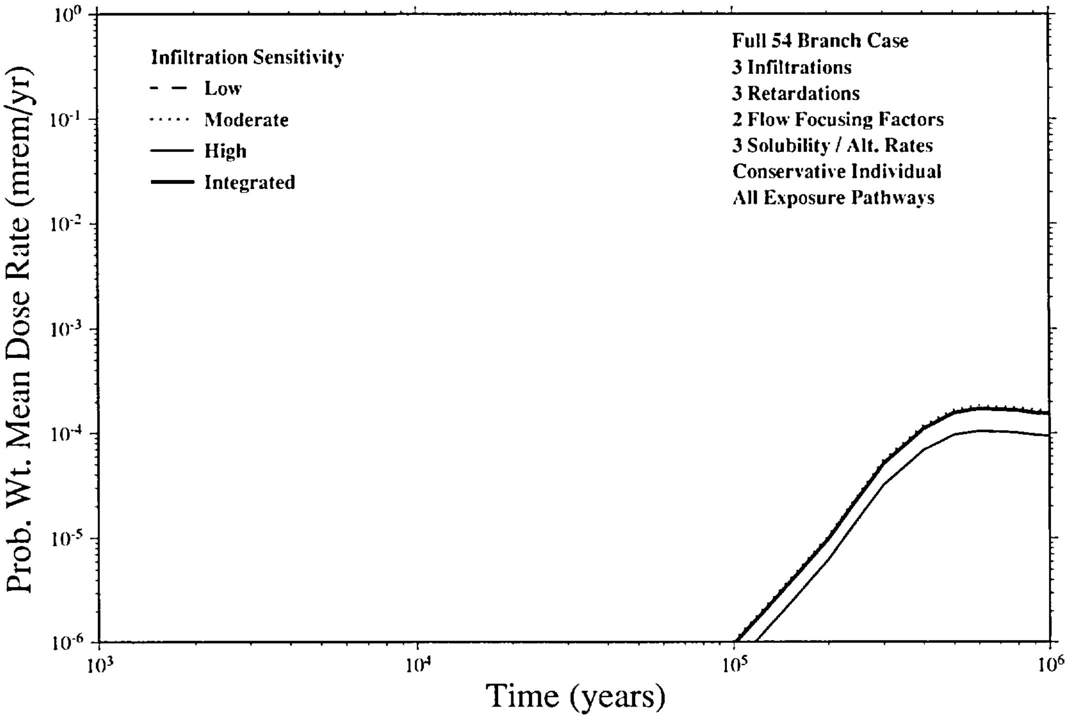

Figure 10-9
Sensitivity of the Probability-Weighted Mean Annual Dose from ^{129}I to Infiltration Rate

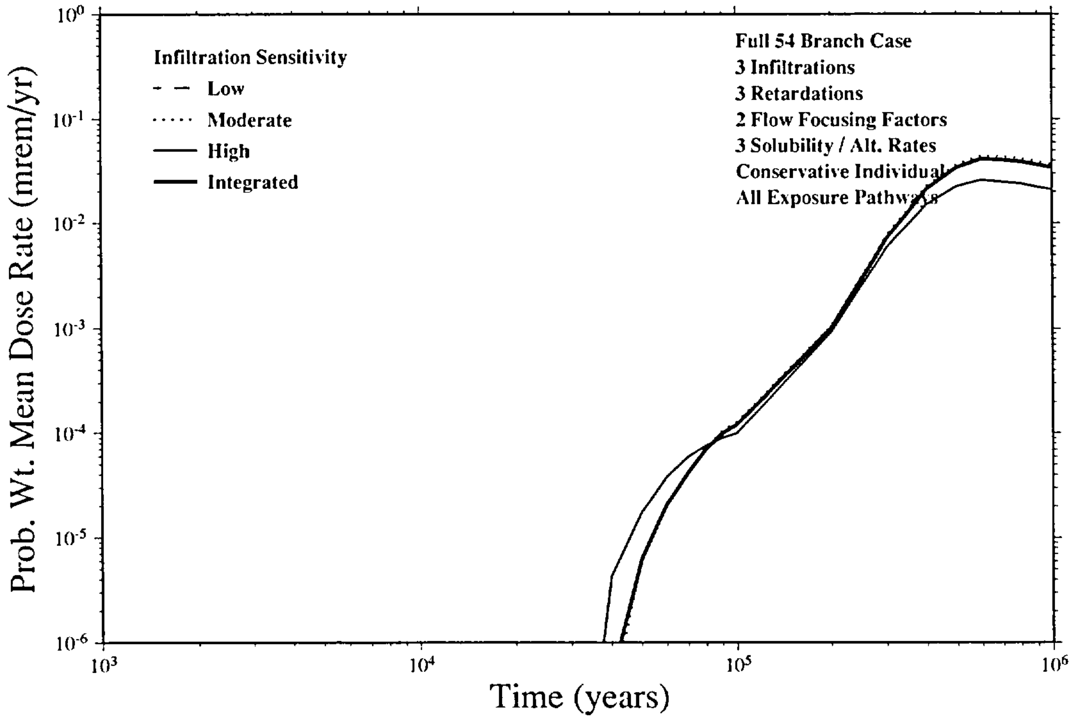

Figure 10-10
Sensitivity of the Probability-Weighted Mean Annual Dose from ^{237}Np to Infiltration Rate

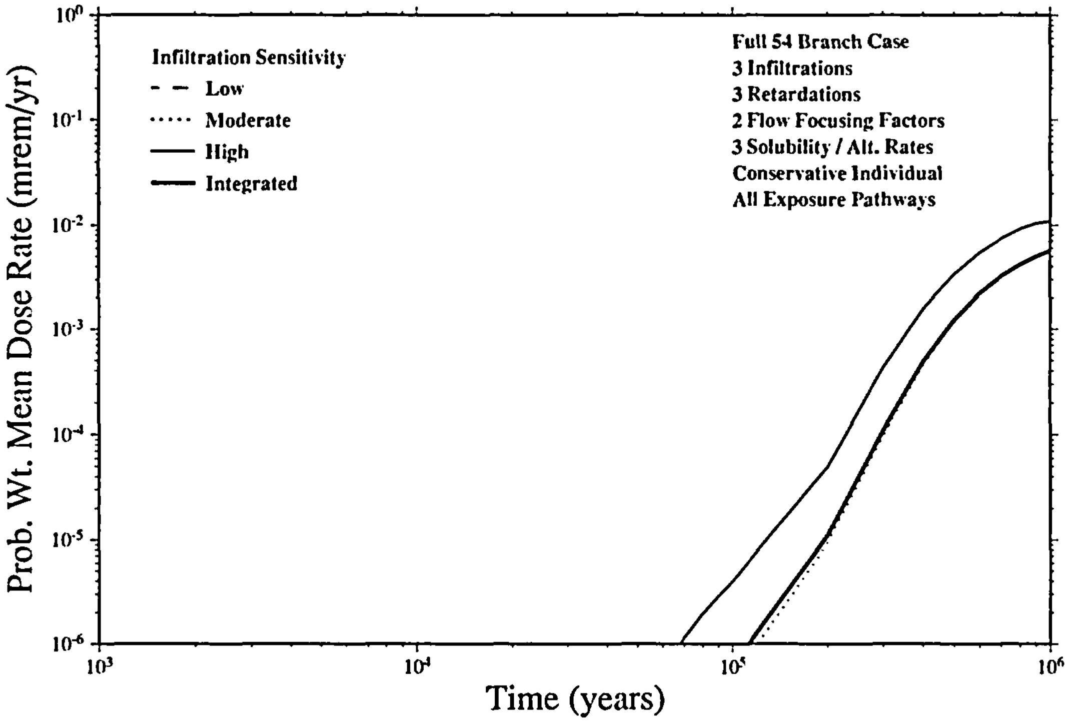

Figure 10-11
Sensitivity of the Probability-Weighted Mean Annual Dose from ^{238}U to Infiltration Rate

Figures 10-12 and 10-13 are the annual dose sensitivities from ^{129}I and ^{237}Np, respectively, due to variations in the focused flow factor. The curve for ^{238}U looks similar in shape to that for ^{237}Np. There is only a slight difference between the two figures shown here. This is not surprising since the dose rates are highly dependent on the fraction of the repository that is 'wet'. In the no flow focusing case (focused flow factor of 1), it is assumed that none of the repository is 'wet' for any of the three infiltration scenarios. As was discussed in Chapter 9, it is thought that the rock and drift properties are such that, even for the highest net infiltration rate, no drips are expected to enter the drifts. For the case of focused flow with a flow-focusing factor of 4, only 25% of the repository are assumed to have active flow within the region such that the average percolation rate in this active flow region is four times the average infiltration rate. For this higher percolation rate, it is assumed about 5% of the containers would be dripped on for the 'moderate' and 'high' infiltration rates. Thus, the only curve that appears in Figures 10-12 and –13 is that for the focused flow factor of 4. The "integrated" curve adjusts the dose rate in accordance with the probability of occurrence of the focused flow factor of 4 case – 13.5%.

Almost no sensitivity to solubility or waste form alteration time was seen for ^{129}I and ^{237}Np. However, a significant sensitivity to solubility for ^{238}U is shown in Figure 10-14. In this case, the effect on the dose rate due to significant uncertainty in uranium solubility is evident.

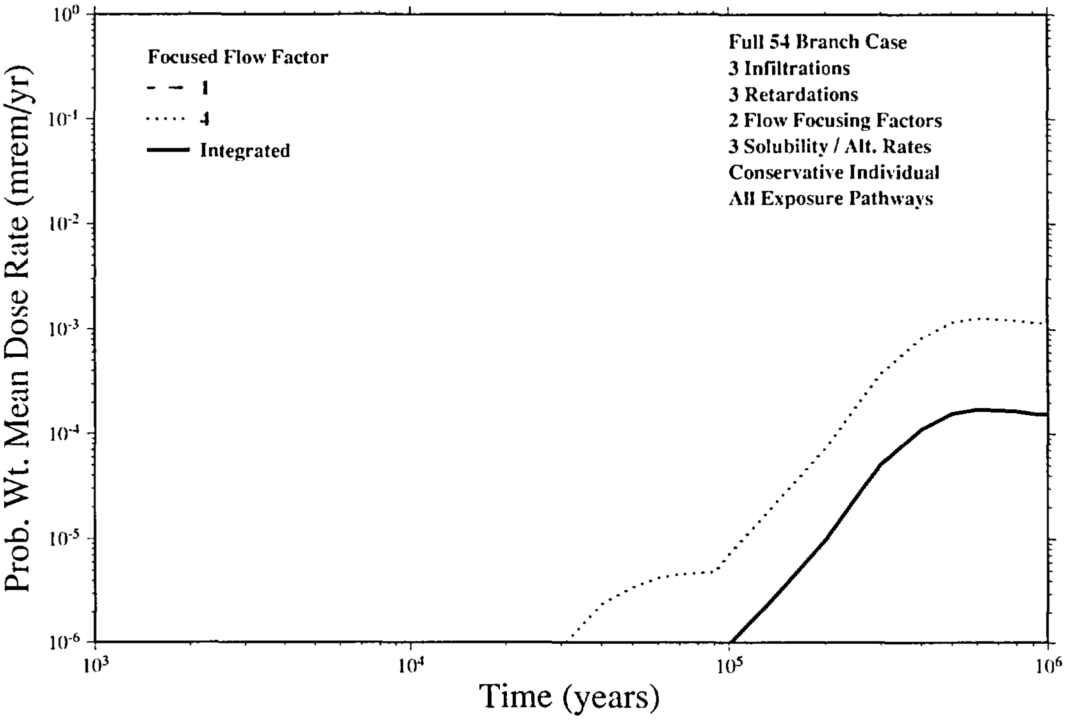

Figure 10-12
Sensitivity of the Probability-Weighted Mean Annual Dose from ^{129}I to the Focused Flow Factor

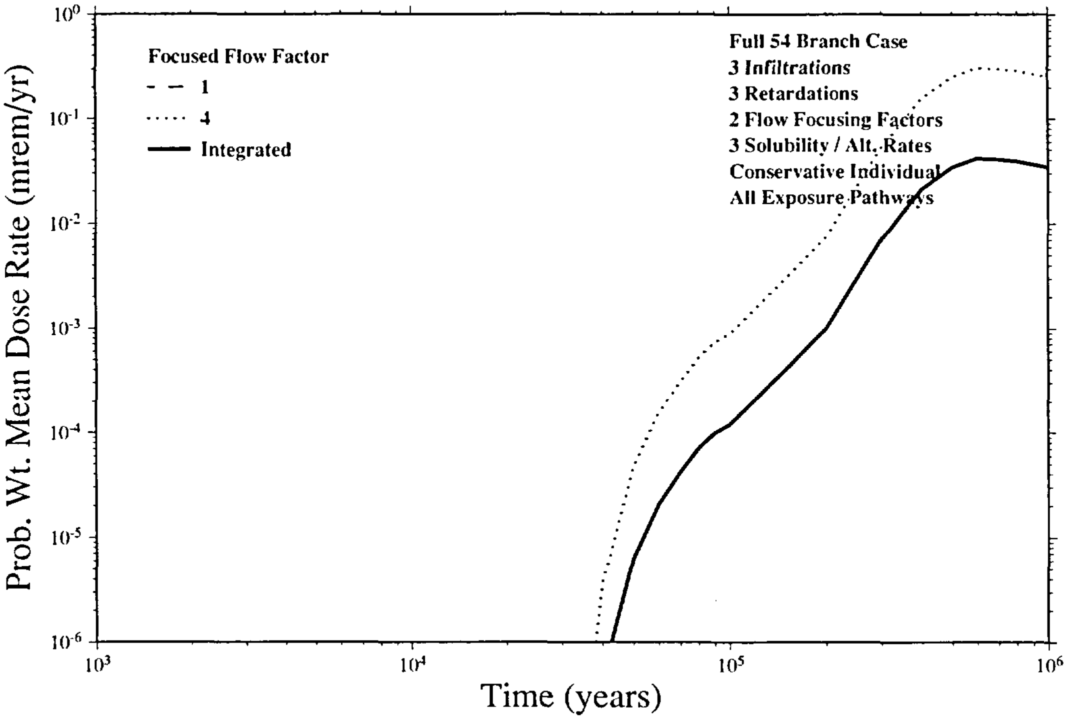

Figure 10-13
Sensitivity of the Probability-Weighted Mean Annual Dose from ^{237}Np to the Focused Flow Factor

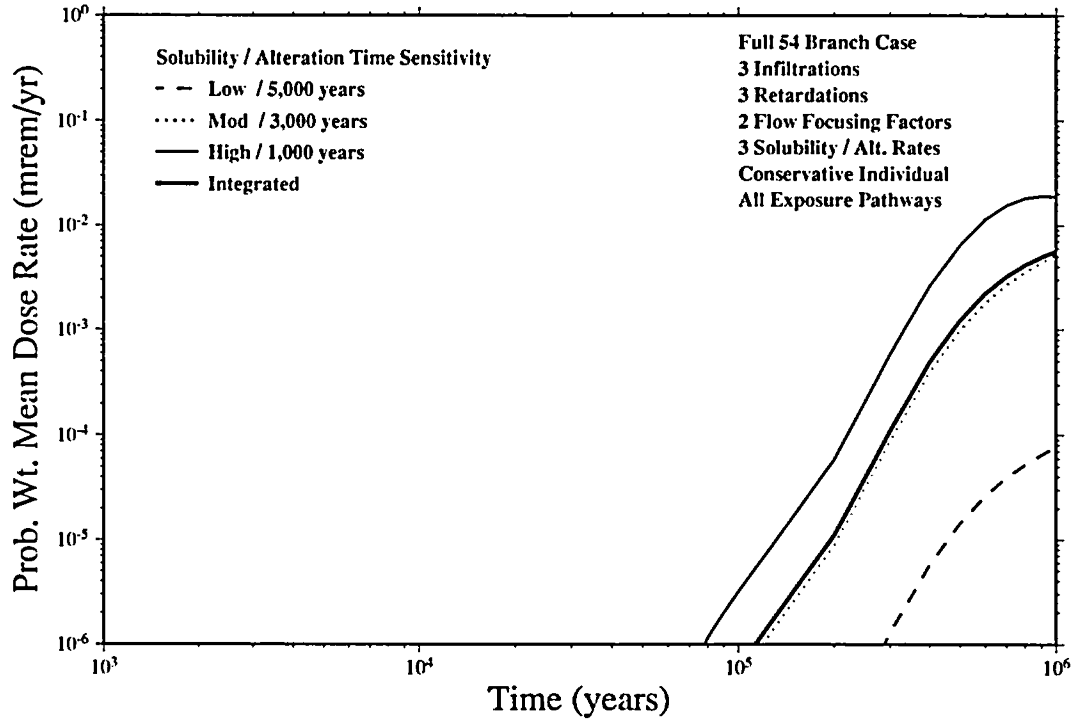

Figure 10-14
Sensitivity of the Probability-Weighted Mean Annual Dose from ^{238}U to Uranium Solubility

The sensitivity to annual drinking water dose from ^{237}Np and ^{238}U due to matrix retardation in the unsaturated (UZ) and saturated (SZ) zones is shown in Figures 10-15 and 10-16, respectively. The time of initial arrival of the radionuclide at 18 km varies by several tens of thousands of years for ^{237}Np, and by about one hundred thousand years for ^{238}U. The time of the peak dose arrival varies by less than one hundred thousand years between the 'low' and 'high' matrix retardation case for ^{237}Np; the ^{238}U peak arrival time appears to be somewhat beyond one million years due to the relatively higher matrix retardation for uranium and the longer half-life for ^{238}U. No sensitivity of ^{129}I to matrix retardation is noted since iodine has zero or near zero Kd's on tuff matrix materials.

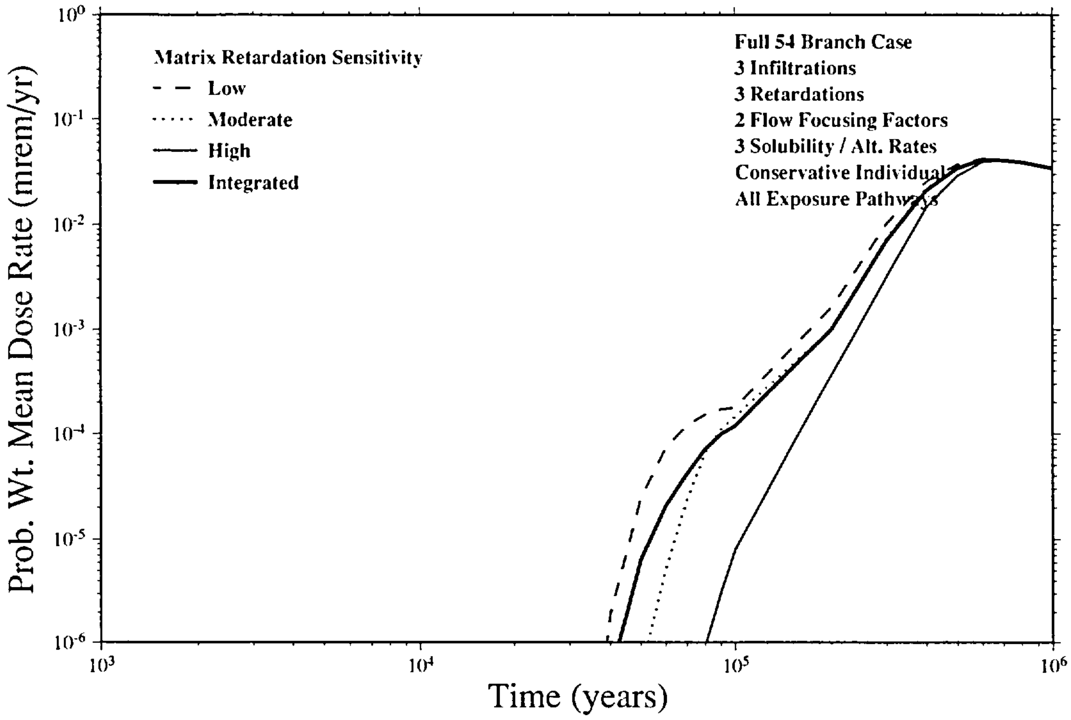

Figure 10-15
Sensitivity of the Probability-Weighted Mean Annual Dose from ^{237}Np to UZ/SZ Matrix Retardation

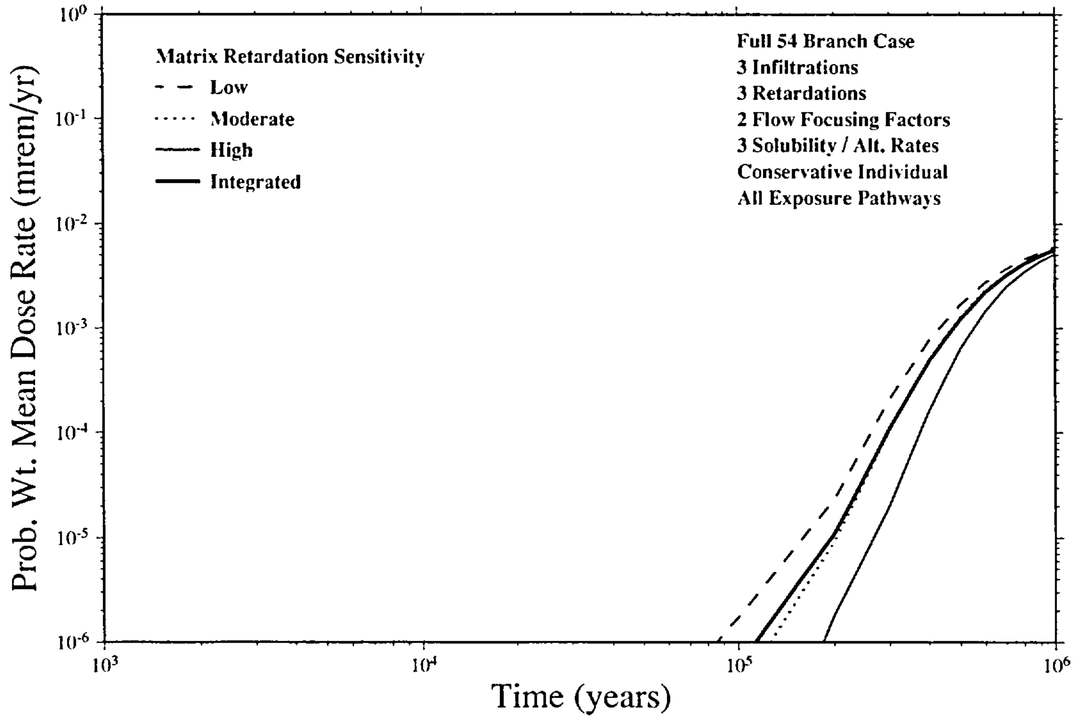

Figure 10-16
Sensitivity of the Probability-Weighted Mean Annual Dose from ^{238}U to UZ/SZ Matrix Retardation

10.2 Evaluation of Whether Multiple Barriers Exist at Yucca Mountain

A key aspect of evaluating the suitability of the Yucca Mountain repository system is to identify the key barriers to radionuclide release in the system. In their final regulation for Yucca Mountain, 10 CFR Part 63 [NRC, 2001], the US Nuclear Regulatory Commission (NRC) states:

> §63.102 (h): "*Multiple barriers.* §63.113(a) requires that the geologic repository include multiple barriers, both natural and engineered. Geologic disposal of HLW is predicated on the expectation that one or more aspects of the geologic setting will be capable of contributing to the isolation of radioactive waste and thus be a barrier important to waste isolation. ... A description of each barrier's capability (e.g., retardation of radionuclides in the saturated zone, waste package lifetime, matrix diffusion in the unsaturated zone), as reflected in the performance assessment, provides and understanding of how the natural system and engineered barriers work in combination to enhance the resiliency of the geologic repository. The Commission believes that this understanding can increase confidence that the performance objectives ... will be achieved and that DOE's design includes a system of multiple barriers."

Thus, multiple barriers are required, some of which must be natural, and some must be engineered. The barriers important to waste isolation must be identified, quantified, and defended. For the purposes of analysis in this chapter, a "barrier" is assumed to be any single or readily distinguishable suite of features, events, and processes (FEPs) that act to:

- prevent or substantially delay[4] movement of the radionuclides to the biosphere; and/or
- substantially reduce their concentration[5] by action of either radioactive decay *or dilution*

The purpose of this section is to provide analyses using the IMARC code to potentially identify a set of natural and engineered 'barriers' upon which to build a safety case for Yucca Mountain. While admittedly artificial, the numerical device of barrier neutralization is useful for shedding light, in a conceptual manner, on the true importance of individual barriers. The analyses in this chapter use the barrier neutralization technique. Like a 'partial' neutralization or 'degraded' barrier performance analysis, none of these techniques represent the 'expected' behavior of the repository system, so they can all be considered artificial. The advantage of a full barrier neutralization approach is that it sometimes helps identify other barriers that are thought to be of only minor importance using more traditional sensitivity analyses, such as those presented in the previous section. As will be shown in this section, this approach has identified potentially important barriers that may have otherwise been ignored.

The neutralization analyses presented here take on two forms. The first is the more common approach to barrier neutralization where a single or, at most, a handful of related barriers are assumed to be non-functional. The second form is what we termed a "Hazard Index" approach when we first presented it two years ago [EPRI, 1998, chapter 14], with revisions in Chapter 13 of EPRI [2000]. This second form is the successive addition of barrier after barrier until the

---

[4] A 'substantial' delay may be on the order of 10^4 years or longer since both EPA and NRC have proposed that the time period of regulatory compliance be 10,000 years.

[5] A 'substantial' concentration reduction is arbitrarily assumed to be a factor of ten or larger.

entire suite of repository FEPs have finally been added. We note whether the magnitude or timing of the peak theoretical dose rate is changed by the addition of each barrier to gauge the potential importance of each of the barriers added.

10.2.1 Barrier Identification Studies Involving a Single Branch of the Logic Tree

In addition to the sensitivity of calculated doses to alternatives in the logic tree calculations, it is instructive to examine the effect on doses of alternative assumptions to other input parameters. This allows for some additional combinations of effects that were not included directly into the IMARC logic tree.

The following branch from the logic tree was selected for specific sensitivity studies (probability of the particular branch given in parentheses):

- Net infiltration rate: "moderate" (P=0.9);
- Flow focusing factor: 4 (P=0.135);
- Solubility/alteration rate: "moderate" (P=0.9);
- Matrix retardation: "moderate" (P=0.5)

This represents the "wet" branch with the maximum likelihood (referred to as the "Max. Likelihood Wet Branch" in subsequent figures in this section). We needed to choose the branch with the flow focusing factor of 4 and either a net infiltration rate of "moderate" or "high" to achieve conditions that cause at least some of the drifts to experience active dripping of groundwater. Without active dripping, there is no release from the containers even if they eventually fail. This is because releases due to diffusion only are thought to be negligible. Note that the majority of the branches are thought to not have any active dripping at all. The probability of dripping conditions is only the probability of a flow focusing factor of four (0.135) times the probability of either "moderate" or "high" net infiltration (0.95), or approximately 13%.[6] In the case of active dripping, only 5% of the drip shield/containers are assumed to be dripped on within the 25% of the area with focused flow. Thus, the probability that a particular drip shield or container gets dripped on is 0.135 x 0.95 x 0.05 x 0.25 = 0.0016.

Relative Importance of the "Engineered" versus "Natural" Barriers

Figures 10-17 through 10-45 evaluate the relative importance of the engineered and natural barriers. These figures directly address the concern expressed by some that the "engineered" barriers are relied on too heavily and that the "natural" barriers do not contribute significantly to safety. The "barrier neutralization" technique is used in these figures. When we refer to "barrier neutralization", we make the assumption that the *function* that particular barrier provides (e.g., radionuclide isolation, lower radionuclide release rate, dilution) has been neutralized. We do not assume the physical barrier itself is eliminated. A few examples of barrier neutralization are:

---

[6] Thus, the dose rates for this branch are approximately 1/0.13 = 7.8 times higher than for the probability-weighted mean dose rate shown in Figure 10-1.

- Drip shield: we assume groundwater dripping into the drift directly above a "neutralized" drip shield drips directly onto the waste container below. We assumed the waste container failure rate remained unaffected by this;
- Waste container: we assume any groundwater dripping above the "neutralized" container is free to contact the cladding surrounding the waste form, or the waste form directly when the cladding has failed. We assumed the cladding failure rate remained unaffected. We do not assume that the used fuel assemblies are lying in a pile on top of the invert;
- Cladding: we assume any groundwater dripping onto a "neutralized" cladding will contact the waste form directly. We assume the alteration rate of the waste form (the UO_2 pellets) is unaffected. We do not assume the pellets are lying in a pile at the bottom of the container;
- Saturated zone: we assume, in some cases that none of the radionuclides are retarded due to radionuclide sorption onto the surfaces of the rock or alluvium in the saturated zone. In this case, the radionuclides will travel at the same rate as the average groundwater velocity in the flowing zone within the saturated zone. Alternatively, we "neutralize" the entire saturated zone (or part of the zone) by assuming any radionuclides entering the saturated zone from the unsaturated zone instantly appear either five or 18 kilometers downstream. We do not assume the saturated zone is physically removed from the Yucca Mountain system, however.

Figure 10-17 shows the effect of neutralizing just the drip shields on the single branch case. This effectively assumes that the drip shields have all failed at emplacement and that any groundwater dripping into the drifts will drip directly on the waste containers underneath the drip shields. This figure suggests that failure of the drip shields only will make little difference to the dose rate – assuming all the other barriers perform as anticipated. This demonstrates that container performance is not thought to be very dependent on whether active dripping occurs directly onto the container surface.

Figure 10-18 shows the case in which all the waste packages are assumed to be "neutralized". This figure shows that neutralizing the performance of the waste packages causes the peak dose rate to increase about a factor of ten. The time of peak dose is also moved forward by about 500,000 years. However, even with the containers completely removed, the peak dose rate for this maximum likelihood "wet" branch is still less than 10 mrem/year[7], and does not occur until about 100,000 years – well after the time period during which the regulatory limits apply.

---

[7] Converted to the probability-weighted mean annual dose, the peak dose rate would be approximately one millirem per year, or roughly 100 times lower than natural background levels.

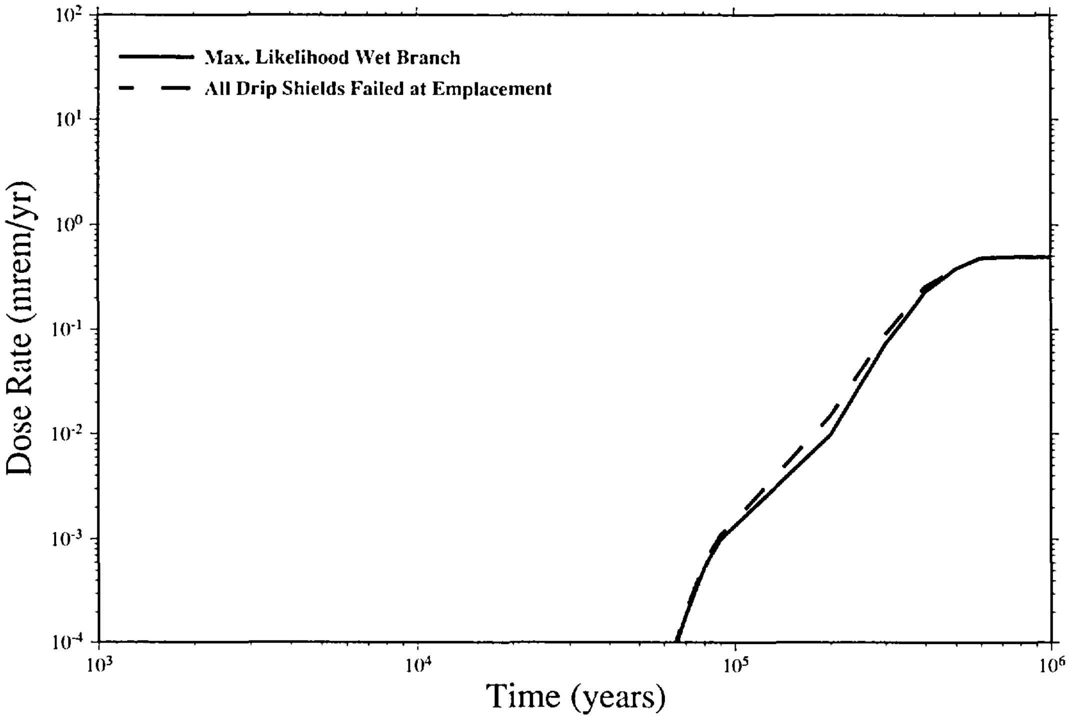

Figure 10-17
Annual Dose from the Maximum Likelihood "Wet" Branch Assuming the Drip Shield Barrier is Neutralized

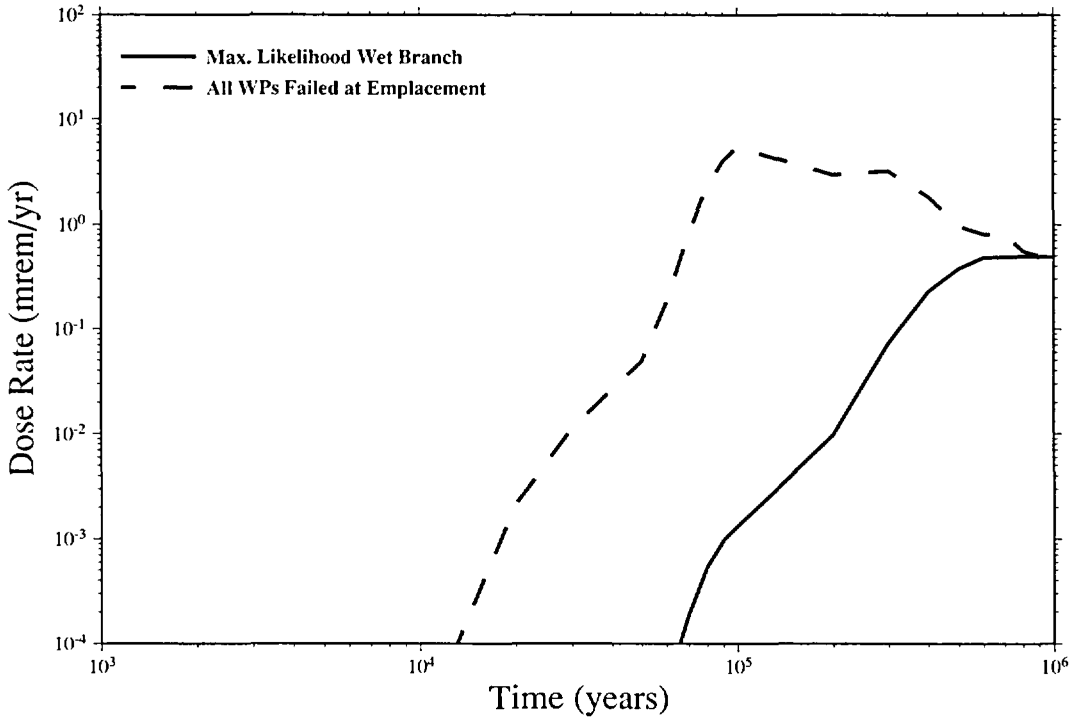

Figure 10-18
Annual Dose from the Maximum Likelihood "Wet" Branch Assuming the Waste Package Barrier is Neutralized

Figure 10-19 shows the case for which all the cladding performance is assumed to be neutralized. As for the drip shield, it appears in this case that, as long as all the other barriers perform as anticipated, then the loss of the cladding barrier function does not significantly affect overall performance.

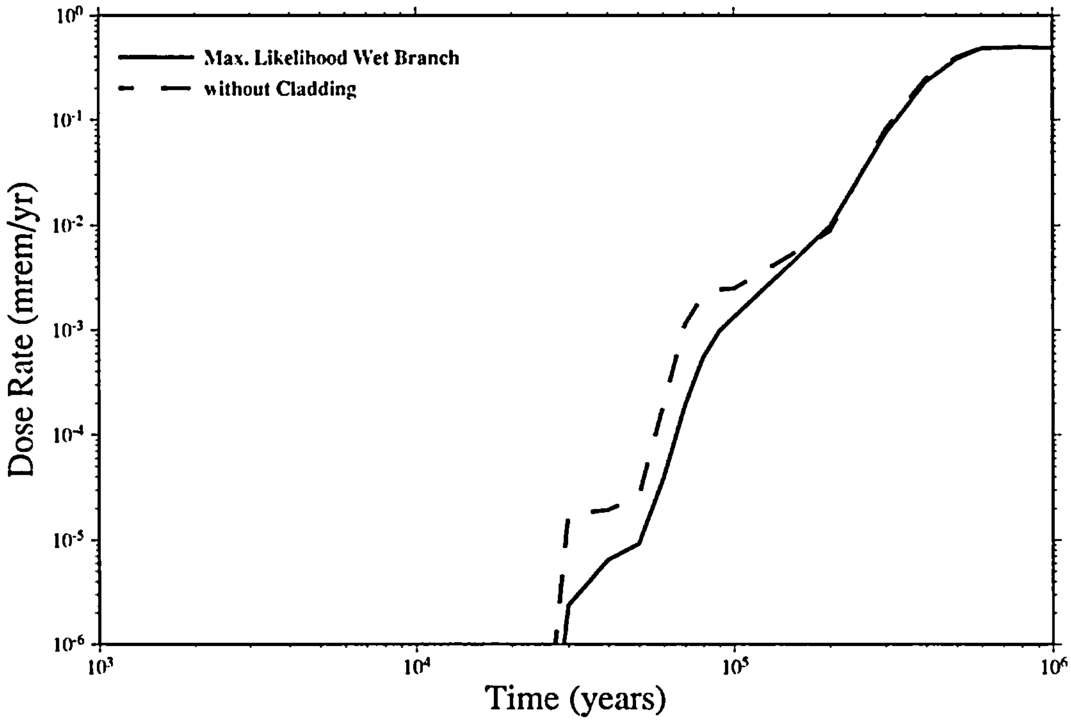

Figure 10-19
Annual Dose from the Maximum Likelihood "Wet" Branch Assuming the Cladding Barrier is Neutralized

Figure 10-20 shows the case for which both the drip shield and the container functions have been neutralized. In this case, the peak dose rate also increases by about a factor of ten, with the time of the initial plume arrival moved forward to about 10,000 years. It is interesting to note that even with both the drip shield and the waste containers neutralized, the peak dose is almost the same as in Figure 10-18 in which only the waste container is neutralized. The main difference between figures 10-20 and 10-18 is the earlier arrival of the radionuclide plume at 18 km when both engineered barriers are failed. This implies that the drip shield is not a greatly effective "backup" barrier to the containers if the cladding is still functioning as anticipated.

Figure 10-21 shows the case where all three of the major engineered barriers (drip shield, container, cladding) have had their functions neutralized. The peak dose rate increases by a factor of about 10^2 and the time of the first peak arrival is reduced to just under 10,000 years when compared to the case where all three barrier functions are behaving as anticipated. The two peaks are caused by the separation of the radionuclides that are and are not retarded in the unsaturated and saturated zones. Those that are not retarded (e.g., ^{99}Tc and ^{129}I) are represented in the first peak. Those that are retarded (e.g., the ^{237}Np chain and the uranium isotopes) comprise the second peak.

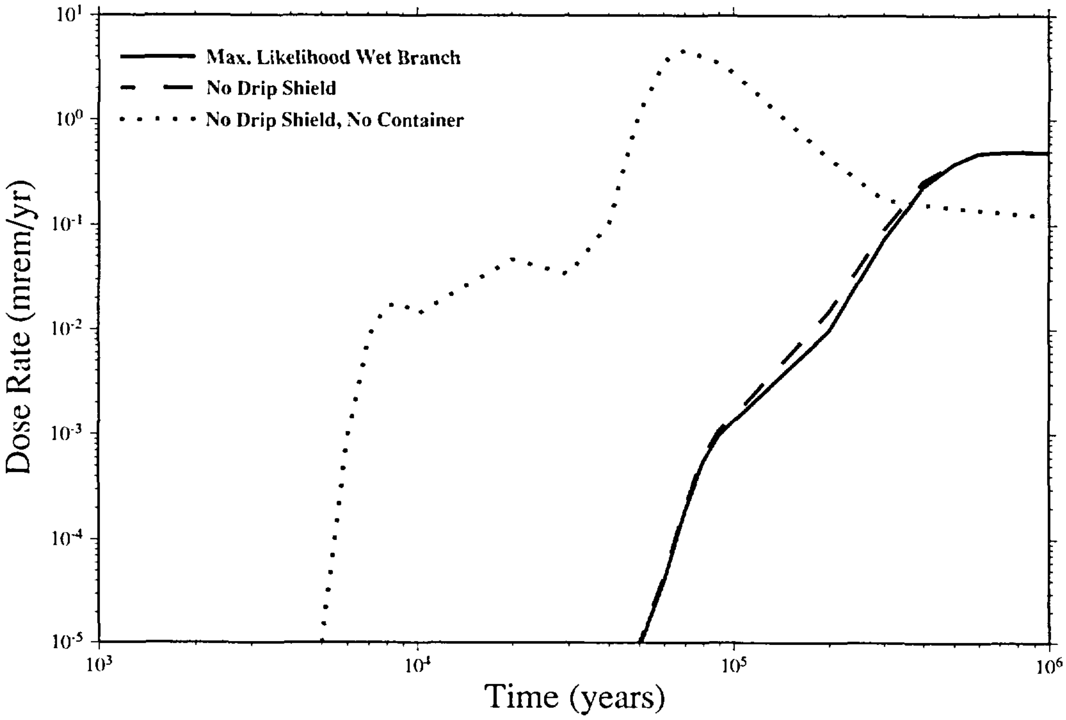

Figure 10-20
Annual Dose from the Maximum Likelihood "Wet" Branch Assuming the Drip Shield and the Waste Container are Both Neutralized

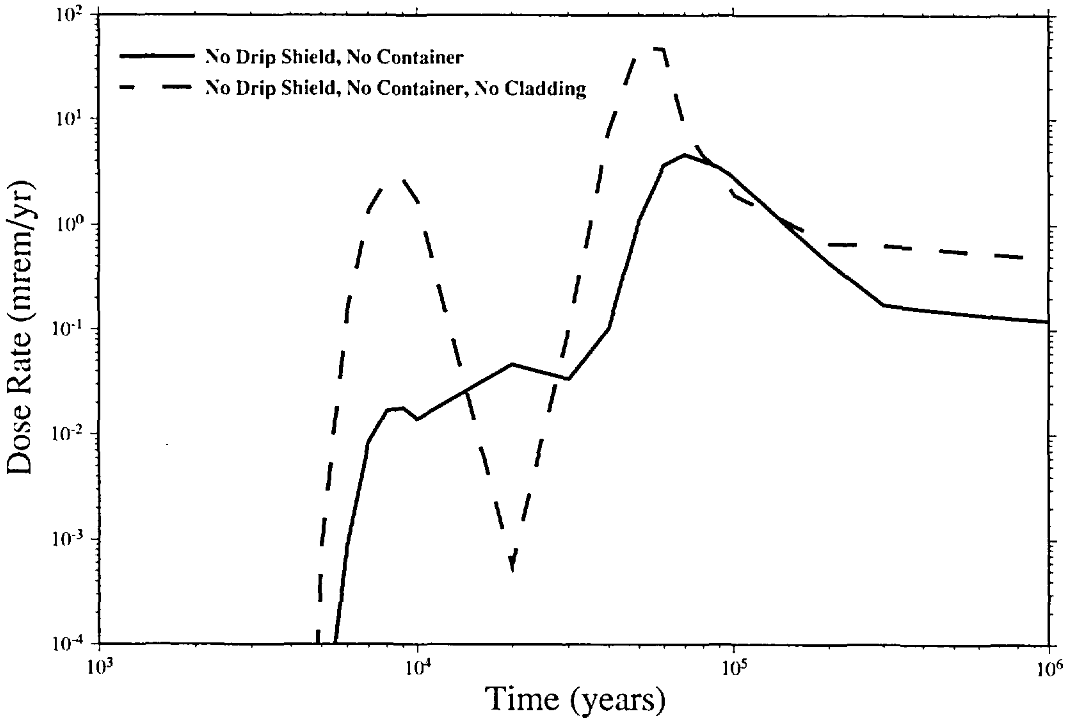

Figure 10-21
Annual Dose from the Maximum Likelihood "Wet" Branch Assuming the Drip Shield, the Waste Container, and Cladding Barriers are All Neutralized

Comparing the two curves in Figure 10-21, it can be seen that the barrier effect of the cladding is more pronounced when the other two major engineered barriers have been neutralized. This suggests that the cladding barrier is acting as another "backup" barrier in case the drip shield and waste container barriers do not function as anticipated.[8]

What is even more remarkable about Figure 10-21 is that the peak dose rate for the maximum likelihood 'wet' branch even with all three barriers removed is still under 100 mrem/yr. Thus, the natural barriers alone are able to reduce the peak dose rate to less than that of natural background.[9] If one corrects for the probability of the 'wet' branch, the probability-weighted mean annual dose rate would have a peak that is still less than the individual dose limit of 15 mrem/yr, and would still occur well after 10,000 years. This strongly supports the idea that the natural barriers contribute very significantly to safety.

10.2.2 'Hazard Index' Analyses to Identify Multiple Barriers

The purpose of the "Hazard Index" analyses provided in this section is to provide rough, quantitative estimates of the importance of the major Features, Events, and Processes (FEPs) in reducing the potential hazard due to the full inventory of disposed spent fuel and HLW at the candidate Yucca Mountain facility. The approach used is to artificially "turn off" the function of all FEPs initially, then add successive FEPs (in as logical an order as possible) one at a time to gauge their contribution to the total Hazard Index reduction. The FEPs will also be identified as being either due to "engineered" or "natural" features, or both.

10.2.2.1 Starting Point Assumptions for the IMARC Hazard Index Calculations

In order to "turn off" the function of *all* of the FEPs involved with deep geologic disposal of HLW, the following, admittedly unrealistic starting assumptions are used:

- The repository contains 70,000 MTU spent fuel at some reasonable average burnup and a decay time of 2,000 years.[10] The same inventory data used in the IMARC runs presented in earlier sections were used for the Hazard Index calculations, plus some additional inventory data, for the additional radionuclides we added, to illustrate the hazard reduction due to decay of some shorter-lived radionuclides;
- The entire inventory of radionuclides (from all 70,000 MTU) is assumed to be dissolved in 0.6 m^3 of "drinking water". This assumes infinite solubility, and the entire inventory is concentrated in one small location;

---

[8] The effect of the drip shield as a "backup" barrier for the cladding and container could also be shown.

[9] The only "engineered" barriers that are still included in this figure are the waste form (the UO_2 pellets) themselves, and the drifts. However, the drifts can be considered to be partially a "natural" barrier since it is the combination of the natural rock properties and the engineered drift that act to reduce the amount of groundwater that can freely drip from the drift ceiling.

[10] IMARC starts with a decay time of 1,000 years, but requires its first single, 1,000-year time step to calculate the initial peak values.

- The 0.6 m^3 (containing the entire 70,000 MTU inventory of dissolved radionuclides) is drunk by a single, adult individual over the course of one year at the beginning of its adult life (age 20);
- It is acceptable to use the drinking water pathway concentration-to-dose conversion factors found in Chapter 8- even for artificially high radionuclide concentrations.

Based upon the above assumptions, the starting Hazard Index for all radionuclides, HI_{tot}, in the 70,000 MTU inventory is nearly 10^{17} mrem (Figure 10-29). Thus, the peak HI_{tot} will need to be reduced roughly 16 orders of magnitude to be in the range of the dose limits in the final NRC regulations. Since the "base case" dose rate-versus-time curve for the current IMARC analysis, Figure 10-1, does show that peak individual dose rates at 20 km have been lowered to ~10^{-1} mrem/yr, it would be appropriate to be able to suggest what FEPs contribute to this dose reduction by 18 orders of magnitude.

The above starting point assumptions can be attacked for being extremely non physical. However, the intent is to neglect *all* barriers initially, such as solubility, dissolution rate constraints, and the fact that it is impossible for all of the water to pass through the system and then flow into a small enough volume to be drunk by a single individual in a single year. Solubility and dissolution rate constraints are two of the many potential barriers to assign benefit to. Furthermore, the fact that engineering design can dictate how concentrated or spread out the waste is should also have a place in the calculations about how concentrated the water flow paths can get. To start with some more "real" set of assumptions would begin to neglect some of the FEPs that are in play. Since one of the purposes of these Hazard Index calculations is to show there are many barriers that contribute to hazard reduction, it is undesirable to exclude any initially. The introduction of Hazard Reduction Factors later on will allow the reader to start at a more "realistic" point, if desired.

A starting time of 1,000 years was used to avoid difficulties with including shorter-lived radionuclides that would contribute greatly to the initial Hazard Index, such as Cs-137 and Sr-90. Because IMARC's smallest time step used is 1,000 years, this means that the initial calculation is actually made for 2,000 years.

10.2.2.2 Release Scenario

Because these represent scoping calculations, and because it is necessary to strictly control the FEPs that are introduced into the calculations, a single "scenario" was investigated having the same properties as the "Maximum Likelihood Wet Branch" used above. When the groundwater flux distribution through the distributed repository was included, a constant 19.6 mm/yr infiltration (moderate infiltration value for the full glacial maximum climate) was assumed in these calculations.

10.2.2.3 General Description

Results are presented in terms of "Hazard Index" versus time for a series of individual radionuclides, and a HI_{tot} for the total of 22 of the radionuclides contributing the most to long-term HI.

Figures 10-22 through 10-29 show the Hazard Index versus time for the starting case and for 13 sets of FEPs successively added that act to change the Hazard Index. Figures 10-22 through 10-28 are for individual radionuclides. Figure 10-29 is for the total Hazard Index summed over the 22 radionuclides contributing the most to the individual dose rate. The 14 curves shown on these figures are as follows:

- "Hazard Index" (starting case – all barrier functions "turned off"): All radionuclides from 70,000 MTU of spent fuel are assumed dissolved in 0.6 m^3 of water in year 1,000, which is then drunk in a single year at year 2,000.[11] An "alteration time", the time required to dissolve the fuel, was set to one year to allow the IMARC code to calculate the dissolved inventory without becoming unstable. Since the fuel is dissolved in the first time step it does not affect the results. The figure is artificial in the sense that the dose is calculated at 2,000 years only. Since all the radionuclides are assumed to be consumed in year 2,000 the curves go back to zero at the next time step (3,000 years). Thus, only the dose rates at the peak have meaning.
- "1.25% of Repository Wet": This figure differs from the previous figure by a factor of 0.0125. This accounts for the suite of individual FEPs that cause only a portion of the containers to come into contact with groundwater. The remaining 98.75% of the containers were assumed to remain dry due to the following assumptions:
  - For the smaller local percolation rates, the fact that the drifts are air-filled and curved causes the vast majority of the percolating water (for the lower local percolation rates only) to be diverted around the drifts;
  - Groundwater flow through the repository horizon is heterogeneous. So, on average, only 1.25% of the repository area has local percolation rates high enough to allow water to drip into the drifts and onto containers. Both of these processes were discussed in Section 9.

  The FEPs contributing to the assumption that only 1.25% of the waste will ever be dissolved are mostly due to natural features of the repository (flow heterogeneity due to the presence of fractured, porous rock). However, the engineered feature of the drift being placed in the unsaturated zone with a drift radius small enough to divert low percolation rates around, rather than through, the drift also is an important FEP. These natural and engineered FEPs act in concert, so cannot be separated further.

  For these FEPs, the "Hazard Reduction Factor" is 80 for all radionuclides. That is, these FEPs act to reduce the HI by a factor of 80.
- "3,000 yr Alteration Time": This is representative of the barrier provided by the waste form itself. For this barrier addition it is assumed that the waste form dissolves uniformly over 3,000 years, and all radionuclides are released congruently. Because the dissolution rate has been increased by over three orders of magnitude from the previous cases, and because individuals are assumed to drink 0.6 m^3 of water every year, peak concentrations have been reduced by a factor of 3000.

---

[11] This neglects the roughly 100 years of decay time before final closure of the repository.

Again, alteration time is a function of both natural and engineered features acting in concert. That is, the dissolution rate is a function of "engineered" features, such as the waste form properties (e.g., the UO_2 matrix), and the degree to which the rest of the waste package and any other engineered materials in the engineered barrier system affect the chemistry or flow rate of the ingressing groundwater. The alteration time must also be considered a function of the "natural" features of groundwater chemistry and flow rate.

- "Moderate Solubility": For these curves, solubility limits are added to those causing only 1.25% of the repository to be wet and a 3,000-year waste form alteration time. This 'barrier' can be considered due to the "natural" system in the sense that natural groundwater chemistry is assumed to control the solubility limits. An exception to this may be if an "engineered" feature, such as the presence of reducing or chelating agents, affected the local solubility limits. In the IMARC base case, three sets of solubility limits were considered. For the Hazard Indices presented here, the "moderate" solubility values were used.
- "Cladding Fails over Time": This represents adding in the cladding barrier. It is assumed cladding begins to fail during the first time step. Mean cladding lifetime is several tens of thousands of years. This is considered an engineered barrier.
- "Containers Fail over Time": This represents adding in the container barrier. As discussed in Section 9, containers are assumed to fail over many thousands of years. One container is assumed to be failed at emplacement. This is an engineered barrier.
- "Drip Shields Fail over Time": This represents adding in the drip shield barrier. One drip shield is assumed failed at emplacement; the rest fail over many thousands of years. This is an engineered barrier.
- "WPs Dispersed Throughout the Repository": In all the curves preceding this one, all of the flow was assumed to be limited to 0.6 m^3 per year. Furthermore, this flow was assumed to pass through ALL of the containers that were exposed to groundwater, then focused back into a small enough volume that it could be consumed by a single individual in one year.

  In this curve, this assumption is removed. That is, it is assumed the waste packages are evenly dispersed throughout the "wet" zone in the repository such that the flow is no longer limited to 0.6 m^3 per year, nor refocused back into a small volume. Based on assumptions of a reasonable percolation rate over the base case repository area, actual annual flow volumes are roughly 10^4 times larger than 0.6 m^3 per year. This reduces ALL individual HI values uniformly by roughly 10^4. The peak HI_{tot} is now reduced to approximately 10^4.

  This effective dilution factor of 10^4 is mostly due to an "engineering" decision to spread out the HLW over a large area (compared to the flow area associated with just 0.6 m^3/yr flow rate). While this is not a *physical* 'barrier' per se, it does cause a major reduction in the hazard index, so is an important barrier.
- "EBS Sorption": These curves show that adding sorption on container corrosion products (iron oxyhydroxides) and backfill (crushed tuff) reduces the peak HI's for those radionuclides that sorb. This can also be considered mostly an "engineered" FEP.
- "AE [Accessible Environment] at 5 km": In all the previous curves, the HI's at the repository exit were considered. In this figure, the travel time through the UZ and the first five kilometers of the SZ are considered. Sorption in the UZ and SZ are still neglected. This

causes the peak HI_w to be reduced by another factor of over 10^2 due to additional dispersion in the SZ. This FEP can be considered mostly "natural".

- "UZ/SZ Moderate Retardation": These curves introduce "moderate" sorption values to the tuff. This can be considered a "natural" FEP.
- "AE in front of Alluvium": These curves add in the effect of another 11 km of travel time in the SZ through volcanic tuff. The additional hazard reduction is about a half an order of magnitude due to additional dilution (and decay for some radionuclides). This is a natural barrier.
- "AE at 18 km": The effect of moving the measurement point another 2 km downstream is to now include the 2 km of alluvium in the SZ. While the additional amount of dispersion on hazard reduction between 16 and 18 km is nearly negligible, the effect is more dramatic for those radionuclides that strongly sorb onto alluvium. This is a "natural" FEP.
- "Dose from All Pathways": These curves *add* in all the non-drinking water pathways to the total dose estimate (see Chapter 8 for a detailed treatment of these other biosphere pathways). When this is done, the HI's *increase* rather than decrease. HI's for Tc-99, I-129, and the Np-237 chain increase by roughly a factor of $10^{1\text{ to }2}$. This suggests that the drinking water pathway is a minor contributor to the total HI.

The effective positions at which the HI calculations are made change as more barriers are added:

1. Inside the container: "Hazard Index"; "1.25% of Repository Wet"; "3,000 yr Alteration Time"; "Moderate Solubility"
2. Immediately outside the containers: "Cladding Fails over Time"; "Containers Fail over Time"; "Drip Shields Fail over Time"
3. Just below the repository in the UZ: " "WPs Dispersed Throughout the Repository"; "EBS Sorption"
4. 5 km downstream in the SZ: "AE at 5 km"; "UZ/SZ Moderate Retardation"
5. 16 km downstream in the SZ: "AE in front of Alluvium"
6. 18 km downstream in the SZ: "AE at 18 km"; "Dose from All Pathways"

10.2.2.4 Presentation of Individual Hazard Index Estimates

The following three subsections will step through three different ways of presenting the hazard index estimates. The purpose of repeating the analysis three different ways is to better explore how the presence of some barriers affects how much other barriers contribute to hazard reduction. The first set of presentations adds the barriers in a roughly "inside out" order. That is, barriers nearest the waste itself are added first, followed by additional barriers successively farther away from the waste. The second set of hazard index figures add the barriers in a "natural barriers first" order. The third set of hazard index figures add them in an "engineered barriers first" order. It will be seen that the order in which individual barriers are added affects the relative importance of each barrier.

10.2.2.4.1 Barriers Added from the "Inside Out"

^{129}I (Figure 10-22)

Figure 10-22 presents the HI curves for ^{129}I. The initial HI for ^{129}I starts at about 10^{12}, and is reduced by a factor of 80 for "1.25% of Repository Wet", and another factor of 3,000 when "3,000 yr Alteration Time" is added. These HI reductions apply to all radionuclides as discussed earlier.

The "Moderate Solubility" curve for ^{129}I lies directly on top of the "3,000 yr Alteration Time" curve because iodine has a relatively high 'moderate' solubility. Thus, iodine is alteration rate-limited.

Adding the cladding barrier lowers the HI by approximately two orders of magnitude, and also spreads out the HI in time.

Restoring the container barrier function has the major effect of delaying the onset of radionuclide release to beyond 10^4 years. The HI peak position is now pushed back to 600,000 years and the HI is reduced about another order of magnitude at this time. The rapid rise at 20,000 years in the HI curve for the container barrier added is a numerical artifact based on the IMARC model that doesn't allow any radionuclides to release from the EBS until the container failure fraction exceeds 0.001.

Adding the drip shield hardly changes the HI from that with the container function restored. This demonstrates that the average lifetime of the container is significantly longer than that of the drip shield.

Adding the effect of dilution in the UZ by dispersing the waste packages throughout the repository "wet" zone has a dramatic effect in lowering the Hazard Index by more than four orders of magnitude. This is because it is now assumed radionuclides exiting the EBS are mixed with all the groundwater passing through 25% of the repository cross section.

There is a no sorption of iodine on container corrosion products, so adding the EBS sorption barrier does not change the HI for ^{129}I.

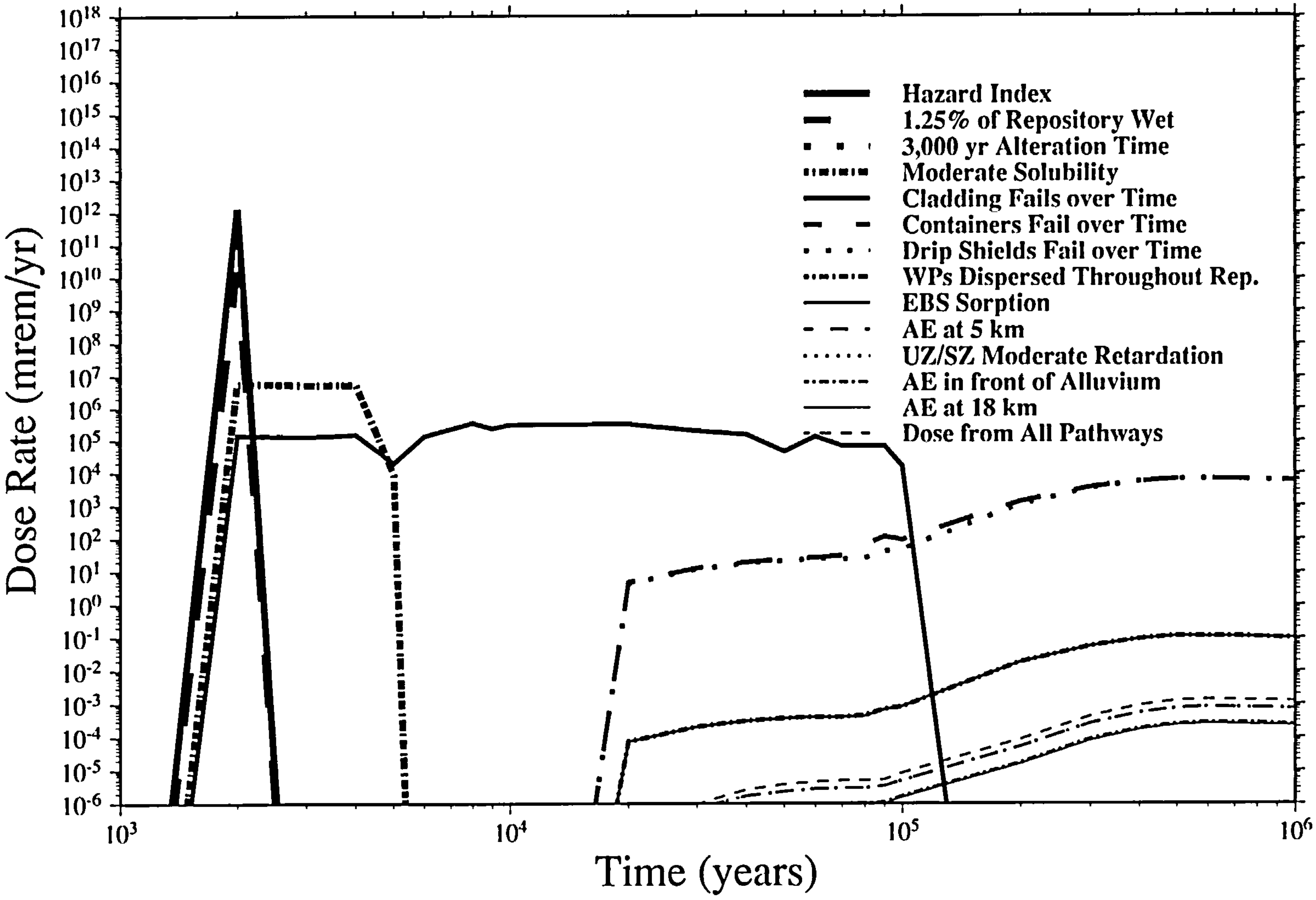

Figure 10-22
Hazard Index Curves for ^{129}I. Barrier Functions Added "Inside Out"

Restoring the effects of transport delay and dilution in the UZ and the first five kilometers in the SZ ("AE at 5 km") lowers the HI by almost another three orders of magnitude and delays the arrival of the ^{129}I plume. The HI reduction is due almost entirely to dilution in the SZ.

Including the barrier of sorption on the UZ and SZ ("UZ/SZ Moderate Retardation") makes no difference since iodine is not thought to sorb on either UZ or SZ minerals.

Extending the SZ to 16 km ("AE in front of Alluvium") further delays the ^{129}I plume by another 50,000 years and lowers the HI another factor of 5 or so. This is because there is not much additional dilution between 5 km and 16 km.

For ^{129}I adding in the 2 km of alluvium ("AE at 18 km") has almost no additional effect since sorption of iodine on alluvium is zero.

The last set of FEPs considered, "Dose from All Pathways" raises the HI by about a factor of ten. This is because the agricultural pathways in the assumed biosphere provide more dose than simply the drinking water pathway used in all the previous FEPs.

Table 10-1 provides a summary of the Hazard Reduction factors (HR) for ^{129}I at both 10,000 years and at the time of peak HI (whenever the peak occurs). This table suggests that the total hazard reduction is approximately 15 orders of magnitude and that several 'natural' and 'engineered' barriers (dilution also considered a 'barrier' in this case) contribute to the hazard reduction. The range of Hazard Reduction factors shown for the "engineered" and "natural" FEPs toward the bottom of the table are determined by assuming the hazard reduction to those FEPs that are a combination of engineered and natural are either all engineered or all natural. The HI is increased by almost one order of magnitude when one considers all the other biosphere exposure pathways rather than just the drinking water pathway.

Table 10-1
Hazard Reduction Factors for ^{129}I with Barrier Functions Added "Inside Out"

10,000 Years	At Time of Peak	Time of Peak [yr]	FEPs	"Engineered" or "Natural"?
10^2	10^2	2000	1.25% of repository wet	both
10^3	10^3	3000	3,000 year alteration time	both
10^0	10^0	3000	Moderate solubility	natural
10^2	10^2	8000	Cladding fails over time	engineered
∞	10^1	600,000	Containers fail over time	engineered
	10^0	600,000	Drip shields fail over time	engineered
	10^5	600,000	WPs dispersed throughout repository	both
	10^0	600,000	EBS sorption	mostly engineered
	10^2	700,000	AE at 5 km	natural
	10^0	700,000	UZ/SZ moderate retardation	natural
	$10^{0.5}$	700,000	AE in front of alluvium	natural
	10^{-0}	700,000	AE at 20 km	natural
∞	*10^{-16}*		*Total Hazard Reduction*	
	10^{3-13}		*Hazard reduction due to "engineered" features*	
	10^{3-13}		*Hazard reduction due to "natural" features*	
10^{-1}	10^{-1}		Hazard "reduction" (i.e., increase) due to all pathways	

Figures 10-23 through 10-26 are the Hazard Index curves for each successive member of the decay chain: ^{241}Am→^{237}Np→^{233}U→^{229}Th.

^{241}Am (Figure 10-23)

The Hazard Index curves for ^{241}Am are shown in Figure 10-23. This radionuclide has a relatively short half-life, 432 years. The Hazard Index curves show that even just adding the 3,000-year alteration time is enough to show the effect of decay on the HI curve. With the addition of the cladding barrier, decay of ^{241}Am is complete.

^{237}Np (Figure 10-24)

Figure 10-24 shows the Hazard Index curves for ^{237}Np. A few aspects of the Hazard Index curve are of note for this moderately soluble, slightly sorbing species. Adding in "Moderate Solubility" for ^{237}Np does not lower the HI from the previous curve. Other than small delays in the time of arrival of the hazard caused by a small amount of sorption on UZ and SZ materials, the effects of adding successive barriers to the ^{237}Np Hazard Index is similar to that for ^{129}I. This suggests that neptunium is, like iodine, soluble enough to be alteration-rate limited, and shows little sorption effects. Table 10-2 shows the Hazard Reduction factors for ^{237}Np.

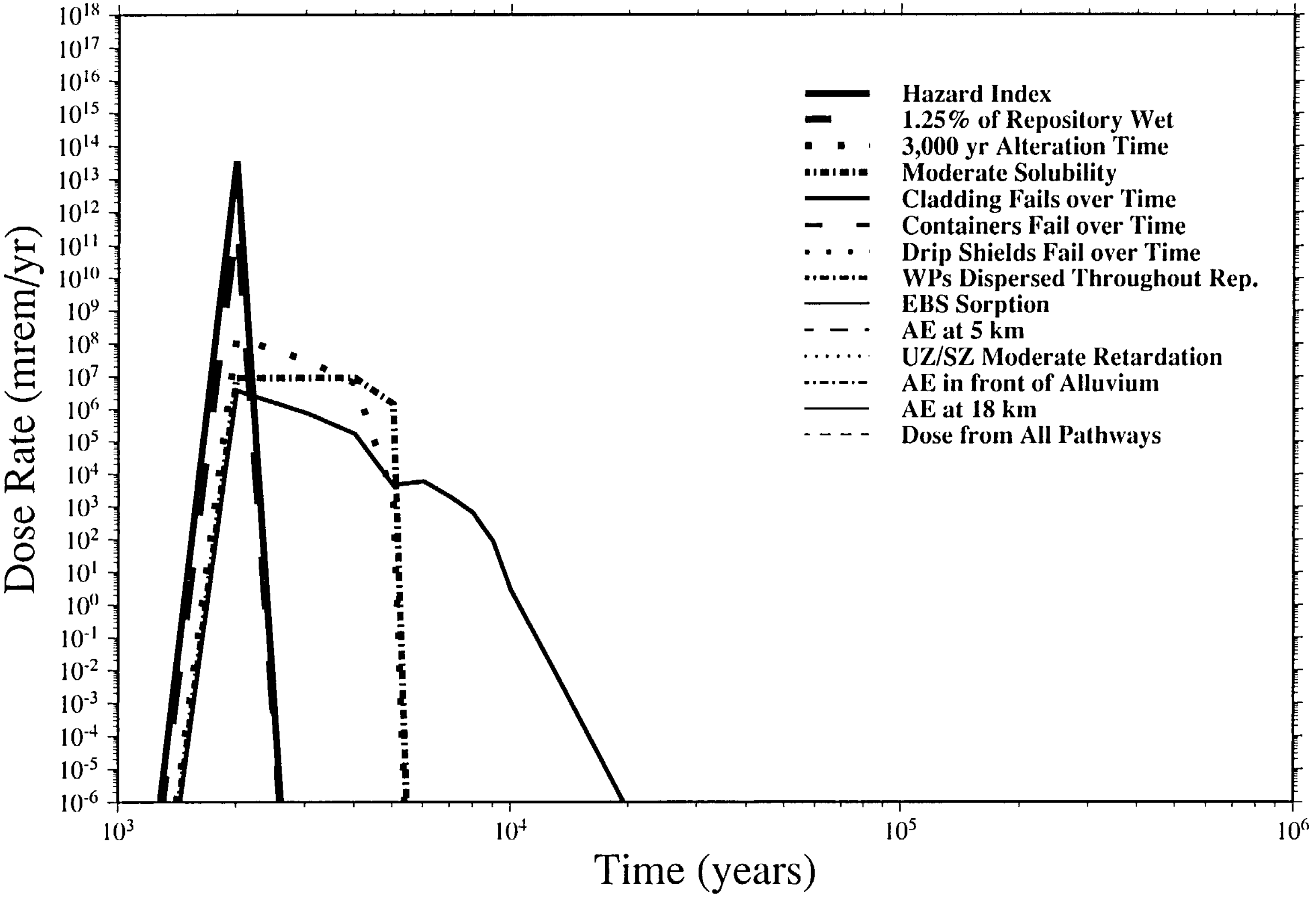

Figure 10-23
Hazard Index Curves for ^{241}Am. Barrier Functions Added "Inside Out".

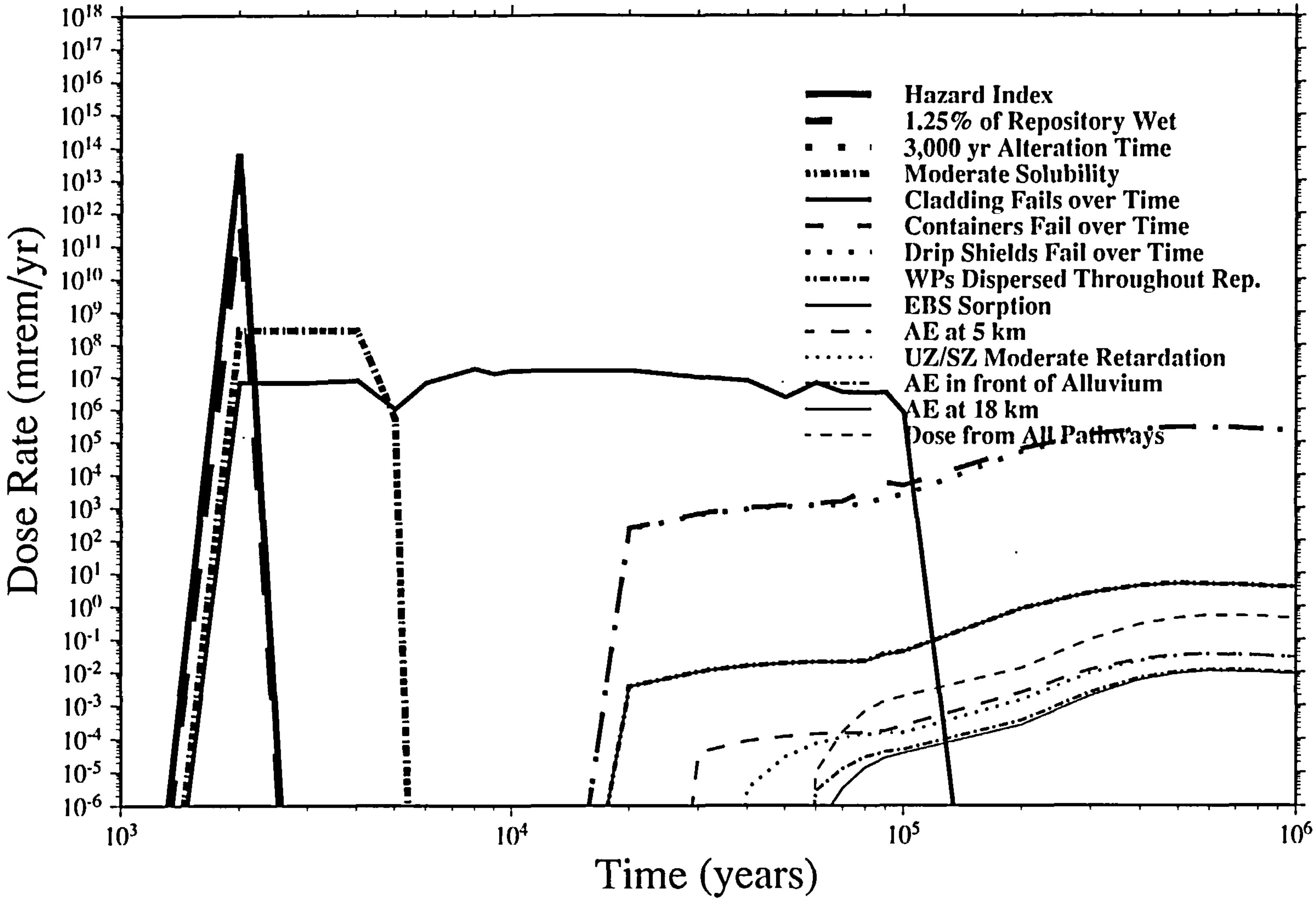

Figure 10-24
Hazard Index Curves for ^{237}Np. Barrier Functions Added "Inside Out".

Table 10-2
Hazard Reduction Factors for ^{237}Np with Barrier Functions Added "Inside Out"

Hazard Reduction	Time of Peak [yr]	FEPs	"Engineered" or "Natural"?
10^2	2000	1.25% of repository wet	both
10^3	3000	3,000 year alteration time	both
$10^{\sim 0}$	3000	Moderate solubility	natural
10^1	7000	Cladding fails over time	engineered
10^2	500,000	Containers fail over time	engineered
$10^{\sim 0}$	500,000	Drip shields fail over time	engineered
10^5	500,000	WPs dispersed throughout rep.	both
10^0	500,000	EBS sorption	mostly engineered
10^2	600,000	AE at 5 km	natural
$10^{\sim 0}$	600,000	UZ/SZ moderate retardation	natural
$10^{0.5}$	600,000	AE in front of alluvium	natural
$10^{\sim 0}$	600,000	AE at 18 km	natural
$10^{\sim 16}$		*Total Hazard Reduction*	
10^{3-13}		*Hazard reduction due to "engineered" features*	
10^{3-13}		*Hazard reduction due to "natural" features*	
$10^{-1.5}$		Hazard "reduction" (i.e., increase) due to all pathways	

^{233}U (Figure 10-25)

The Hazard Index curves for ^{233}U, a moderately soluble, moderately long lived radionuclide, show signs of ingrowth from its parent, ^{237}Np. These curves are shown in Figure 10-25. The Hazard Index curve for "Cladding Fails over Time" is actually higher than the previous curve, which shows that the additional holdup of the ^{237}Np parent inside the unfailed cladding actually increases the inventory of ^{233}U. This same effect is shown by the increase in the HI when "UZ/SZ Moderate Retardation" is restored. Table 10-3 shows the Hazard Reduction Table for ^{233}U.

^{229}Th (Figure 10-26)

Figure 10-26 presents the Hazard Index curves for ^{229}Th. This radionuclide is interesting because it has a fairly low solubility, is a fairly strong sorber, and has a half-life of only 7300 years. Yet its behavior in this figure is strongly influenced by the decay of its parents. The initial set of HI curves are similar to that of its parent, ^{233}U. However, adding in EBS sorption lowers the HI for ^{229}Th about a factor of ten.

Table 10-3
Hazard Reduction Factors for ^{233}U with Barriers Added "Inside Out"

Hazard Reduction	Time of Peak [yr]	FEPs	"Engineered" or "Natural"?
10^{2}	2000	1.25% of repository wet	both
10^{3}	3000	3,000 year alteration time	both
10^{1}	3,000	Moderate solubility	natural
10^{1}	9,000	Cladding fails over time	engineered
$10^{\sim 0}$	1,000,000	Containers fail over time	engineered
$10^{\sim 0}$	1,000,000	Drip shields fail over time	engineered
10^{5}	1,000,000	WPs dispersed throughout rep.	both
$10^{\sim 0}$	1,000,000	EBS sorption	mostly engineered
10^{2}	1,000,000	AE at 5 km	natural
$10^{\sim 0}$	1,000,000	UZ/SZ moderate retardation	natural
$10^{\sim 0.5}$	1,000,000	AE in front of alluvium	natural
$10^{\sim 0}$	1,000,000	AE at 18 km	natural
10^{16}		*Total Hazard Reduction*	
10^{1-11}		*Hazard reduction due to "engineered" features*	
10^{4-13}		*Hazard reduction due to "natural" features*	
10^{-2}		Hazard "reduction" (i.e., increase) due to all pathways	

^{238}U (Figure 10-27)

Figure 10-27 presents the Hazard Index curves for ^{238}U. This uranium isotope provides a significant contribution to the total dose rate, and is indicative of the behavior of a very long-lived, solubility-limited, sorbing radionuclide with a very large initial inventory. The fact that this radionuclide is long-lived, of low to moderate solubility, and has a large inventory is shown by the fact that introducing the "moderate solubility" limit causes the HI for this barrier to remain constant up to (and presumably well beyond) one million years. The fact that it sorbs somewhat on both the EBS corrosion products and on the rock in the UZ and SZ is shown by the curves where sorption from these two barriers is added in. The effect of sorption is to delay the arrival of the ^{238}U plume, but does not affect the dose peak since the half-life is so long. Table 10-4 shows the HI reduction table for ^{238}U.

^{239}Pu (Figure 10-28)

Figure 10-28 presents the Hazard Index curves for ^{239}Pu. This plutonium isotope provides the greatest contribution to the initial Hazard Index. It is also indicative of the behavior of a moderately long-lived, solubility-limited, highly sorbing radionuclide. The combination of its low solubility and strong sorption onto EBS corrosion products and natural rock and alluvium is shown by the fact that these two effects cause ^{239}Pu to decay to insignificant levels before it reaches 18 kilometers.

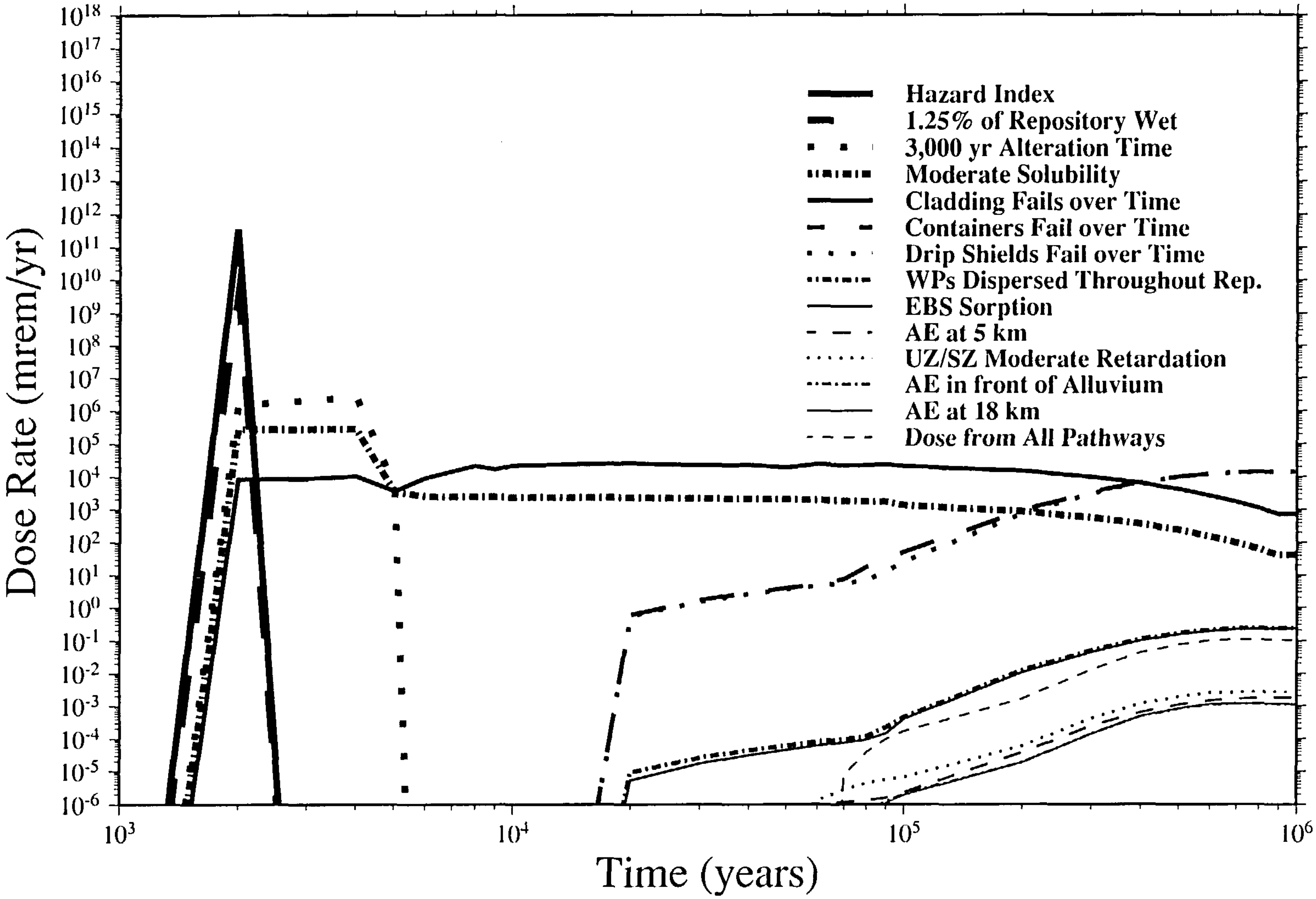

Figure 10-25
Hazard Index Curves for ^{233}U. Barrier Functions Added "Inside Out".

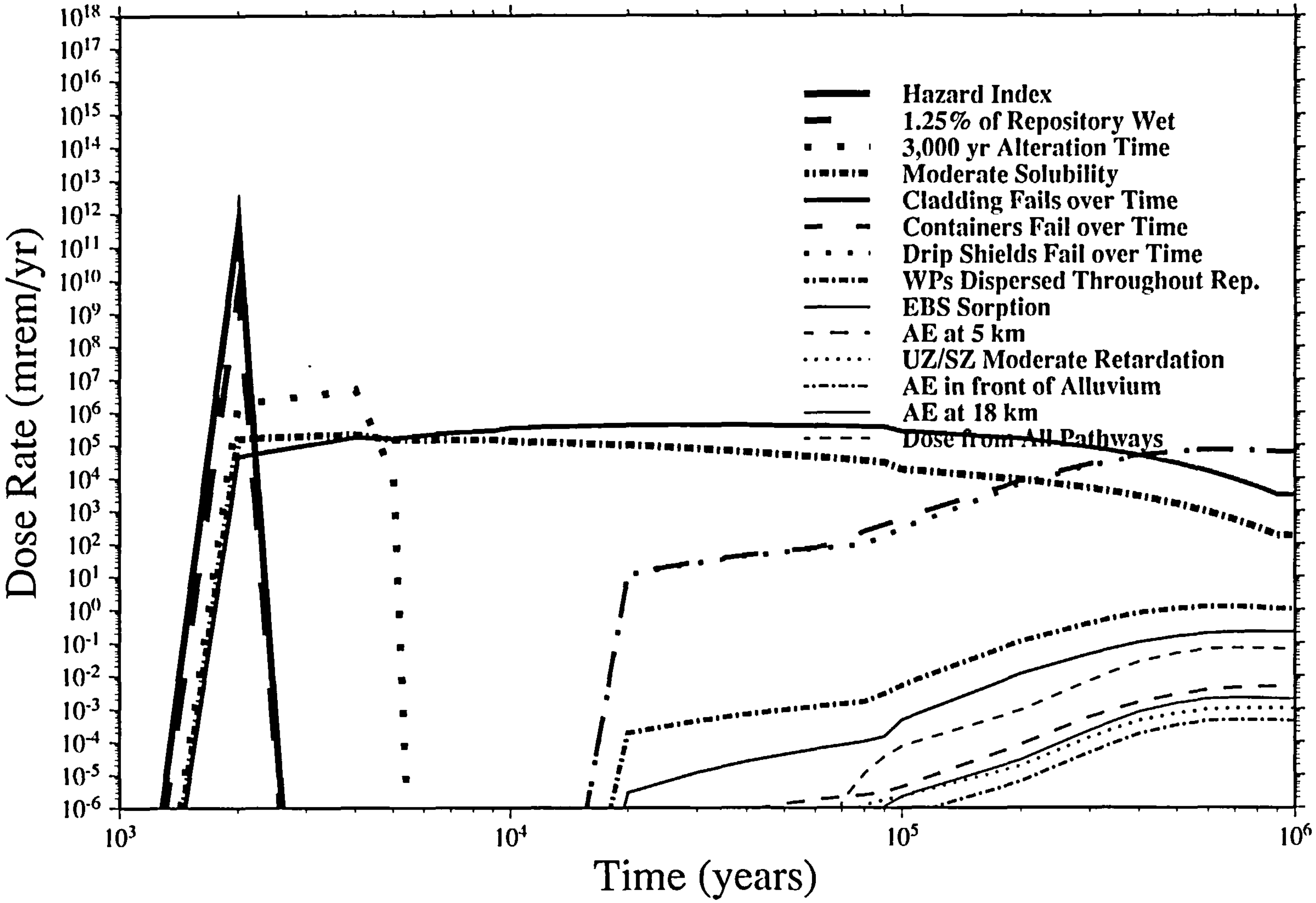

Figure 10-26
Hazard Index Curves for ^{229}Th. Barrier Functions Added "Inside Out".

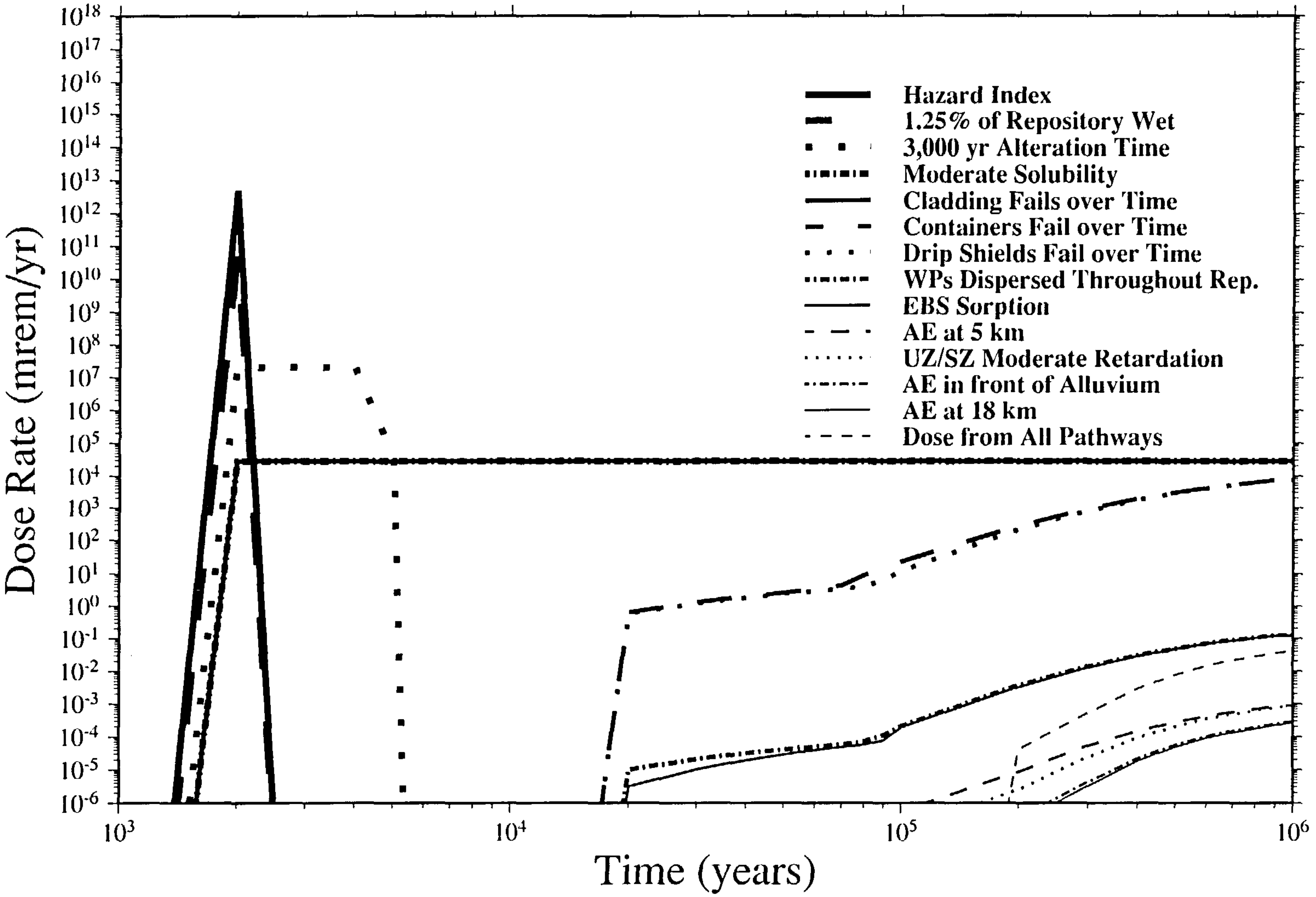

Figure 10-27
Hazard Index Curves for ^{238}U. Barrier Functions Added "Inside Out".

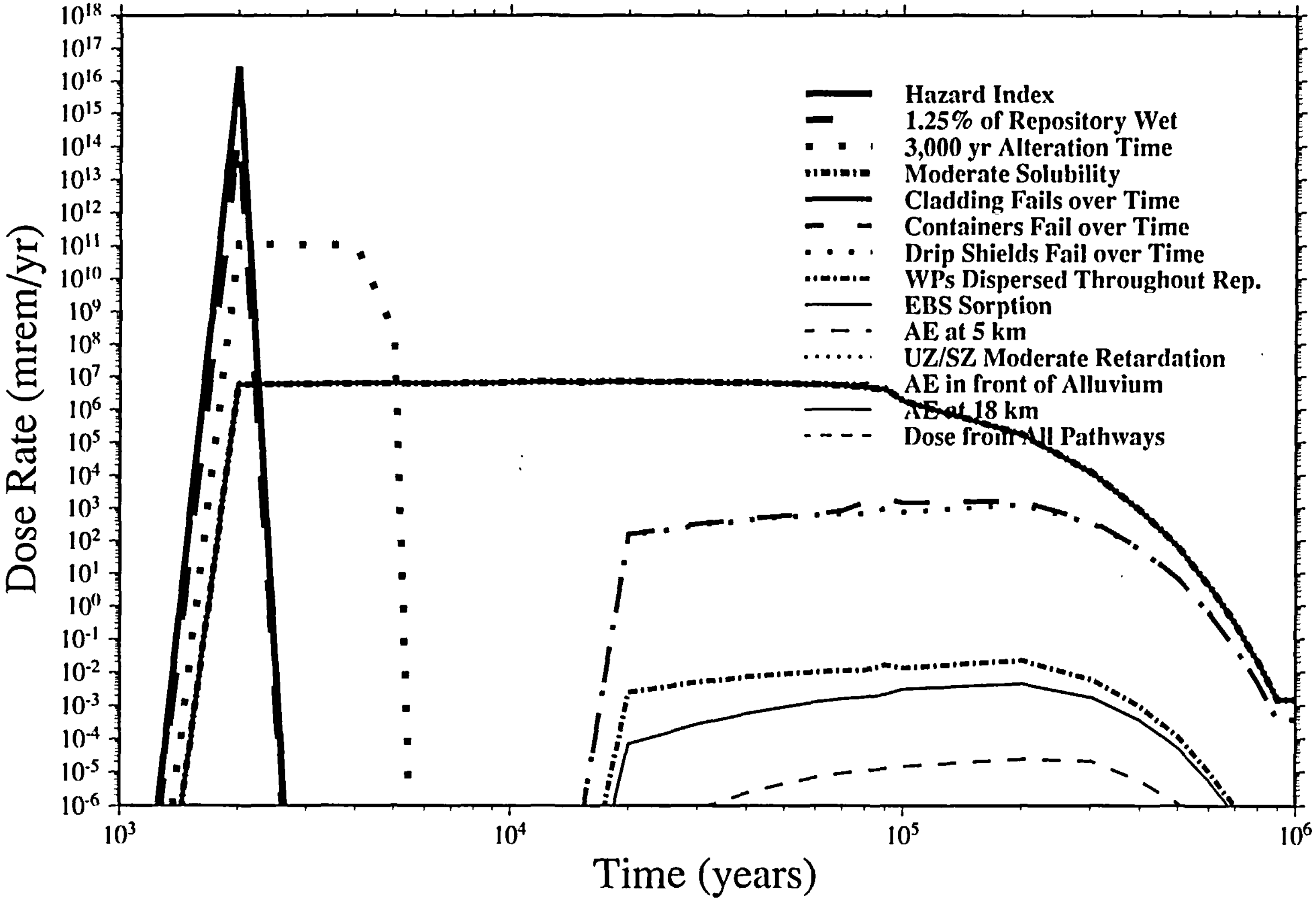

Figure 10-28
Hazard Index Curves for ^{239}Pu. Barrier Functions Added "Inside Out".

Table 10-4
Hazard Reduction Factors for ^{238}U with Barriers Added "Inside Out"

Hazard Reduction	Time of Peak [yr]	FEPs	"Engineered" or "Natural"?
10^{2}	2000	1.25% of repository wet	both
10^{3}	2000	3,000 year alteration time	both
10^{3}	2000	Moderate solubility	natural
$10^{\sim 0}$	2000	Cladding fails over time	engineered
$10^{0.5}$	1,000,000	Containers fail over time	engineered
$10^{\sim 0}$	1,000,000	Drip shields fail over time	engineered
10^{5}	1,000,000	WPs dispersed throughout rep.	both
$10^{\sim 0}$	1,000,000	EBS sorption	mostly engineered
10^{2}	1,000,000	AE at 5 km	natural
$10^{\sim 0}$	1,000,000	UZ/SZ moderate retardation	natural
$10^{\sim 0.5}$	1,000,000	AE in front of alluvium	natural
$10^{\sim 0}$	1,000,000	AE at 18 km	natural
10^{16}		*Total Hazard Reduction*	
10^{1-11}		*Hazard reduction due to "engineered" features*	
10^{5-15}		*Hazard reduction due to "natural" features*	
10^{-2}		Hazard "reduction" (i.e., increase) due to all pathways	

Total Hazard Index from All 22 Radionuclides with the Barriers Added "Inside Out"

Figure 10-29 presents the Hazard Index curves for all 22 radionuclides considered. The behavior of the suite of radionuclides is most affected by those radionuclides that contribute the greatest to total dose rate. Thus, the initial "Hazard Index" curve mostly reflects ^{239}Pu behavior. This is why introducing the "moderate solubility" barrier reduces the HI in this case (plutonium is solubility-limited). Additional effects of EBS sorption and UZ/SZ retardation can be seen since plutonium also sorbs significantly on these materials. The majority of the curves increase with time, which reflects a steady buildup of daughter products, as well as the steady increase in the number of containers that fail over time. Table 10-5 summarizes the reduction of the HI contributed by each barrier. This table shows that both "engineered" and "natural" barriers contribute strongly to overall Hazard Index reduction with the "natural" barriers contributing more than the "engineered" barriers.

Table 10-5
Hazard Reduction Factors for All 22 Radionuclides with Barriers Added "Inside Out"

Hazard Reduction	Time of Peak [yr]	FEPs	"Engineered" or "Natural"?
10^2	2000	1.25% of repository wet	both
10^3	2000	3,000 year alteration time	both
10^3	2000	Moderate solubility	natural
$10^{\sim 0}$	100,000	Cladding fails over time	engineered
10^1	1,000,000	Containers fail over time	engineered
$10^{\sim 0}$	1,000,000	Drip shields fail over time	engineered
10^5	1,000,000	WPs dispersed throughout rep.	both
10^1	1,000,000	EBS sorption	mostly engineered
$10^{2.5}$	1,000,000	AE at 5 km	natural
10^1	600,000	UZ/SZ moderate retardation	natural
$10^{0.5}$	600,000	AE in front of alluvium	natural
$10^{\sim 0}$	600,000	AE at 18 km	natural
10^{19}		*Total Hazard Reduction*	
$10^{2\text{-}12}$		*Hazard reduction due to "engineered" features*	
$10^{7\text{-}17}$		*Hazard reduction due to "natural" features*	
$10^{-1.5}$		Hazard "reduction" (i.e., increase) due to all pathways	

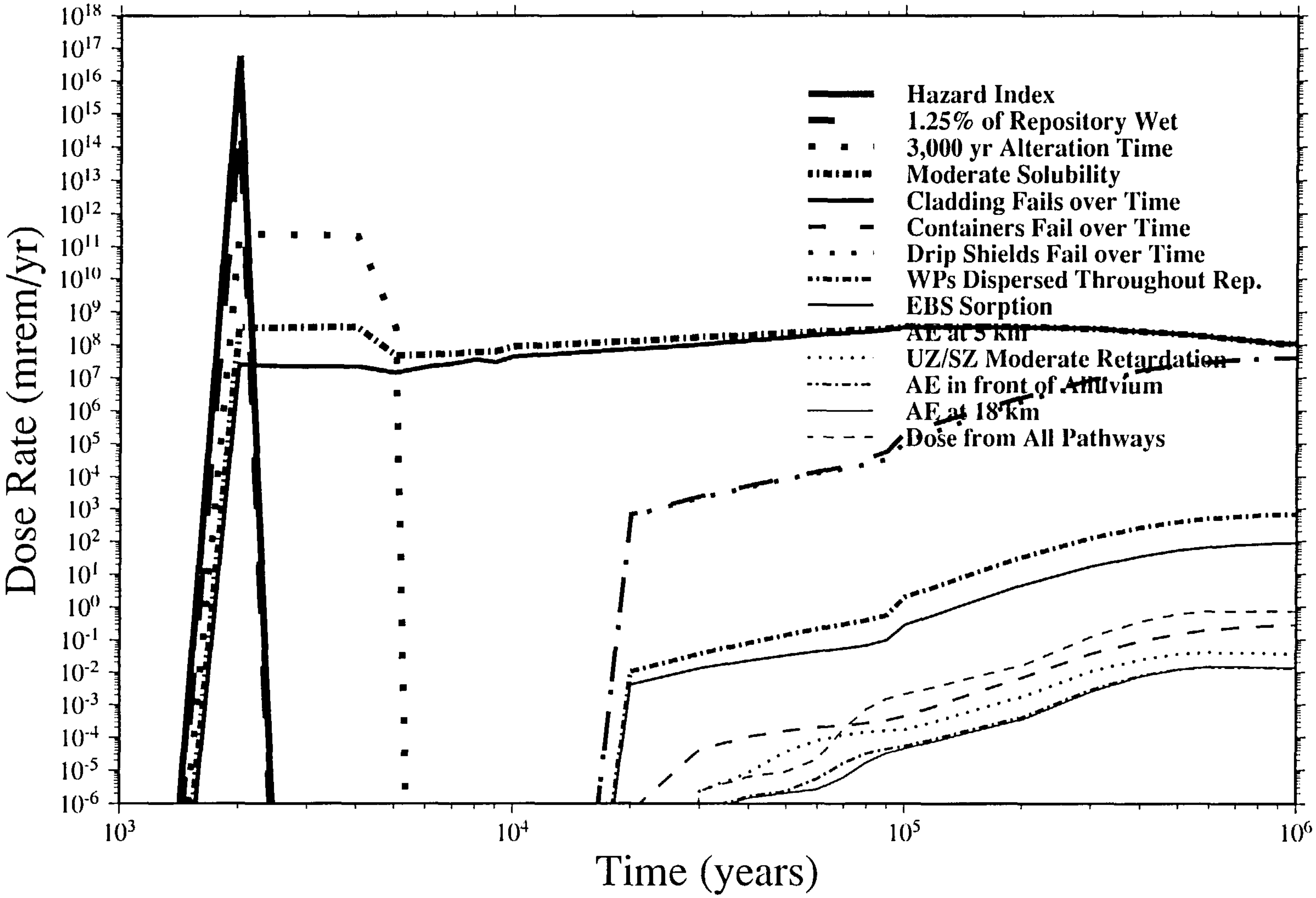

Figure 10-29
Hazard Index for all 22 Radionuclides Considered with the Barriers Added 'Inside Out"

10.2.2.4.2 "Natural" Barriers Added First

^{129}I (Figure 10-30)

Figure 10-30 presents the HI curves for ^{129}I with the "natural" barriers added first. The initial HI for ^{129}I starts at about 10^{12}, and is reduced by a factor of 80 for "1.25% of Repository Wet". With the natural barriers added first, the next to be added this time is "Moderate Solubility". The fact that this curve goes down between 2000 and 3000 years is a modeling artifact since the solubility for iodine is very high.

Adding the functions of the UZ and the first five kilometers of the SZ causes about six orders of magnitude reduction in the Hazard Index. This compares to only about a two order of magnitude reduction for this barrier when it was added later in the "inside out" case above. No reduction is found for adding sorption since iodine is not thought to sorb on any of the materials of interest.

Adding in the rest of the SZ in front of the alluvium causes the dose peak to be shifted back about 1000 to 2000 years, and lowers the Hazard Index by a factor of five. The only effect that can be seen by adding in the two kilometers of alluvium is another approximately 1000-year delay in the initial arrival of the plume.

As in all cases, dispersing the waste packages throughout the "wet" zone in the repository lowers the Hazard Index by about five orders of magnitude.

Introducing the 3,000 year alteration time for the waste form (instead of assuming instantaneous alteration) appears to have little effect when added after all the natural barriers. This compares to the three order of magnitude reduction adding this barrier caused when the barriers were introduced "inside out" above.

The reduced apparent effect of the remainder of the "engineered" barriers when they are introduced after all the "natural" barriers can now be seen clearly in the remaining curves in this figure. The cladding, introduced first, retains a significant effect: the HI is reduced about two orders of magnitude and the peak dose is pushed back in time well over 10,000 years. In this analysis the drip shield barrier function was added ahead of the container function to see what effect this would have. In this case, the drip shield barrier clearly has a significant effect on moving back, by another 40,000 years, the time of the peak dose. There is also a slight dose reduction (factor of about four). Adding in the container barrier function moves the dose peak back several hundred thousand years, almost about a factor ten reduction in the HI is realized.

The last set of FEPs considered, "Dose from All Pathways" raises the HI by about a factor of ten. This will be true no matter what order the other barriers are introduced.

Table 10-6 provides a summary of the Hazard Reduction factors (HR) for ^{129}I at both 10,000 years and at the time of peak HI (whenever the peak occurs). Comparing this table to Table 10-1, in which the barriers were added "inside out" for ^{129}I, shows some significant differences in the relative HI reduction for particular barriers.

Table 10-6
Hazard Reduction Factors for ^{129}I with "Natural" Barrier Functions Added First

10,000 Years	At Time of Peak	Time of Peak [yr]	FEPs	"Engineered" or "Natural"?
10^2	10^2	2000	1.25% of repository wet	Both
$10^{\sim 0}$	$10^{\sim 0}$	3000	Moderate solubility	Natural
10^5	10^5	5000	AE at 5 km	Natural
10^0	10^0	5000	UZ/SZ moderate retardation	Natural
10^1	10^1	6000	AE in front of alluvium	Natural
$10^{\sim 0}$	$10^{\sim 0}$	6000	AE at 18 km	Natural
10^5	10^5	6000	WPs dispersed throughout repository	Both
$10^{0.5}$	$10^{0.5}$	7000	3,000 year alteration time	Both
10^0	10^0	7000	EBS sorption	Mostly engineered
	10^1	20,000	Cladding fails over time	Engineered
	$10^{0.5}$	60,000	Drip shields fail over time	Engineered
	10^1	600,000	Containers fail over time	Engineered
∞	*10^{-16}*		*Total Hazard Reduction*	
	10^{2-9}		*Hazard reduction due to "engineered" features*	
	10^{6-14}		*Hazard reduction due to "natural" features*	
10^{-1}	10^{-1}		Hazard "reduction" (i.e., increase) due to all pathways	

Figures 10-31 through 10-34 are the Hazard Index curves for each successive member of the decay chain: ^{241}Am→^{237}Np→^{233}U→^{229}Th.

^{241}Am (Figure 10-31)

The Hazard Index curves for ^{241}Am with the "natural" barriers added first are shown in Figure 10-31. The Hazard Index curves show that just adding the unretarded travel time to five kilometers downstream in the SZ is enough to completely decay away the ^{241}Am.

^{237}Np (Figure 10-32)

Figure 10-32 shows the Hazard Index curves for ^{237}Np with the "natural" barriers added first. A few aspects of the Hazard Index curve are of note for this moderately soluble, slightly sorbing species. Adding in "Moderate Solubility" for Np early causes all the Np to be released from the EBS in just 3000 years. As opposed to the "outside in" application of successive barriers, for which no Hazard Index reduction was provided by solubility limits, adding in the "moderate solubility" early causes the HI to be reduced by about three orders of magnitude. Adding in the travel time to five kilometers downstream caused the HI to reduce by another two orders of magnitude and delays the peak dose 3000 years. Introducing retardation in the UZ and SZ further delays the dose peak another 15,000 years, and lowers the peak height another factor of ten. More delay in the peak is caused by adding in the rest of the SZ to 18 km. While each successive engineered barrier adds to the delay of the peak dose, very little additional dose reduction is realized (no more than about two orders of magnitude) after all the natural barriers have been added. Table 10-7 shows the Hazard Reduction factors for ^{237}Np when natural barriers are added first.

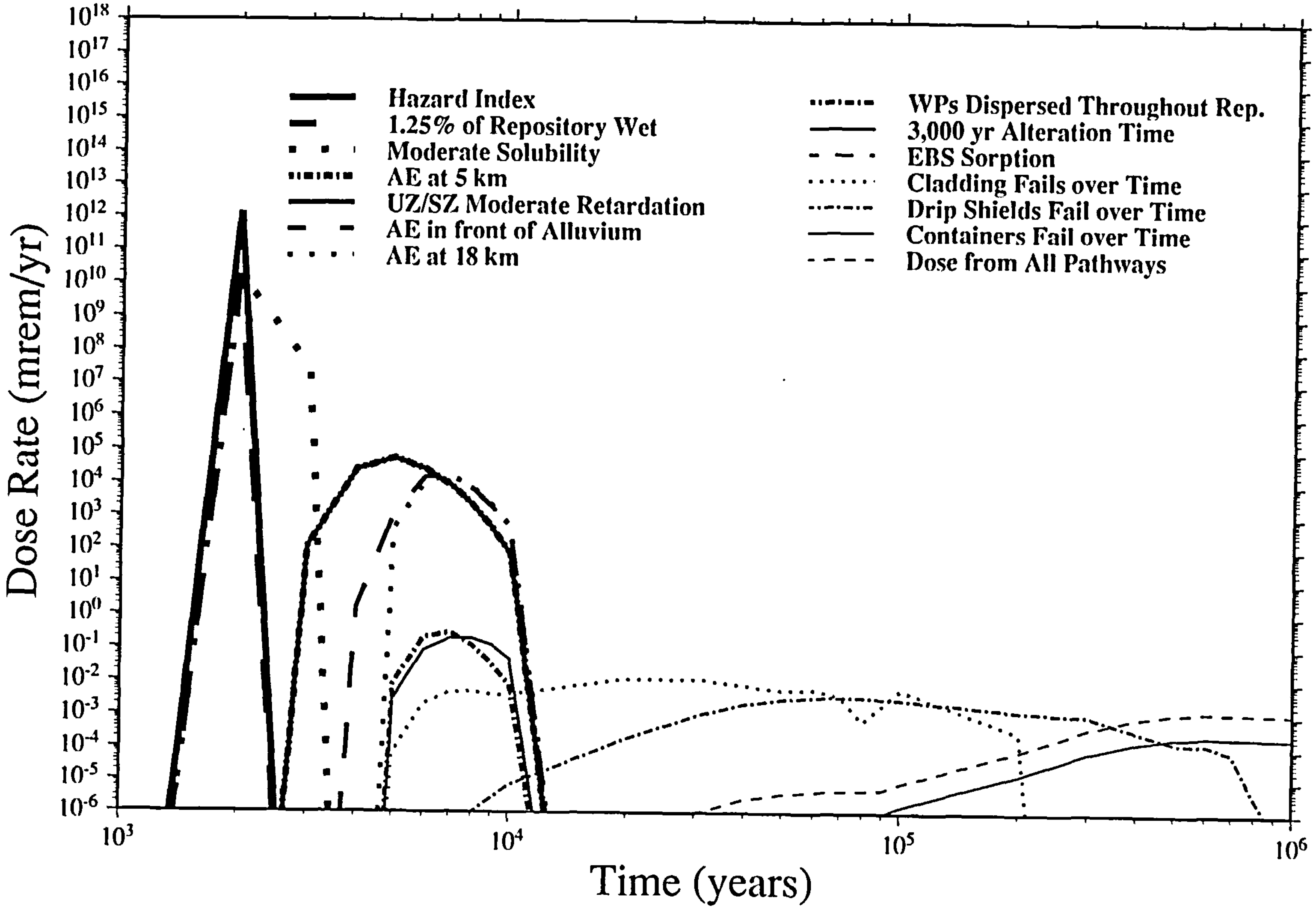

Figure 10-30
Hazard Index Curves for ^{129}I. "Natural" Barrier Functions Added First.

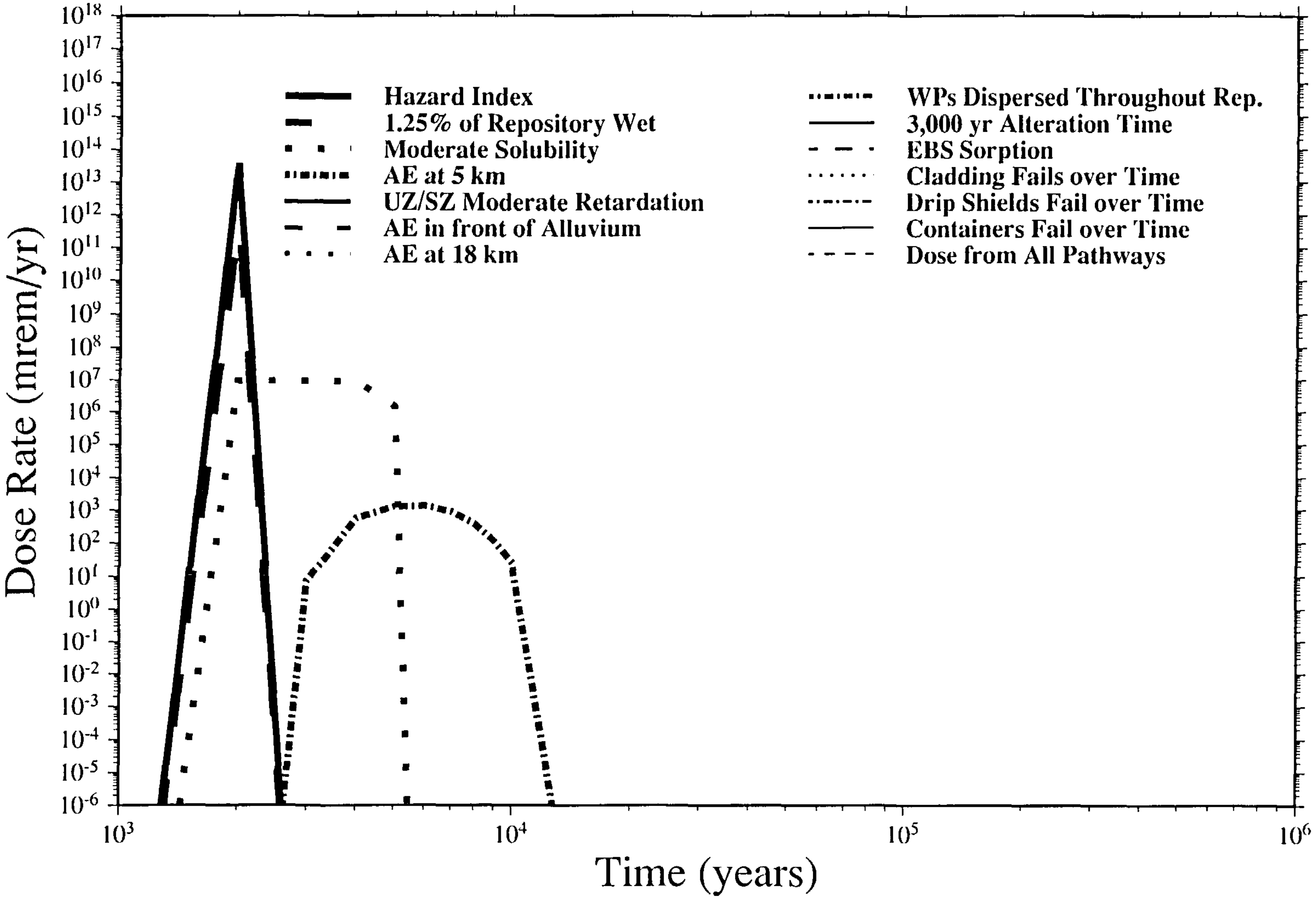

Figure 10-31
Hazard Index Curves for ^{241}Am. "Natural" Barrier Functions Added First.

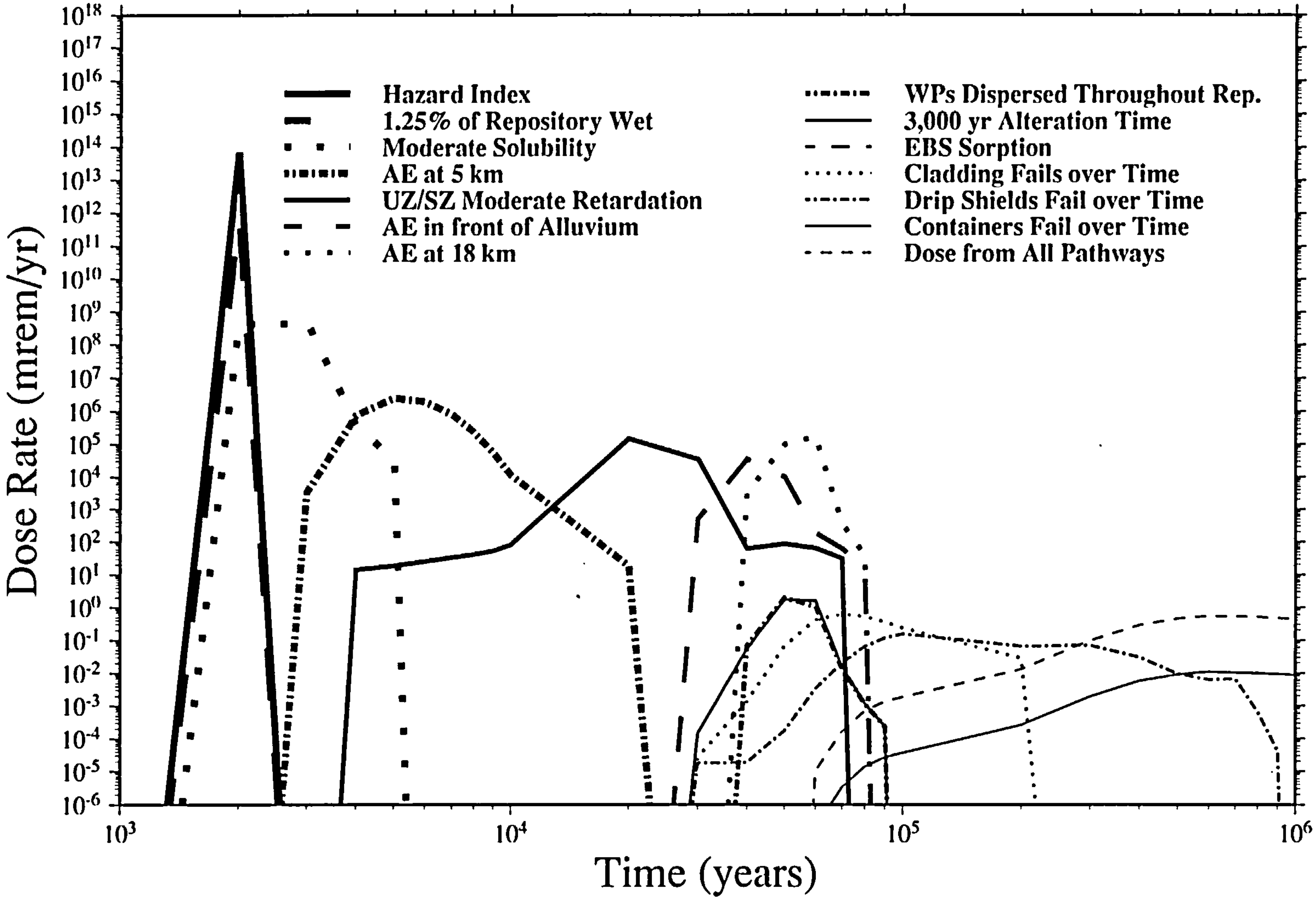

Figure 10-32
Hazard Index Curves for ^{237}Np. "Natural" Barrier Functions Added First.

Table 10-7
Hazard Reduction Factors for ^{237}Np with “Natural” Barrier Functions Added First

HR at Peak	Time of Peak [yr]	FEPs	“Engineered” or “Natural”?
10^{2}	2000	1.25% of repository wet	Both
$10^{3.5}$	2000	Moderate solubility	Natural
10^{2}	5000	AE at 5 km	Natural
10^{1}	20,000	UZ/SZ moderate retardation	Natural
10^{1}	40,000	AE in front of alluvium	Natural
$10^{\sim 0}$	60,000	AE at 18 km	Natural
10^{5}	60,000	WPs dispersed throughout repository	Both
$10^{\sim 0}$	50,000	3,000 year alteration time	Both
10^{0}	60,000	EBS sorption	Mostly engineered
$10^{0.5}$	70,000	Cladding fails over time	Engineered
10^{1}	100,000	Drip shields fail over time	Engineered
10^{1}	600,000	Containers fail over time	Engineered
$10^{\sim 16}$		*Total Hazard Reduction*	
$10^{3\text{-}10}$		*Hazard reduction due to “engineered” features*	
$10^{8\text{-}14}$		*Hazard reduction due to “natural” features*	
$10^{-1.5}$		Hazard “reduction” (i.e., increase) due to all pathways	

^{233}U (Figure 10-33)

The Hazard Index curves for ^{233}U when natural barriers are added first is shown in Figure 10-33. The fact that uranium sorbs well on the natural rock and alluvium is evident by the significant delay in the peak HI that is caused when successive parts of the SZ with sorption are added as barriers. The Hazard Reduction for ^{233}U attributed to each barrier is given in Table 10-8.

^{229}Th (Figure 10-34)

Figure 10-34 presents the Hazard Index curves for ^{229}Th with the “natural” barriers added first. As was the case for the lower solubility, sorbing ^{233}U, the delays in the peak arrival can be seen when the sorbing natural barriers are added and solubility limits are imposed.

^{238}U (Figure 10-35)

Figure 10-35 presents the Hazard Index curves for ^{238}U when “natural” barriers are added first. Adding solubility limits, dispersing the waste packages throughout the “wet” zone contribute the most to Hazard Index reduction. Retardation in the natural system, and adding the container barrier contribute the most to delay of the peak. Table 10-9 shows the HI reduction table for ^{238}U.

Table 10-8
Hazard Reduction Factors for ^{233}U with "Natural" Barriers Added First

HR at Peak	Time of Peak [yr]	FEPs	"Engineered" or "Natural"?
10^{2}	2000	1.25% of repository wet	Both
10^{4}	2000	Moderate solubility	Natural
$10^{1.5}$	5000	AE at 5 km	Natural
$10^{\sim 0}$	40,000	UZ/SZ moderate retardation	Natural
$10^{0.5}$	50,000	AE in front of alluvium	Natural
$10^{\sim 0}$	60,000	AE at 18 km	Natural
10^{5}	60,000	WPs dispersed throughout repository	Both
$10^{\sim 0}$	60,000	3,000 year alteration time	Both
10^{0}	60,000	EBS sorption	Mostly engineered
$10^{0.5}$	80,000	Cladding fails over time	Engineered
10^{1}	100,000	Drip shields fail over time	Engineered
10^{1}	900,000	Containers fail over time	Engineered
$10^{\sim 15}$		*Total Hazard Reduction*	
10^{3-10}		*Hazard reduction due to "engineered" features*	
10^{6-13}		*Hazard reduction due to "natural" features*	
10^{-2}		Hazard "reduction" (i.e., increase) due to all pathways	

Table 10-9
Hazard Reduction Factors for ^{238}U with "Natural" Barriers Added First

HR at Peak	Time of Peak [yr]	FEPs	"Engineered" or "Natural"?
10^{2}	2000	1.25% of repository wet	Both
10^{6}	2000	Moderate solubility	Natural
10^{2}	5000	AE at 5 km	Natural
$10^{\sim 0}$	60,000	UZ/SZ moderate retardation	Natural
$10^{0.5}$	100,000	AE in front of alluvium	Natural
$10^{\sim 0}$	100,000	AE at 18 km	Natural
10^{5}	100,000	WPs dispersed throughout repository	Both
$10^{\sim 0}$	100,000	3,000 year alteration time	Both
$10^{\sim 0}$	200,000	EBS sorption	Mostly engineered
$10^{\sim 0}$	200,000	Cladding fails over time	Engineered
$10^{\sim 0}$	400,000	Drip shields fail over time	Engineered
10^{1}	1,000,000	Containers fail over time	Engineered
$10^{\sim 17}$		*Total Hazard Reduction*	
10^{1-8}		*Hazard reduction due to "engineered" features*	
10^{9-16}		*Hazard reduction due to "natural" features*	
10^{-2}		Hazard "reduction" (i.e., increase) due to all pathways	

^{239}Pu (Figure 10-36)

Figure 10-36 presents the Hazard Index curves for ^{239}Pu for the “natural” barriers added first. This plutonium isotope provides the greatest contribution to the initial Hazard Index. It is also indicative of the behavior of a moderately long-lived, solubility-limited, highly sorbing radionuclide. The combination of its low solubility and the delay due to travel time in the first five kilometers of the UZ and SZ is shown by the fact that these two effects cause ^{239}Pu to decay to insignificant levels before it reaches even five kilometers when UZ/SZ retardation is applied.

Total Hazard Index from All 22 Radionuclides with the “Natural” Barriers Added First

Figure 10-37 presents the Hazard Index curves for all 22 radionuclides considered when the “natural” barriers are added first. The behavior of the suite of radionuclides is most affected by those radionuclides that contribute the greatest to total dose rate. Thus, the initial “Hazard Index” curve mostly reflects ^{239}Pu behavior. This is why introducing the “moderate solubility” barrier reduces the HI in this case (plutonium is solubility-limited). Table 10-10 summarizes the reduction of the HI contributed by each barrier.

Table 10-10
Hazard Reduction Factors for All 22 Radionuclides with “Natural” Barriers Added First

HR at Peak	Time of Peak [yr]	FEPs	“Engineered” or “Natural”?
10^2	2000	1.25% of repository wet	Both
10^6	3000	Moderate solubility	Natural
10^2	5000	AE at 5 km	Natural
10^{-1}	20,000	UZ/SZ moderate retardation	Natural
$10^{0.5}$	40,000	AE in front of alluvium	Natural
$10^{-0.5}$	60,000	AE at 18 km	Natural
10^5	50,000	WPs dispersed throughout repository	Both
10^{-0}	50,000	3,000 year alteration time	Both
$10^{\sim 0}$	50,000	EBS sorption	Mostly engineered
$10^{0.5}$	70,000	Cladding fails over time	Engineered
10^1	90,000	Drip shields fail over time	Engineered
10^1	700,000	Containers fail over time	Engineered
10^{-19}		*Total Hazard Reduction*	
10^{3-10}		*Hazard reduction due to “engineered” features*	
10^{9-16}		*Hazard reduction due to “natural” features*	
10^{-2}		Hazard “reduction” (i.e., increase) due to all pathways	

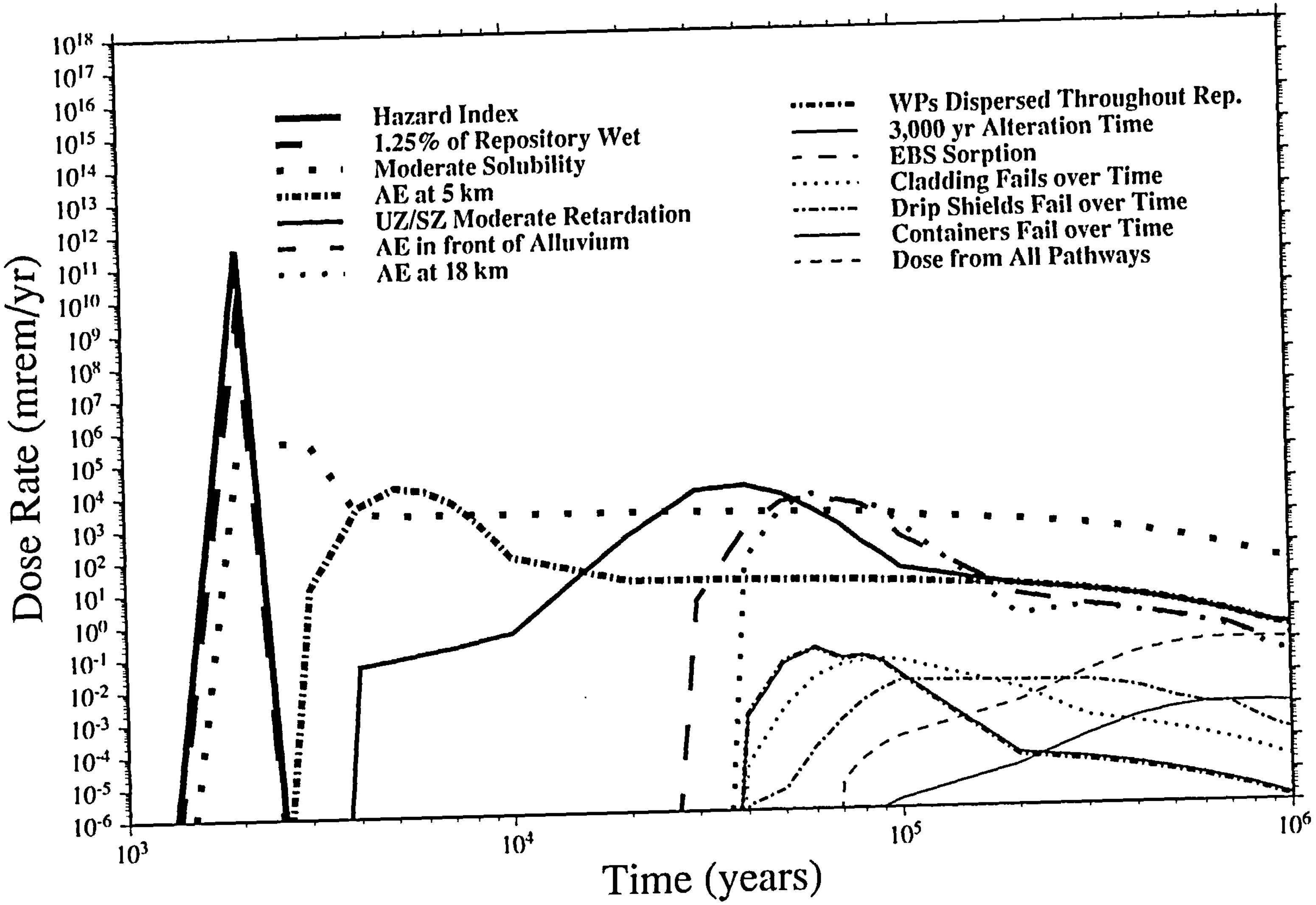

Figure 10-33
Hazard Index Curves for ^{233}U. "Natural" Barrier Functions Added First.

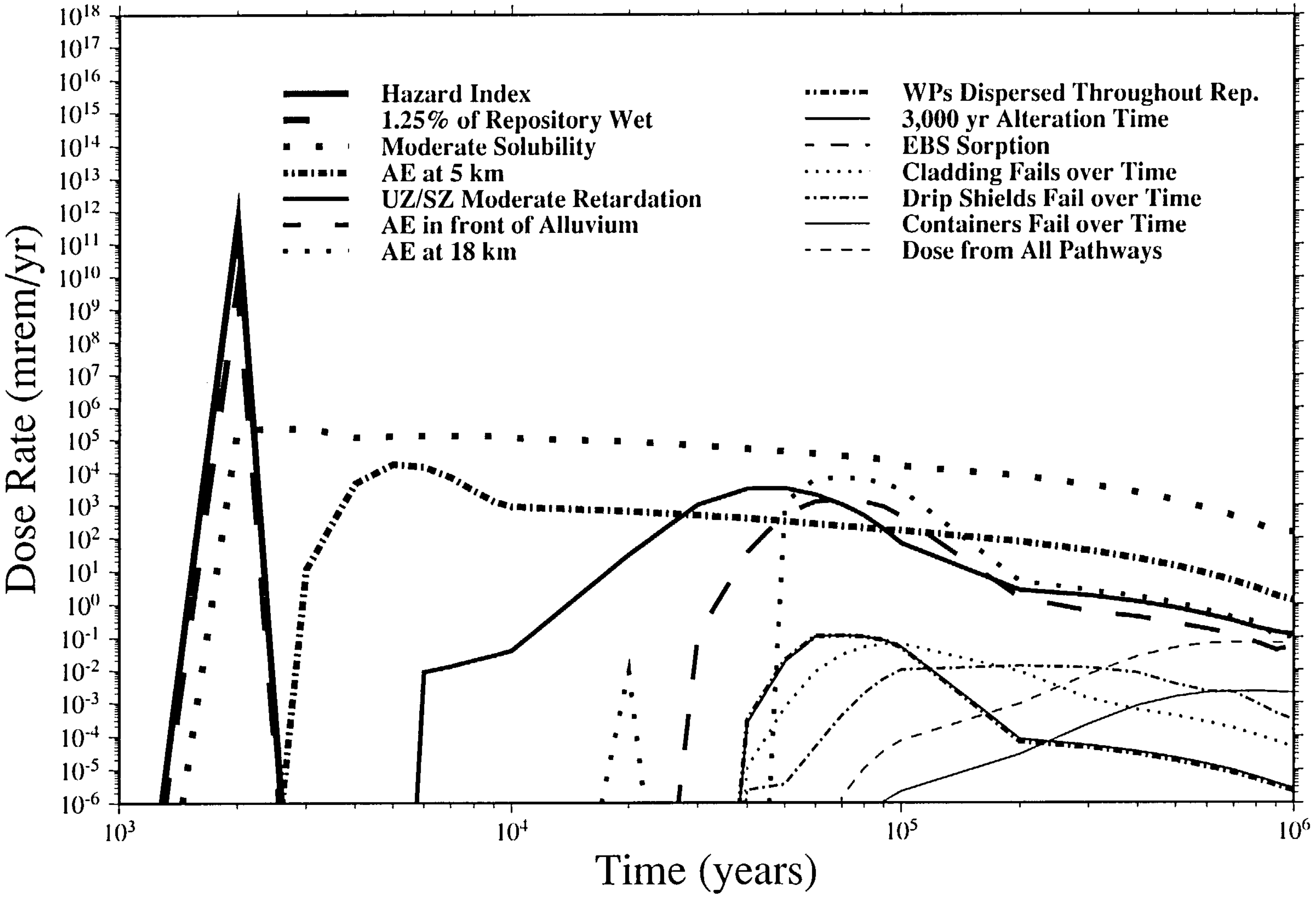

Figure 10-34
Hazard Index Curves for ^{229}Th. "Natural" Barrier Functions Added First.

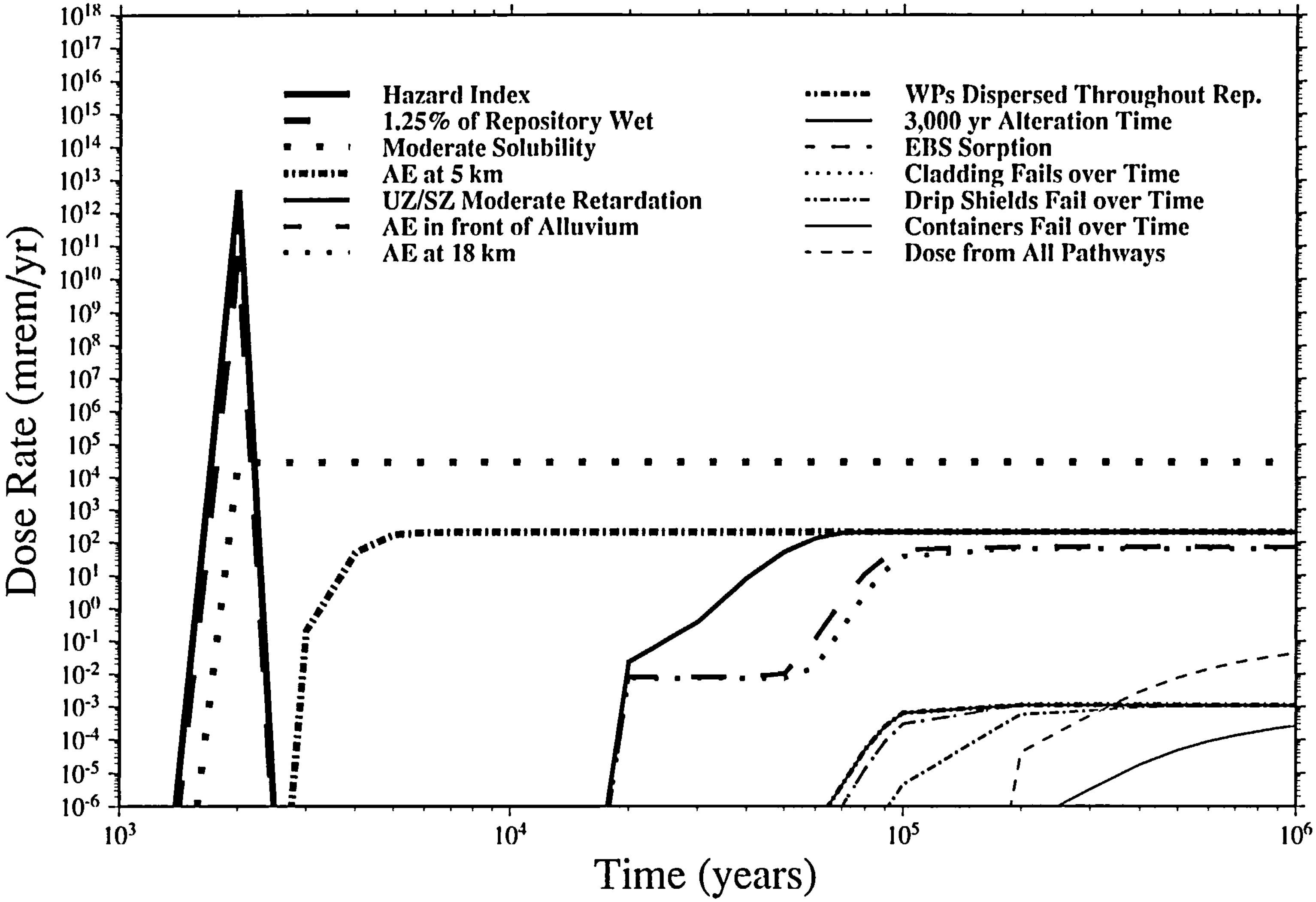

Figure 10-35
Hazard Index Curves for ^{238}U. "Natural" Barrier Functions Added First.

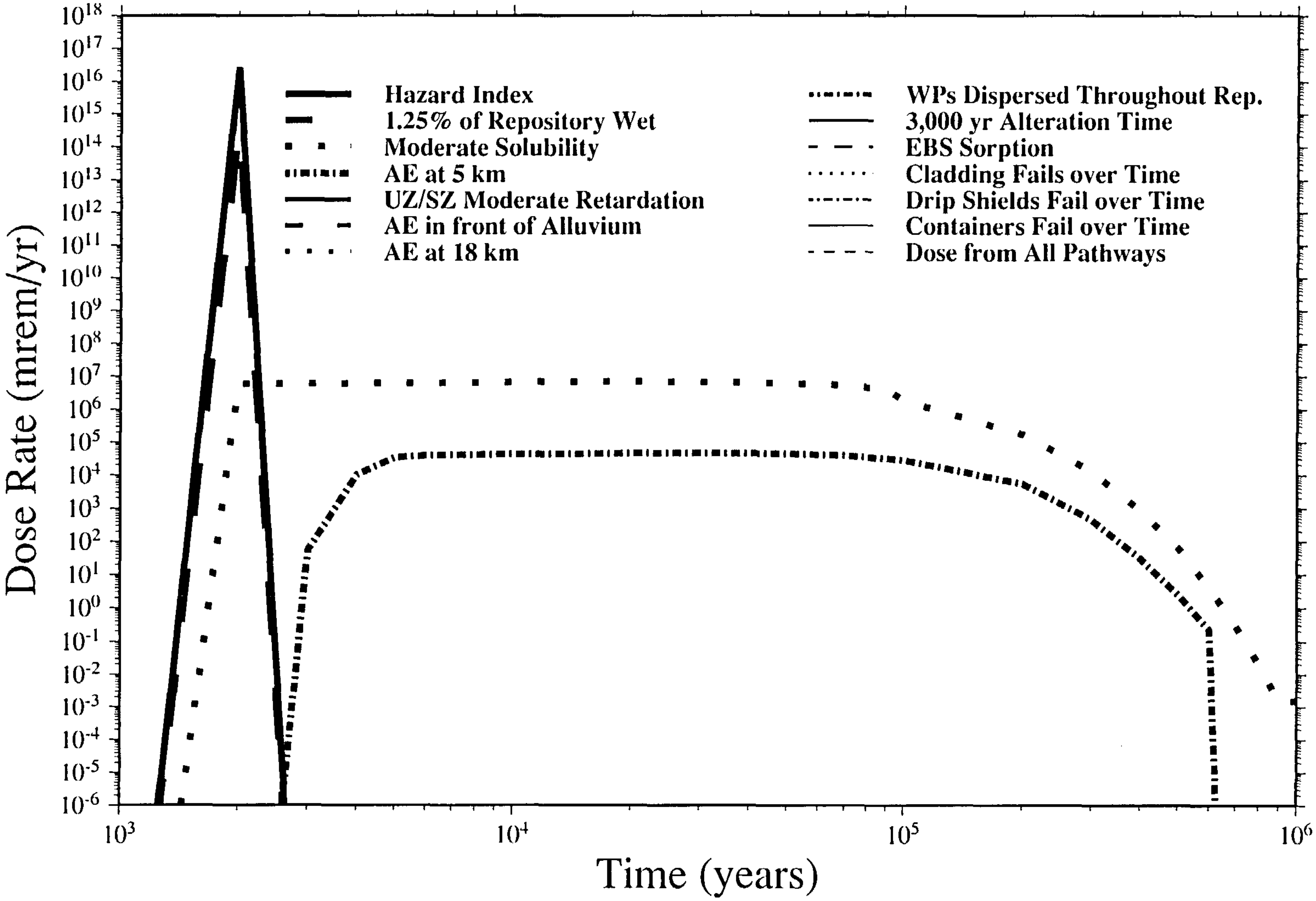

Figure 10-36
Hazard Index Curves for ^{239}Pu. "Natural" Barrier Functions Added First.

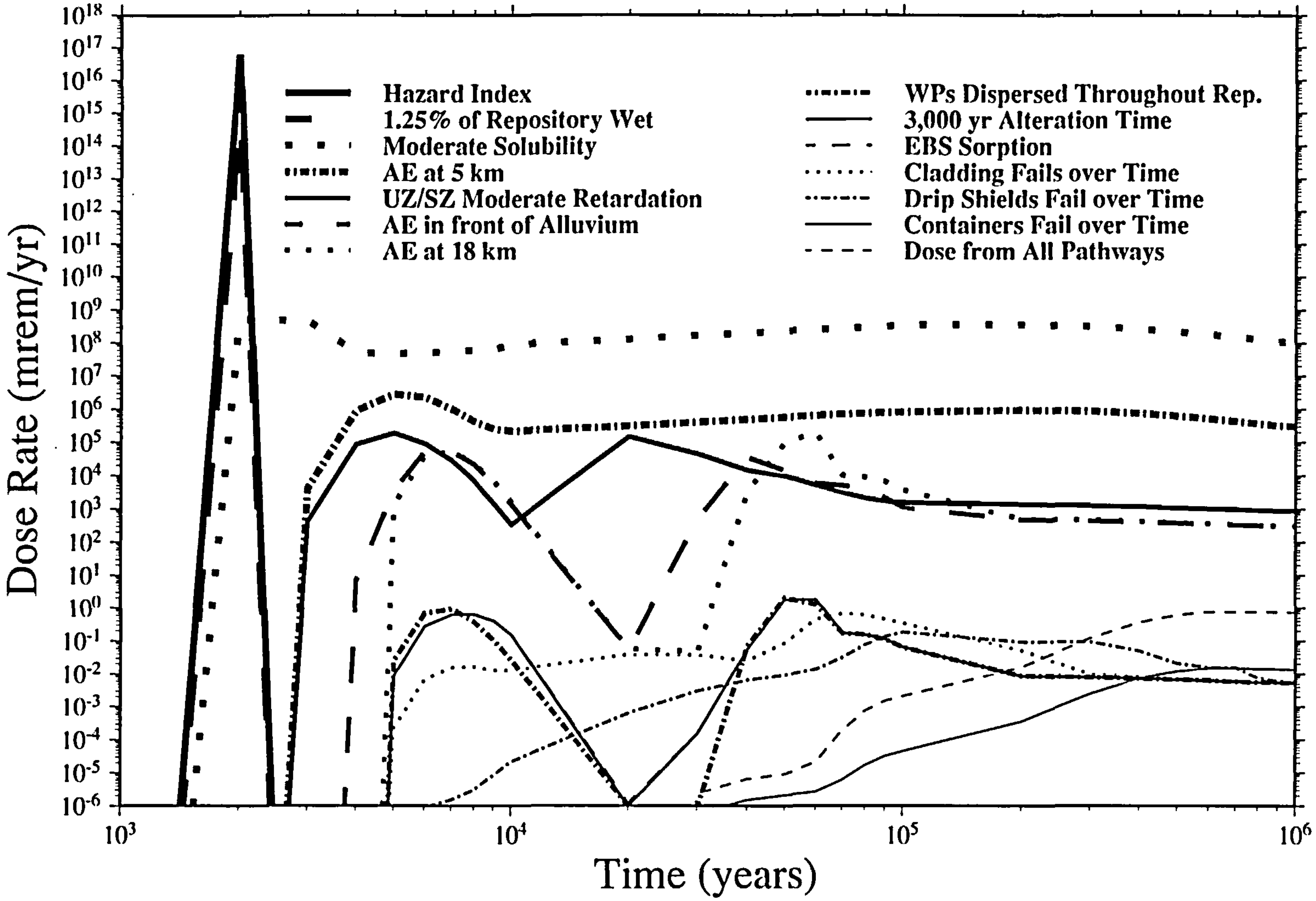

Figure 10-37
Hazard Index for all 22 Radionuclides Considered with the "Natural" Barriers Added First

10.2.2.4.3 "Engineered" Barriers Added First

^{129}I (Figure 10-38)

Figure 10-38 presents the HI curves for ^{129}I with the "engineered" barriers added first. The initial HI for ^{129}I starts at about 10^{12}, and is reduced by a factor of 80 for "1.25% of Repository Wet". With the engineered barriers added first, the next to be added this time is "3000 yr Alteration Time". This reduced the HI by a factor of 3000. Since iodine is non-sorbing, adding the "EBS Sorption" barrier has no effect on the Hazard Index.

Adding the function of the cladding barrier acts to reduce the peak HI by two orders of magnitude and delays the peak until about 7000 years. Adding the drip shield function lowers the HI by about a factor of ten, but delays the peak until about 50,000 years. Adding the effect of the container barrier lowers the peak HI by more than a factor of ten, and delays the peak until about 500,000 years.

The remaining "natural" barriers only contribute additional dilution, and contribute no more than about another 100,000 years of delay.

Table 10-11 provides a summary of the Hazard Reduction factors (HR) for ^{129}I at both 10,000 years and at the time of peak HI (whenever the peak occurs) for the case when "engineered" barriers are added first. Comparing this table to Table 10-1, in which the barriers were added "inside out" or "natural" barriers first for ^{129}I, shows some significant differences in the relative HI reduction for particular barriers.

Figures 10-39 through 10-42 are the Hazard Index curves for each successive member of the decay chain: $^{241}\text{Am} \rightarrow ^{237}\text{Np} \rightarrow ^{233}\text{U} \rightarrow ^{229}\text{Th}$.

^{241}Am (Figure 10-39)

The Hazard Index curves for ^{241}Am with the "engineered" barriers added first are shown in Figure 10-39. The Hazard Index curves show that just allowing the containers to fail over time is enough to completely decay away the ^{241}Am.

^{237}Np (Figure 10-40)

Figure 10-40 shows the Hazard Index curves for ^{237}Np with the "engineered" barriers added first. Table 10-12 shows the Hazard Reduction factors for this case.

Table 10-11
Hazard Reduction Factors for ^{129}I with "Engineered" Barrier Functions Added First

10,000 Years	At Time of Peak	Time of Peak [yr]	FEPs	"Engineered" or "Natural"?
10^2	10^2	2000	1.25% of repository wet	Both
10^3	10^3	2000	3,000 year alteration time	Both
10^0	10^0	2000	EBS sorption	Mostly engineered
10^2	10^2	7000	Cladding fails over time	Engineered
	10^1	50,000	Drip shields fail over time	Engineered
	$10^{1.5}$	500,000	Containers fail over time	Engineered
	$10^{\sim 0}$	500,000	Moderate solubility	Natural
	10^2	600,000	AE at 5 km	Natural
	10^0	600,000	UZ/SZ moderate retardation	Natural
	$10^{0.5}$	600,000	AE in front of alluvium	Natural
	$10^{\sim 0}$	600,000	AE at 18 km	Natural
	10^5	600,000	WPs dispersed throughout repository	Both
∞	$10^{\sim 15}$		*Total Hazard Reduction*	
	$10^{5\text{-}14}$		*Hazard reduction due to "engineered" features*	
	$10^{3\text{-}13}$		*Hazard reduction due to "natural" features*	
10^{-1}	10^{-1}		Hazard "reduction" (i.e., increase) due to all pathways	

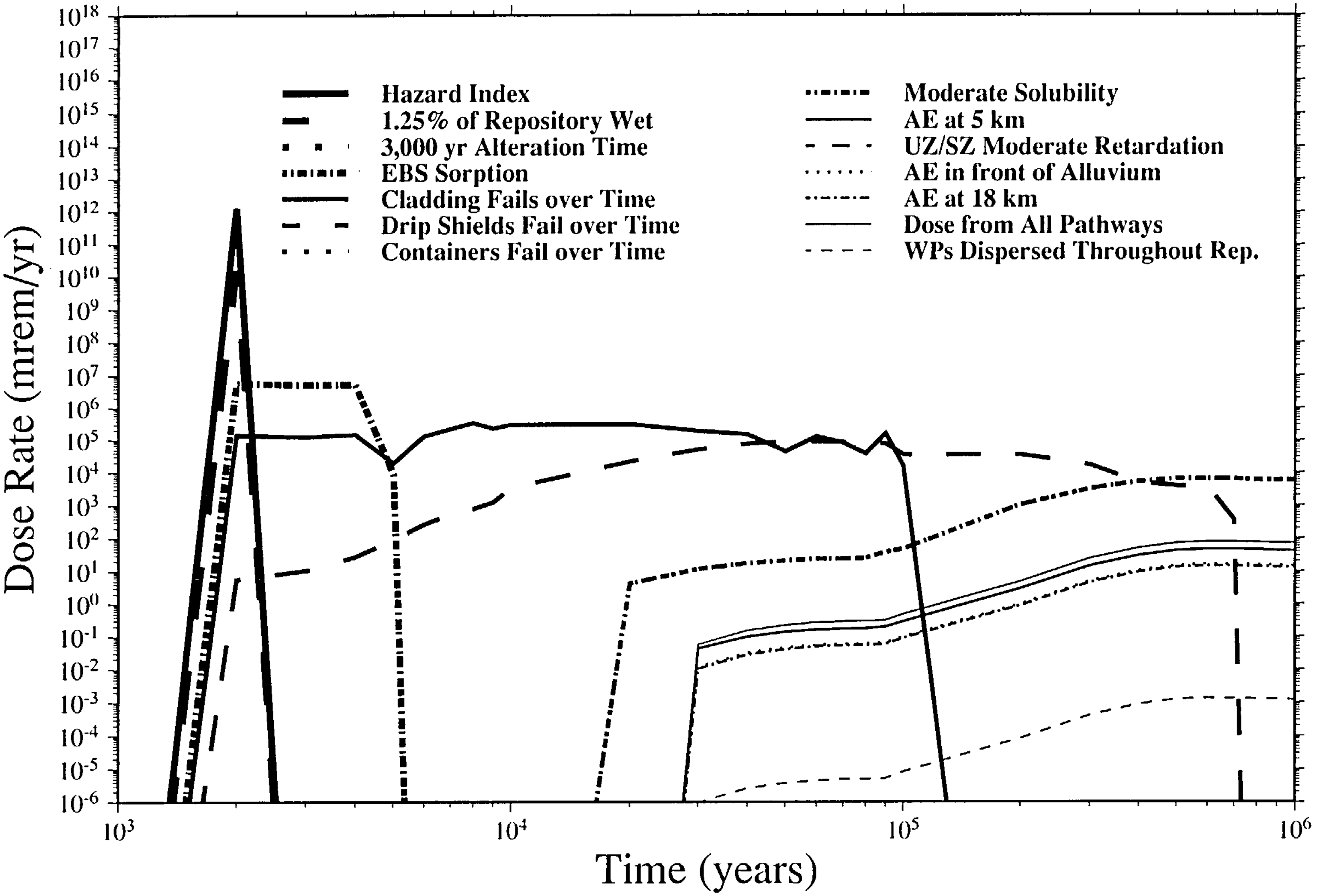

Figure 10-38
Hazard Index Curves for ^{129}I. "Engineered" Barrier Functions Added First.

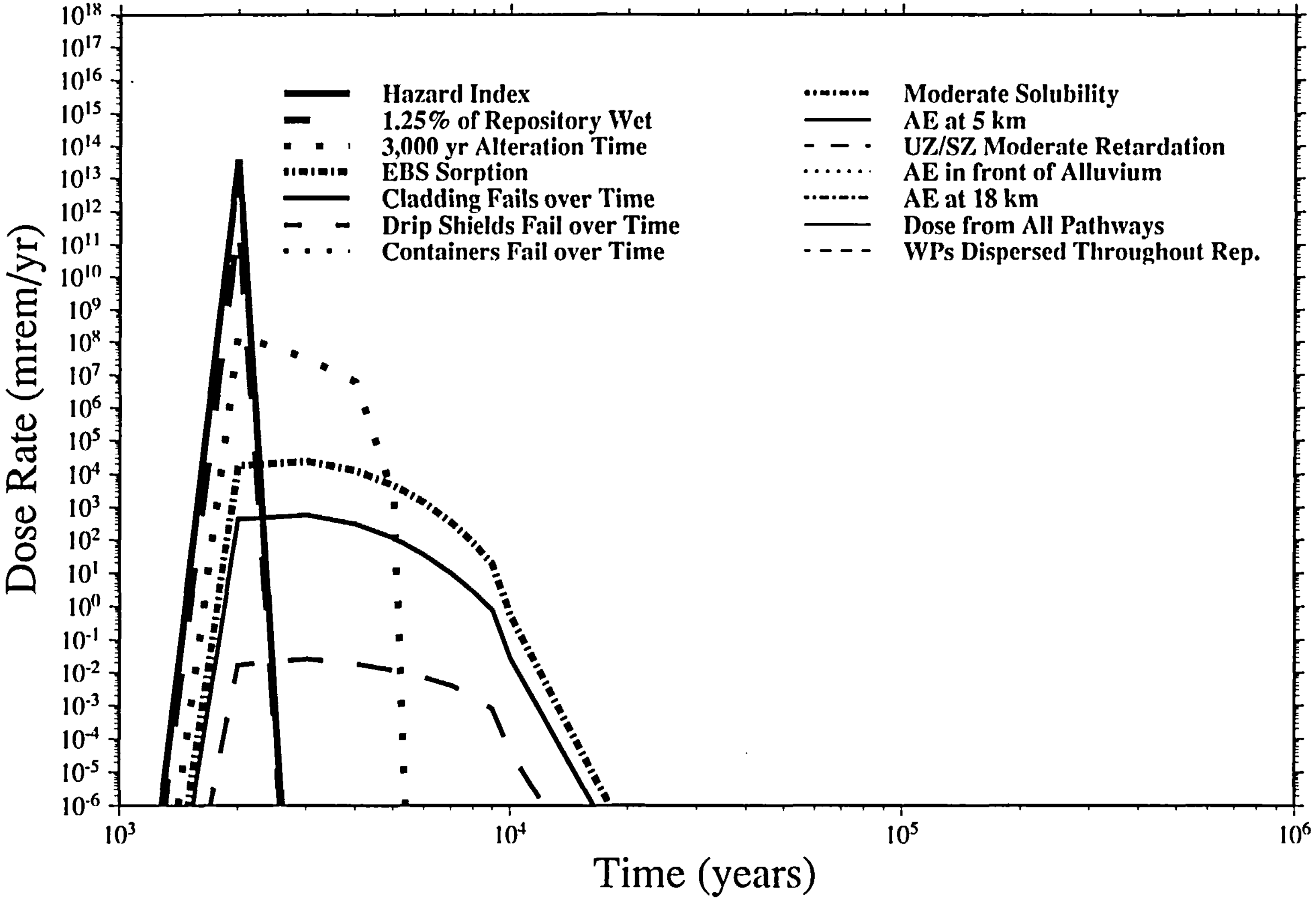

Figure 10-39
Hazard Index Curves for ^{241}Am. "Engineered" Barrier Functions Added First.

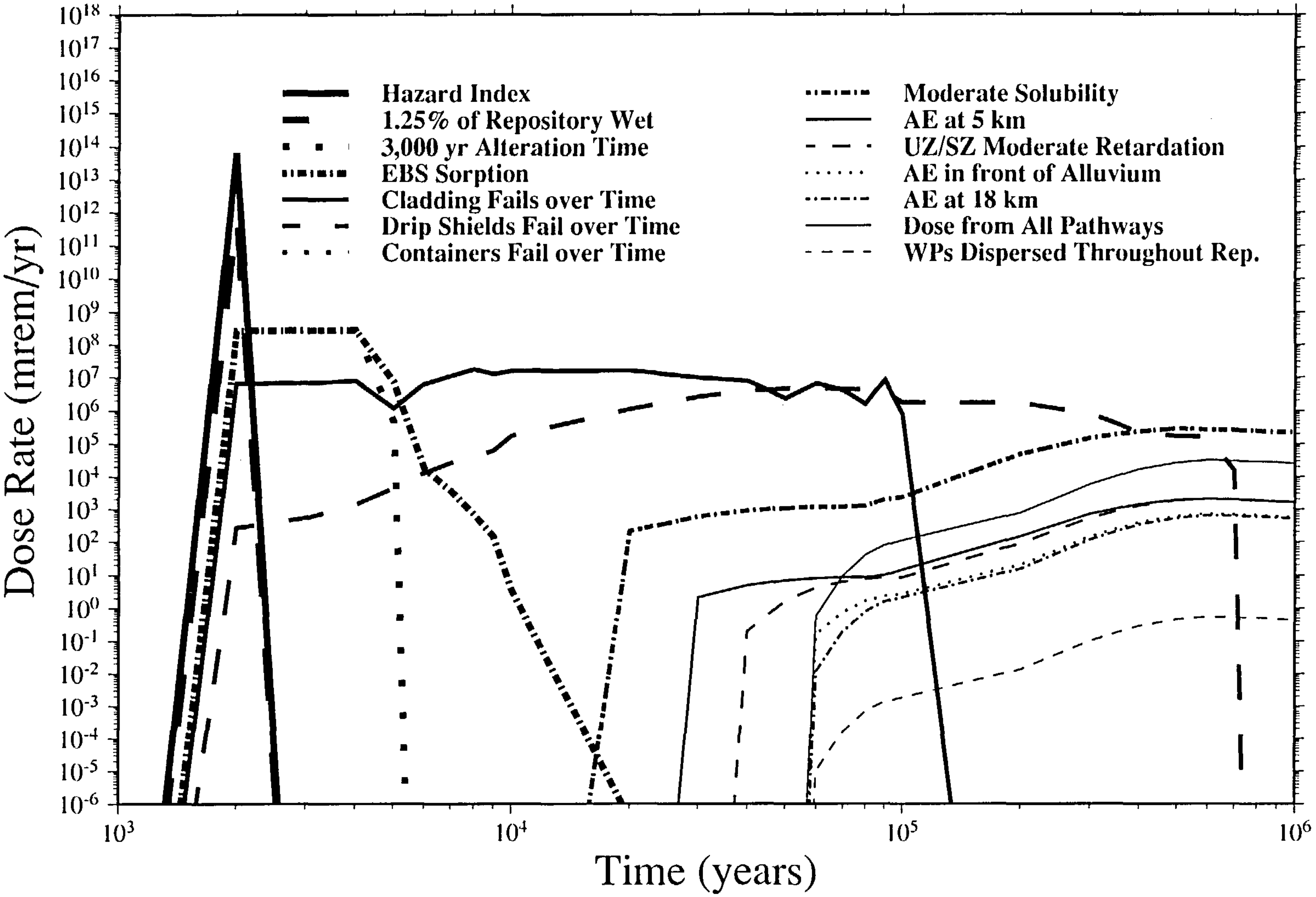

Figure 10-40
Hazard Index Curves for ^{237}Np. "Engineered" Barrier Functions Added First.

Table 10-12
Hazard Reduction Factors for ^{237}Np with "Engineered" Barrier Functions Added First

At Time of Peak	Time of Peak [yr]	FEPs	"Engineered" or "Natural"?
10^{2}	2000	1.25% of repository wet	Both
10^{3}	2000	3,000 year alteration time	Both
10^{0}	2000	EBS sorption	Mostly engineered
10^{2}	7000	Cladding fails over time	Engineered
10^{1}	50,000	Drip shields fail over time	Engineered
$10^{1.5}$	500,000	Containers fail over time	Engineered
$10^{\sim 0}$	500,000	Moderate solubility	Natural
10^{2}	600,000	AE at 5 km	Natural
10^{0}	600,000	UZ/SZ moderate retardation	Natural
$10^{0.5}$	600,000	AE in front of alluvium	Natural
$10^{\sim 0}$	600,000	AE at 18 km	Natural
10^{5}	600,000	WPs dispersed throughout repository	Both
10^{-15}		*Total Hazard Reduction*	
10^{5-14}		*Hazard reduction due to "engineered" features*	
10^{3-13}		*Hazard reduction due to "natural" features*	
10^{-1}		Hazard "reduction" (i.e., increase) due to all pathways	

^{233}U (Figure 10-41)

The Hazard Index curves for ^{233}U when engineered barriers are added first are shown in Figure 10-41. What is notable about this figure is that it shows that engineered barriers that cause delay in the release of ^{233}U's parent radionuclides act to prevent the Hazard Index for ^{233}U from being lowered very much. This is because the delay allows for more ingrowth of the ^{233}U daughters. The Hazard Reduction for attributed to each barrier is given in Table 10-13.

^{229}Th (Figure 10-42)

Figure 10-42 presents the Hazard Index curves for ^{229}Th with the "engineered" barriers added first. As was the case for the lower solubility, sorbing ^{233}U, the delays in the peak arrival can be seen when the sorbing natural barriers are added and solubility limits are imposed. Ingrowth from the parents of ^{229}Th is also evident.

^{238}U (Figure 10-43)

Figure 10-43 presents the Hazard Index curves for ^{238}U when "engineered" barriers are added first. Table 10-14 shows the HI reduction table for ^{238}U.

Table 10-13
Hazard Reduction Factors for ^{233}U with "Engineered" Barriers Added First

At Time of Peak	Time of Peak [yr]	FEPs	"Engineered" or "Natural"?
10^{2}	2000	1.25% of repository wet	Both
10^{3}	4000	3,000 year alteration time	Both
$10^{0.5}$	4000	EBS sorption	Mostly engineered
$10^{\sim 0}$	60,000	Cladding fails over time	Engineered
$10^{\sim 0}$	70,000	Drip shields fail over time	Engineered
10^{1}	500,000	Containers fail over time	Engineered
10^{1}	1,000,000	Moderate solubility	Natural
10^{2}	1,000,000	AE at 5 km	Natural
10^{0}	700,000	UZ/SZ moderate retardation	Natural
$10^{\sim 0}$	700,000	AE in front of alluvium	Natural
$10^{\sim 0}$	700,000	AE at 18 km	Natural
10^{5}	700,000	WPs dispersed throughout repository	Both
10^{-14}		*Total Hazard Reduction*	
10^{2-12}		*Hazard reduction due to "engineered" features*	
10^{3-13}		*Hazard reduction due to "natural" features*	
10^{-2}		Hazard "reduction" (i.e., increase) due to all pathways	

Table 10-14
Hazard Reduction Factors for ^{238}U with "Engineered" Barriers Added First

At Time of Peak	Time of Peak [yr]	FEPs	"Engineered" or "Natural"?
10^{2}	2000	1.25% of repository wet	Both
10^{3}	2000	3,000 year alteration time	Both
10^{1}	5000	EBS sorption	Mostly engineered
10^{1}	30,000	Cladding fails over time	Engineered
10^{1}	70,000	Drip shields fail over time	Engineered
10^{1}	600,000	Containers fail over time	Engineered
10^{1}	1,000,000	Moderate solubility	Natural
10^{2}	1,000,000	AE at 5 km	Natural
$10^{\sim 0}$	1,000,000	UZ/SZ moderate retardation	Natural
$10^{0.5}$	1,000,000	AE in front of alluvium	Natural
$10^{\sim 0}$	1,000,000	AE at 18 km	Natural
10^{5}	1,000,000	WPs dispersed throughout repository	Both
10^{-16}		*Total Hazard Reduction*	
10^{4-14}		*Hazard reduction due to "engineered" features*	
10^{4-14}		*Hazard reduction due to "natural" features*	
10^{-2}		Hazard "reduction" (i.e., increase) due to all pathways	

^{239}Pu (Figure 10-44)

Figure 10-44 presents the Hazard Index curves for ^{239}Pu for the "engineered" barriers added first. This plutonium isotope provides the greatest contribution to the initial Hazard Index. It is also indicative of the behavior of a moderately long-lived, solubility-limited, highly sorbing radionuclide. The combination of its low solubility and the delay due to travel time in the first five kilometers of the UZ and SZ is shown by the fact that these two effects cause ^{239}Pu to decay to insignificant levels before it reaches even five kilometers.

Total Hazard Index from All 22 Radionuclides with the "Engineered" Barriers Added First

Figure 10-45 presents the Hazard Index curves for all 22 radionuclides considered when the "engineered" barriers are added first. Table 10-15 summarizes the reduction of the HI contributed by each barrier.

Table 10-15
Hazard Reduction Factors for All 22 Radionuclides with "Engineered" Barriers Added First

At Time of Peak	Time of Peak [yr]	FEPs	"Engineered" or "Natural"?
10^2	2000	1.25% of repository wet	Both
10^3	2000	3,000 year alteration time	Both
$10^{1.5}$	6000	EBS sorption	Mostly engineered
10^1	20,000	Cladding fails over time	Engineered
10^1	60,000	Drip shields fail over time	Engineered
10^1	500,000	Containers fail over time	Engineered
$10^{\sim0}$	1,000,000	Moderate solubility	Natural
10^2	1,000,000	AE at 5 km	Natural
10^1	600,000	UZ/SZ moderate retardation	Natural
$10^{0.5}$	600,000	AE in front of alluvium	Natural
$10^{\sim0}$	600,000	AE at 18 km	Natural
10^5	600,000	WPs dispersed throughout repository	Both
10^{-18}		*Total Hazard Reduction*	
10^{5-15}		*Hazard reduction due to "engineered" features*	
10^{4-14}		*Hazard reduction due to "natural" features*	
$10^{-1.5}$		Hazard "reduction" (i.e., increase) due to all pathways	

The above analyses show that many natural and engineered barriers contribute to hazard reduction. The degree to which any individual barrier contributes depends on the presence of other barriers. Often the "potential" benefit of a barrier cannot be seen until other barriers are removed.

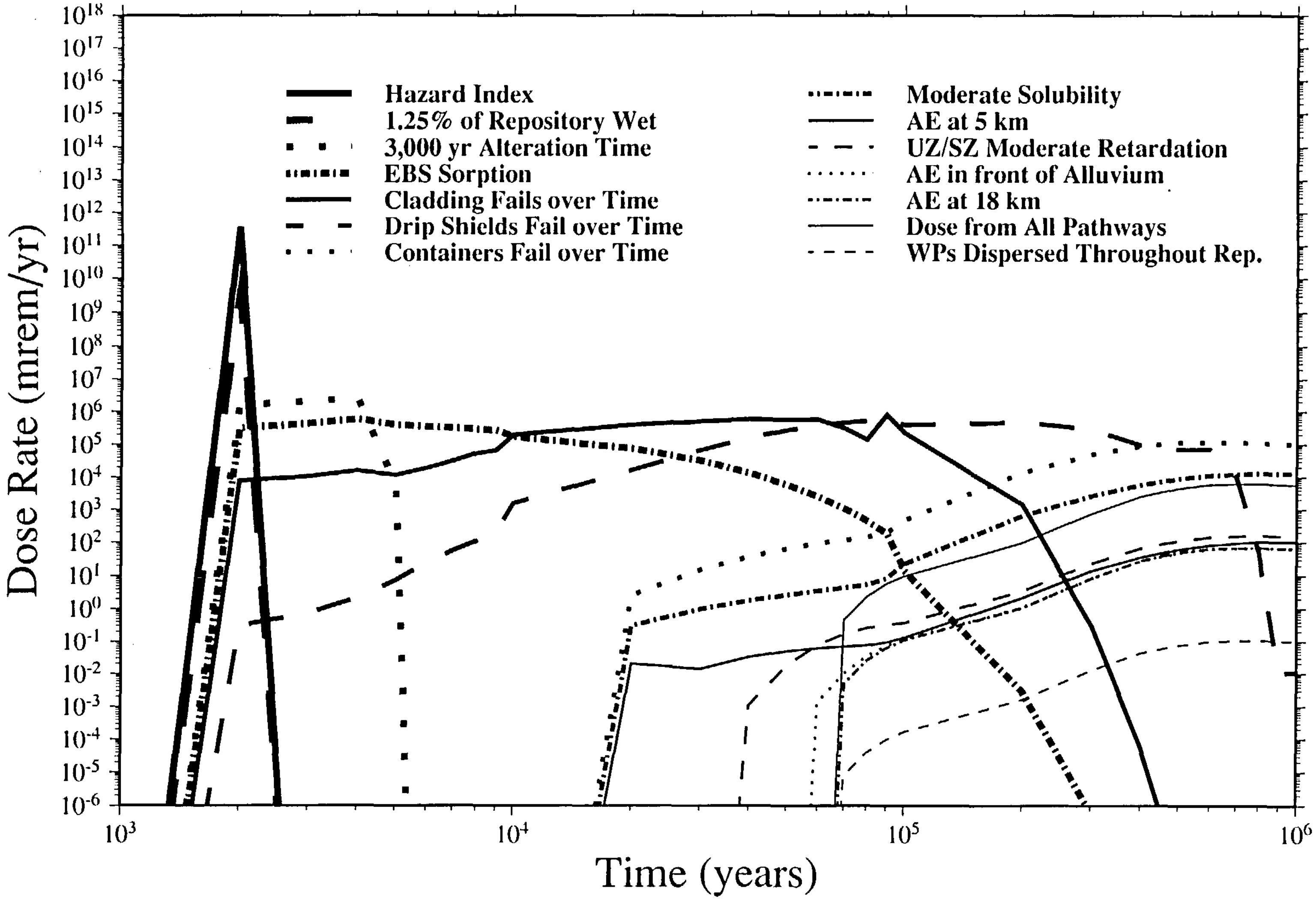

Figure 10-41
Hazard Index Curves for ^{233}U. "Engineered" Barrier Functions Added First.

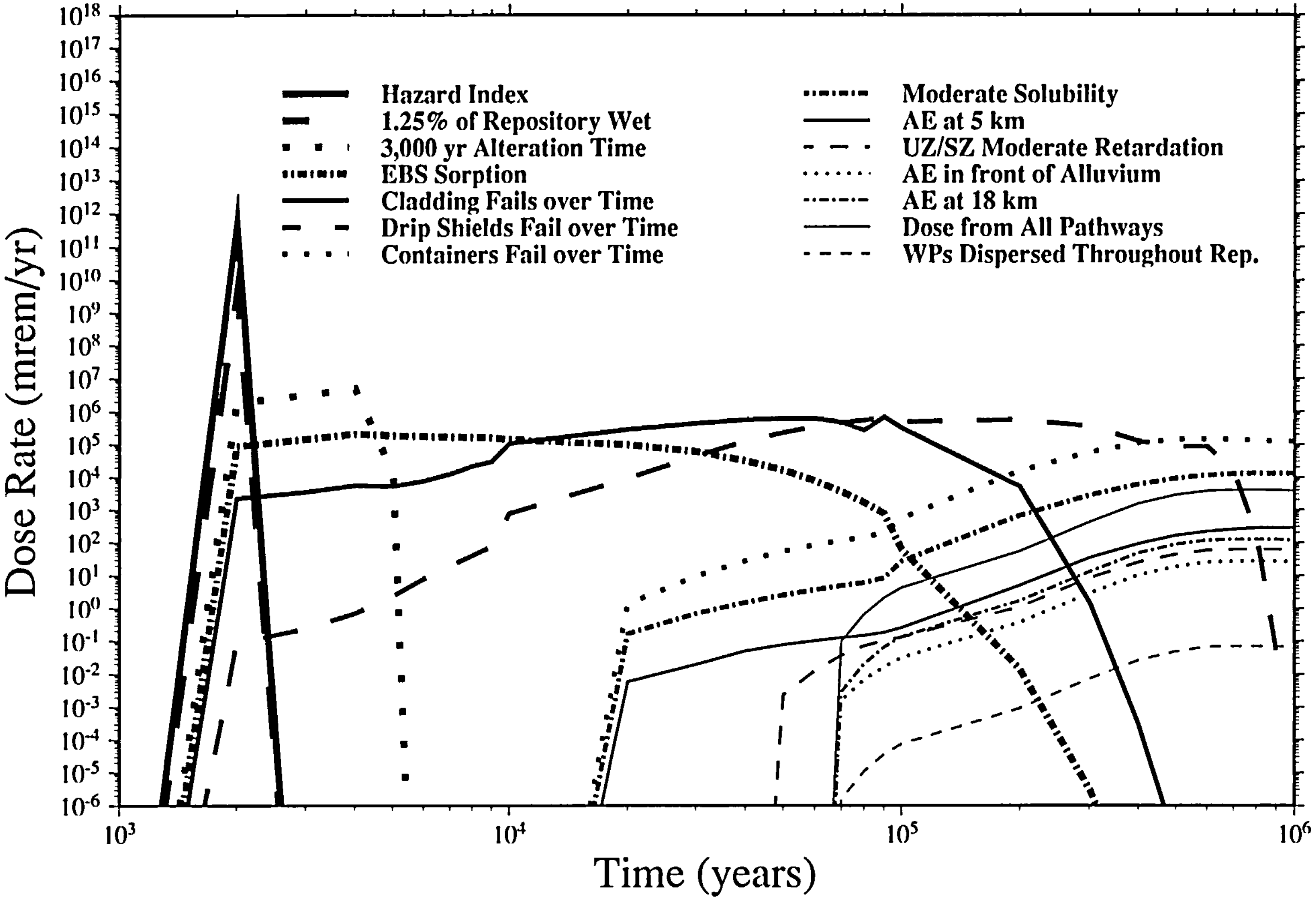

Figure 10-42
Hazard Index Curves for ^{229}Th. "Engineered" Barrier Functions Added First.

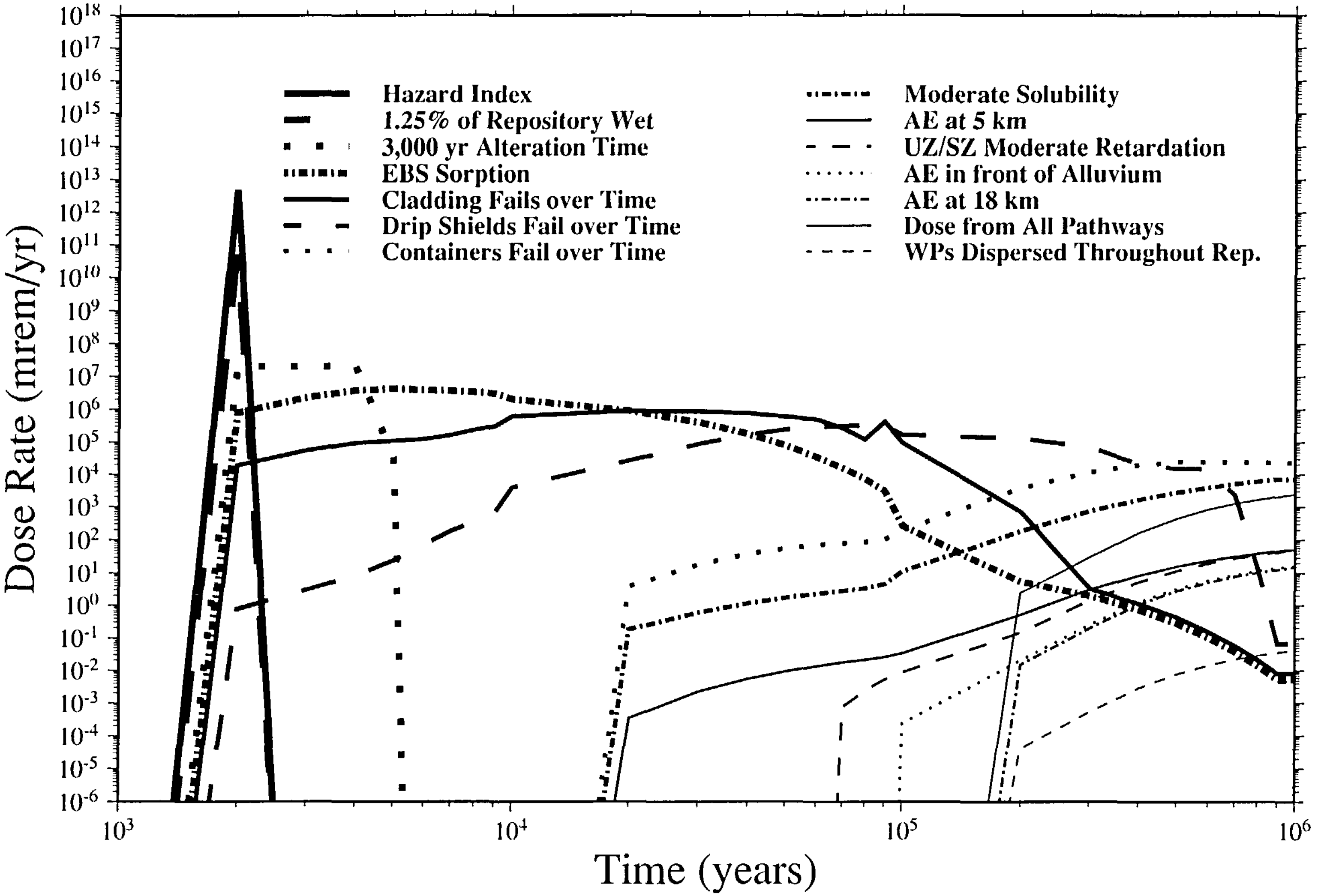

Figure 10-43
Hazard Index Curves for ^{238}U. "Engineered" Barrier Functions Added First.

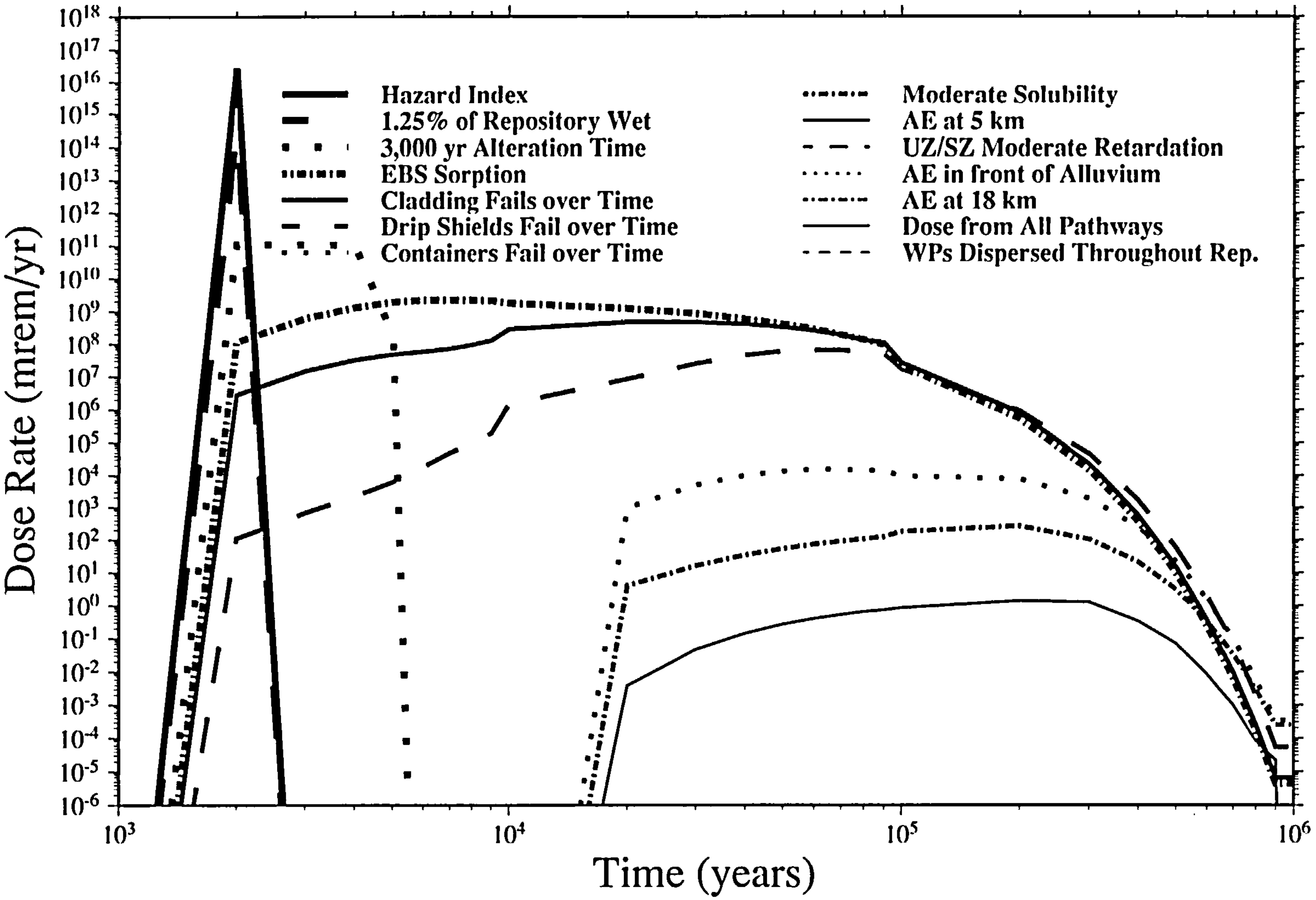

Figure 10-44
Hazard Index Curves for ^{239}Pu. 'Engineered" Barrier Functions Added First.

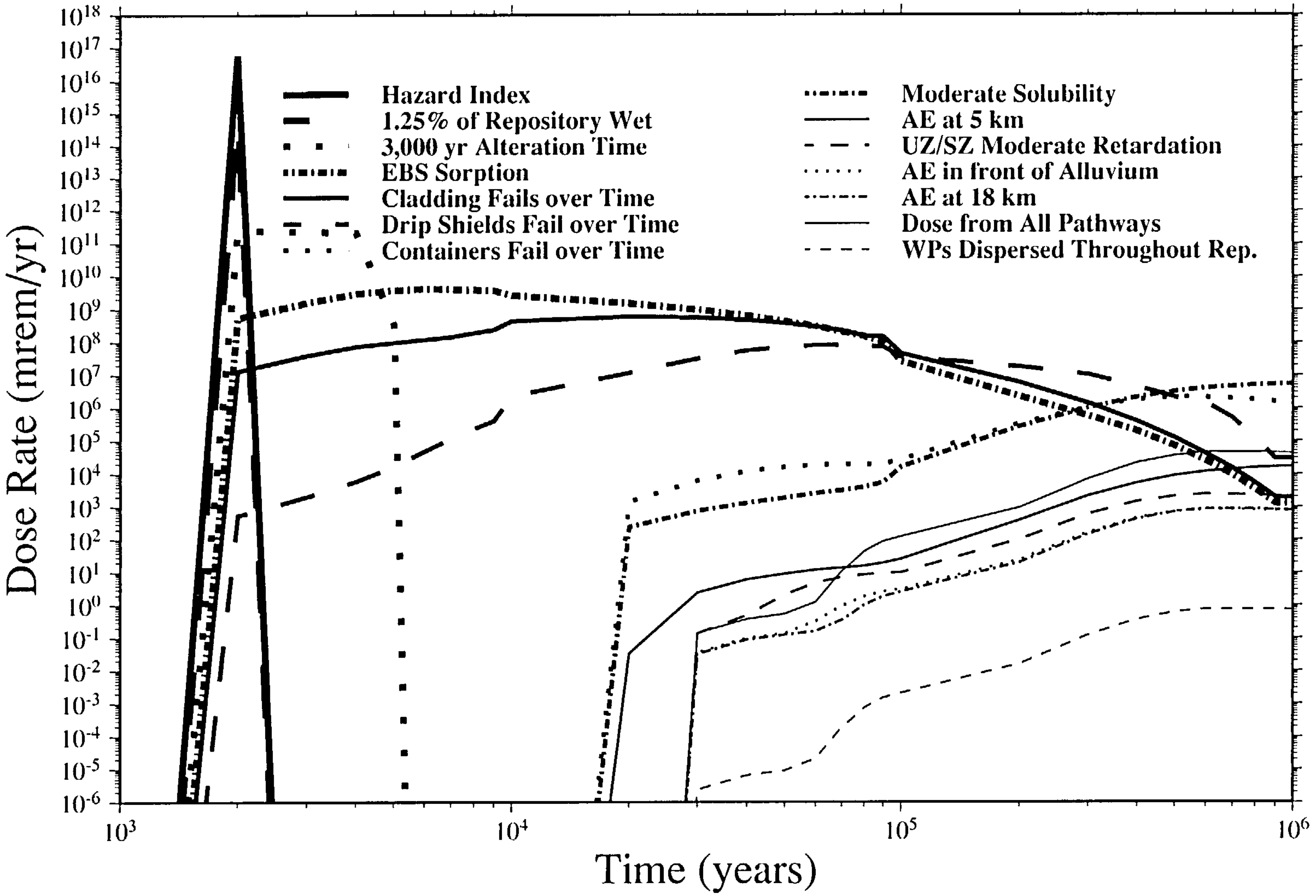

Figure 10-45
Hazard Index for all 22 Radionuclides Considered with the "Engineered" Barriers Added First

10.2.2.5 Comparison of Relative Importance of Individual Barriers Depending on the Order of Addition

Table 10-16 compares the Hazard Reduction each barrier contributes as a function of the order the barrier was added: "inside out", "natural" barriers first, or "engineered" barriers first. Table 10-16 is for all radionuclides, so is a compilation of Tables 10-5, 10-10, and 10-15. This table shows that the relative importance of many of the barriers is dependent on the presence of other specific barriers. That is, many of the barriers' functions are partially or fully masked by the presence of the other barriers. The table shows that if "natural" barriers are added first (i.e., no "engineered" barriers added initially), then the "natural" barriers can contribute more to overall dose reduction. The opposite is also true if the "engineered" barriers are added first. However, no matter what order the barriers are added, both "natural" and "engineered" barriers contribute significantly to overall dose reduction.

Table 10-16
Comparison of Hazard Reduction Factors for All 22 Radionuclides Depending on the Order of Addition of the Individual Barriers

Hazard Reduction			FEPs	"Engineered" or "Natural"?
Barriers added "Inside out"	"Natural" barriers added first	"Engineered" barriers added first		
10^2	10^2	10^2	1.25% of repository wet	both
10^3	$10^{\sim 0}$	10^3	3,000 year alteration time	both
10^3	10^6	$10^{\sim 0}$	Moderate solubility	natural
$10^{\sim 0}$	$10^{0.5}$	10^1	Cladding fails over time	engineered
10^1	10^1	10^1	Containers fail over time	engineered
$10^{\sim 0}$	10^1	10^1	Drip shields fail over time	engineered
10^5	10^5	10^5	WPs dispersed throughout rep.	both
10^1	$10^{\sim 0}$	$10^{1.5}$	EBS sorption	mostly engineered
$10^{2.5}$	10^2	10^2	AE at 5 km	natural
10^1	10^1	10^1	UZ/SZ moderate retardation	natural
$10^{0.5}$	$10^{0.5}$	$10^{0.5}$	AE in front of alluvium	natural
$10^{\sim 0}$	$10^{0.5}$	$10^{\sim 0}$	AE at 18 km	natural
10^{19}	10^{19}	10^{19}	*Total Hazard Reduction*	
$10^{2\text{-}12}$	$10^{3\text{-}10}$	$10^{5\text{-}15}$	***Hazard reduction due to "engineered" features***	
$10^{7\text{-}17}$	$10^{9\text{-}16}$	$10^{4\text{-}14}$	***Hazard reduction due to "natural" features***	
$10^{-1.5}$	$10^{-1.5}$	$10^{-1.5}$	Hazard "reduction" (i.e., increase) due to all pathways	

10.3 Other Single-Branch Sensitivity Studies

Two additional sensitivity studies on engineered barriers are given in Figures 10-46 and 10-47. The effect of changing the alteration time of the waste form on the maximum likelihood 'wet' branch is shown in Figure 10-46. As expected, there is very little sensitivity to the alteration time since the variations in alteration times (1,000 to 5,000 years) are small compared to the time it takes for the other barriers to fail or travel times through some of the natural barriers.

In some of the previous figures, complete neutralization of the waste package or drip shield function was assumed. In Figure 10-47, only a few of the containers or drip shields are assumed to have failed at the time of emplacement. In the "maximum likelihood wet branch" base case, it is assumed that one drip shield and one waste package are assumed failed at emplacement. Each failure is assumed to be randomly positioned within the repository such that the initially failed drip shield is not located above the initially failed container. Figure 10-47 considers three additional cases: no drip shields or containers failed at emplacement; no drip shields, but ten waste packages failed at emplacement; and one drip shield and ten waste packages failed at emplacement in 11 different locations throughout the repository. Assuming no failures at emplacement does not significantly change the dose rates. Assuming ten containers failed at emplacement for either the case of zero or one drip shield failed at emplacement increases the dose rates at early times by roughly a factor of ten, although the peak dose rate is unchanged.

Figures 10-48 through 10-57 explore some single-branch sensitivities to some of the details of the natural system. Figure 10-48 shows the small change in the dose rates if a less strong, long-term climate than the Full Glacial Maximum (FGM) is chosen. The "2/3" and "1/3 Full Glacial Maximum" curves are for cases where there is less long-term net infiltration. This is one reason why the long-term climate has been removed from the IMARC logic tree.

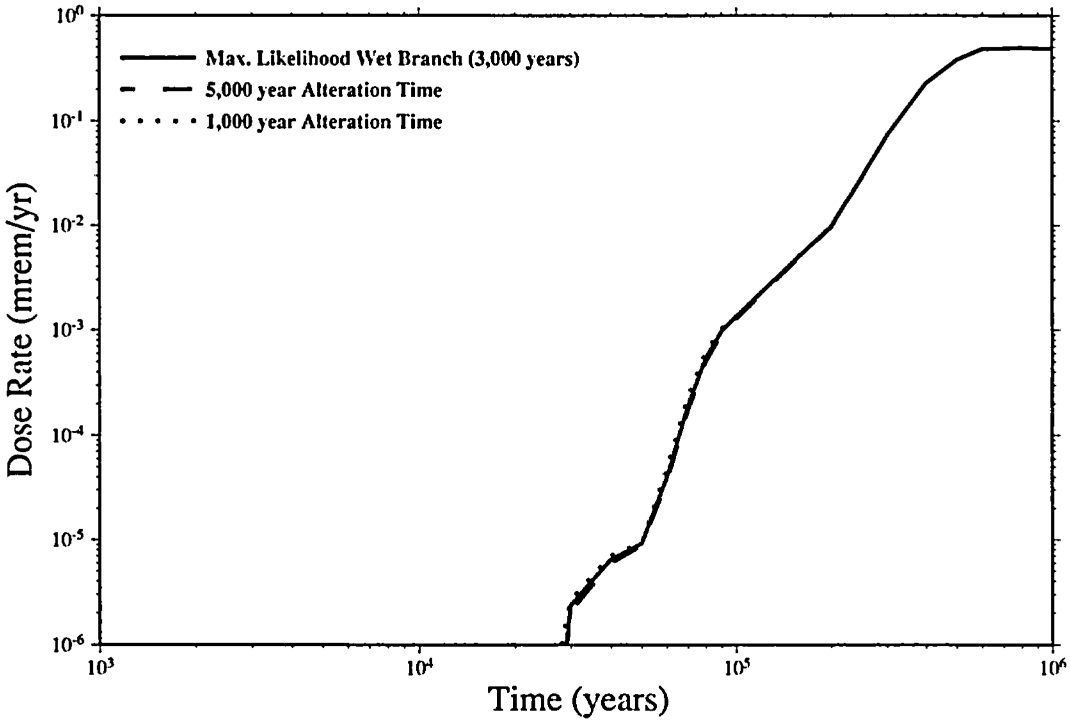

Figure 10-46
Sensitivity of Annual Dose from the Maximum Likelihood "Wet" Branch Due to Variations in the Waste Form Alteration Time

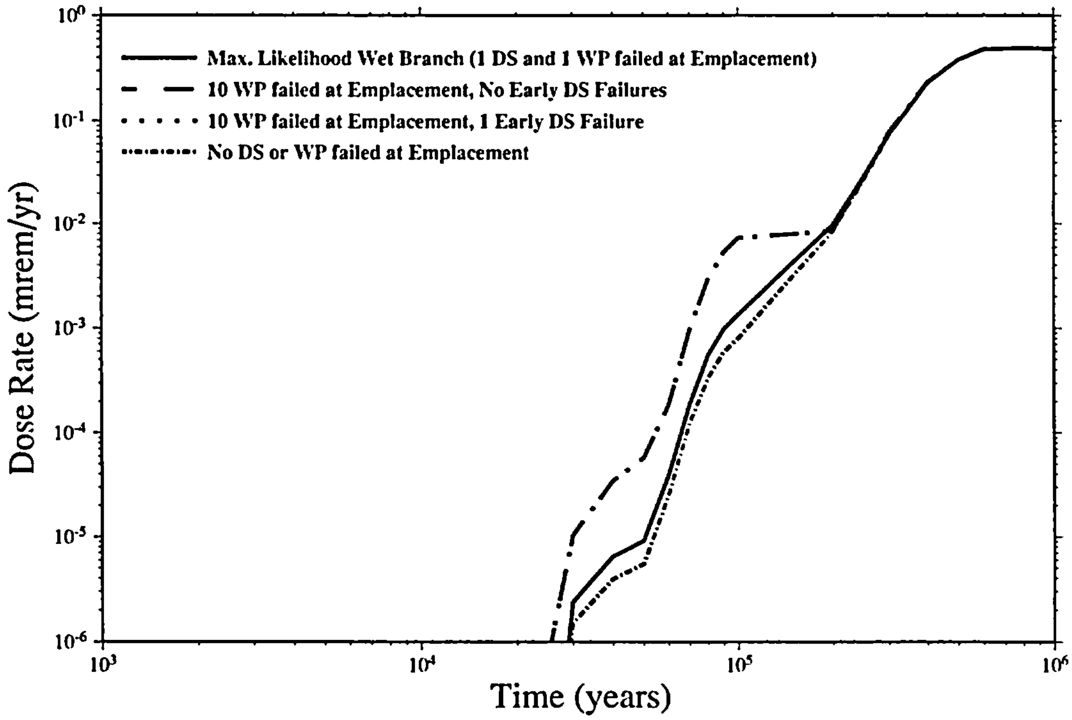

Figure 10-47
Sensitivity of Annual Dose from the Maximum Likelihood "Wet" Branch Due to Variations in the Number of Drip Shields and Containers Assumed to be Failed at Emplacement

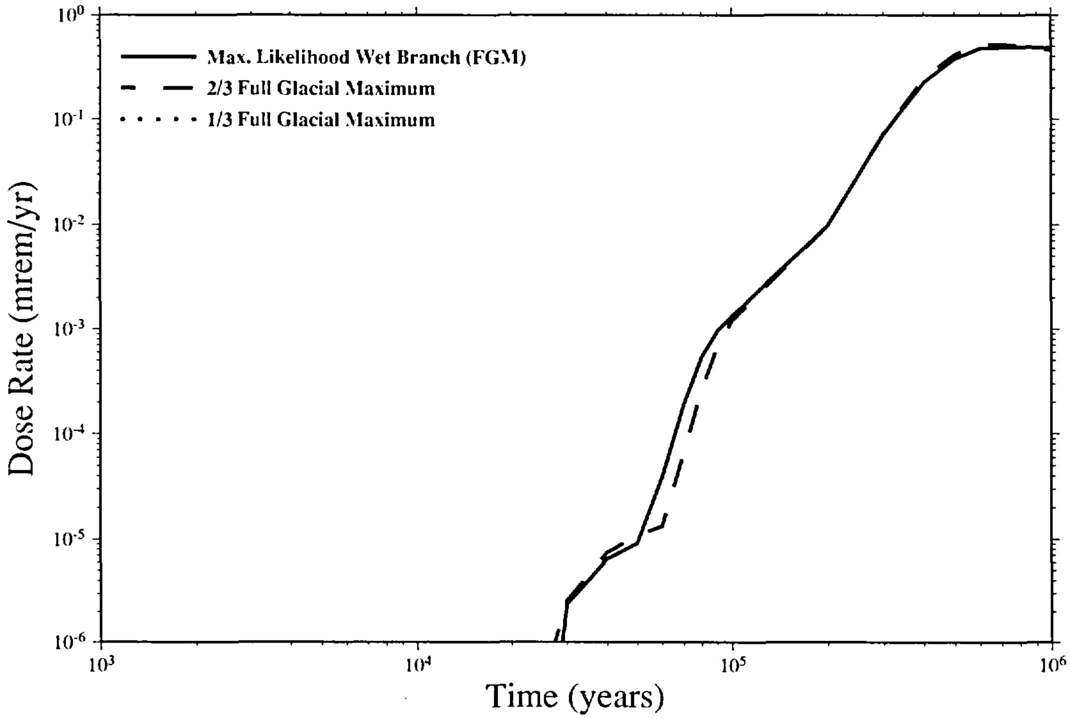

Figure 10-48
Sensitivity of Annual Dose from the Maximum Likelihood "Wet" Branch Due to Variations in the Intensity of the Assumed Long-Term Glacial Climate

The next set of figures explores a few sensitivities for properties of the saturated zone. Figures 10-49 and 10-50 explore the sensitivity due to variations in the matrix retardation caused by sorption of some radionuclides onto the surfaces of the rock matrix. Figures 10-51 and 10-52 consider variations in the parameters within the "flowing interval" (see Section 7) of the saturated zone. Finally, Figure 10-53 investigates the effects of variations in the specific discharge (translates into groundwater velocity) within the saturated zone.

Figure 10-49 shows the sensitivity due to different values of matrix retardation for all radionuclides. As would be expected, if there is less retardation, the plume arrives earlier at 18km. Conversely, if there is higher matrix retardation it takes longer for the radionuclides to arrive at 18km. However, peak dose rates are not affected by the degree of matrix retardation.

Figure 10-50 shows the sensitivity due to different values of matrix retardation just for ^{237}Np, which moderately sorbs onto the rock matrix surfaces and also contributes the greatest to total dose rate. This figure shows that, as might be expected, most of the sensitivity to variations in matrix retardation for all radionuclides shown in Figure 10-49 can be explained by the sensitivity to just ^{237}Np.

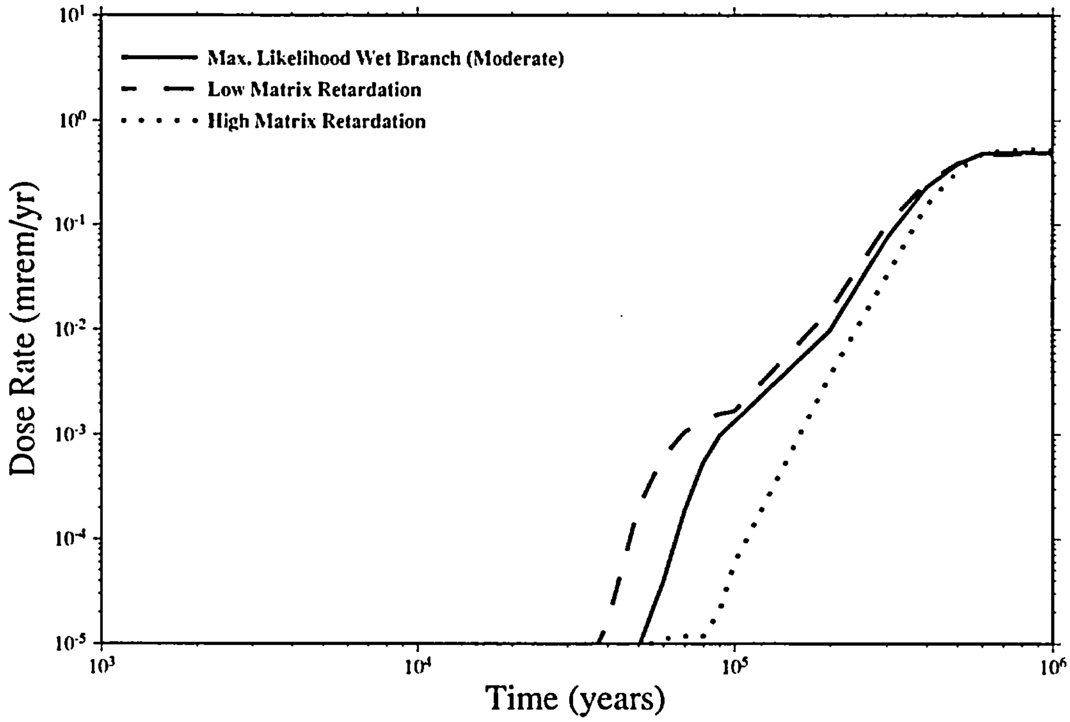

Figure 10-49
Sensitivity of Annual Dose from the Maximum Likelihood "Wet" Branch Due to Variations in the Saturated Zone Matrix Retardation (all radionuclides considered)

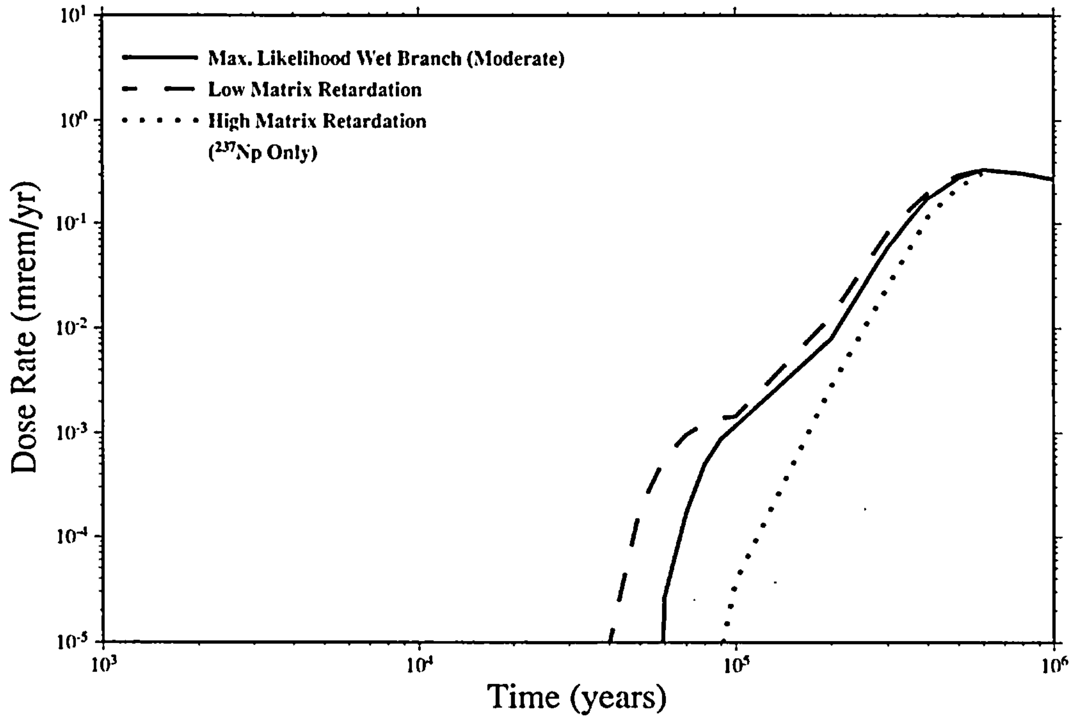

Figure 10-50
Sensitivity of Annual Dose from the Maximum Likelihood "Wet" Branch Due to Variations in the Saturated Zone Matrix Retardation (^{237}Np only)

Figure 10-51 shows the sensitivity to the block radius within the flowing interval. The block radius is similar to the distance between flowing fractures in the saturated zone. If there is a small distance between flowing fractures, then it is more likely that radionuclides initially flowing in the fast flowing fractures could diffuse into the stagnant matrix block.[12] The greater the proportion of the radionuclide that can diffuse into the stagnant matrix block, the slower the average velocity of the radionuclide as a whole. This general trend is borne out in Figure 10-51. As the block radius increases, the average velocity of the radionuclides increases as there is less opportunity for the radionuclides to diffuse into the stagnant matrix. At higher velocities the radionuclides should appear at 18km earlier. Figure 10-51 shows that the initial arrival of the plume can be moved forward in time by several thousand years if a larger block matrix size is assumed. However, the peak height appears unaffected.

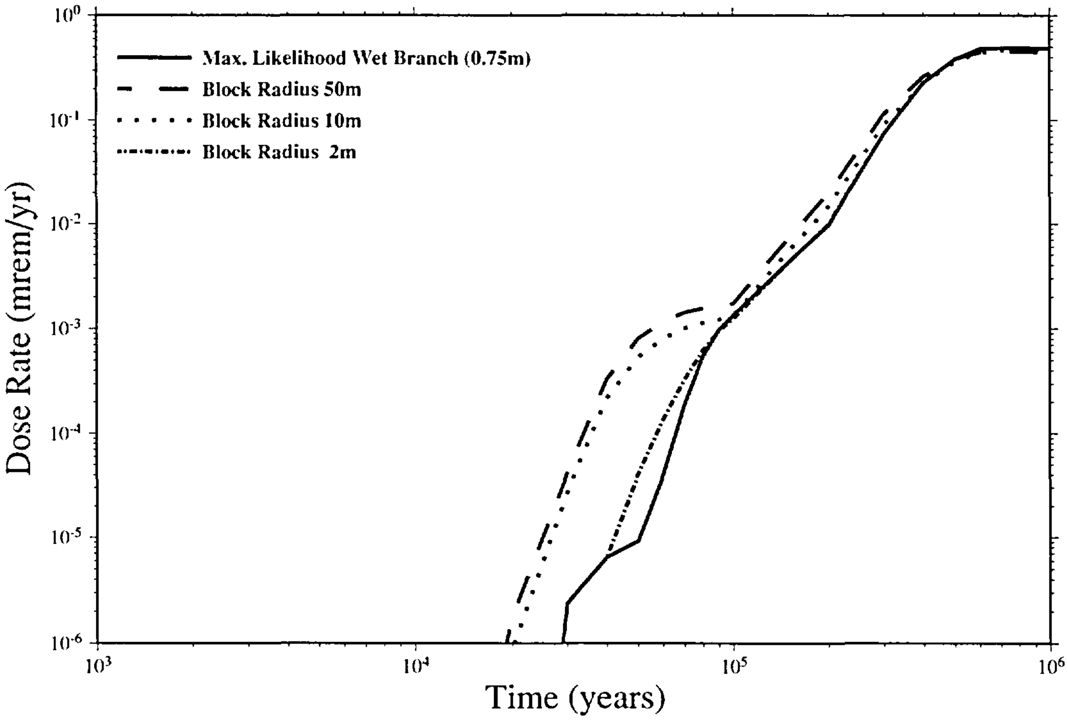

Figure 10-51
Sensitivity of Annual Dose from the Maximum Likelihood "Wet" Branch Due to Variations in the Saturated Zone Matrix Block Size

In a similar manner, the amount of the radionuclide that can diffuse into the matrix blocks from the fractures is also controlled by the effective diffusion coefficient. A lower diffusion coefficient could result in more of the radionuclide remaining in the flowing fractures, causing earlier arrival of the radionuclide at 18km. This is shown in Figure 10-52. A lower diffusion coefficient is shown to move ahead the arrival time of the plume by several thousand years. Increasing the diffusion coefficient does not seem to have much effect. This is because the combination of matrix block radius (0.75m) and diffusion coefficient (3.2×10^{-11} m^2/s) assumed in

---

[12] The matrix blocks are assumed to be porous, but the groundwater velocity within the block is assumed to be zero. Only groundwater within the flowing fractures is assumed to move downstream.

the base case is sufficient for the main radionuclides contributing to dose to fully penetrate the matrix blocks.

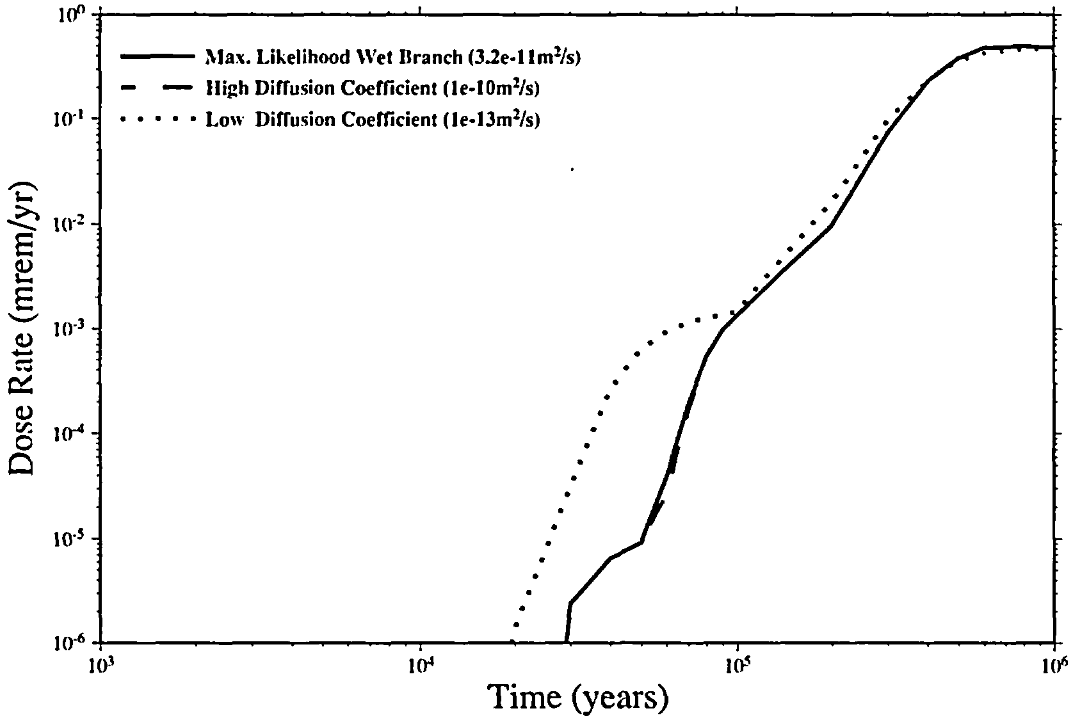

Figure 10-52
Sensitivity of Annual Dose from the Maximum Likelihood "Wet" Branch Due to Variations in the Saturated Zone Diffusion Coefficient

Figure 10-53 shows the sensitivity to saturated zone specific discharge values that are four times larger and four times smaller than the base case value of 0.15 m/yr. These variations cause the time of the initial plume arrival to shift by a few thousand years, which is consistent with our understanding of effective radionuclide travel times through the saturated zone.

The IMARC base case assumes the fraction of the repository that is 'wet' (experiences active dripping of groundwater into the drifts) is only 5% of that part of the repository experiencing "focused flow" (average percolation rate that is four times the area-averaged rate). For the focused flow case (probability of 0.135), 25% of the total repository area is in the "focused flow" zone. If, instead, one assumes that 100% of the zone of "focused flow" experiences dripping, the fraction of the repository that is 'wet' in the flow focusing case is increased from 1.25% to 25% - a 20-fold increase. This case is shown in Figure 10-54. The increase in dose rate is almost perfectly correlated to the increase in the fraction of the repository that is assumed 'wet'.

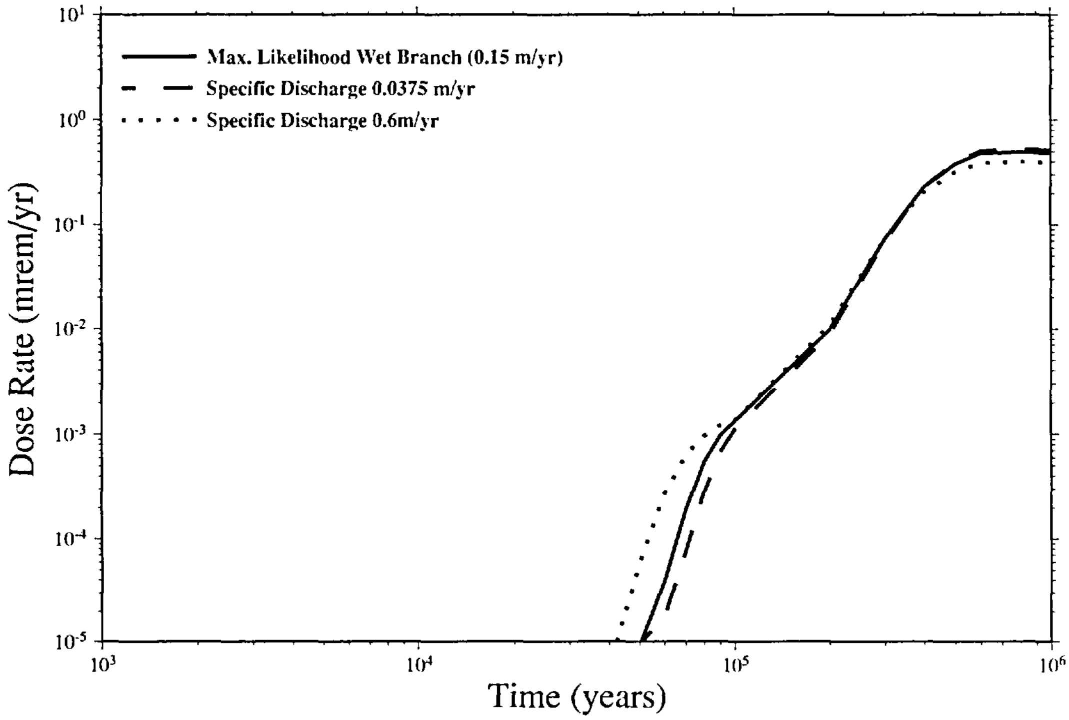

Figure 10-53
Sensitivity of Annual Dose from the Maximum Likelihood "Wet" Branch Due to Variations in the Saturated Zone Specific Discharge

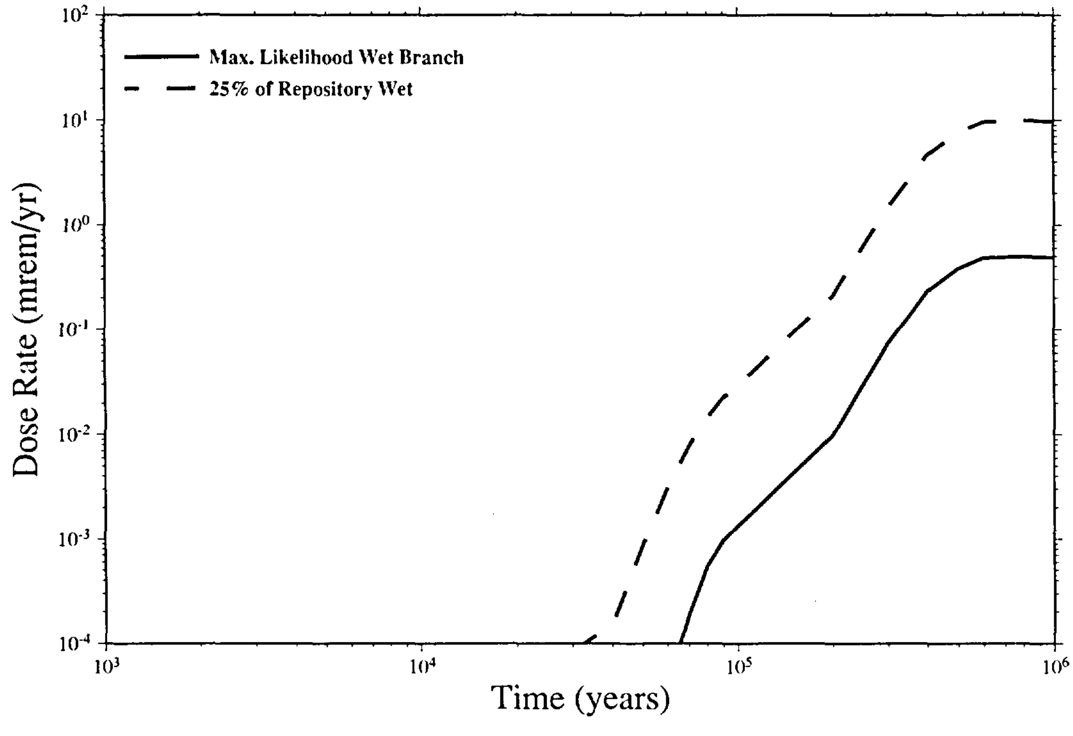

Figure 10-54
Sensitivity of Annual Dose from the Maximum Likelihood "Wet" Branch to Increasing the Fraction of the Repository that is Assumed "Wet"

Figure 10-55 shows the sensitivity to radionuclide solubility for the case for which no solubility limit for any of the radionuclides is assumed. The effect is to increase the peak dose rate only slightly. This is expected since earlier figures suggested that neptunium is not solubility-limited for the base case conditions, with ^{237}Np and its daughters contributing the most to total dose. Increasing solubility limits for the uranium isotopes will increase their release from the engineered barriers somewhat, so a small increase in the peak dose rate is expected.

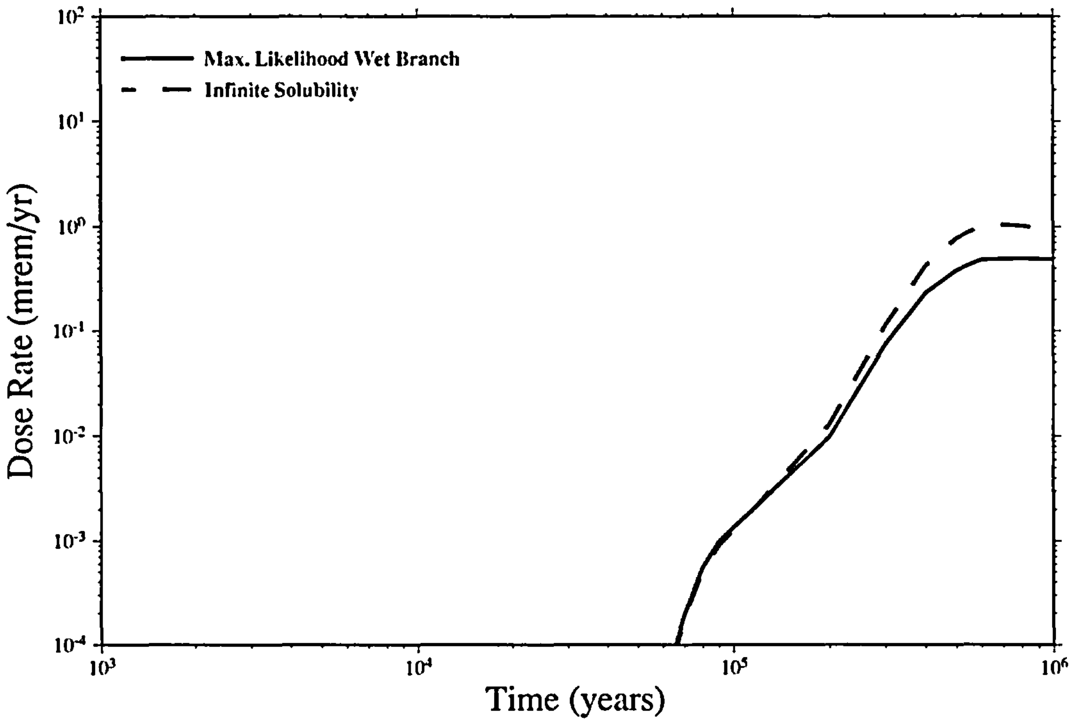

Figure 10-55
Sensitivity of Annual Dose from the Maximum Likelihood "Wet" Branch to Increasing the Solubility of all Radionuclides to Infinity

A significant amount of dilution of radionuclides is expected to occur as they move through the natural system to a position 18 kilometers downstream. For the base case from all exposure pathways, the groundwater flux within the plume at 18 kilometers was estimated to be 750 acre-feet per year. Figure 10-56 attempts to illustrate the major effect the combination of engineered and natural features has on reducing the estimated dose rates. The reasonably maximally exposed individual (RMEI) is assumed to drink approximately 0.6 cubic meters of contaminated groundwater. The "Dilution in 0.6 m^3/yr" curve illustrates the theoretical dose rate the RMEI would receive if all the radionuclides exiting the engineered barrier system annually were to remain concentrated in this amount of water. Thus, this figure illustrates that the effects of dilution reduce this theoretical dose rate by a factor of nearly 100,000.

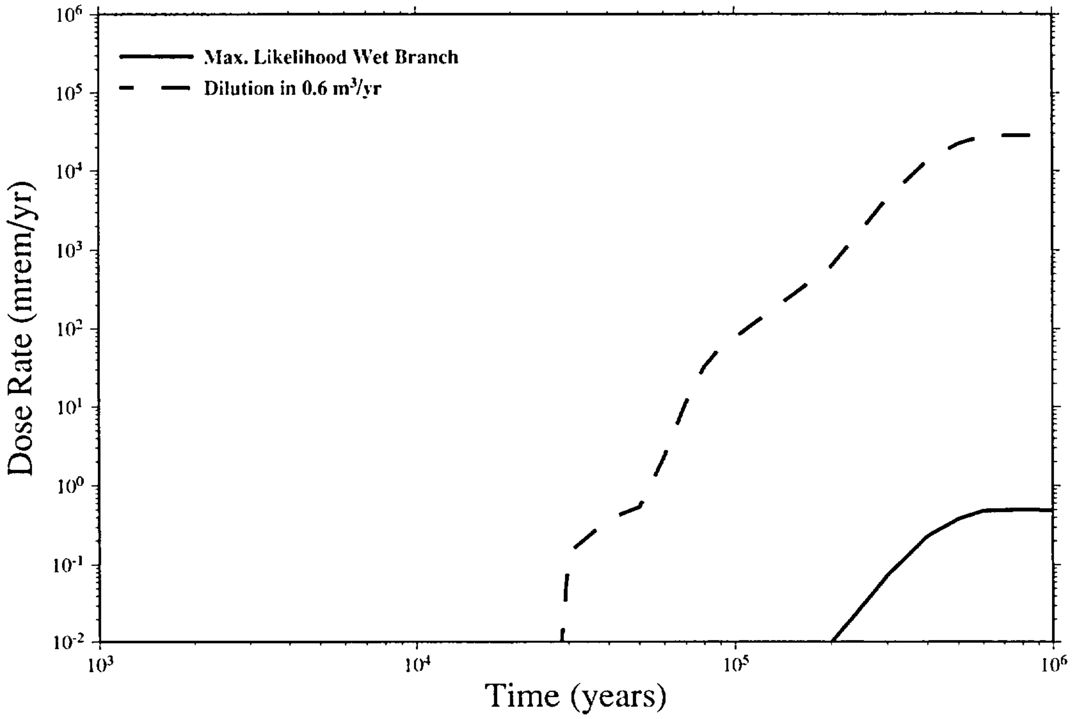

Figure 10-56
Theoretical Annual Dose from the Maximum Likelihood "Wet" Branch by Assuming No Dilution in the Natural System

The combined effect of dilution and additional travel time in the saturated zone between five and 18 kilometers downstream is illustrated in Figure 10-57. This figure suggests that the travel time for the radionuclides contributing to dose between these two positions is greater than 20,000 years.[13] The amount of additional dilution between 5 and 18 kilometers is a factor of three to four. This is likely an underestimate of the amount of dilution between these two positions based on the way that IMARC divides up the contributions from dilution. The IMARC code assumes radionuclides exiting the repository are well mixed across the entire repository cross-section by the time they reach the saturated zone. This is likely a significant overestimate of dilution in the unsaturated zone. However, studies conducted earlier [EPRI, 1998] suggest that a contaminant source of limited area entering the saturated zone will spread across the saturated zone to roughly the same degree by the time the contaminants have traveled several kilometers downstream. Thus, the amount of dilution in the total system shown in Figure 10-57 is reasonably accurate.

---

[13] While both ^{99}Tc and ^{129}I would be expected to travel through the saturated zone at a rate faster than this, neither radionuclide contributes greatly to the total dose rate.

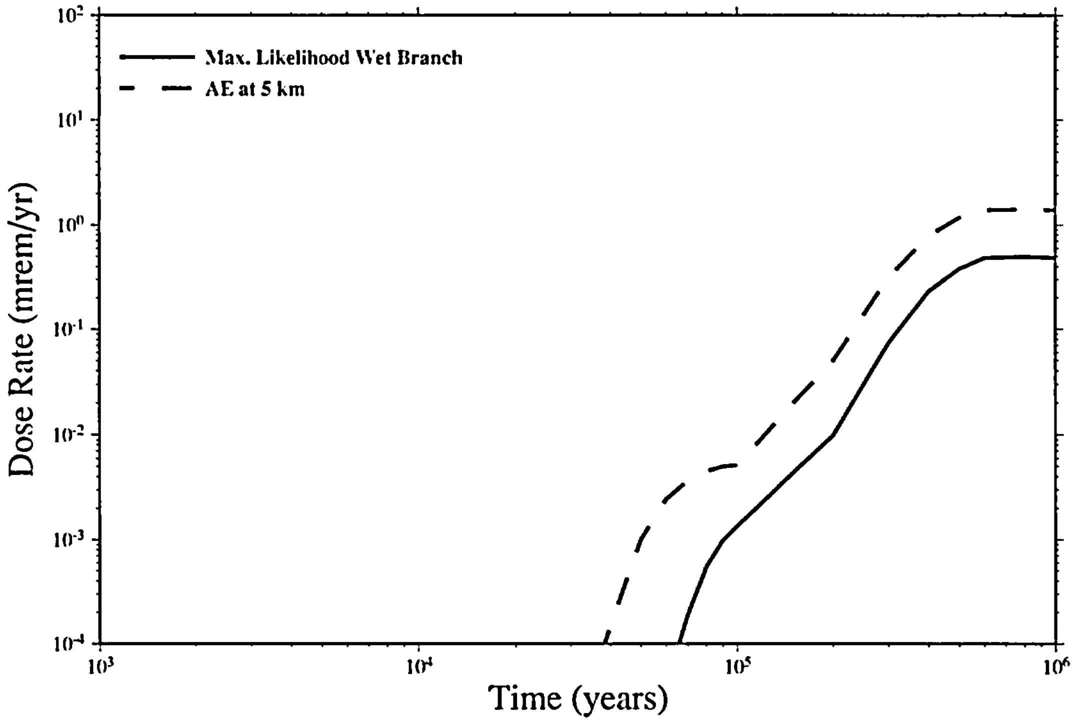

Figure 10-57
Annual Dose from the Maximum Likelihood "Wet" Branch 5 and 18 ("Max. Likelihood Wet Branch") Kilometers Downstream

10.4 References

EPRI, 1996. Smith, G. M., Watkins, B. M., Little, R. H., Jones, H. M., and Mortimer, A. M. Mortimer, *Biosphere Modeling and Dose Assessment for Yucca Mountain,* EPRI TR-107190, Electric Power Research Institute, Palo Alto CA, December 1996.

EPRI, 1998. Kessler, J. H., McGuire, R. K., Vlasity, J. A., Long, A., Childs, S., Ross, B., Schwartz, F., Shoesmith, D., Kolar, M., Apted, M., Zhou, W., Sudicky, E., Smith, G., Kozak, M., Salter, P., Klos, R., Venter., A., Stenhouse, M., Watkins, B., and R. Little, *Alternative Approaches to Assessing the Performance and Suitability of Yucca Mountain for Spent Fuel Disposal,* EPRI TR-108732, Electric Power Research Institute, Palo Alto CA, November 1998.

EPRI, 2000. Kessler, J. H., Doering, T., McGuire, R., Vlasity, J., Long, A., Childs, S., Ross, B., Schwartz, F., Shoesmith, D., Apted, M., Zhou, W., Sudicky, E., Smith, G., Stenhouse, M., and Sheridan, M., *Evaluation of the Candidate High-Level Radioactive Waste Repository at Yucca Mountain Using Total System Performance Assessment,* 100802, Electric Power Research Institute, Palo Alto CA, November 2000.

NRC, 2001. Federal Register, 66(213), 55732-55816, November 2.

A

GRAPHICAL REPRESENTATIONS OF DEFENSE-IN-DEPTH

A.1 Purpose

The purpose of this appendix is to develop a series of graphical representations of the multiple natural and engineered barriers that provide the *defense-in-depth* basis for assuring long-term safety and isolation of the geological repository at the Yucca Mountain Site. In part, ideas and concepts from various international repository programs are drawn upon.

Defense-in-depth (DID) provided by multiple barriers is internationally recognized as a guiding principle in geological disposal of nuclear waste. Furthermore, the US Nuclear Regulatory Commission (NRC) expects a final license for a geological repository to be based on at least one natural barrier and at least one engineered barrier to provide a defense-in-depth basis for the safety analysis. It would be extremely useful, therefore, if simple DID graphical representations can be developed to illustrate the type and effectiveness of various barriers within the Yucca Mountain safety concept.

A.2 Introduction

Total system performance assessment (TSPA) analyses, by definition, are comprehensive analyses. TSPA attempts to integrate all of the various features, events, and processes (FEPs) contributing to long-term isolation over the entire gamut of radionuclides that exist in nuclear waste disposed a repository. There are limitations, however, to applying TSPA to defense-in-depth analysis.

Sensitivity analyses can be performed with TSPA codes, such as IMARC, to separately investigate the impact of individual FEPs, such as infiltration rate, solubility or groundwater flow rate, on safety indicators such as dose rate or radionuclide flux at a specific position in space. While such analyses are useful, they are sometimes limited because of the different response of different dose-contributing nuclides when certain FEPs are changed. In addition, numerical calculations of dose are not readily interpretable by both technical and non-technical stakeholders. Furthermore, the linkage and coupling between two or more FEPs acting together is often not clearly identifiable from sensitivity analyses.

This report presents a series of simple graphical methods for illustrating the specific defense-in-depth basis provided by the natural and engineered barriers at Yucca Mountain. While data previously published for various sub-system performances are used in these illustrations, the actual data do not necessarily reflect the most up-to-date data or conceptual models for the

Yucca Mountain site. The purpose of this report is to illustrate how such DID graphics might be reported. The examples of this report should be considered as a beginning point for further attempts to develop simple, clear and transparent illustrations of the fundamental basis for the Yucca Mountain safety concept.

A.3 Defense-in-Depth Concepts

Although there are many different barriers and processes that contribute to any specific repository, there are two basic concepts by which safety is assured:

- delay and decay, and
- concentration constraints

As will be discussed in subsequent chapters, all of the myriad of different defense-in-depth concepts can be assigned to one (or both) of these two concepts.

A.3.1 Delay and Decay

Perhaps the simplest DID concept is related to the well-established principle of "delay and decay". That is, the longer a nuclide is contained within the repository prior to its release to the accessible environment, the greater will be the degree of radioactive decay. We can simply relate this "delay time", t_d, to the characteristic half-life of a given nuclide $i, t^i_{1/2}$, as:

$$a = \frac{t_d}{t^i_{1/2}}$$

where a is the *delay ratio* of the delay time for a given nuclide i to the characteristic half life, evaluated within a defined repository system (or barrier subsystem). By the basic physics of radioactive decay (neglecting any potential ingrowth) the mass of a radionuclide at a given time t, $m(t)$, is related to the initial mass of the same nuclide, m_0, via the half life $t_{1/2}$ as follows:

$$m(t) = m_o e^{[t(-\ln 2/t_{1/2})]}$$

Substituting for t_d and the delay ratio a gives

$$m_o e^{[t_d(-\ln 2/t_{1/2})]} = m_o e^{[a(-\ln 2)]}, \quad a \geq 0$$

Thus, if the time that a nuclide is delayed within a repository (or individual barrier) corresponds to $a = 2$, then the initial mass of a given radionuclide will have decreased by a factor of 4. If $a = 10$ (i.e., the time of containment is equal to 10 times the half life of a given radionuclide), the initial nuclide mass will decrease by a factor of 1024. For $a = 20$, the reduction factor in mass is over one million.

There are two leading types of 'delay and decay' factors that commonly arise for natural and engineered barriers; delay during *transport across a barrier* and delay in release because of *total containment.*

A.3.1.1 Delay and Decay: Transport across a Barrier

Aqueous transport paths are the most common and credible of release pathways for radionuclides from a deep geological repository. Transport may occur by

- diffusion-only, or by
- combined diffusion-advection.

The diffusive transit time, t_D, can be simply computed by the following equations:

$$t_D = R\, b^2 / D$$

$$R = 1 + \rho K_d(1-\varepsilon / \varepsilon)$$

where R is the retardation coefficient, b is the thickness of the diffusive barrier, D is the effective diffusion coefficient, ρ is the bulk density of the barrier, K_d is the sorption coefficient, and ε is the effective porosity of the barrier.

For fractured rock, the advective-diffusive transit time, $t_{A\text{-}D}$, is given as (Nagra, 1994):

$$t_{A\text{-}D} = \rho K_d\, V / Ti$$

where V is the mineral volume per unit channel width of the diffusion-accessible matrix, T is the transmissivity of the channels, and i is the hydraulic gradient[1].

For porous rock the relevant timescale for $t_{A\text{-}D}$ is:

$$t_{A\text{-}D} = R\, L / v$$

where L is the path length through the porous barrier and v is the pore velocity.

Of course for unsaturated conditions, the above diffusion and diffusion-advection equations would need to be adjusted for effects such as degree of saturation, episodic flow behavior, etc.

Figure A-1 shows a general plot of transit time[2], t_t, across a hypothetical barrier vs. half-life. The dashed, sloped line represents the condition

---

[1] In systems with distributions of characteristic flow times over different channels or fracture networks, the 50th percentile of calculated travel time could be substituted as an index for transit time.

[2] Transport by either diffusion or diffusion-advection, depending on the barrier.

$t_t = t_{1/2}$

That is to say, where the transit time for a given radionuclide equals the nuclide's half-life (i.e., the delay ratio a=1). This would lead to a rather insignificant reduction in the original mass of the nuclide by a factor of 2.

Also shown in Figure A-1 is a thick, "exclusionary" line representing the condition

$t_t = 10\ t_{1/2}$

In this case of a=10, there would be over a 1000-fold reduction in mass of the migrating radionuclide during its transit across this hypothetical barrier. As a rough rule of thumb, the mass reduction represented by this "exclusionary" line (and all of the region above this line) would eliminate any effective release of such a radionuclide at the outer side of the hypothetical system or barrier[3]. Thus, if a barrier restricts transit time for any nuclide to a region above this "exclusionary" line, the barrier provides a significant delay and decay barrier for defense-in-depth.

A.3.1.2 Delay and Decay: Total Containment

Figure A-2 shows a different type of delay and decay associated with total containment, typically provided by a canister, container, or overpack barrier immediately surrounding a nuclear waste form. The key relationship is essentially the same as for transit time. For a given containment time of t_c, the following impacts can be assured;

$t_c = t_{1/2}$;	2-fold reduction in original nuclide mass (insignificant), and
$t_c = 10\ t_{1/2}$;	1000-fold reduction in original nuclide mass (significant).

---

[3] Alternatively, a more conservative value of 20 instead of 10 half-lives would lead to a reduction in mass during transport of greater than a factor of one million.

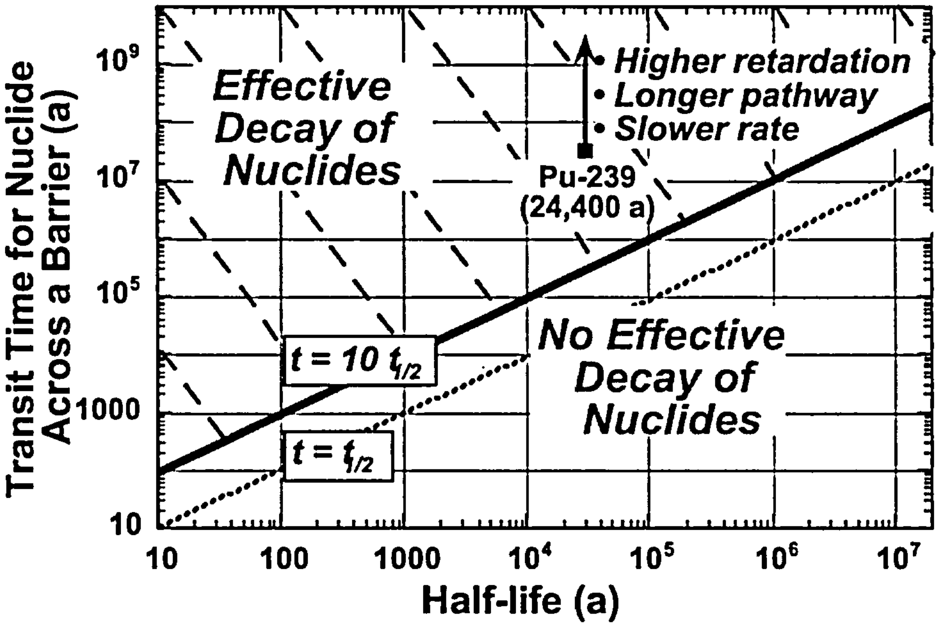

Figure A-1
Graphical Representation of Delay and Decay for Transport Phenomena through a Single Barrier.

These two conditions are represented by the dashed vertical line and the solid vertical line in Figure A-2, respectively. Nuclides with half-lives to the left of solid "exclusionary" line are, therefore, effectively eliminated from significant release by total containment[4].

---

[4] Waste form dissolution time, t_{wr}, provides an analogous but materially different factor compared to total containment time. To achieve a 1000-fold reduction in released mass because of delay arising from an extended t_{wr}, the relevant condition is approximately

$$t_{wr} > 1000\, t_{1/2}$$

Thus, it can be seen that significant reductions in radionuclide release rates attributable to delay and decay by long waste-form dissolution time (i.e., slow dissolution rate) are difficult to achieve. As noted later, however, long waste-form dissolution time may contribute to repository performance via constraints on radionuclide concentrations.

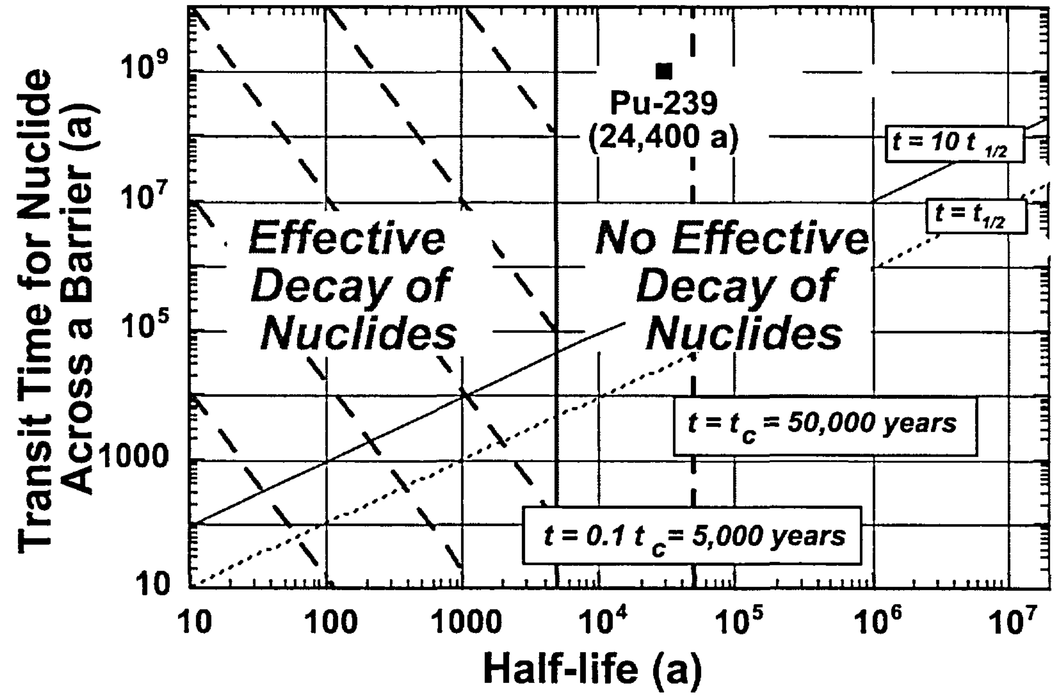

Figure A-2
Graphical Representation of Delay and Decay for a Total Containment Barrier.

A.3.1.3 Decay and Delay: Caveats on Interpretations of Diagrams

It is important to realize that the "exclusionary" lines in delay and decay plots are always the same (independent of repository system concept or given nuclide), whereas the locations of points representing specific nuclides varies from plot-to-plot depending on the type of transport, porosity, retardation, etc. That is to say, the ordinate (y-axis) values of transit time vary from case to case for each nuclide, while the abscissa (x-axis) values of half-life, of course, remain unchanged.

Note that the impacts arising from delay and decay effects are not, *per se*, relative to any particular initial mass for any nuclide. Hence, no normalization to inventory per package or number of packages is applicable. Nor are any additional impacts arising from a barrier (for example, mass-transfer constraints of pinholes in containers) accounted for in these simple diagrams. The intent is to isolate single delay and decay effects arising from specific barriers.

Furthermore, nuclides that are shown to lie outside of the regions of elimination do not necessarily imply that such nuclides will be released from the repository system at hazardous levels. For example, multiple transport barriers in series may act to further delay and decay the eventual release of such nuclides. Also, constraints to the concentrations of such nuclides are not included in these simple defense-in-depth plots (see Section A.3.2). Conversely, some actinides that nominally lie in the excluded zone do appear in safety assessment calculations. This is because of decay ingrowth from longer-lived parents that are not effectively eliminated by delay and decay.

A.3.1.4 Delay and Decay: Illustrative Example for Yucca Mountain

Figures A-3 to A-6 present some illustrations of various delay and decay barrier functions for the Yucca Mountain repository concept. These figures are meant to be illustrative, and do not reflect the latest data and conceptual models for the current repository concept.

Figure A-3 shows the case for an assumed 50,000-year total-containment time combined with estimated unsaturated advective-transport times through a 300-m thick unsaturated zone of tuff. In this case, the unsaturated zone transport was simply modeled as an equivalent porous flow, with infiltration rates of 1 mm/yr and 10 mm/yr to illustrate sensitivity.

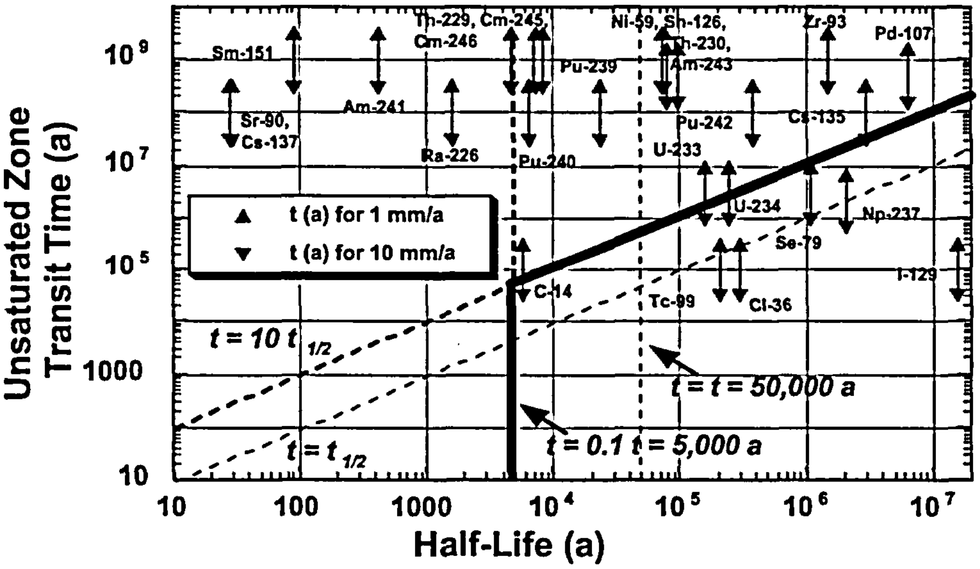

Figure A-3
Illustrative Example of Defense-in-Depth Diagram for an Assumed 300-m Unsaturated Zone Transport at Yucca Mountain. Two calculations for infiltration rate of 1 mm/yr. and 10 mm/yr. are made. A 50,000-year total containment time, provided by the integrated set of containment barriers, is also assumed.

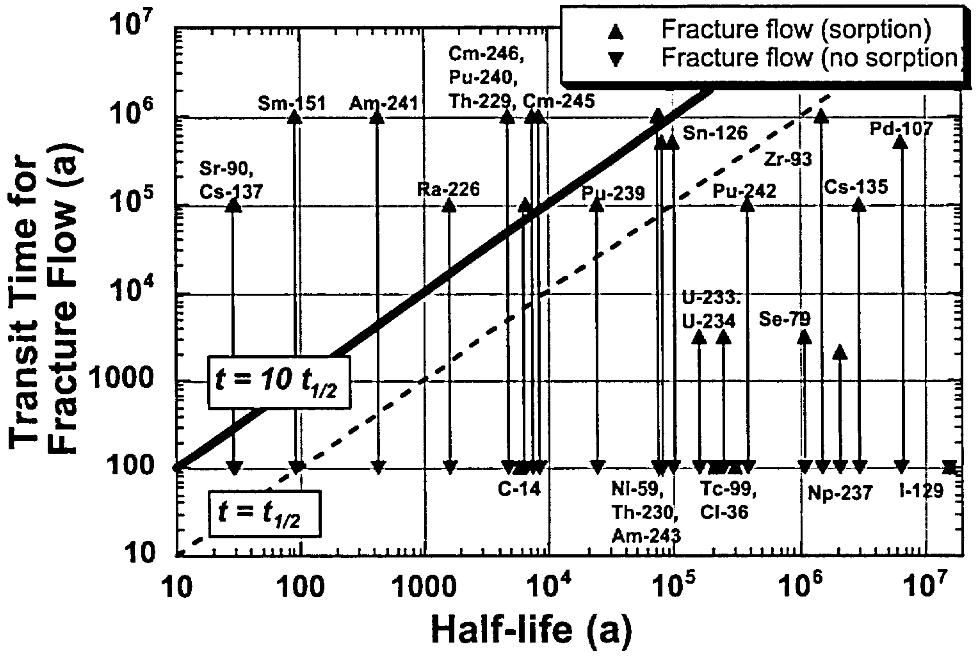

Figure A-4
Illustrative Example of Defense-in-Depth Diagram for an Assumed 300-m Unsaturated Zone Transport at Yucca Mountain with Postulated Rapid Fracture Flow. Two calculations are made for the case of normal sorption and a speculative case of no sorption.

Figure A-4 shows the same 50,000-yr containment time combined with the potential impact of fast fracture flow in this same 300-m unsaturated zone. If the assumed high flow of 20 mm/yr., the transit times for cases with and without sorptive retardation are illustrated.

Figure A-5 presents delay and decay effects potentially attributable to transit through either 5-km or 20-km saturated zone with a 10 m/yr. assumed flow rate and including retardation. The same 50,000-yr. total containment time is also shown.

Finally, a delay and decay case from the 1995 Total System Performance Assessment report (CRWMS M&O, 1995) is presented in Figure A-6 for a capillary-breaking backfill (Richards barrier). Also shown are defense-in-depth contributions arising from an assumed 50,00-yr. containment time and a rather bounding value for dissolution time of the spent fuel matrix equal to 450 years. There are several features and interpretations to note. First, even a 50,000-year containment time does little to eliminate key nuclides (except for that 50,000 years of containment, of course), whereas a capillary backfill will effectively eliminate all radionuclides except I-129 and Cl-36. Also note that if either the capillary backfill or the 50,000-year total containment time is robustly assured (for example, by consideration of multiple containment barriers), then the matrix dissolution time of spent fuel provides a negligible defense-in-depth "barrier".

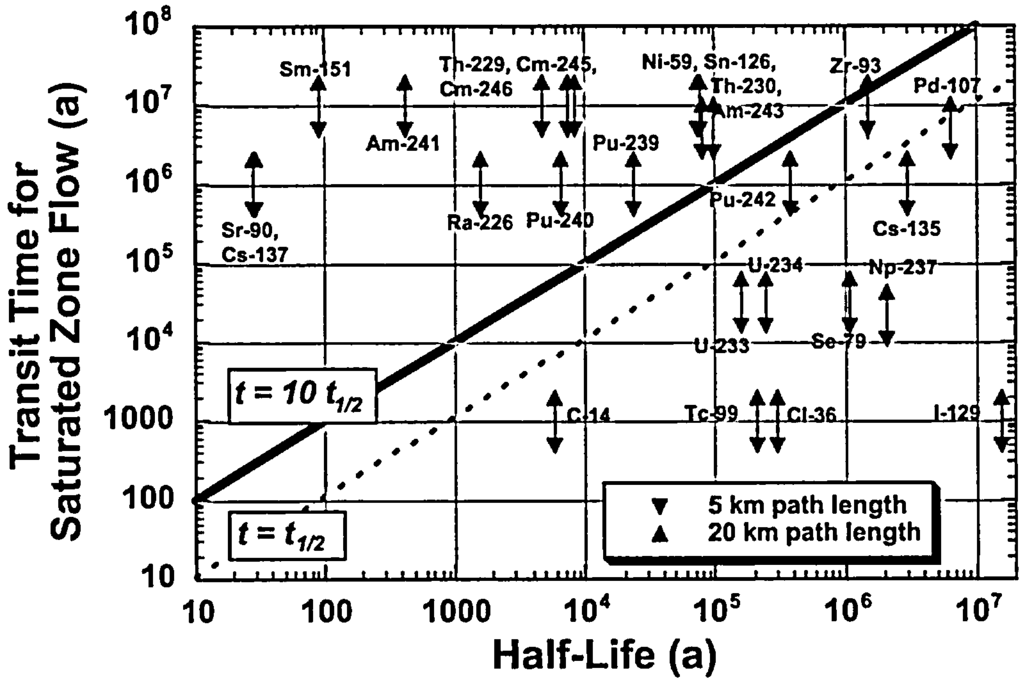

Figure A-5
Illustrative Example of Defense-in-Depth Diagram for Saturated Zone Transport at Yucca Mountain. Two calculations for path lengths of 5 km and 20 km are made.

In Figure A-6, two transit times for I-129, a persistent problem nuclide, are shown. The lower "I-129" represents transport assuming $K_d = 0\ kg/m^3$ for the capillary barrier material (crushed and sized tuff). The "I-129*" point represents transit time if an extremely small, yet non-zero value of $K_d = 0.0001\ kg/m^3$ is used for this same material in the calculations. There is, at this time, limited evidence for such a non-zero K_d. The purpose of this speculative calculation, however, is to shown the potential sensitivity and importance of testing the conventional assumption that anionic species have no sorptive behavior toward repository materials.

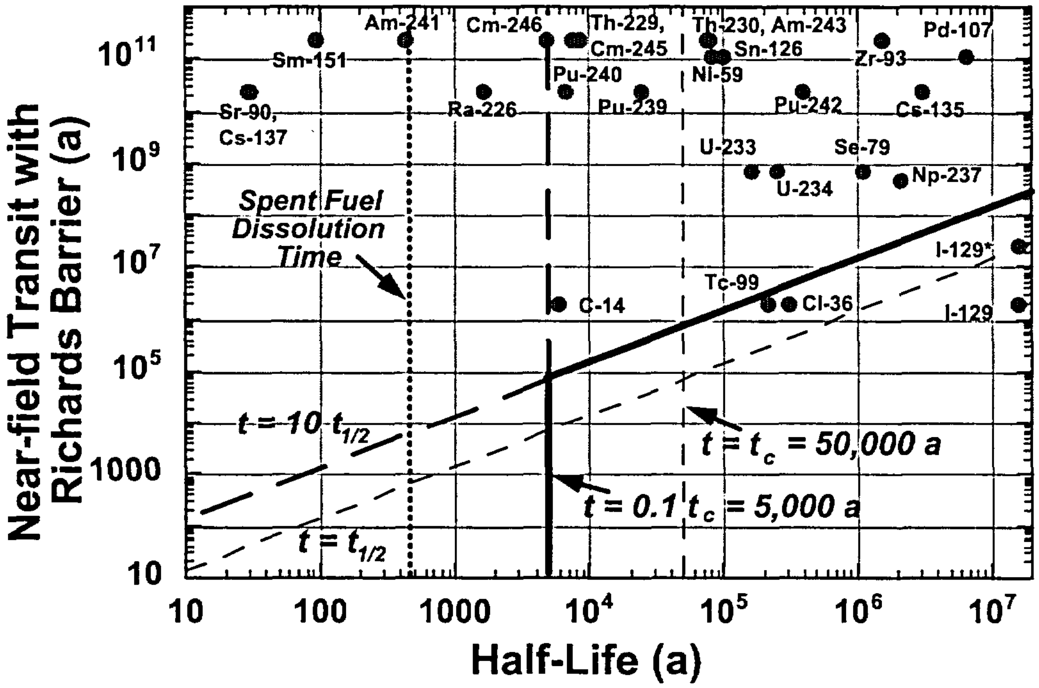

Figure A-6
Illustrative Example of Defense-in-Depth Diagram for the TSPA-95 Capillary Barrier Concept at Yucca Mountain. Two calculations for path lengths of 5 km and 20 km are made. Note that the "I-129*" point assumes a K_d = 0.0001 kg/m^3 for the capillary barrier, rather than K_d = 0 kg/m^3. A 50,000-year total containment time, provided by the integrated set of containment barriers, is also assumed. Also shown is a highly conservative dissolution time for the spent fuel matrix of 450 years.

A.3.1.5 Delay and Decay: Yucca Mountain Results in Perspective

Based on Figures A-3 to A-6, it is clear that the delay and decay functions of either natural or engineered barriers are unlikely to assure the elimination of *all* radionuclides based on a 1000-fold or more decay in the original inventory. In particular, extremely long-lived (half lives > 10^5 years) radionuclides, such as Np-237, Tc-99, Se-79, Cs-135, Cl-36 and I-129, may not be eliminated. Indeed, these are typically the key radionuclides that appear in safety assessments for a repository at Yucca Mountain.

A.3.2 Concentration Constraints

As Section A.3.1 has illustrated, various delay and decay functions and barriers can promote effectively complete decay of the original inventory of many radionuclides within the repository.

There remain, however, a category of long-lived, typically low-sorbing and high-solubility radionuclides for which delay and decay cannot fully assure safe isolation within a geological repository.

The initial concentrations of such long-lived radionuclides within spent fuel and HLW (mass of nuclide per mass of waste form) are unacceptably high to meet compliance levels (e.g., dose rate, drinking water concentration, annual flux) for direct release to the environment. In some manner, these initially high concentrations must be reduced to target compliance levels. Clearly such reduction must be associated with the release and migration necessary to transport the nuclides from the emplaced waste form to the accessible environment.

Figure A-7 qualitatively shows potential factors that may reduce the concentrations of radionuclides during release and migration. At this stage no simple graphical concepts have yet been devised to quantitatively illustrate these concentration constraints. Figure A-7 attempts to show the gradual decrease in radionuclide concentration by showing how the concentration in each successive box represents a dilution (by an arbitrary factor of 1000) attributable to the stated processes or barriers.

The following sub-sections review FEPs associated with each step in Figure A-7, although it must be stressed that many of these factors are speculative with respect to Yucca Mountain and have not been formally introduced into most repository safety assessments. Thus, the following text is intended to serve as a beginning point for further discussions and sensitivity analyses.

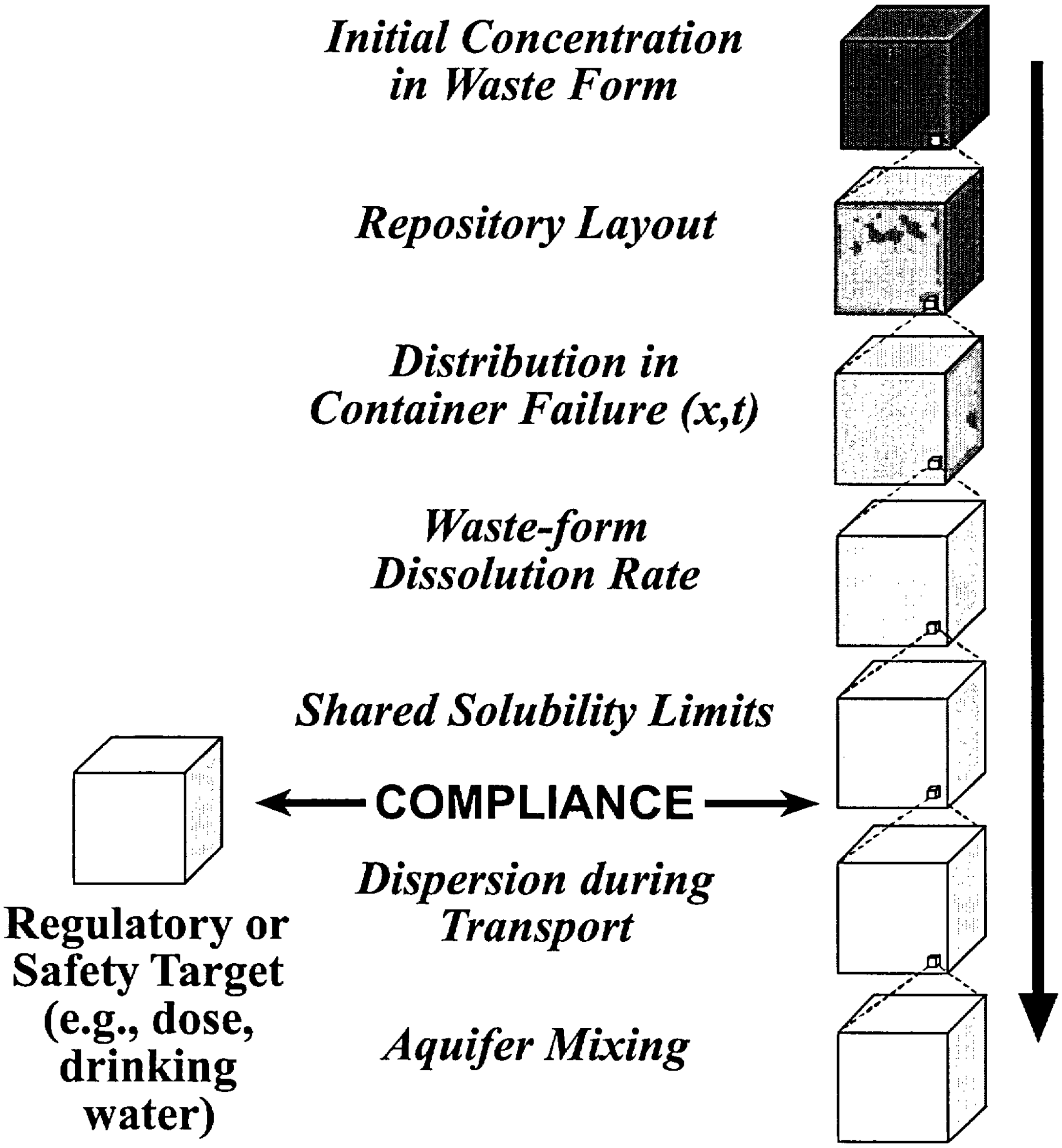

Figure A-7
Illustration of Factors that Constrain and Reduce the Concentration of radionuclides during Release and Migration from a Geological Repository.

A.3.2.1 Repository Layout

The spatial distribution of waste packages (package pitch, spacing between emplacement tunnels, etc.) provides the first factor in the reduction of radionuclide releases. The simplest method for repository total system performance assessment is to calculate the performance of a single package, then multiply by the number of packages to get a source term. While such a simplification may be satisfactory for repositories with a small number (<1000) of waste packages, as the number of waste packages becomes several thousand or more this pessimistic assumption should be reconsidered.

First, although each package retains the same initial solid concentrations of radionuclides in the waste form, the spatially averaged concentrations of radionuclides decreases. In the case of Yucca Mountain, there may be some reduction in release because of this repository layout consideration, for example reducing the number of packages that will be encountered by dripping water from fractures.

Second, the release plumes of adjoining failed packages may overlap. If there is a diffusive transport step, release may be reduced because of this overlap. This is because the rate of diffusive transport will scale with the gradient in concentration; the effect of overlapping release plumes from adjoining packages will be to reduce concentration gradients, hence reduce the rate of diffusive transport.

A.3.2.2 Distribution in Containment Failure over Time and Space

The release of certain radionuclides is not constrained by either waste-form dissolution rate or shared solubility limits (see later sections), for example the instant release fraction (IRF) of I-129, Cs-135 and other volatile fission products produced in spent fuel. Because the abundance of these IRFs can be several percent of their total inventory, their release as a "pulse" can dominate both the early, as well as peak, release rates for the repository system.

The KBS-3 analysis of disposal of spent fuel in long-lived (about one million years) copper containers was the first to identify and deal with this issue of pulse release of long-lived IRF nuclides, notably I-129. It was assumed that the containment failure of waste packages began at 100,000 years and proceeded to 1,000,000 years at a uniform rate of failure. This assumed (and arbitrary) distribution over time of containment failures effectively decreased the calculated peak dose to an acceptable value.

The Environmental Impact Statement report by the Atomic Energy of Canada in 1994 (Johnson et al, 1994) also explored the impacts of a distributed containment failure. In this case, a more defensible basis was proposed for this distribution; the different temperature-time histories of waste packages located in the center (hottest location), edge (cooler location), and corners (coolest location) of a repository. These different temperature-time histories were then factored into corrosion-rate models for the container material (Ti in this case) to generate a distribution of container failures over both time and space.

To be effective, the time-distribution of failures must be broader than the characteristic time interval for the pulse of released radionuclide. Say that the characteristic width (i.e.,, time interval of the half maximum in peak concentration) of I-129 reaching the accessible environment is 20,000 years because of dispersion and other factors. Thus, consideration of distributed container failure will only be effective in reducing peak concentration (hence, dose rate) if the failures occur over a time significantly greater than 20,000 years.

A.3.2.3 Waste-form Dissolution Rate

It was noted in Section A.3.1 that the dissolution time for a nuclear waste form is not a particularly effective delay and decay factor. It can, however, be effective in limiting the concentration of radionuclides. A simple model for contrasting the waste-form dissolution rate, j_{WF}, and the rate of mass transfer away from the waste-form surface, m_{WF}, (Zavoshy et al , 1985) evaluates the relative as a "flux ratio", R_f, such that:

$$R_f = j_{WF}/ m_{WF},$$

When R_f is large (typically when m_{WF} is small), the long-term concentration at the waste form surface will equal the shared solubility limit for that nuclides (see next section). However, when R_f is small, the long-term concentration of radionuclides at the waste form surface is controlled by the waste-form dissolution rate at a value much lower than the shared solubility limit.

Thus, depending on the relative magnitudes of shared solubility limit and dissolution rate of the waste-form matrix, the concentration of a specific radionuclide may be constrained at the waste-form surface by either mechanism. Note that other factors, such as concentration of the nuclide within the waste-form matrix, mass transport process and rate, porosity, etc., also will effect which mechanism controls the long term-concentration of a nuclide at a waste-form surface.

A.3.2.4 Shared Solubility Limits

As noted in the previous section, the influence (or lack of influence) of solubility limits on the release behavior of radionuclides is strongly related to the relative magnitude of the waste-form dissolution rate and the rate of mass-transport away from the waste-form surface. Nonetheless, because the type and reliability of data between dissolution rate and solubility limits are much different, it is worthwhile to separately examine solubility constraints on radionuclide concentrations.

This section is called "Shared Solubility Limits" for several important reasons. First, it is assumed that all radioisotopes of a radioelement (e.g., Pu) will behave in a chemically identical manner. In particular, that any solid phase that incorporates one radioisotope of a radioelement will equally incorporate all other radioisotopes in ratios determined by their absolute mass abundances in the system at any specified time. Because the different radioisotopes of a radioelement decay at different rates, the relative abundances of radioisotopes in a solid will change over time. With increasing time, the proportion of the longer-lived radioisotopes will increase because of the relatively faster decay of the shorter-lived radioisotopes. Thus, there can be an actual increase over time for the effective solubility of long-lived nuclides because of this shared solubility phenomena.

Second, stable isotopes for radioelements must also be considered. There are, for example, stable isotopes of Ni, Nb, Zr, Se, Sr, Pd, Sn and Sm all exist in spent nuclear fuel components. The shared solubility limits of phases that incorporate both stable isotopes with radioisotopes leads to a reduction in the effective solubility limit for the radioisotopes.

Third, the concept of co-precipitation of multiple radioelements within relatively few alteration solids is getting more and more attention internationally. It is unreasonable to assume that each radioelement to form its own solubility-limiting phases, which is currently the assumed conceptual model for shared solubility in most performance assessment calculations. All radioelements other than U occur at trace abundances, plus many have similar ionic size and charge (e.g., actinides) allowing for ready substitution within solid precipitated phases. Furthermore, natural glasses and minerals are found to breakdown under hydrous conditions to form relatively few phases containing extensive solid-solutions of trace elements. It seems more likely, therefore, that most, if not all radionuclides, will be co-precipitated into one or two alteration phases arising from irreversible dissolution of chemically unstable waste forms.

These few co-precipitated phases, rather than the multitude of postulated individual solid phases, will imposed shared solubility constraints on radionuclide concentrations. The potential, as yet undemonstrated anywhere, is that co-precipitation may lead to lower (perhaps by many orders of magnitude) concentration constraints for radionuclides. This mechanism may be of extreme importance to nuclides such as Np-237 and Cs-135 that are long-lived yet are assumed to have high solubility limits in current assessment of Yucca Mountain.

A.3.2.5 Dispersion during Transport

Dispersion during transport is a well-known process. The extent that this occurs for Yucca Mountain will be a function of a number of factors, such as matrix interactions, path length, etc. It is recommended that the portions of the IMARC code now involved with calculating far-field transport be modified to calculate such dispersive effects on concentration, perhaps making a ratio of the concentration at the "inlet" side of a natural; barrier and the calculated steady-state concentration at the "outlet" side.

A.3.2.6 Aquifer Mixing

In certain repository concepts there can be a significant reduction in the concentration of radionuclides during the final "extraction" or removal from the geological setting. In the recent H12 safety assessment in Japan, for example, a dilution factor of 10^9 was assumed for the mixing in both a near-surface aquifer prior to well extraction, as well as dilution for direct discharge into a river system. Obviously, whether such a mechanism and large dilution factor is applicable to Yucca Mountain, and to what extent (i.e., dilution factor), will depend on a number of repository and regulatory factors.

A.4 Conclusions

This report describes some new ideas on how to graphically portray the defense-in-depth performance of individual engineered and natural barriers at Yucca Mountain. Concepts for *delay and decay* functions readily lend themselves to graphical representation, including transport and containment times.

A.5 References

CRWMS M&O, 1995, Total System Performance Assessment-1995: An Evaluation of the Potential Yucca Mountain Repository, B00000000-01717-2200-00136, REV 01, Us. Department of Energy, Las Vegas, NV.

JNC, 1999, H12: Project to Establish the Scientific and Technical basis for HLW Disposal in Japan, Japan Nuclear Cycle Development Institute, Tokyo, Japan.

Johnson, L., D. LeNeveu, D. Shoesmith, D. Oscarson, M. Gray, R. Lemire and N. Garisto, 1994, The Disposal of Canada's Nuclear Fuel Waste: The Vault Model for Postclosure Assessment, AECL-10714, Atomic Energy of Canada, Limited, Pinawa, Manitoba, Canada.

Nagra, 1994, Kristallin-I Safety Assessment Report, Technical Report 93-22, National Cooperative for the Disposal of Radioactive Waste, Baden, Switzerland.

Posiva, 1999, Safety Assessment of Spent Fuel Disposal in Hastholmen, Kivetty, Olkiluoto and Romuvaara: TILA-99, Posiva 99-07, Posiva Oy, Helsinki, Finland.

Zavoshy, S., P. Chambre and T. Pigford, 1995, Mass Transfer in a Geological Repository, Mat. Res. Soc. Symp. Vol. 44, Materials Research Society, Pittsburgh, PA, pp. 311-322.

B

VENTILATION EFFICIENCY

If the initial heat output is Q_0 and it decays with a half-life $t_{½}$, the heat output at any time is $Q_0e^{-\lambda t}$ where

$$\lambda = \frac{\ln 2}{t_{1/2}} \tag{B-1}$$

For ventilation efficiency F [The ventilation efficiencies in the TSPA and IMARC are constants. However, they are derived by averaging over the results of temperature-dependent simulations.] and duration T, the total amount of heat removed is

$$H = F\int_0^T Q_0\, e^{-\lambda t} dt = \frac{F\ Q_0}{\lambda}\left[1 - e^{-\lambda T}\right] \tag{B-2}$$

Inserting the cesium-137 half-life of 30.17 yr, the assumed ventilation efficiency of 80%, and the cold-repository ventilation period of 300 yr, we obtain

$$\frac{H}{Q_0} = 34.8\,\text{yr} \tag{B-3}$$

To calculate the time needed to remove the same amount of heat with 94% ventilation efficiency, we rearrange Eq. (B-2) as

$$T = \frac{-1}{\lambda}\ln\left(1 - \frac{H\lambda}{F\,Q_0}\right) \tag{B-4}$$

For $F = 0.94$ and $H/Q_0 = 34.75$, this yields

$$T = 82.6 \tag{B-5}$$

C

REVIEW OF MODELLING OF UPTAKE OF RADIONUCLIDES INTO FRUIT

C.1 Introduction

An initial biosphere assessment methodology had been developed for EPRI in 1996 [Smith et al, 1996]. Further assessment studies were undertaken in 1998, to take account of releases via natural groundwater discharges, instead of via a well sunk into a contaminated aquifer [EPRI, 1998]. The crops considered in these assessments were grain, root vegetables, green vegetables, fruit and pasture.

Many new data are available now concerning the Yucca Mountain site itself and other more generically defined parts of the system under assessment. For instance, modelling of the processes of interception and subsequent weathering and transfer into and within irrigated crops could be improved, taking account of the BIOMASS ERB2A model which has been subject to review by modelling groups in several countries [BIOMASS 2001a]. Also, in the assessments undertaken for Yucca Mountain, the interception and uptake of radionuclides by fruit were modelled in the same way as those for green vegetables. These could be improved by taking account of the work undertaken by the BIOMASS Fruits Working Group on modelling the uptake of radionuclides by fruit, in particular the conceptual fruits model developed by 18 participants from several countries [BIOMASS 2001b].

This annex describes the work of the BIOMASS Fruits WG with respect to modelling the uptake of radionuclides into fruit and the relative importance of processes that should be included in a fruit model. The formulation for uptake of radionuclides by crops in the BIOMASS ERB2A model is reviewed to assess its suitability for modelling the uptake of radionuclides into fruit by comparing it to the matrix developed by the BIOMASS Fruits WG. Parameter values specific to fruit are provided for the ERB2A model.

C.2 The BIOMASS Fruits Conceptual Model

The transfer of radionuclides to fruit is complex and involves many interactions between biotic and abiotic components. The BIOMASS Fruits Working Group therefore adopted a systemic approach based on the RES matrix methodology to develop a conceptual fruit model [BIOMASS, 2001b]. The matrix that was developed for atmospheric deposition of radionuclides and subsequent uptake into fruit is shown in Figure C-1. Although the matrix is based on atmospheric deposition as source of contamination, it can also be applied to irrigation water as source term.

Air	deposition, interception rainfall	Deposition, interception rainfall	Deposition, interception, rainfall	deposition, interception, rainfall			deposition intercept., rainfall	deposition intercept. rainfall
resusp.	**Leaf**	translocation	wash-off	wash-off			leaf-fall, pruning	translocation
resusp.	translocation	**Wood & stem**	throughfall + stemflow	throughfall + stemflow	translocation		leaf-fall, pruning	translocation
resusp.	splash	splash	**Soil**	root uptake	root uptake	uptake		resusp.
resusp.	splash	splash	migration	**Ground cover**			leaf-fall, dieback	splash/ resusp.
		translocation	exudation	exudation, root uptake	**Roots**	exudate transfer, mycorrhiza	dieback	
			bioturbation	bioturbation, excretion	mycorrhizal processes	**Micro-orgs**	excretion	
resusp.	resusp.	splash	dissolution	root uptake, breakdown		uptake	**Debris**	resusp.
resusp.	translocation		fruit-fall	fruit-fall			wash-off	**Fruit**

Figure C-1
Interaction matrix with 9 diagonal elements describing the contamination of fruit trees following a deposit from atmosphere

The elements of the leading diagonals in the matrix represent the components of a fruit system. The interactions between these components are represented in the off-diagonal elements. The selection of the diagonal elements is an essential part of this methodology. The Fruits WG adopted an iterative approach over several meetings and the 18 members eventually reached consensus on the components that would be included. The final matrix was used to collect participants' views on the relative strength of the interactions. Although it was recognised that the relative importance of different processes would be nuclide dependent, the intention was to develop guidance for a generic model. The strength of the interactions were ranked on a scale of zero to five:

0	**no interaction**
1	**weak**
2	**light**
3	**medium**
4	**strong**
5	**critical**

The results are listed in Table C-1.

The ranking in Table C-1 was used as a basis for assessing whether the formulation for calculating uptake of radionuclides by crops in the BIOMASS ERB2A model was adequate for calculating the uptake of radionuclides by fruit.

C.3 The BIOMASS ERB2A model

This model has been developed for calculation of the dose resulting from radionuclide contamination of groundwater. In the case where water from a contaminated well is used for irrigation of crops, the radionuclide concentration in the bulk cultivated soil compartment, C_s, for radionuclide N, Bq m^{-3}, is calculated using equation (8-6) in Section 8.2.5.2.1 of the main text.

The annual individual dose from the consumption of agricultural crops is given by equation (8-7) in Section 8.2.5.2.2 in the main text.

The C_{crop} term (the radionuclide concentration in the edible part of the crop, Bq kg^{-1} (fresh weight of crop)) is calculated using equation (8-9) in the main text.

It should be noted that it is assumed that the crop can be contaminated due to:

- internal uptake of contaminants from the cultivated soil compartment into the crop via the roots (represented by the $\frac{CF_{crop}C_s}{(1-\theta_t)\rho}$ term);
- external contamination of the crop due to deposition of re-suspended sediment from the surface soil compartment (represented by the $\frac{S_{crop}C_s}{(1-\theta_t)\rho}$ term);
- irrigation (represented by the $I_{crop}V_{irr}C_w$ term).

It is assumed that contamination can be lost due to:

- food preparation (represented by F_{p1}, F_{p2} and F_{p3} terms);
- weathering of the external contamination to the soil (represented by the e^{-WT} term).

The parameters in the above equations were compared with the processes in the BIOMASS Fruits Matrix (Table C-1). Of the 30 processes in the Fruits Matrix, 16 are represented in the ERB2A model (either explicitly or implicitly). The processes that are not represented mostly have a ranking of 2-3 (light to medium interaction), i.e. the most important processes (ranking 2.8 to 4.9, medium to critical interaction) are all represented in the ERB2A model. The processes that are not represented mostly relate to the omission of ground cover component and action of micro-organisms in the ERB2A model. The BIOMASS Fruits WG defined ground cover as 'non-fruit' vegetation within the stand'. This relate to certain agricultural practices and may not be necessarily applicable to fruit cultivation in the Yucca Mountain area. As to the action of micro-organisms, although it is known that that they are important within the rhizosphere and on the phylloplane, we do not have yet a good understanding of these interactions. There is also a lack of data to allow modelling of these interactions.

It can therefore be concluded that the formulation for modelling uptake of radionuclides by crops in the BIOMASS ERB2A model is adequate for modelling the uptake of radionuclides by fruit. The only change that would be required is to add 'fruit' as a crop type. For the purposes of this type of assessment, it is not considered necessary to distinguish between different fruit types, a general (generic) classification of fruit will suffice. This assumption is based on the results of the model intercomparison exercises undertaken by the BIOMASS Fruits WG [BIOMASS 2001b]. Modelling of the transfer of Cs-137, Sr-90 and I-129 to apples (tree fruit), blackcurrants (shrub fruit) and strawberries (herbaceous fruit) was based on continuous annual atmospheric deposition of 1 kBq m^{-2} uniform deposition to soil plus plant as source term. The modelled radionuclide concentrations in fruit are presented in Table C-2 as the average of the modelled results. For each radionuclide, the concentration in the various fruits differs only by about a factor of 2.

Table C-1
Comparison of the ERB2A Formulation with the Processes in the BIOMASS Fruits Interaction Matrix

Influence of	On	STRENGTH OF INTERACTION (0=NONE; 5="CRITICAL") (n=18)	Represented in ERB2a
Air	Leaf	4.9	Yes
Soil	Roots	4.2	(yes)
Air	Soil	4.1	Yes
Air	Ground Cover	3.8	No
Leaf	Fruit	3.5	Yes
Leaf	Soil	3.4	Yes
Leaf	Debris	3.2	(Yes)
Leaf	Wood & Stem	3.1	(Yes)
Wood & Stem	Fruit	3.1	(Yes)
Roots	Wood & Stem	2.9	(Yes)
Air	Wood & Stem	2.9	(Yes)
Soil	Micro-organisms	2.9	No
Air	Fruit	2.8	(Yes)
Debris	Soil	2.8	Yes
Ground Cover	Wood & Stem	2.8	No
Soil	Ground Cover	2.7	No
Wood & Stem	Leaf	2.6	(Yes)
Wood & Stem	Soil	2.6	No
Micro-organisms	Roots	2.5	No
Wood & Stem	Roots	2.4	No
Leaf	Ground Cover	2.4	No
Air	Debris	2.3	No
Wood & Stem	Debris	2.3	(Yes)
Soil	Fruit	2.3	(Yes)
Debris	Ground Cover	2.3	No
Soil	Wood & Stem	2.2	(Yes)
Fruit	Soil	2.2	No
Soil	Air	2.0	No
Roots	Micro-organisms	2.0	No
Micro-organisms	Debris	2.0	No

(Yes): Process is implicitly represented

Table C-2
Radionuclide Concentration in Fruit as the Average of Modelled Results

Radionuclide	Averaged radionuclide concentration (modelled)		
	Apples	Blackcurrants	Strawberries
Cs-137	45	83.5	102.5
Sr-90	55	73	100
I-129	5.5	8.9	16.6

C.4 Application of the updated BIOMASS ERB2A approach to EPRI

The current formulation in the ERB2A model for modelling the uptake of radionuclides by crops will be adequate for modelling the uptake of radionuclides by fruit. The only change that is required is to add 'fruit' as a crop type. Parameter values relating to fruit also need to be entered in the model. This may present a problem, as, apart from Cs-137 and, to a lesser extent, Sr-90, there is a general lack of data on the uptake and behaviour of radionuclides in fruit [FWG, 2001]. The required parameters, with parameter values for fruit, are listed in Table C-3. In the absence of fruit specific values, those for green vegetables have been substituted.

Table C-3
Parameter Values for Fruits

Parameter	Symbol	Value for fruit				Ref	Note
		I-129	Tc-99	Se-79	Np-237		
fraction of radionuclide in spray irrigation water that is initially deposited on standing biomass	I_{crop}	3.0E-1	3.0E-1	3.0E-1	3.0E-1	1	(1)
fraction of absorbed activity that is translocated to the edible portion of the plant by the time of harvest (translocation fraction),	F_{trans}	1.0E0	1.0E0	1.0E0	1.0E0	3	(2)
fraction of intercepted radionuclide initially deposited onto the plant surface that is absorbed from external surfaces into plant tissues	F_{abs}	4.8E-1	4.8E-1	4.8E-1	4.8E-1	3	(3)
is the fraction of external soil contamination on the edible part of the crop retained after food processing	F_{p1}	1.0E-1	1.0E-1	1.0E-1	1.0E-1		(4)
fraction of the internal contamination associated with the edible part of the plant at harvest that is retained after food processing has occurred	F_{p2}	8.0E-1 to 1.0E0	(5)	(5)	(5)	1, 2	(6) (5)
fraction of external contamination from interception that is retained on the edible part of the crop after food processing	F_{p3}	1.0E0	1.0E0	1.0E0	1.0E0	2	(7)
Removal rate of radionuclide deposited on plant surface by irrigation by weathering processes (weathering rate) including mechanical weathering, wash-off and leaf fall, y^{-1}	W	3.2E1	3.2E1	3.2E1	3.2E1	4	(8)
Crop concentration factor	C_f	1E-2	1.0E+1 (9)	1.0E0 (4)	1E-3 (10)	5	

1. BIOMASS, 2001b
2 Green, 2001
3. Carini and Bengtsson, 2001
4. Mitchell, 2001
5. Carini, 2001

(1) Generic value for fruit (fruit plus plant).
(2) Most of the available data on translocation from the aboveground part of the plant to fruit do not differentiate between absorption of radionuclides from the external to internal plant parts and subsequent translocation to fruit.
(3) Values vary as a function of fruit type and radionuclide, but the listed value is considered appropriate for general use.
(4) No specific data for fruit, taken to be the same as for green vegetables.
(5) Assumed to be the same as for I-129.
(6) The lower value is for canned/stewed fruit, or fruit juice. The higher value is for washed fruit consumed raw.
(7) Cautious value that is considered appropriate for general use.

(8) Default value in the SPADE model (UK Food Standards Agency).
(9) In the absence of data for Tc, data for Mn is substituted.
(10) Value derived from decreasing trend in fruit CF for U, Pu and Am (from Carini, 2001).

C.5 References

BIOMASS (2001a) ERB2A revised mathematical model and results. BIOMASS Theme 1, Task Group 6, Note 5, Version 2. February 2001. International Atomic Energy Agency, Vienna.

BIOMASS (2001b). Transfer of radionuclides to fruit. BIOMASS Theme 3, Fruits Working Group TECDOC (in print). International Atomic Energy Agency, Vienna.

Carini F and Bengtsson G (2001). Post-deposition transport of radionuclides in fruit.. Journal of Environmental Radioactivity, **52** p 215-236.

Carini F (2001). Radionuclide transfer from soil to fruit. Journal of Environmental Radioactivity, **52** p 237-279.

EPRI (1998). Alternative approaches to assessing the performance and suitability of Yucca Mountain for spent fuel disposal. EPRI Report No TR-108732. Electric Power Research Institute, Palo Alto.

Green, N (2001). The effect of storage and processing on radionuclide content of fruit. Journal of Environmental Radioactivity, **52** p 281-290.

Mitchell N G. (2001). Model for radionuclide transfer to fruits and data requirements. Journal of Environmental Radioactivity, **52** p 291-307.

Smith G M, Watkins B M, Little R H, Jones H M and Mortimer A M. (1996) Biosphere modelling and dose assessment for Yucca Mountain. EPRI report Not TR-107190 3294-18. Electric Power Research Institute, Palo Alto.

D

BIOSPHERE SYSTEM DESCRIPTION

D.1 Screening of System Characteristics

The first step of the biosphere description procedure is to identify those characteristics and properties of each component of the biosphere system identified above that are relevant to providing an assessment-oriented description of the system. This is achieved by working through a checklist of common general characteristics, descriptive of potentially relevant features for each Principal Component defined in the previous section and selecting specific items for their relevance to the overall assessment objective according to the assessment context and any additional assumptions invoked in the preceding system identification.

Climate Characteristics

Consideration of climate characteristics contributes to providing a coherent overall description of the biosphere system, especially in so far as precipitation is an important contribution to the availability and quality of local surface resources (and hence demands on aquifer use). Other components of climate are important in determining the growth regime of plants, animal husbandry practices, water demand, etc. Table D-1 summarises the screening arguments that have been deployed in respect of the climate characteristics of the biosphere system.

Table D-1
Climate Characteristics

Principal Component Type	Characteristic	Relevant ?	Comments
Climate characteristics	Temperature	Y	Temperature and precipitation determine basic productivity and need for irrigation
	Precipitation	Y	
	Pressure	N	Pressure not relevant (no gas release assumed)
	Wind	N	Wind speed ruled out on basis of low importance
	Solar radiation	N	Effects covered in temperature
Temporal variability of climate	Diurnal	Y	Probably not represented explicitly in models
	Seasonal	Y	Seasonal because it determines the growing season and need for irrigation
	Interannual	N	Longer term variations ruled out on basis of low relevance to lifetime average exposure
	Decadal	N	
Spatial variability of climate	Latitude	N	Spatial extent too small for climatic variation
	Longitude	N	No significant variation in a plains area
	Altitude	N	
	Aspect	N	Aspect not relevant for a plains area

The assessment context specifies no biosphere change. Nevertheless, relatively short-term variability may be relevant to the radiological assessment, insofar as the use of water (and evapotranspiration, and other related factors) will be influenced by climate fluctuations over diurnal and seasonal timescales. Interannual and decadal variabilities have limited relevance to the determination of lifetime average exposures. However, it is assumed that they can be addressed through the selection of appropriate annual-average parameter values based on measurements over decades.

The geographical extent of the biosphere system is restricted to the region within which agricultural practices involving the use of well water are carried out by the local community. There is unlikely to be any significant spatial variability in climate over the domain of the biosphere system. This factor can therefore be considered irrelevant to the system description.

Geology, Soil and Topography Characteristics

As the geosphere/biosphere interface is restricted to abstraction of water via a well, the only function of the saturated zone is to act as a sink for percolating water. Detailed characteristics of the underlying geology are therefore largely irrelevant, except if they influence the properties of the soil and variably saturated zone. Soil characteristics are relevant to providing a description of the structure and composition of the substrate within which crops are grown. Table D-2 summarises the screening arguments deployed with respect to these aspects of the biosphere system.

The topography does not have a major influence on the overall system description, although its characteristics may be relevant to considerations such as the description of field drainage. Table D-2 summarises the screening arguments deployed in respect of this component of the biosphere system description.

Hydrology Characteristics

Identified water bodies present within the biosphere system include a well, variably saturated zone and saturated zone. There is also the possibility of including consideration of a small reservoir, or pond, to distribute water for irrigation and animal watering. Table D-3 summarises the screening arguments deployed with respect to these aspects of the biosphere system.

It can be inferred from the assessment context that technological development is sufficient to allow for abstraction of water to take place. The actual technology required would depend on the specific situation in which abstraction takes place. Simple excavation into a shallow aquifer requires less technology than pumping from a borehole drilled into a deep, relatively impermeable, formation.

Table D-2
Geology Soil and Topography Characteristics

Principal Component Type	Characteristic	Relevant?	Comments
Consolidated/ Solid Geology	Lithostratigraphy	Y	Only relevant insofar as it affects the past development and present type of soil.
	Fracture systems	Y	
	Degree of weathering	Y	
	Erodability	Y	
	Mineralogy	Y	
Unconsolidated / Drift Geology	Lithostratigraphy	Y	Only relevant insofar as it affects the type of soil and as a host for the variably saturated zone. An unspecified transmissivity is required to allow sufficient water movement.
	Fracture systems	Y	
	Degree of weathering	Y	
	Erodability	Y	
	Deposition rates	Y	
	Mineralogy	Y	
Soil	Stratification (e.g. soil horizons)	Y	Modified by cultivation and irrigation practice.
	Composition (organic content, mineralogy)	Y	Modified by cultivation practice.
	Texture	Y	Apart from breaking up any possible hard pan by ploughing and cultivation effects on humus content, the properties of the cultivated soil will be largely those of unmodified chernozems.
	Areal variation	N	Potentially relevant to extensive agricultural region.
Topography	Altitude	Y	Low enough to permit agriculture.
	Slope	Y	0-5% according to plain topography.
	Erodability	N	Limited significance in region of low relief with no surface water courses.
	Deposition Rate	N	Assessment context requires that biosphere system should be constant. [You'll need to add a caveat about this to explain how you will handle dust deposition/resuspension.]

Table D-3
Hydrology Characteristics

Biosphere System Component	Characteristic	Relevant?	Comments
Well	Geometry	N	Excluded by assessment context
	Flow Rate	N	Excluded by assessment context [Would be better to explain what this means – that the flow rate is specified by the regulations.]
	Suspended Sediment	Y	
	Freeze/Thaw Phenomena	N	
	Hydrochemistry	Y	Composition and load, pH, Eh
Variably Saturated Zone	Geometry		
	▸ Level	Y	Seasonal variation
	▸ Basal	N	Not relevant to irrigation
	Flow Rate	N	Not relevant given source term in assessment context
	Freeze/Thaw Phenomena	N	Too warm
	▸ Ground Freezing		
	▸ Water Body Freezing	N	Not relevant
	Hydrochemistry	N	Too warm
Saturated Zone	Geometry	N	Only role of saturated zone within conceptualised system is as a sink for infiltrating water. Characteristics are irrelevant to *biosphere* assessment context.
	Flow Rate	N	
	Freeze/Thaw Phenomena	N	
	Hydrochemistry	N	

Although consideration of population size does not necessarily influence the biosphere system description, it may be important in applying and interpreting the results. For example, the size should be consistent with the underlying geosphere characteristics, insofar as radionuclide concentrations in well water are assumed to be unaffected by withdrawal rates, or variations in withdrawal rates. It might also be inferred from the assessment context that, if water abstraction is to be sustainable over an indefinite period, water use should be compatible with the capacity of the aquifer. Moreover, the overall community context (combined with local lithostratigraphy) may affect the type of well that is constructed, and hence the potential (as well as the realised) abstraction rates in any given situation. Predication of a particular abstraction rate (necessary to guide the geosphere calculations) will constrain the type of well that can be used.

Based on the above information, Tables D-4 and D-5 identify and describe the biosphere system. Inspection shows only few differences from Example 2A of BIOMASS Theme 1 [IAEA, 2001]. These relate primarily to the drier and warmer climate.

Table D-4
Biosphere System Identification

System Component	Classification	Reasons
Geographical Extent	Minimum area sufficient to meet the purpose of the assessment, consistent with the assumed use of well water. Precise definition depends on assumed size of the exposure group.	Precise definition is to be based on the diversity of foodstuffs and other practices assumed for the RMEI, according to surveys of current occupation and habits of occupants in the area.
Climate	ZBVIII [Walker, 1984]	Average rainfall less than 200mm/y, variable.
Geographical Context and Topography	Inland	From context
	Lowland	A contaminated aquifer at accessible depth in an agricultural setting is more likely to be associated with a lowland location.
	Flat Limited localised erosion	Consistent with requirement for irrigation and use of land for agricultural purposes.
Human Activities	Agricultural land use with production of animal products and crops for human and animal consumption. Residents with gardens.	Production of a variety of products consistent with mixture of commercial agricultural practice and gardening.
Geology	Alluvium (but not a critical assumption and could be any of the other classes listed)	Consistent with the presence of an aquifer, as required by the assessment context. Unconsolidated sediments not specifically identified.
Water Bodies	Wells Variably saturated zone Saturated zone as a fixed source and sink	No permanent, useable open water bodies.
Soils	Chernozem (primary requirement is consistency with assumed climate, geographical context and land use) See Soils entry in Table 2.6 for full description	Soil type should provide a reasonably robust estimate of potential transfer pathways (i.e. with respect to bioavailablity and sorption)
Ecology	Cultivated crops and gardens dependent on irrigation	All managed terrestrial ecosystems can be excluded by reference to the assessment context and assumed human activities, with the exception of those identified here.

Table D-5
Biosphere System Description

Biosphere System Component	Descriptive Class	In?	Reason
Climate characteristics	Temperature	Y	Temperature and precipitation determine basic productivity and need for irrigation
	Precipitation	Y	
	Pressure	N	Pressure not relevant
	Wind speed/direction	N	Wind speed ruled out for the 'normal' scenario on basis of low consequence (can determine evapotranspiration without it), but it may be important when considering dust issues for the 'igneous' scenario.
	Solar radiation	N	
Temporal variability of climate	Diurnal	Y	Probably not represented explicitly in models
	Seasonal	Y	Seasonal because it determines the growing season and need for irrigation
	Interannual	N	Longer term variations ruled out on basis of low relevance to lifetime average exposure
	Decadal	N	
Spatial variability of climate	Latitude	N	Spatial extent too small for climatic variation
	Longitude	N	
	Altitude	N	No significant variation in a plains area
	Aspect	N	Aspect not relevant for a plains area
Consolidated/ Solid Geology	Lithostratigraphy	N	Only relevant insofar as it affects the type of soil, but this is substantially modified by the cultivation practice
	Fracture systems	N	
	Degree of weathering	N	
	Erodability	N	
	Deposition rates	N	
	Mineralogy	N	
Unconsolidated/ Drift Geology	Lithostratigraphy	N	Only relevant insofar as it affects the type of soil, but this is substantially modified by the cultivation practice
	Fracture systems	N	
	Degree of weathering	N	
	Erodability	N	
	Deposition rates	N	
	Mineralogy	N	
Soil	Stratification (e.g. soil horizons)	Y	Well mixed to 30 cm thickness due to ploughing/filling
	Composition (organic content, mineralogy)	Y	Assume entire root zone is in contaminated zone Sub soil consistent with sedimentary geology
	Texture	Y	Will be affected by the farming practice.
	Areal variation	N	Some areal variation that can be explored using a range of parameter values
Topography		Y	Flat (i.e., no need to consider runoff)
Human Activities	Chemical changes to the environment	N	Have described environment (e.g. soil) so we do not need to consider chemical and physical changes. Limited effect if small changes, and large changes not included in a constant biosphere.
	Physical changes to the environment including construction of ponds, demolition of buildings	N	
	Land reclamation	N	
	Ploughing	Y	
	Well	Y	
	Other water	N	Well water is sole source

Biosphere System Component	Descriptive Class	In?	Reason
	Irrigation	Y	
Water Bodies	*Recycling of bulk solid materials*		
	Artificial mixing of water bodies	N	Well water is sole source
	Dredging	N	Not relevant
	Controlled ventilation	Y	Incorporated in air exchange rates
	Redistribution of trace materials		
	Water treatment		
	Waste water	N	Not significant
	treatment	Y	As soil improvement
	Air filtration	Y	Passive effects in enclosed spaces
	Food processing	Y	Can decrease or increase concentrations
	Sea level	N	Not relevant
	Basal characteristics	N	Not relevant
	Suspended sediments	N	
	Freeze thaw phenomena	N	Not relevant
	Infiltration	Y	
	Runoff	N	Flat topography
	Ground water	N	Assessment context
	discharge	Y	
	Porous medium	N	
	Fracture flow	Y	
	Macropore flow		
	Surface water flows	N	No, only need flow through soil - above
	Ice sheet	N	Inconsistent with assessment context
Water Balance	Hydrochemistry		
	Major ions	Y	
	Minor ions	Y	
	Organic compounds	Y	
	Colloids	Y	
	Sorption	Y	
	Precipitation/dissolution	Y	
	Mineralisation	Y	
	pH and Eh	Y	
	Precipitation	N	Minor in this climate compared with irrigation
	Irrigation	Y	
Land surface	Subsurface water flows	N	Not applicable at site
	Interception	N	Incorporated in evaporation and transpiration
	Leaf drip	N	Incorporated in evaporation and transpiration
	Stemflow	N	Incorporated in evaporation and transpiration
	Interflow (throughflow)	N	Incorporated in evaporation, transpiration and infiltration
	= storage	N	
	Evaporation	Y	
	Transpiration	Y	

E

POTENTIAL EXPOSURE MODES, POTENTIAL EXPOSURE ROUTES AND EXAMPLES OF TYPICAL ACTIVITIES

Source/ medium	Exposure mode	Example exposure route	Examples of typical activities	Assumed parameters
Soil	inhalation	***gaseous release to air***	***outdoor activities***, indoor activities	A, B, E
		resuspension of soil particulates	***ploughing, walking, misc. outdoor activities, indoor exposure resulting from soil brought inside***	A, B, E
	ingestion	***incidental soil ingestion***	***gardening, fresh fruit and veg. consumption, recreational activities, occupational activities***	A, B, H
		deliberate soil ingestion	soil pica	B, H
	external	***external radiation exposure***	***activities over/near contaminated soil, including dermal contact***, living in buildings made of contaminated soil	A, C, F, G
Water	inhalation	***spray/aerosols/volatiles***	***spray (irrigation,*** surface water***), recreation, domestic (showering, sauna, cooking),*** recreation/fishing	A, B, E
	ingestion	***deliberate water intake***	***drinking, as a component of diet in other foods (cooking)***	B
		incidental water intake	during swimming, bathing, showering	A, B
	external	**submersion in water**	***bathing, swimming***	A, C, F, G
		external exposure from water bodies	working near bulk water (storage tanks, filtration systems), recreational activities near water bodies	A C, F, G
	dermal absorption	submersion in water	farming activities, interception of spray irrigation, swimming, bathing	A, B
Sediments	inhalation	gaseous release to air	outdoor activities on exposed sediments, and sediments transferred to soil by dredging	A, B, E
		(re)suspension of dried sediments	dredging, maintenance of water distribution system, farming, activities on shorelines and near perennial lakes	A, B, E
		spray including suspended sediments	irrigation spray, showering	A, B
	ingestion	incidental ingestion	dried/exposed sediments as deposits on food, or fingers, suspended sediment with water	B

Potential Exposure Modes, Potential Exposure Routes and Examples of Typical Activities

Source/ medium	Exposure mode	Example exposure route	Examples of typical activities	Assumed parameters
		deliberate ingestion	sediment pica (dried exposed sediments only)	B, H
	external	•-irradiation from bulk sediments	activities (recreational and occupational) near exposed sediments, dried sediments, swimming, bathing	A, C, F, G
Air (pathways covered by releases from soils and water bodies	inhalation	breathing	all activities (indoor, outdoor, including sleeping)	A, B
	ingestion	particulate deposition on surfaces/foodstuffs	eating, recreational activities	B, D, H
	external	submersion dose	exposure from airborne concentrations (all types of activity)	A, C, F, G
Plants and plant products	inhalation	***particulates from combustion, from plant processing***	***burning of plant material*** (wood, ***stubble,*** specific crops, e.g.., tobacco), milling	A, B, E
	ingestion	***food consumption***	***eating, drinking plant material as part of the diet, root veg., green veg, cereals, fruit, etc.***	B
	external	***exposure from plants and plant products***	***Working/ recreation in fields, storage of plants, wearing clothes derived from plants,*** building materials	A, C, F, G
Animals and animal products	inhalation	inhalation of animal derived particulates	derived from domestic activities (cooking), occupational activities (incineration, butchery, tanning)	A, B, E
	ingestion	***food consumption***	***animal products consumed include meat, milk, offal, eggs, dairy products, other products (e.g., gelatin)***	B
	external	***•-exposure from animals and animal products***	***animal husbandry, processing/storage of animal products and materials***	A, C, F, G

Legend:

A - Exposure duration (hours a^{-1})
B - Rate of intake (kg a^{-1})
C - Shielding of source (yes/no, shielding factor)
D - Deposition rate (kg m^{-2} a^{-1})
E - Resuspension/release rate [(kg soil) (m^3 air)$^{-1}$, m^{-1}, kg $hour^{-1}$, etc.]
F - Source geometry (infinite plane, line, sphere, semi-infinite cloud, etc.)
G - Relation to source (distance, orientation – above, beside, below, immersed, etc.)
H - Age specific information relevant

About EPRI

EPRI creates science and technology solutions for the global energy and energy services industry. U.S. electric utilities established the Electric Power Research Institute in 1973 as a nonprofit research consortium for the benefit of utility members, their customers, and society. Now known simply as EPRI, the company provides a wide range of innovative products and services to more than 1000 energy-related organizations in 40 countries. EPRI's multidisciplinary team of scientists and engineers draws on a worldwide network of technical and business expertise to help solve today's toughest energy and environmental problems.

EPRI. Electrify the World

♻ *Printed on recycled paper in the United States of America*

1003031

EPRI • 3412 Hillview Avenue, Palo Alto, California 94304 • PO Box 10412, Palo Alto, California 94303 • USA
800.313.3774 • 650.855.2121 • askepri@epri.com • www.epri.com